ELECTROCHEMICAL REACTION FOR DIRECT SYNTHESIS OF AMIDES FROM ALDEHYDES

Mr. Tanawat Rerkrachaneekorn

A Thesis Submitted in Partial Fulfillment of the Requirements
for the Degree of Master of Science in Chemistry
Department of Chemistry
FACULTY OF SCIENCE
Chulalongkorn University
Academic Year 2020

ปฏิกิริยาเคมีไฟฟ้าสำหรับการสังเคราะห์เอไมด์โดยตรงจากแอลดีไฮด์

นายธนวัฒน์ ฤกษ์รัชนีกร

วิทยานิพนธ์นี้เป็นส่วนหนึ่งของการศึกษาตามหลักสูตรปริญญาวิทยาศาสตรมหาบัณฑิต
สาขาวิชาเคมี ภาควิชาเคมี
คณะวิทยาศาสตร์ จุฬาลงกรณ์มหาวิทยาลัย
ปีการศึกษา 2563

Thesis Title	ELECTROCHEMICAL REACTION FOR DIRECT SYNTHESIS OF AMIDES FROM ALDEHYDES
By	Mr. Tanawat Rerkrachaneekorn
Field of Study	Chemistry
Thesis Advisor	Professor Doctor SUMRIT WACHARASINDHU
Thesis Co Advisor	Professor Doctor MONGKOL SUKWATTANASINITT

Accepted by the FACULTY OF SCIENCE, Chulalongkorn University in Partial Fulfillment of the Requirement for the Master of Science

..... Dean of the FACULTY OF SCIENCE
(Professor Doctor POLKIT SANGVANICH)

THESIS COMMITTEE

..... Chairman
(Professor Doctor VUDHICHAI PARASUK)

..... Thesis Advisor
(Professor Doctor SUMRIT WACHARASINDHU)

..... Thesis Co-Advisor
(Professor Doctor MONGKOL SUKWATTANASINITT)

..... Examiner
(Associate Professor Doctor VIWAT VCHIRAWONGKWIN)

..... Examiner
(Assistant Professor Doctor TANATORN KHOTAVIVATTANA)

..... External Examiner
(Assistant Professor Doctor Punlop Kuntiyong)

ธนวัฒน์ ฤกษ์รัชนีกร : ปฏิกิริยาเคมีไฟฟ้าสำหรับการสังเคราะห์เอไมด์โดยตรงจากแอลดีไฮด์. (ELECTROCHEMICAL REACTION FOR DIRECT SYNTHESIS OF AMIDES FROM ALDEHYDES) อ.ที่ปรึกษาหลัก : ศ. ดร.สัมฤทธิ์ วัชรสินธุ์, อ.ที่ปรึกษาร่วม : ศ. ดร.มงคล สุขวัฒนาสินิทธิ์

การสังเคราะห์เอไมด์แบบดั้งเดิมเกี่ยวข้องกับการใช้ปฏิกิริยาที่รุนแรง ใช้ตัวออกซิไดซ์ที่รุนแรง ใช้ตัวเร่งปฏิกิริยาโลหะที่มีราคาแพง หรือใช้สารตั้งต้นที่ผ่านการสังเคราะห์หลายขั้นตอน เพื่อที่จะเอาชนะปัญหาเหล่านี้ ในงานวิจัยนี้เราพัฒนาปฏิกิริยาสังเคราะห์เอไมด์ด้วยกระบวนการออกซิเดชันเชิงไฟฟ้าเคมีที่ไม่รุนแรงจากเบนซิลแอลกอฮอล์และแอลดีไฮด์กับเอมีนที่สามารถซื้อขายได้ทั่วไป การศึกษาสภาวะที่เหมาะสมที่สุดบ่งบอกว่าปฏิกิริยาสังเคราะห์เอไมด์ด้วยกระบวนการออกซิเดชันเชิงไฟฟ้าเคมีสามารถดำเนินปฏิกิริยาได้ด้วยการใช้โซเดียมไอโอไดด์เป็นสารอิเล็กโทรไลต์และเมดิเอเตอร์ในสารละลายน้ำซึ่งแสดงปฏิกิริยาในเซลล์ไฟฟ้าเคมีแบบไม่แบ่งแยกภายใต้อุณหภูมิห้องที่ไม่มีการใช้สารเติมแต่งเพิ่มเติม ภายใต้การศึกษาสภาวะที่เหมาะสมที่สุดเราสามารถแสดงปฏิกิริยาสังเคราะห์เอไมด์ด้วยกระบวนการออกซิเดชันเชิงไฟฟ้าเคมีกับเบนซิลแอลกอฮอล์หลายชนิดและอะโรมาติกแอลดีไฮด์หลายชนิดกับเอมีน เพื่อจะเตรียมเอไมด์ที่มีความสอดคล้อง (จำนวน 29 ตัวอย่าง) ซึ่งมีร้อยละผลได้ของผลิตภัณฑ์ตั้งแต่ปานกลางจนถึงดี มากไปกว่านั้นปฏิกิริยาสังเคราะห์เอไมด์ด้วยกระบวนการออกซิเดชันเชิงไฟฟ้าเคมีของเราสามารถเพิ่มปริมาณสารตั้งต้นไปถึงหนึ่งกรัมได้ นอกจากนี้แหล่งพลังงานสำรองแบบพกพาได้สามารถใช้เป็นแหล่งให้กระแสไฟฟ้าทางเลือกซึ่งจะให้การจัดตั้งปฏิกิริยาอิเล็กโทรลิซิสที่สะดวกขึ้น การศึกษากลไกปฏิกิริยาเปิดเผยว่าไอโอดีนคือสารออกซิไดซ์ที่แท้จริงซึ่งเป็นตัวแทนของปฏิกิริยาอิเล็กโทรลิซิสแบบทางอ้อม กุญแจสำคัญของปฏิกิริยาสังเคราะห์เอไมด์ด้วยกระบวนการออกซิเดชันเชิงไฟฟ้าเคมีคือ การตั้งปฏิกิริยาแบบหม้อเดียว การใช้สภาพปฏิกิริยาแบบอากาศเปิด ไม่ต้องการอิเล็กโทรไลต์ เบส หรือตัวออกซิไดส์เพิ่มเติม ซึ่งจะให้กระบวนการสังเคราะห์เอไมด์ที่เป็นมิตรต่อสิ่งแวดล้อม

สาขาวิชา เคมี ลายมือชื่อนิสิต .....

ปีการศึกษา 2563 ลายมือชื่อ อ.ที่ปรึกษาหลัก .....

ลายมือชื่อ อ.ที่ปรึกษาร่วม .....

6171963823 : MAJOR CHEMISTRY

KEYWORD: Amide, Electrochemical oxidative amidation, Mediator, Portable power charger, Undivided cell

Tanawat Rerkrachaneekorn : ELECTROCHEMICAL REACTION FOR DIRECT SYNTHESIS OF AMIDES FROM ALDEHYDES. Advisor: Prof. Dr. SUMRIT WACHARASINDHU Co-advisor: Prof. Dr. MONGKOL SUKWATTANASINITT

Conventional synthesis of amide involves the use of harsh condition, strong oxidizing agents, high value metal catalysts or multiple step synthesis of starting materials. To overcome these problems, in this research, we develop a mild electrochemical oxidative amidation directly from commercially available benzyl alcohols and aldehydes with amines. Optimization studies indicate that this electrochemical oxidative amidation can be proceeded via the use of sodium iodide as both electrolyte and mediator in aqueous solution performing in undivided cell at room temperature without additional additive. Under the optimized condition, we are able to perform electrochemical oxidative amidation of various benzyl alcohols and aromatic aldehydes with amines to prepare corresponding amide products (29 examples) in moderate to good yields. Moreover, our electrochemical oxidative amidation can be scaled to one gram synthesis. In addition, portable power charger can be used as alternative electrical source offering a convenience electrolysis setup. The mechanistic investigations reveal that molecular iodine is true oxidizing agent representing in indirect electrolysis fashion. The key benefits of this process are one-pot operation, open air condition, no requirement of external electrolyte, base and oxidizing agent providing an environmentally friendly process for amide synthesis.

Field of Study: Chemistry
Academic Year: 2020

Student's Signature .....
Advisor's Signature .....
Co-advisor's Signature .....

ACKNOWLEDGEMENTS

First of all, I would like to express my sincere gratitude to my generous advisor, Professor Dr. Sumrit Wacharasindhu and my gracious co-advisor, Professor Dr. Mongkol Sukwattanasinitt, Department of Chemistry, Faculty of Science, Chulalongkorn University for their valuable advices and suggestions throughout this research.

Sincere thanks are also extended to the chairperson: Professor Dr. Vudhichai Parasuk, Department of Chemistry, Faculty of Science, Chulalongkorn University; the thesis examiners: Associate Professor Dr. Viwat Vchirawongkwin, Assistant Professor Dr. Tanatorn Khotavivattana, Department of Chemistry, Faculty of Science, Chulalongkorn University and Assistant Professor Dr. Punlop Kuntiyong, Department of Chemistry, Faculty of Science, Silpakorn University for their valuable comments and suggestions.

I would like to thank National Research Council of Thailand (NRCT), National Nanotechnology Centre (NANOTEC) and Center of Excellence on Petrochemical and Materials Technology (PETROMAT) for financial support.

In addition, my appreciation is also given to my friends, SW members, Material Advancement via Proficient Synthesis (MAPS) group members, Dr. Theeranon Tankam, Dr. Komthep Slipcharu, Dr. Wittawat Kaewsongsaeng and Mr. Vasin Thummasorn for their kind support and good friendship. I also thank to an amazing singer and song-writer, Taylor Swift for her inspirations from first to latest studio albums. I hope that your latent will lead me to do something excepting only study. I promise.

Finally, I am deeply appreciated to my family and my felines (Cherry, Cake, Cookie, Butter and Brownie) for their positive supports and encouragements throughout my M.Sc. journey.

Tanawat Rerkrachaneekorn

TABLE OF CONTENTS

Page

LIST OF SCHEMES

Page

LIST OF TABLES

Page

LIST OF FIGURES

Page

LIST OF ABBREVIATIONS

^{1}H-NMR	proton nuclear magnetic resonance
^{13}C-NMR	carbon-13 nuclear magnetic resonance
^{19}F-NMR	fluorine-19 nuclear magnetic resonance
BHT	butylated hydroxytoluene
$CDCl_3$	deuterated chloroform solvent
CD_3CN	deuterated acetonitrile solvent
CH_2Cl_2	dichloromethane
DCE	dichloroethane
DIB	(diacetoxyiodo)benzene
DMSO	dimethyl sulfoxide
ESI-HRMS	electrospray ionization high resolution mass spectrometry
EtOAc	ethyl acetate
EtOH	ethanol
FT-IR	Fourier transform infrared spectroscopy
MeCN	acetonitrile
ppm	part per million
TBHP	*tert*-butyl hydroperoxide
TEA	triethylamine
THF	tetrahydrofuran
TOF	time-of-flight (mass spectrometry)
br	broad (NMR)
cm	centimeter (s)
d	doublet (NMR)
dd	doublet of doublet (NMR)
eq	equivalent (s)
Hz	Hertz
h	hour (s)
J	coupling constant
m	multiplet (NMR) or milimeter (s)

mA	milliampere
mg	milligram (s)
mL	milliliter (s)
mmol	millimole (s)
mV	millivolt
M	molar
MHz	megahertz
m/z	mass per charge
s	singlet (NMR) or second (cyclic voltammetry)
TLC	thin layer chromatography
V	voltage
^{o}C	degree Celsius
Ø	diameter
μm	micrometer (s)
δ	chemical shift
% yield	percentage yield
AOP	(7-azabenzotriazol-1-yl)oxy-tris-(dimethyl-amino)phosphonium hexafluorophosphate
AOMP	5-(7-azabenzotriazol-1-yloxy)-3,4-dihydro-1-methyl-2*H*-pyrrolium hexachloroantimonate
BDP	benzotriazol-1-yl diethylphosphate
BEP	2-bromo-1-ethyl pyridinium tetrafluoroborate
BOI	2-(benzotriazole-1-yl)oxy-1,3-dimethylimidazolidinium hexafluorophosphate
BOP-Cl	*N*,*N*'-bis(2-oxo-3-oxazolidinyl)-phosphinic chloride
BTC	bis(trichloromethyl)carbonate
BDMP	5-(1-*H*-benzotriazol-1-yloxy)-3,4-dihydro-1-methyl 2*H*-pyrrilium hexachlorideantimonate
BEMT	2-bromo-3-ethyl-4-methyl thiazolium tetrafluoroborate
BEPH	2-bromo-1-ethyl pyridinium hexachloroantimonate

BMPI	2-bromo-1-methylpyridinium iodide
BMP-Cl	*N*,*N*'-bismorpholinophosphinic chloride
BOMI	benzotriazole-1-yloxy-*N*,*N*-dimethyl-methaniminium hexachloroantimonate
BPMP	(1*H*-benzotriazol-1-yloxy)phenyl-methylene pyrrilidinium hexachloroantimonate
BroP	bromotris(dimethylamino)phosphonium hexafluorophosphate
BTFFH	bis(tetramethylene)fluoroformamidinium hexafluorophosphate
CDI	1,1'-carbonyldiimidazole
CIB	2-chloro-1,3-dimethylimidazolidinium tetrafluoroborate
CIC	*N*-cyclohexyl-*N*'-isopropylcarbodiimide
CIP	2-chloro-1,3-dimethylimidazolidinium hexafluorophosphate
CBMIT	1,1'-carbonylbis(3-methyl-imidazolium)-triflate
CDMT	2-chloro-4,6-dimethoxy-1,3,5-triazine
CloP	chlorotris(dimethylamino)phosphonium hexafluorophosphate
CMBI	2-chloro-1,3-dimethyl-1*H*-benzimidazolium hexafluorophosphate
CMPI	2-chloro-1-methylpyridinium iodide
Cpt-Cl	1-oxo-chlorophospholane
DCC	*N*,*N*'-dicyclohexylcarbodiimide
DIC	*N*,*N*'-diisopropylcarbodiimide
DPP-Cl	diphenylphosphinic chloride
DEBP	diethyl-2-(3-oxo-2,3-dihydro-1,2-benzisosulfonazolyl)phosphonate
DECP	diethylcyanophosphonate
DEPB	diethyl phosphorobromidate
DEPC	diethyl phosphorochloridate
DFIH	ethyl-2-fluoro-4,5-dihydro-1*H*-imidazolium hexafluorophosphate
DOMP	5-(3',4'-dihydro-4'-oxo-1',2'3'-benzotriazin-3'-yloxy)-3,4-dihydro-1-methyl 2*H*-pyrrolium hexachloroantimonate

DPPA	diphenylphosphoryl azide
EDC	1-[3-(dimethylamino)propyl]-3-ethyl-carbodiimide hydrochloride
ENDPP	phosphoric acid 3,5-dioxo-10-oxa-4-azatricyclo[5.2.1.$0^{2,6}$]dec-8-en-4-yl ester diphenyl ester
FEP	2-fluoro-1-ethyl pyridinium tetrafluoroborate
FDPP	pentafluorophenyl diphenyl phosphinate
FEPH	2-fluoro-1-ethyl pyridium hexachloroantimonate
FOMP	5-(pentafluorophenyloxy)-3,4-dihydro-1-methyl 2*H*-pyrrolium hexachloroantimonate
HBTU	*O*-(benzotriazole-1-yl)-1,1,3,3-tetramethyluronium hexafluorophosphate
HDTU	*O*-(3,4-dihydro-4-oxo-1,2,3-benzotriazin-3-yl)-1,1,3,3-tetramethyluronium hexafluorophosphate
HOAt	1-hydroxy-7-azabenzotriazole
HOBt	1-hydroxybenzotriazole
HOCt	ethyl-1-hydroxy-1*H*-1,2,3-triazole-4-carboxylate
HODhbt	3,4-dihydro-3-hydroxy-4-oxo-1,2,3-benzotriazine
MPTA	dimethylphosphinothioyl azide
MPTO	3-dimethylphophinothioyl-2(3*H*)-oxazolone
NDPP	norborn-5-ene-2,3-dicarboximidodiphenylphosphate
pyAOP	[(7-azabenzotriazol-1-yl)oxy]tris-(pyrrolidino)phosphonium hexafluorophosphate
PyBOP	benzotriazole-1-yloxytri(pyrrolidino)phosphonium hexafluorophosphate
PyBroP	bromotri(pyrrolidino)phosphonium hexafluorophosphate
PyCloP	chlorotri(pyrrolidino)phosphonium hexafluorophosphate
SOMP	5-(succinimidyloxy)-3,4-dihydro-1-methyl 2*H*-pyrrolium hexachloroantimonate
TBTU	*O*-benzotriazol-1-yl-1,1,3,3-tetramethyluronium tetrafluoroborate

TDBTU	2-(3,4-dihydro-4-oxo-1,2,3-benzotriazin-3-yl)1,1,3,3-tetramethyluronium tetrafluoroborate
TFFH	tetramethylfluoroformamidinium hexafluorophosphate
TNTU	2-(5-norbornene-2,3-dicarboximido)-1,1,3,3-tetramethyluronium tetrafluoroborate
TPTU	1-((dimethylamino)(dimethyliminio)methoxy)-2-hydroxypyridinium tetrafluoroborate
TSTU	2-succinimido-1,1,3,3-tetramethyluronium tetrafluoroborate

CHAPTER I

INTRODUCTION

1.1 Overview

Amide is not only backbone of protein but it is also found in medical compounds and materials [1-4]. There are many methods for amide synthesis such as classical methods [5-11] and non-classical methods [12-60]. However, such processes require harsh reaction, multiple step synthesis starting materials, toxic oxidizing agents, high value metal catalysts and long reaction times. Those will cause poor atom economy and non-environmental process. In recent years, there are numerous reports on the electrochemical oxidation process to replace the typical oxidation reactions [61-82]. These processes utilize electrons or non-toxic additive as oxidizing agent which are less toxic comparing to tranditional oxidizing agent. Therefore, in this research, we aim to develop a new electrochemical oxidative amidation process to prepare amide as shown in Scheme 1.1. We plan to use the commercially available benzyl alcohols and aldehydes as starting materials in the presence of less toxic natural salt as both electrolyte and mediator without external additives.

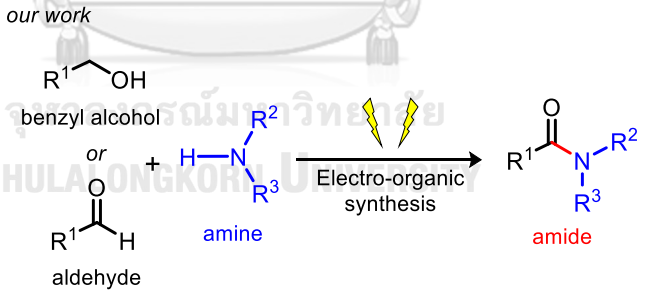

Scheme 1.1 Synthesis of amide between benzyl alcohol/aldehyde and amine

1.2 Introduction to amide

Amide is an important nitrogen-containing compounds which is also subclass of carbonyl compounds. It is a versatile group which can be found in blockbuster drugs such as Captopril **1** (treatment of hypertension) [1], Atorvastatin **2** (cholesterol lowering drug) [2], Diltiazem **3** (calcium channel blocker for treatment of angina and hypertension) [3] or in material such as Nylon-6,6 **4** (high performance fiber) [4] or in polymer such as protein **5** as shown in Figure 1.1.

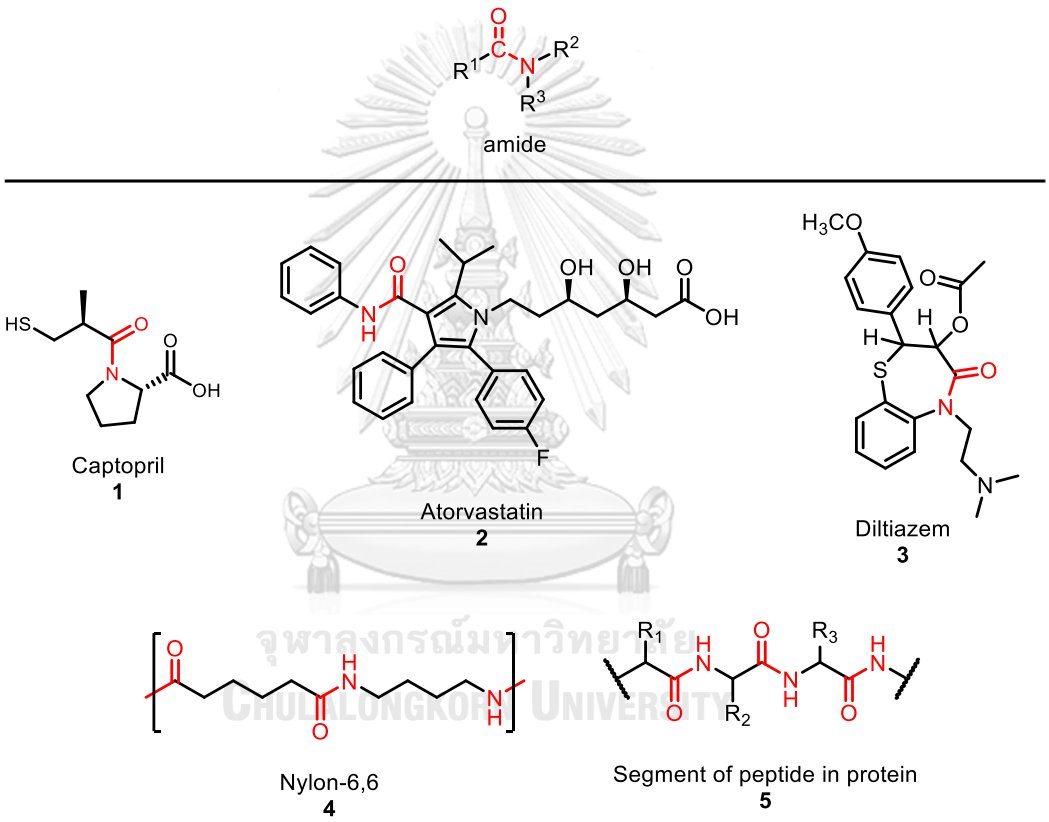

Figure 1.1 Structure of amide functional group and its important compounds

1.3 Literature reviews on amide synthesis

The amide synthetic process or amidation can be categorized into two main methods as shown in Scheme 1.2. First method is so called "classical methods" composing of 1) thermal method which is the reaction between carboxylic acid and amine and 2) the use of coupling reagent. These methods will be discussed in section 1.3.1. Second method is also known as "non-classical methods" which can be divided into four processes including 1) catalytic amidation directly from carboxylic acid and amine, 2) ligations, 3) the use of amino surrogates with carboxylic acid and 4) the use of carboxylic acid surrogates with amines. These processes will be fully explained in section 1.3.2.

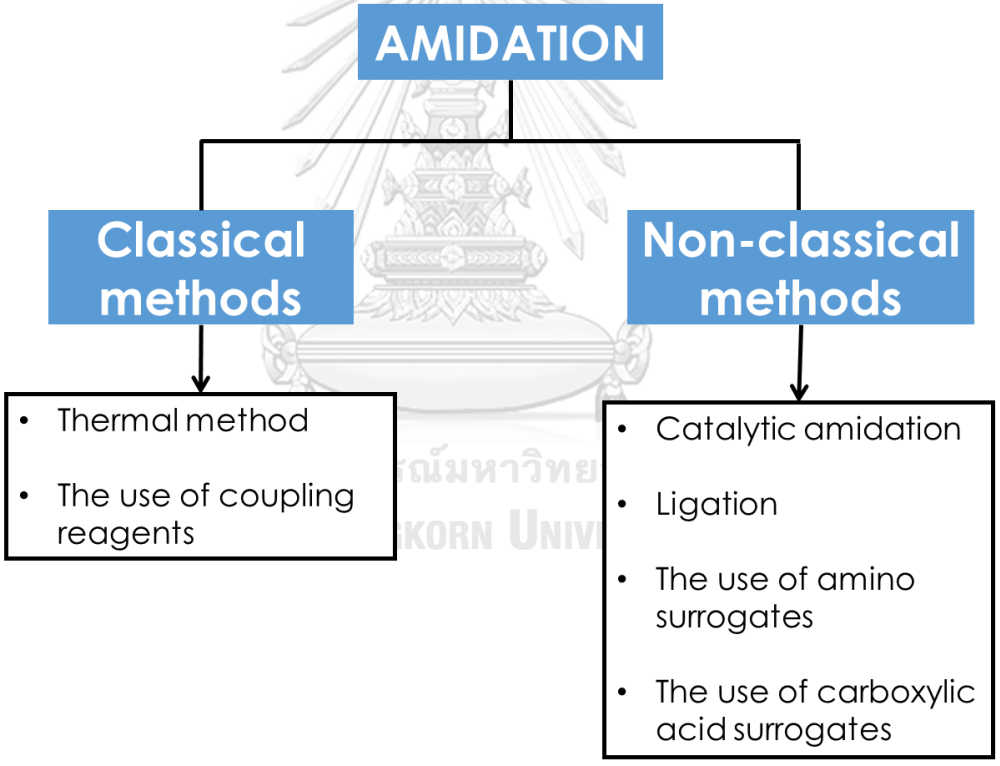

Scheme 1.2 Reaction types for amide synthesis

1.3.1 Classical methods for amide synthesis

The classical methods or traditional methods for amide synthesis using carboxylic acid and amine as starting materials are well-known reaction and have been used for the past centuries. These reactions can be classified into two main methods including thermal method and the use of coupling reagents.

The thermal method was shown in Scheme 1.3. Both carboxylic acid **6** and amine **7** starting materials were stirred under high temperature (normally more than 150 °C) in either non-polar solvent or neat reaction [5-7]. Although the satisfactory yields of amide product **8** were isolated from the thermal method, the danger from harsh condition is concerned. The high temperature from thermal method caused by the less reactivity of carboxylic acid starting material and production of water as byproduct. Therefore, the reaction equilibrium of this method shifted backward under thermal condition.

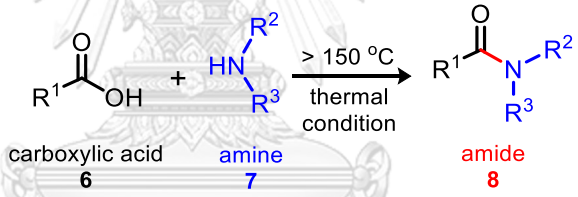

Scheme 1.3 Thermal method for amide synthesis

To avoid the use of such harsh conditions, the use of coupling reagents to activate carboxylic acid has been developed. This method still uses carboxylic acid **6** as starting material reacting with amine **7** in the presence of various coupling reagent to produce amide linkage. The reaction was demonstrated in Table 1.1 [8, 9]. We can categorize coupling reagents for amidation into eight types such as phosphonium reagents (Table 1.1, no. 1), uronium reagents (Table 1.1, no. 2), immonium reagents (Table 1.1, no. 3), carbodiimide reagents (Table 1.1, no. 4), imidazolium reagents (Table 1.1, no. 5), organophosphorous reagents (Table 1.1, no. 6), acid halogenating reagents (Table 1.1, no. 7) and chloroformate/pyridinium reagents (Table 1.1, no. 8) [10, 11]. The use of coupling reagent provided mild condition under one-pot condition starting from

carboxylic acid **6**. However, the disadvantage of these processes was requirement for using coupling reagent in stoichiometric amount which generated large amount of byproduct. Therefore, this process was poor atom economy.

Table 1.1 Examples of commonly used coupling reagents for amide synthesis

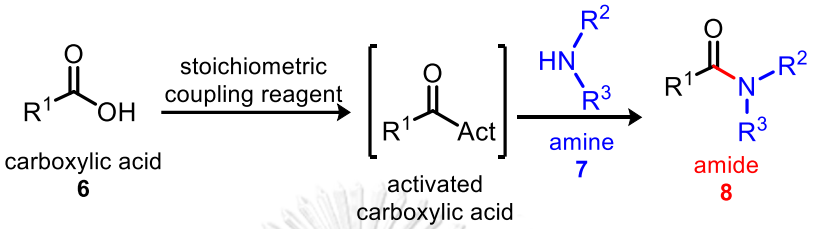

	Coupling reagents	Structure
1.	Phosphonium reagents	CloP (X = Cl) BroP (X = Br); BOP (X = CH) AOP (X = N); PyCloP (X = Cl) PyBroP (X =Br); PyBOP (X = CH) PyAOP (X = N)
2.	Uronium reagents	HBTU (X = PF_6) TBTU (X = BF_4); HDTU (X = PF_6) TDBTU (X = BF_4); TNTU; TSTU; TPTU

(Table 1.1 continued)

	Coupling reagents	Structure
3.	Immonium reagents	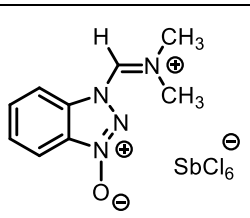 BOMI 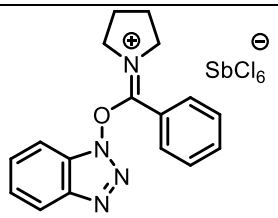 BPMP 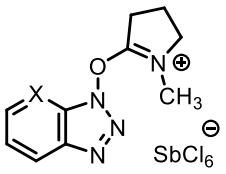 BDMP (X = CH) AOMP (X = N) 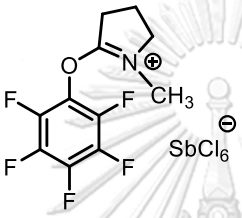 FOMP 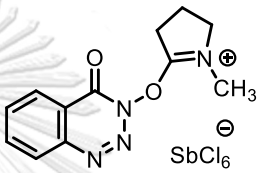 DOMP 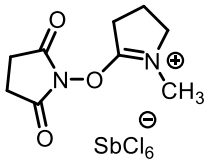 SOMP
4.	Carbodiimide reagents	 DCC 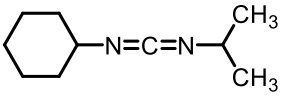 CIC 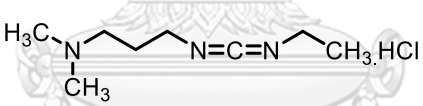 EDC 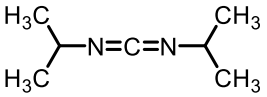 DIC additives 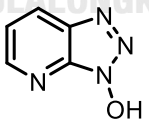 HOAt 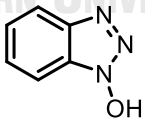 HOBt 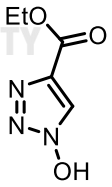 HOCt 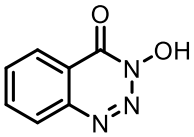 HODhbt

(Table 1.1 continued)

	Coupling reagents	Structure
5.	Imidazolium reagents	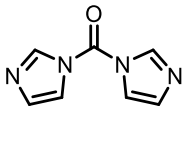 CDI 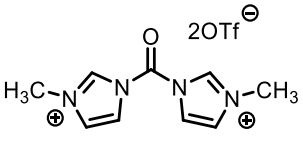 CBMIT 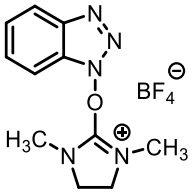 BOI 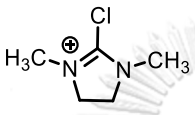 CIP (X = PF_6) CIB (X = BF_4) 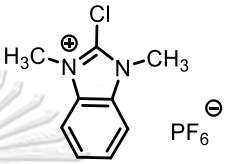 CMBI 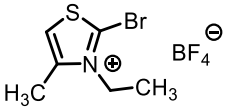 BEMT
6.	Organo-phosphorous reagents	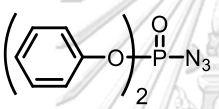 DPPA 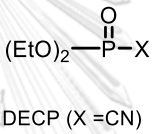 DECP (X =CN) DEPB (X = Br) DEPC (X = Cl) 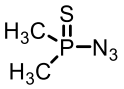 MPTA 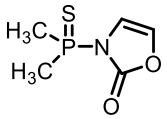 MPTO 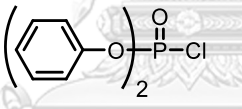 DPP-Cl 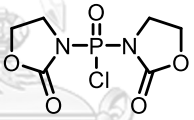 BOP-Cl 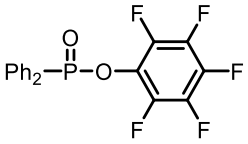 FDPP 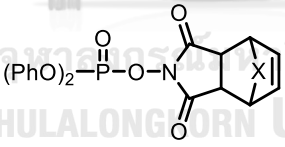 ENDPP (X =O) NDPP (X = CH_2) 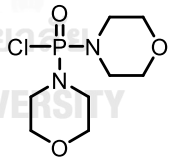 BMP-Cl 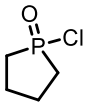 Cpt-Cl 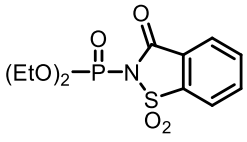 DEBP 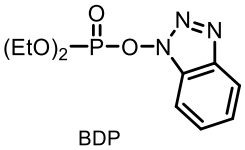 BDP

(Table 1.1 continued)

	Coupling reagents	Structure
7.	Acid halogenating reagents	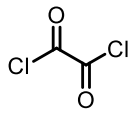 oxalyl chloride 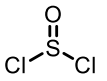 thionyl chloride 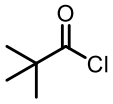 pivaloyl chloride 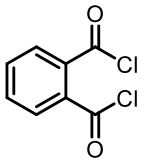 phthaloyl dichloride 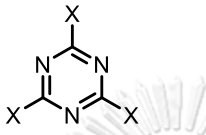 cyanuric chloride (X = Cl) cyanuric fluoride (X = F) 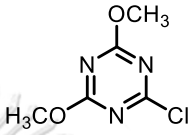 CDMT 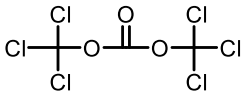 BTC 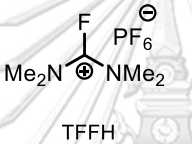 TFFH 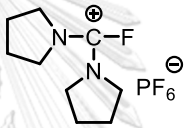 BTFFH 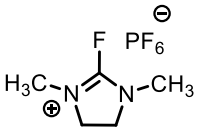 DFIH
8.	Chloroformate and pyridinium reagents	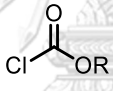 ethyl chloroformate (R = Et) phenyl chloroformate (R = Ph) isopropyl chloroformate (R = *i*-Pr) 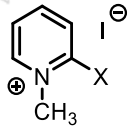 BMPI (X = Br) CMPI (X = Cl) 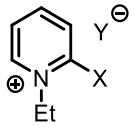 BEP (X = Br, Y = BF_4) BEPH (X = Br, Y = $SbCl_6$) FEP (X = F, Y = BF_4) FEPH (X = F, Y = $SbCl_6$)

1.3.2 Non-classical methods for amide synthesis

To avoid the drawbacks of classical methods for amidation, non-classical methods for amidation were developed as a predominant reaction in organic synthesis field for past decade [12]. These methods can be classified into four pathways as shown in Scheme 1.4. Such pathways are catalytic amidation between carboxylic acid **6** and amine **7** (pathway 1), ligations using hydroxylamine **9** as amino surrogates (pathway 2), the use of amino surrogates with carboxylic acid **6** (pathway 3) and the use of carboxylic acid surrogates with amine [**7**] (pathway 4). All details will be further discussed in section 1.3.2.1-1.3.2.4 and 1.4, respectively.

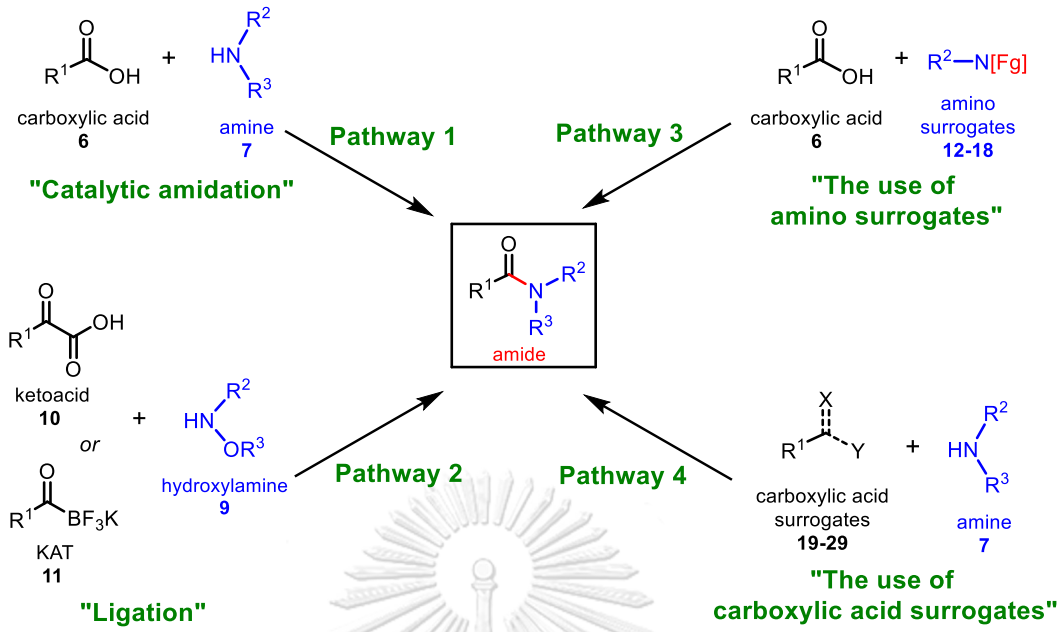

Scheme 1.4 Four pathways of non-classical methods for amide synthesis

1.3.2.1 Non-classical methods (pathway 1: catalytic amidation)

First pathway, the catalytic amidation is the reaction between carboxylic acid **6** and amine **7** which was catalyzed by organoboron or zirconium transition-metal complex to provide amide product **8** in fair to excellent yields as summarized in Scheme 1.5, route A and B [13, 14]. Importantly, both reactions used organoboron or zirconium complex in catalytic amount. Moreover, both reaction templates remained the only catalytic amidation processes until now. Even though, both reactions are the most atom economy process for construction amide linkage, the use of toxic solvent (CH_2Cl_2, THF), high temperature and long reaction time is required.

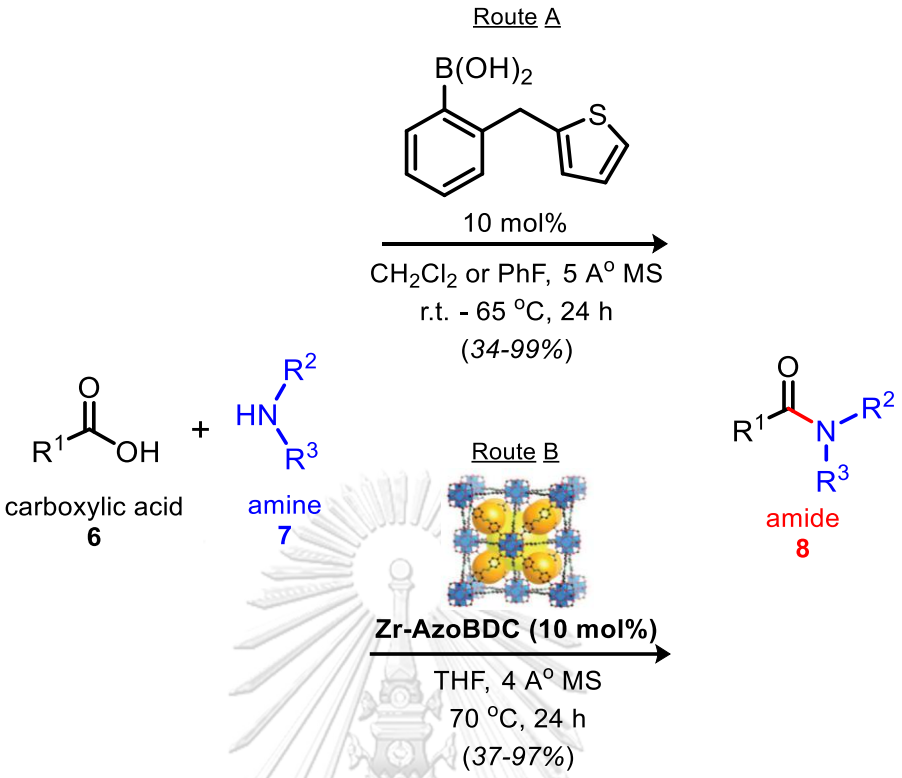

Scheme 1.5 Catalytic amidation between carboxylic acid and amine using a) organoboron and b) zirconium transition-metal complex

1.3.2.2 Non-classical methods (pathway 2: ligation)

The ligation method is the use of carboxylic acid surrogates **10**, **11** with hydroxylamine **9**. In 2006, Bode and coworkers performed the amide synthesis or "KAHA ligation" using α-ketoacid **10** and *N*-alkylhydroxylamine **9** as starting materials as shown in Scheme 1.6., route A [15]. This reaction can proceed with polar solvent at 40 °C for 15 hours providing amide **8** in 58-80% yields. Next, in 2012, Dumas and coworkers successfully synthesized amide product **8** by ligation between potassium acyltrifluoroborate (KAT) **11** and *O*-benzyl hydroxylamine **9** under aqueous phase solvent at room temperature as shown in Scheme 1.6, route B [16]. The amide products **8** were obtained in 68-96% yields. However, both ligation processes shared the same disadvantages which require a multiple step synthesis of α-ketoacid and KAT.

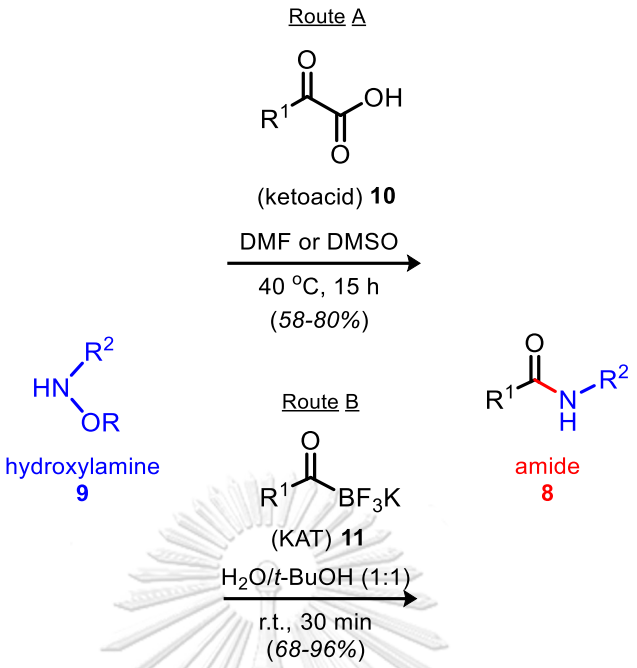

Scheme 1.6 Ligation for amide synthesis using hydroxylamine with a) ketoacid and b) KAT

1.3.2.3 Non-classical methods (pathway 3: the use of amino surrogates)

The third pathway is the use of amino surrogates **12**-**18** as alternative source of amine to react with carboxylic acids **6** which summarized in Table 1.2. The examples of amino surrogates are isocyanate **12** (Table 1.2, entry 1), isonitrile **13** (Table 1.2, entry 2), thioamide **14** (Table 1.2, entry 3), sulfinylamide **15** (Table 1.2, entry 4), azide **16** (Table 1.2, entry 5), tertiary amine **17** (Table 1.2, entry 6) and aromatic imine **18** (Table 1.2, entry 7). The advantages of using amino surrogates are the high stability of amino surrogate providing satisfactory yields of amide products. However, the disadvantages of those reactions are the requirement of multiple step synthesis of amino surrogates, toxic solvent (CH_2Cl_2, DCE, toluene) and additive (CCl_4, NaCN) as well as high reaction temperature.

Table 1.2 Reviews on non-classical methods using amino surrogates for amide synthesis

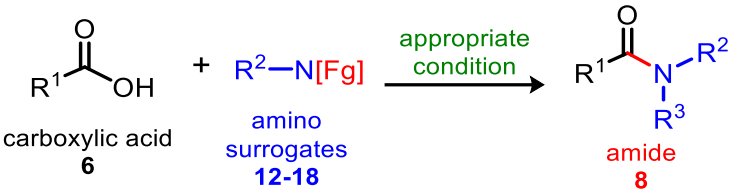

Entry	Amino surrogates	Conditions	Yields	References
1	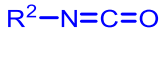 isocyanate **12**	DMAP (15 mol%), CH_2Cl_2 0 °C-r.t., 3 h	61-98%	[17]
2	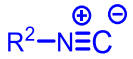 isonitrile **13**	PhSH (4 mol%), DCE 50-80 °C, 48 h	23-50%	[18]
3	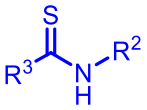 thioamide **14**	Ag_2CO_3 (1.5 eq), CH_2Cl_2, r.t., 2 h	70-99%	[19]
4	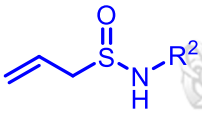 sulfinylamide **15**	DMAP (2 mol%) MeCN, 70 °C, 2-32 h	34-94%	[20]
5	 azide **16**	PySeSePy (20 mol%) PMe_3, toluene, 0 °C 2-48 h	90-99%	[21]
6	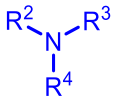 tertiary amine **17**	CuI (5 mol%), CCl_4 (3 eq) DMF, 60 °C, 16 h	28-97%	[22]
7[a]	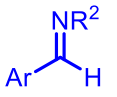 aromatic imine **18**	NaCN (1.1 eq), 4 A° MS DMF, 120 °C, 2 h	56-83%	[23]

[a] using aromatic imine as a sole starting material (DMAP: 4-dimethylaminopyridine, DCE: dichloroethane, PySeSePy: diphenyl diselenide, MS: molecular sieves)

1.3.2.4 Non-classical methods (pathway 4: the use of carboxylic acid surrogates)

The last pathway for non-classical method is the use of carboxylic acid surrogates **19**-**29** as carboxylic acid source to react with amine **7** which displayed in Table 1.3. Various carboxylic acid surrogates include alkene **19**, alkyne **20**, aryl halide **21**, ester **22**, amide **23**, thiocarboxylic acid **24**, ketone **25**, nitrile **26**, aldoxime **27**, benzyl alcohol **28** and aldehyde **29**. Among above carboxylic acid surrogates, the reactions can be catagorized into five types. The first one is "aminocarbonylation" which involved the use of alkene **19**, alkyne **20** and aryl halide **21** reacting with carbon monoxide gas to generate carbonyl intermediate from insertion process *in situ* as shown in Table 1.3, entries 1-3. Those reaction provided amide products from 32 to 99% yields. The second reaction is "catalytic amidation of ester **22**" while the third reaction is "catalytic transamidation of amide **23**" (Table 1.3., entries 4 and 5). Both reactions used metal catalyst such as zirconium and aluminium in catalytic amount to provide amide in 50-99% and 43-66% yields, respectively. The fourth reaction is the conversion of thiocarboxylic acid **24** to amide **8** which is so called "dethioamidation" (Table 1.3, entry 6). These reactions used commercially available thiocarboxylic acid **24** reacting with amine **7** to provide products in 72-90% yields. Although, above four processes are efficient and provide amide **8** under mild condition in satisfactory yields, there are some difficulties in some starting materials requiring extra step synthesis or harsh condition. Therefore, the last reaction which is "oxidative amidation" was developed and heavily used as alternative methods due to the highly available starting materials of these process. Oxidative amidation involves the use of ketone **25**, nitrile **26**, aldoxime **27**, benzyl alcohol **28** and aldehyde **29** as starting materials to react with amine **7** as shown (Table 1.3., entries 7-11). For the oxidative amidation using ketone **25**, nitrile **26** and aldoxime **27**, these reactions provided amide products **8** in good yields upon the treatment of I_2/TBHP, copper(II) acetate and rhodium catalyst, respectively. Although, those three substrates **25**-**27** are readily available, the amine substrate scopes are limited to only primary amine. For past decade, the oxidative amidation processes between benzyl alcohol **28**/aldehyde **29** and amine **7** were attractive among organic chemistry due to their high availability of starting materials

and broad reaction substrate scope. Due to their unique properties, they turned our attention to develop the oxidative amidation between benzyl alcohol/aldehyde and amine. In the following section, we will summarize the previous works on oxidative amidation reaction.

Table 1.3 Reviews on non-classical methods using carboxylic acid surrogates for amide synthesis

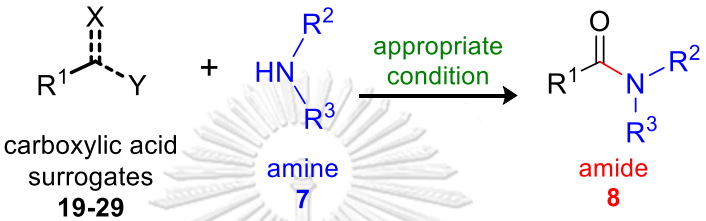

Entry	Carboxylic acid surrogates	Conditions	Yields	References
1	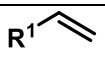 alkene **19**	Pd-610 (5 mol%), H_3PO_4 KI (5 mol%), CO (40 bar) dioxane, 130 °C, 12 h	70-99%	[24]
2	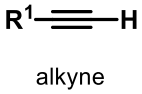 alkyne **20**	$Fe_3(CO)_{12}$ (5 mol%), ligand, TEA, CO (10 bar), THF 120 °C, 16 h	47-96%	[25]
3	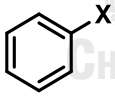 aryl halide **21**	$Pd_2(dba)_3.CHCl_3$ (2 mol%) ligand, TEA, CO (800 psi) H_2 (200 psi), 160 °C 24-42 h	32-65%	[26]
4	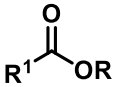 ester **22**	$Zr(Ot\text{-}Bu)_4$ (10 mol%) additive (10 mol%) toluene, r.t.-100 °C, 2-48 h	50-99%	[27]
5	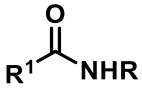 amide **23**	$Al_2(NMe_3)_6$ (5 mol%) toluene, 90 °C, 20 h	43-66%	[28]

(Table 1.3 continued)

Entry	Carboxylic acid surrogates	Conditions	Yields	References
6	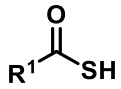 thiocarboxylic acid **24**	$CuSO_4.5H_2O$ (30 mol%) MeOH, r.t., 5 min	72-90%	[29]
7	 ketone **25**	I_2 (1.1 eq), TBHP (6 eq) PE, 0 °C, 12 h	55-86%	[30]
8	 nitrile **26**	$Cu(OAc)_2$ (10 mol%) H_2O, 2-piperidineCOOH (20 mol%), 100 °C, 18 h	50-90%	[31]
9	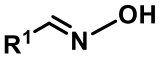 aldoxime **27**	$RhCl(PPh_3)_3$ (5 mol%), solvent, 150 °C, 2-5 h	74-94%	[32]
10	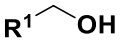 benzyl alcohol **28**	Condition examples will be discussed in section 1.5		
11	 aldehyde **29**			
(TEA: triethylamine, TBHP: *tert*-butyl hydroperoxide)				

1.4 Oxidative amidations between benzyl alcohol/aldehyde and amine

In this section, we will review the use of benzyl alcohol **28** and aldehyde **29** as carboxylic acid surrogates to couple with amine **7**. The oxidative amidation between alcohol **28**/aldehyde **29** and amine **7** can be mediated by three pathways such as 1) transition-metal 2) metal-free process and 3) photocatalyst as depicted in Scheme 1.7.

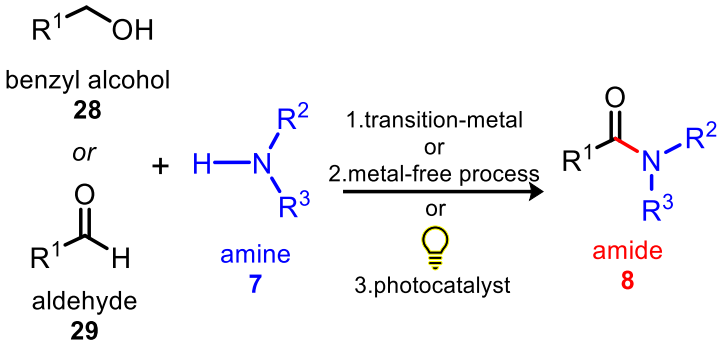

Scheme 1.7 Three pathways for oxidative amidation between benzyl alcohol/aldehyde and amine

1.4.1 Oxidative amidation between benzyl alcohol/aldehyde and amine with transition-metal

In this section, we summarized the use of transition-metal for oxidative amidation between benzyl alcohol **28** and amine **7** in Table 1.4. In 2009, Shimizu and coworkers reported catalytical oxidative amidation between benzyl alcohol **28** and amine **7** with silver supported on alumina as shown in Table 1.4, entry 1. This process used silver as transition-metal catalyst to catalyze oxidative amidation providing amide **8** in moderate to excellent yields. After that, five research groups reported similar process using gold, ruthenium, palladium, iron and copper as transition-metal catalysts as shown in Table 1.4, entries 2-6. Those methods have to use extra oxidizing agent such as oxygen, 3-methyl-2-butanone, H_2O_2 or TBHP, respectively to produce amide **8** in fair to good yields. The benefit of such reactions was the use of catalyst to catalyze oxidative amidation producing amide product in satisfactory yields. However, such processes still required the use of toxic transition-metal, stoichiometric oxidizing agent and long reaction time under high temperature reaction.

Table 1.4 Reviews on oxidative amidations between benzyl alcohol and amine with transition-metal

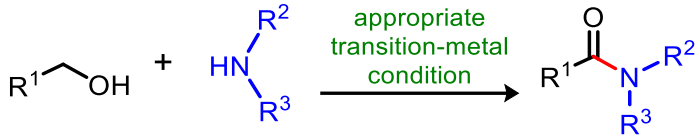

benzyl alcohol **28** | amine **7** | amide **8**

Entry	Conditions	Yields	Refences
1	Ag/Al_2O_3 (4 mol%), Cs_2CO_3, toluene, reflux, 24 h	48-93%	[33]
2	PICB-Au (1.5 mol%), NaOH, O_2 ballon THF:H_2O (9:1), 40 °C, 12 h	59-95%	[34]
3	[Ru(*p*-cymeme)Cl_2]$_2$ (2.5 mol%), dppb (5 mol%) Cs_2CO_3, *t*-BuOH, 3-methyl-2-butanone, 125 °C, 24 h	24-81%	[35]
4	1) SEP_{123}-GO/Pd_{NPS} (1 mol%), H_2O_2 (2 eq), 1.5-2 h 2) SEP_{123}-GO/Pd_{NPS} (1 mol%), H_2O_2 (4 eq), 18-20 h	62-84%	[36]
5[a]	$Fe(OH)_3$@Fe_3O_4 (20 mg), TBHP (3 eq) $CaCO_3$, MeCN, 80 °C, Ar, 6 h	45-82%	[37]
6[a]	MSD/GAA/Cu(II) (20 mg), TBHP (3 eq) eggshell, MeCN, 80 °C, 8 h	37-93%	[38]
[a] using amine hydrochloride salt as amine source (dppb: 1,4-bis(diphenylphosphino)butane, TBHP: TBHP: *tert*-butyl hydroperoxide)			

Moreover, the transition-metals were also used in oxidative amidation between aldehyde **29** and amine **7** which shown in Table 1.5. Nakagawa and Gliman published similar work on oxidative amidation between aldehyde **29** and amine **7** using manganese dioxide and nickel peroxide, respectively in stoichiometric amount as shown in Table 1.5, entries 1 and 2. The results shown that all amide products **8** were successfully obtained in good to excellent yields. Then, in 2001, Tillack and coworkers reported the use of rhodium catalyst for oxidative amidation with aldehyde **29** and amine **7** as shown in Table 1.5, entry 3. Using this condition, the amide products **8**

were obtained in 8-100%. Later, three research groups performed similar oxidative amidation between aldehyde **29** and amine **7** as starting materials by the use of transition-metal in catalytic amount such as gold, palladium, iron and copper in combination with various oxidizing agent such as oxygen, H_2O_2 and TBHP (Table 1.5, entries 4-7). With these methods, they can construct amide products **8** in satisfactory yields. However, the use of expensive transition-metal, hazardous oxidizing agent, toxic additive and long reaction time cannot be avoided.

Table 1.5 Reviews on oxidative amidations between aldehyde and amine with transition-metal

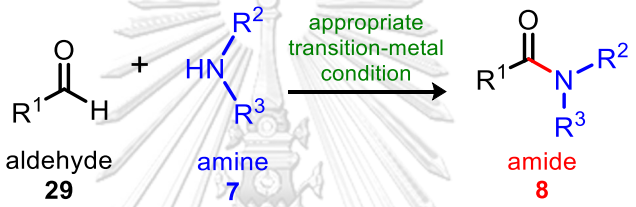

Entry	Conditions	Yields	References
1	MnO_2 (20 eq), NaCN (5 eq), *i*-PrOH, 0 °C, 4 h	64-100	[39]
2[a]	NiO_2 (1.3 eq), ether, -20 °C, N_2, 4 h	58-89%	[40]
3	$[Rh(COD)_2]BF_4$ (2.5 mol%), PPh_3, THF, 100-140 °C, 20 h	8-100%	[41]
4	$KAuCl_4$ (10 mol%), O_2, K_2CO_3 MeCN:H_2O (1:1), 40 °C, 12 h	30-98%	[42]
5	SEP_{123}-GO/Pd_{NPS} (1 mol%), H_2O_2 (4 eq), 18-20 h	62-84%	[36]
6	$FeH_2(PPh_3)_4$ (5 mol%), TBHP (3 eq) NHC **5** (5 mol%), toluene, reflux, 24 h	74-94%	[43]
7[b]	$CuSO_4.5H_2O$ (5 mol%), TBHP (1.1 eq) $CaCO_3$, MeCN, 60 °C, Ar, 6 h	42-92%	[44]

[a] using amine hydrochloride salt as amine source, [b] using ammonia gas as amine source (*i*-PrOH: isopropanol, TBHP: *tert*-butyl hydroperoxide)

1.4.2 Oxidative amidation between benzyl alcohol and amine with metal-free process

To avoid the use of toxic metal, the oxidative amidation via metal-free oxidant between benzyl alcohol **28** and amine **7** were developed as shown in Scheme 1.8. In 2015, Sutar and coworkers shown the oxidative amidation using benzyl alcohol **28** and amine [**7**] to produce amide product **8** as shown in Scheme 1.8, route A [45]. This work replaced the use of transition-metal by (diacetoxyiodo)benzene in the presence of oxidizing agent and provided amide product **8** in 65-88% yields. Additionally, Karimi's research group also reported the similar oxidative amidation between benzyl alcohol **28** and amine hydrochloride salt **30** for constructing amide **8** as shown in Scheme 1.8, route B [46]. This reaction can proceed with NaI cooperating of oxidizing agent, TBHP providing amide products in 53-87% yields. Although both processes can avoid the use of toxic or expensive transition-metal, the use of hazardous stoichiometric oxidizing agent under high temperature still requires.

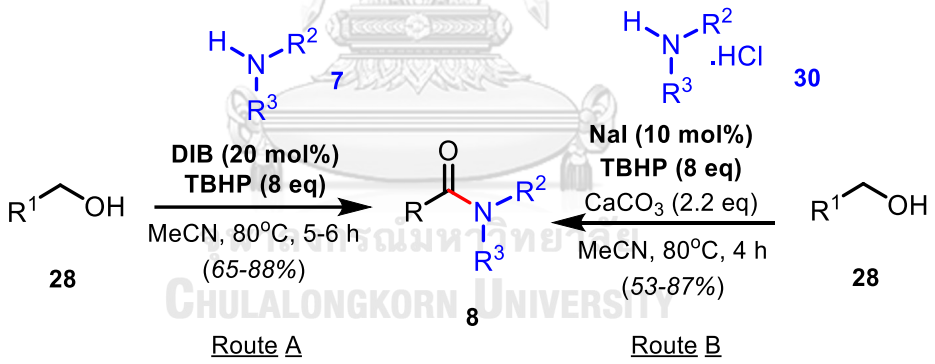

Scheme 1.8 Oxidative amidation between benzyl alcohol and amine with metal-free process

Similar to oxidative amidation from alcohol, the aldehyde starting material **29** was reported under metal-free condition as summarized in Table 1.6. Kekeli and Liang published the metal-free oxidative amidation between aldehyde **29** and amine **7** by the use of TBHP and NaOCl in stoichiometric amount as shown in Table 1.6, entries 1 and 2. Such reactions provided amide products **8** in satisfactory yields. Later, the

catalytic amidation processes were demonstrated by Shie, Reddy and Deshidi (Table 1.6, entries 3-5). They used iodine/iodide in catalytic amount along with oxidizing agents such as TBHP and hydrogen peroxide. They obtained amide product **8** in fair to excellent yields. In 2017, Kumar and coworkers performed NHC-catalyzed oxidative amidation from aldehyde **29** and amine **7** in combination with 1,2,4-triazole as co-catalyst and phenazine as oxidizing agent as shown in Table 1.6, entry 6. The reaction provided amide products **8** under argon atmosphere under room temperature for 24 hours in 70-98%. As reaction condition mentioned above, metal-free oxidative amidations still require the use of hazardous oxidizing agent in large amount.

Table 1.6 Reviews on oxidative amidations between aldehyde and amine with metal-free process

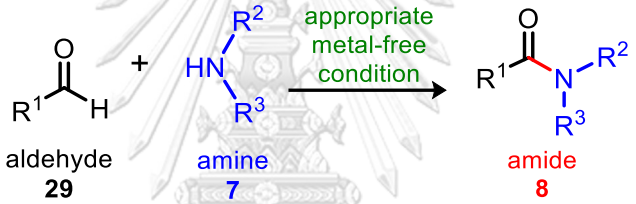

Entry	Conditions	Yields	References
1	TBHP (1.2 eq), MeCN, 80 °C, 5 h	85-99%	[47]
2	NaOCl/Bu_4NHSO_4 (1.5 eq), PEG-400, 120 °C, 12 h	45-94%	[48]
3	1) I_2 (1.1 eq), THF, r.t. then 2) H_2O_2, r.t., 2-4 h	81-98%	[49]
4	KI (5 mol%), TBHP (2.2 eq), H_2O, 80 °C, 15 h	25-83%	[50]
5	TBAI (20 mol%), TBHP (3 eq), MeCN, 80 °C, 6-10 h	45-83%	[51]
6	**17** (15 mol%), 1,2,4-triazole (20 mol%) phenazine (1 eq), THF, Ar, r.t., 24 h	70-98%	[52]

[a] using amine hydrochloride salt as amine source, [b] using ammonia gas as amine source (Bu_4NHSO_4: tetrabutylammonium hydrogensulfate, TBHP: ter*t*-butyl hydroperoxide)

1.4.3 Oxidative amidation between aldehyde and amine via photo-oxidation process

In recent years, the photo reactions under visible light have been utilized in many oxidations including our research group [53-55]. Therefore, the oxidative amidations between aldehyde **29** and amine **7** using photocatalyst have been developed. We summarized all reports in Table 1.7. Phenazenium, BODIPY, quinolizinium, hemicyanine and iridium complex were used as a photosensitizer for C-N bond formation under visible light. These processes used mild condition and eco-friendly visible light source providing amide **8** in good to excellent yields. However, most of photocatalyst are expensive and the reaction time is relatively long comparing to conventional oxidizing agents. Therefore, the need for green and cost-effective process for oxidative amidation still remains of both aldehyde and alcohol substrates.

Table 1.7 Reviews on oxidative amidations via photo-oxidation process

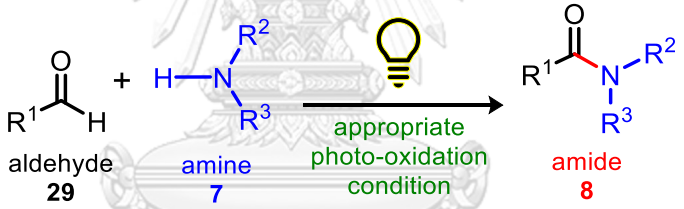

Entry	Photocatalysts	Conditions	Yields	References
1	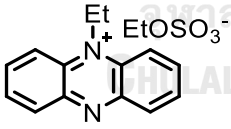 **1i** (phenazenium)	**1i** (1-2 mol%) 24 W household lamp THF, air, r.t. 20 h	58-93%	[56]
2	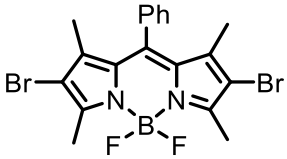 **P2** (BODIPY)	**P2** (2 mol%), 3 W blue LEDs, BHT, MeCN, air r.t., 12 h	35–96%	[57]

(Table 1.7 continued)

Entry	Photocatalysts	Conditions	Yields	References
3	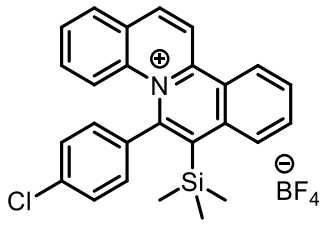 **4e** (Quinolizinium)	**4e** (5 mol%) blue LED, MeCN r.t., air, 48 h	49-84%	[58]
4	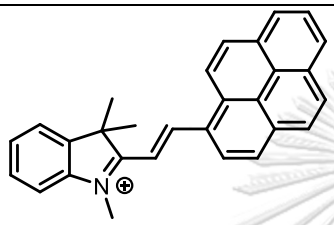 **C4** (hemicyanine)	**C4** (1 mol%), UV light DMSO:H_2O (1:1) air, r.t., 12-30 h	60-80%	[59]
5	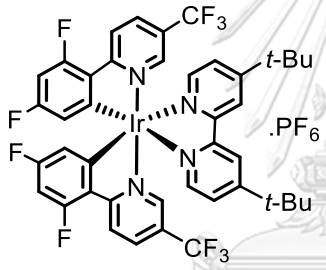 **Ir[df(CF_3)ppy]$_2$(dtbbpy)PF_6**	**Ir complex** (2 mol%) CCl_3Br, blue LED MeCN, Ar, r.t., 20 h	40-86%	[60]
(BHT: butylated hydroxytoluene)				

1.5 Introduction to electro-organic synthesis

Recently, the electro-organic synthesis has been received much attention as sustainable chemistry among organic synthesis [61-64]. To understand the electro-organic synthesis, the details will be fully explained in this section.

1.5.1 Differences between normal chemical reaction and electrochemical reaction

The difference between normal chemical reaction and electrochemical reaction shown in Figure 1.2. For normal chemical reaction in Figure 1.2a, the homogeneous transformation will take place with appropriate distance between

substrate **A** and **B** to generate activated complex first. Then, the electron will move from **A** (reducing agent) to **B** (oxidizing agent) to generate product **C** and **D**. On the other hand, the electrochemical reaction in Figure 1.2b performed the heterogeneous transformation in electrolytic cell between substrate and electrode via single electron transfer (SET) process. At anodic electrode, **A** was oxidized to form product **C** whereas **B** was reduced at cathodic electrode to form product **D**. Although the electrochemical reaction was considered as heterogeneous phase providing slower reaction rate than normal chemical reaction, the electrochemical reaction offers better environmental benefits due to the use of electron as a non-toxic reagent instead of toxic oxidizing or reducing agent.

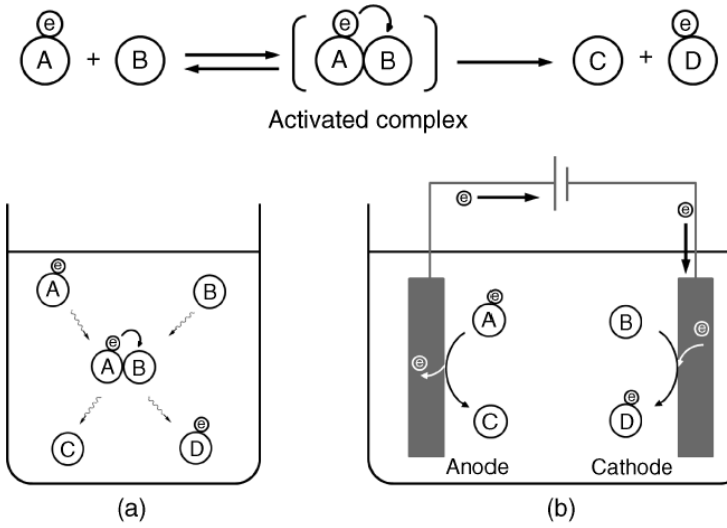

Figure 1.2 Comparison between a) normal chemical reaction and b) electrochemical reaction

For the mechanism of electrochemical process, the single electron transfer process is the main pathway as demonstrated in Figure 1.3 [65]. In general, electro-organic synthesis is the setup using electrolytic cell and applying external potential between two electrodes. Oxidation process occurs at an anodic electrode while reduction process takes place at cathodic electrode, respectively. For oxidation process (Figure 1.3, left), it takes place by applying positive potential at anode. The

atomic energy level of electrode will decrease until it is lower than the highest occupied molecular orbital (HOMO) of substrate. Then, the electron which located at HOMO will transfer to atomic energy level of electrode. For reduction process (Figure1.3, right), this occurs by applying a negative potential at cathode. The atomic energy level of electrode will increase until it is higher than the lowest unoccupied molecular orbital (LUMO) of substrate. After that, the electron from atomic energy level will transfer to LUMO.

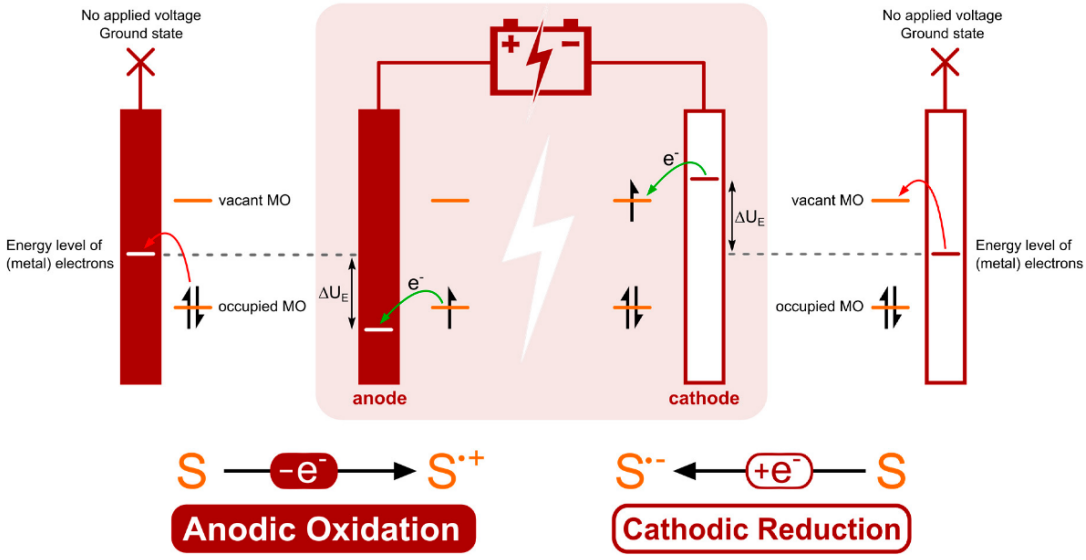

Figure 1.3 Single electron transfer process for left) oxidation and right) reduction in electrochemical reaction

To demonstrate the differences between the normal oxidation using the oxidizing agent such as $KMnO_4$, H_2CrO_4, Swern, PCC and DMP versus electrochemical oxidation [66], the example was shown in Scheme 1.9. Even though all methods provide anticipated product in satisfactory yields, the normal oxidation provide metal byproduct (H_2CrO_3, MnO_2) or toxic gas (CO, CO_2) resulting in contamination in environment. On the other hand, the electrochemical oxidation of alcohol was performed using carbon paper and platinum plate as anode and cathode with the

electrolyte. Importantly, the hydrogen evolution is only the byproduct from this condition providing both high atom economy and green process.

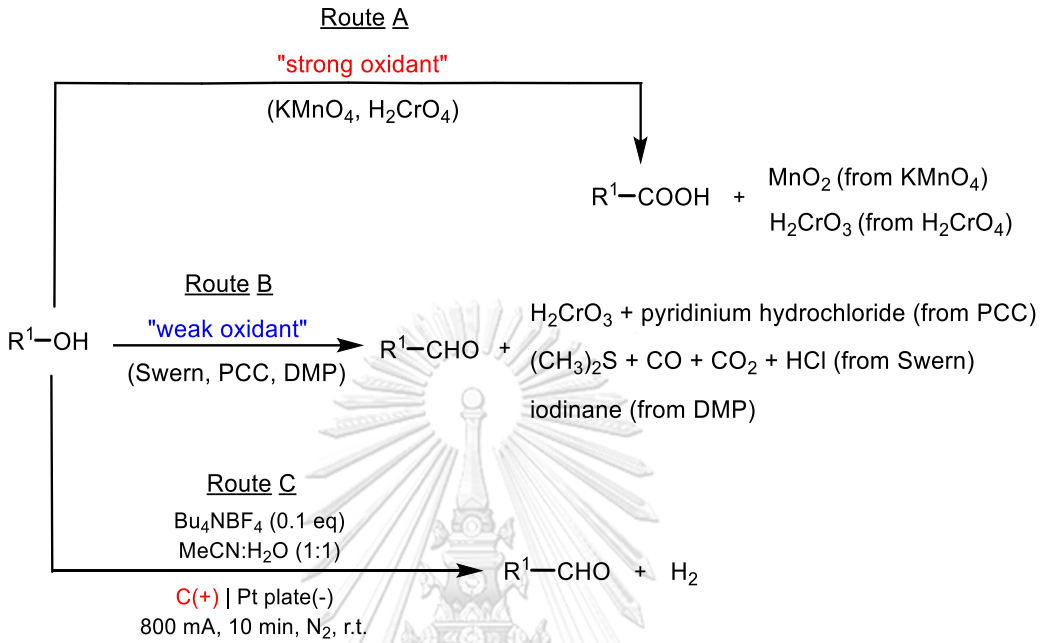

Scheme 1.9 Oxidation of alcohol to carbonyl compound using a, b) oxidizing agents and c) electro-organic synthesis

1.5.2 Component for electro-organic synthesis setup

The component of electro-organic synthesis composes of four main parts such as power source, electrochemical cell, electrodes and supporting electrolyte as shown in Figure 1.4 [67]. The first component is a power supply. Due to the use of electrolytic cell, the external energy source needs to be applied from power supply. In general, power supply can be classified to galvanostat (for controlling current) and potentiostat (for controlling potential) which requires the use of two-electrode and three-electrode configurations, respectively. The second component is an electrochemical cell. Type of electrochemical cell can be classified into two types, divided cell and undivided cell. The difference between such electrochemical cell depends on permeable membrane (sintered glass or Nafion membrane) in divided cell. However, the

advantage of divided cell is avoidance the transformation of sensitive substrate to byproduct and the advantage of undivided cell is convenience for reaction setup. The disadvantage of divided cell is difficulty for reaction setup while the disadvantage of undivided cell is the production of byproduct from sensitive substrate. The third component is electrode. It consists of both anodic and cathodic electrode for oxidation and reduction, respectively. Type of electrodes is classified into sacrificial anodic electrode (i.e. Mg, Cu, Zn, Pb, Fe and Ni) and non-sacrificial anodic electrode (i.e. Pt and carbon material). The most important criteria for choosing electrode are having wide potential window and suitable for chemical reaction. If oxidation is required, both anode and cathode should be non-sacrificial electrode. If reduction is required, anode should be sacrificial anodic electrode while cathode should be non-sacrificial electrode. The fourth component is a supporting electrolyte. This can be classified into organic supporting electrolyte such as ammonium salts and inorganic supporting electrolyte such as halide salts, hydroxide salts and perchlorate salts. Such electrolytes can improve conductivity by giving positive and negative ion and reduce the resistance in reaction. However, the criteria for selection supporting electrolyte are having wide potential window along with good solubility for all chemicals. Importantly, some supporting electrolytes can act as both electrolyte and mediator which will be elaborated in the next section.

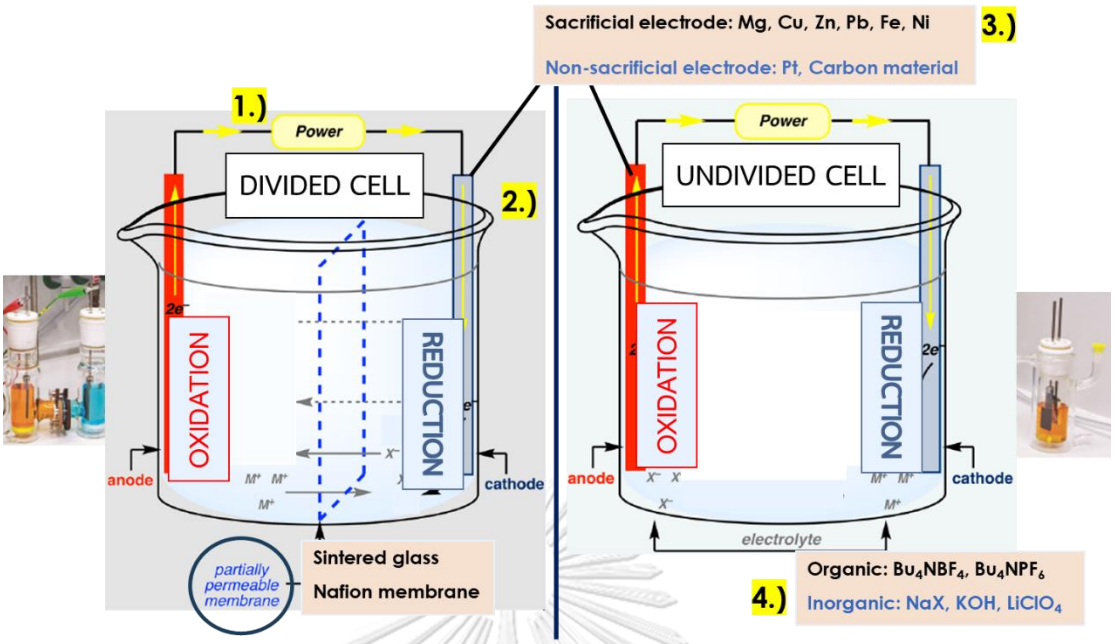

Figure 1.4 Reaction setup for electro-organic synthesis

1.5.3 Modes of electro-organic synthesis

In electrochemical reaction, we can divide modes of electro-organic synthesis into two modes, 1) constant current mode and 2) constant potential mode as shown in Figure 1.5. For constant current mode (Figure 1.5a), the applied current will be held as initial current until electrolysis process finishes. During the course of the reaction between electrode surfaces which face each other, the concentration of starting material decreases while the product is formed and the potential will be increased due to insufficient mass transfer at electrical double layer. For the constant potential mode (Figure1.5b), the applied potential will be maintained throughout reaction. When reaction is applied with potential, the concentration of starting material will be decreased causing limitation of mass transfer. Hence, current intensity will decrease because the potentiostat will maintain the applied potential. Normally, constant current mode is the most commonly used in electro-organic synthesis because it allows to calculate total charge consumption in reaction via relationship between current and time to provide Faraday's efficiency. Moreover, there is no need to use a reference electrode unlike constant potential mode. Due to losing potential through

resistance in electrolytic cell (Ohmic drop), the reaction potential is not stable at constant value. Therefore, the reference electrode is required to serve as a reference for measuring and controlling the potential providing more reliable and reproducible information for electrochemical reaction. The advantage of constant current is convenience to set the reaction with two-electrode configuration while the over-oxidation/reduction can be occurred due to increasing reaction potential. The advantage of constant potential mode is having higher selectivity than constant current mode but the reaction setup with three-electrode configuration is difficult.

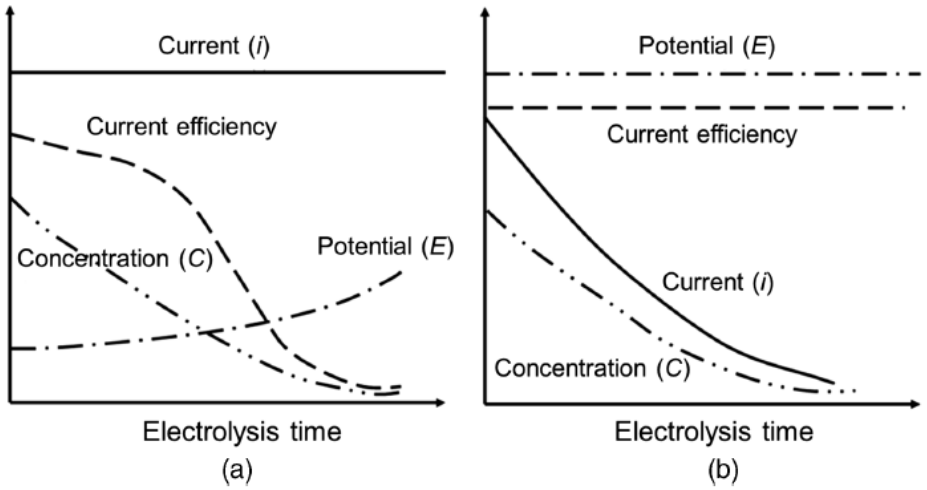

Figure 1.5 Comparison between a) constant current and b) constant potential mode

1.5.4 Electrolysis process

In general, electro-organic synthesis can be divided into 1) direct electrolysis process and 2) indirect electrolysis process as depicted in Scheme 1.10 [68]. The first process (Scheme1.10a) involves the direct electron transfer between electrode and substrate. On the other hand, the second process (Scheme 1.10b) involves the indirect electron transfer between substrate and mediator. The first process requires only electrolyte whereas the second process requires both electrolyte and mediator to complete the electron transfer. The mediator can be divided into two types such as 1) oxidative mediator (i.e. halogen (X^+/X^-), IO_4^-/IO_3^-, $NO_3^{\bullet}/NO_3^-$ Ar_3N^+/Ar_3N, *N*-oxyl

derivatives ($R^1R^2N{=}O$)) and 2) reductive mediator (i.e. polycyclic aromatic hydrocarbon (PAH), viologen). For the direct electrolysis, it offers high atom economy process because no other reagents require. However, the high potential is needed due to heterogeneous electron transfer. Also, the direct interaction between electrode and substrate (starting material) may prodive the decomposition. For indirect electrolysis, it uses an additional mediator to assist the transformation of substrate to reactive intermediate. Therefore, it requires a lower potential along with avoiding the direct contact between substrate and electrode. From the benefits of indirect electrolytic process, we will develop the oxidative amidation based on this process.

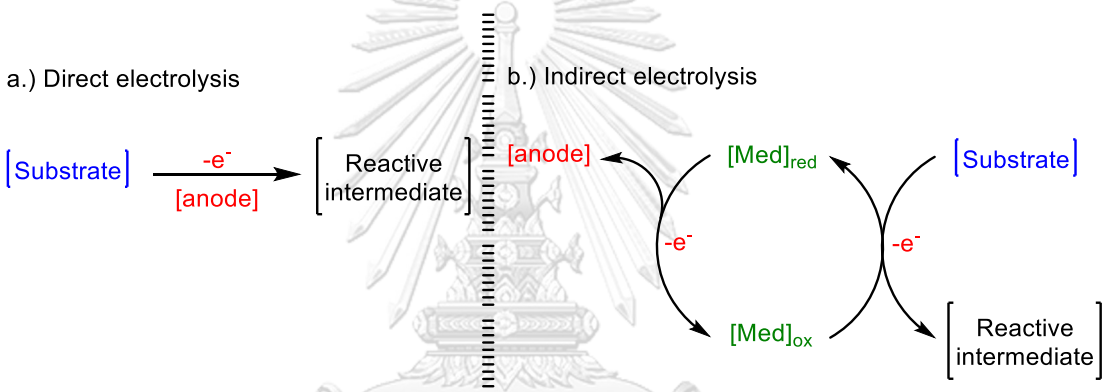

Scheme 1.10 Electrolysis processes a) direct and indirect electrolysis

1.6 Literature reviews on electrochemical reactions for C-N bond formation

Since the discovery of electro-organic synthesis, many synthetic transformations have been reported for past two decades [69-74]. However, the C-N bond formations via electro-organic synthesis have been just realized in recent years. In this section, we will describe the electrochemical reaction for C-N bond formation. The reaction details and the reaction mechanism will be fully explained.

1.6.1 Examples for electrochemical reactions for C-N bond formation via direct electrolysis

In 2019, Tang and coworkers reported the electro-organic synthesis of amide between thiocarboxylic acid **24** and amine **7** via direct electrolytic process as shown in Scheme 1.11 [75]. The reaction demanded tetrabutylammonium tetrafluoroborate

as electrolyte in ethyl acetate solvent, both platinum plate as anode and cathode, 1 mA electrical current for 24 hours at room temperature in undivided cell. This reaction provided amide products **8** in 39-97% yields and hydrogen gas as a sole byproduct.

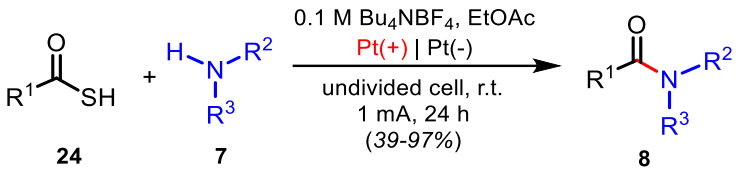

Scheme 1.11 Direct electrochemical amidation of thiocarboxylic acid and amine

The proposed mechanism was shown in Scheme 1.12. First step of reaction is deprotonation of thiocarboxylic acid **24** to thioacetate anion **31**. Then such anion **31** is oxidized at anode to thioacetate radical **32** to couple with another radical forming disulfide intermediate **33**. Finally, amine **7** will attack at carbonyl functional group yielding amide product **8**. Besides, the proton in reaction can be reduced by cathode forming hydrogen gas evolution.

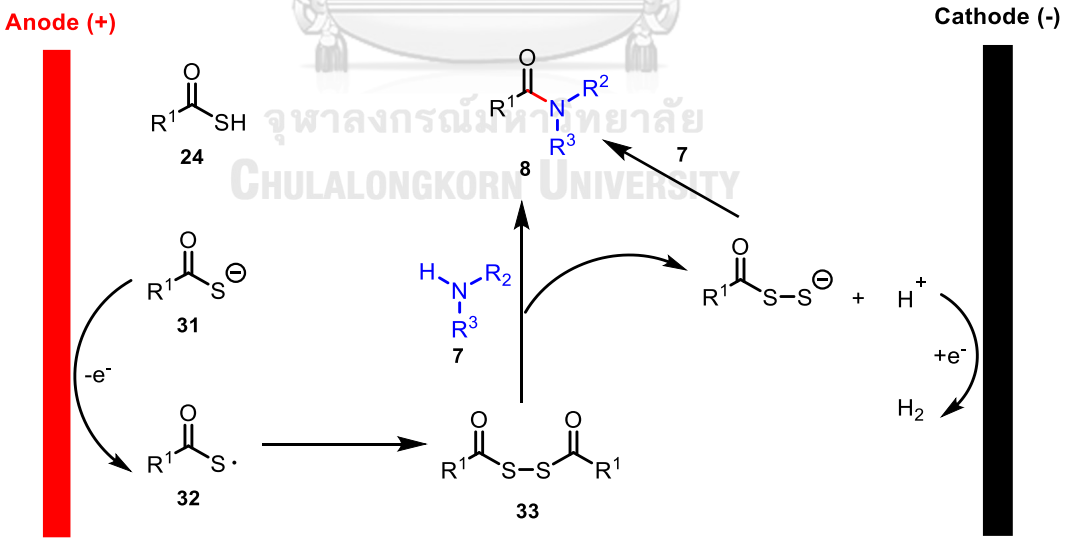

Scheme 1.12 Proposed mechanism for direct electrochemical amidation of thiocarboxylic acid and amine

In 2019, Dissanayake and coworkers developed the reaction which can produce dual products, amide **8** and benzyl ester **36** from acid anhydride **34**, amine **7** and benzyl bromide **35** using direct electrolysis in Scheme 1.13 [76]. Reticulate vitreous carbons (RVC) were used as electrodes in the presence of tetrabutylammonium hexafluorophosphate as electrolyte in anhydrous acetonitrile in divided cell. Amide products **8** were obtained in moderate yields.

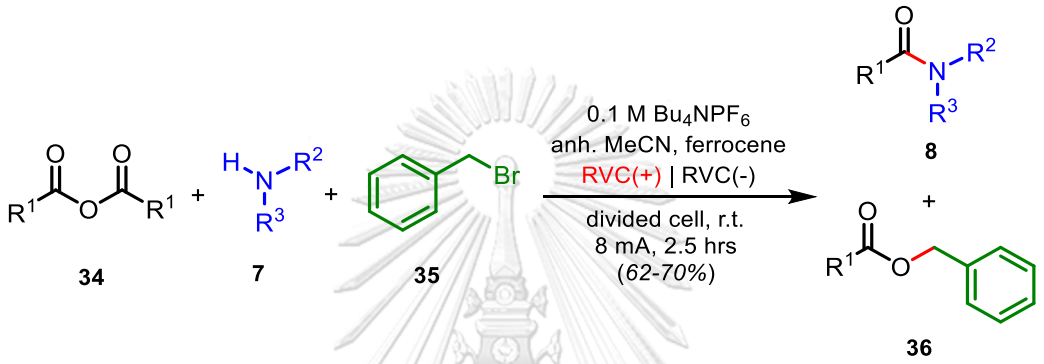

Scheme 1.13 Direct electrochemical amidation of acid anhydride, amine and benzyl bromide

The reaction mechanism was depicted in Scheme 1.14. The process starts from the reduction of amine **7** to form amine anion **37** which consequently attacks acid anhydride **34** to generate amide product **8** and carboxylate anion **38**. Finally, carboxylate anion **38** reacts further with benzyl bromide **35** to give benzyl ester **36** as co-product. In the same time, ferrocene **39** at anode chamber will be oxidized to ferrocenium **40** to complete full circuit of electrolysis process.

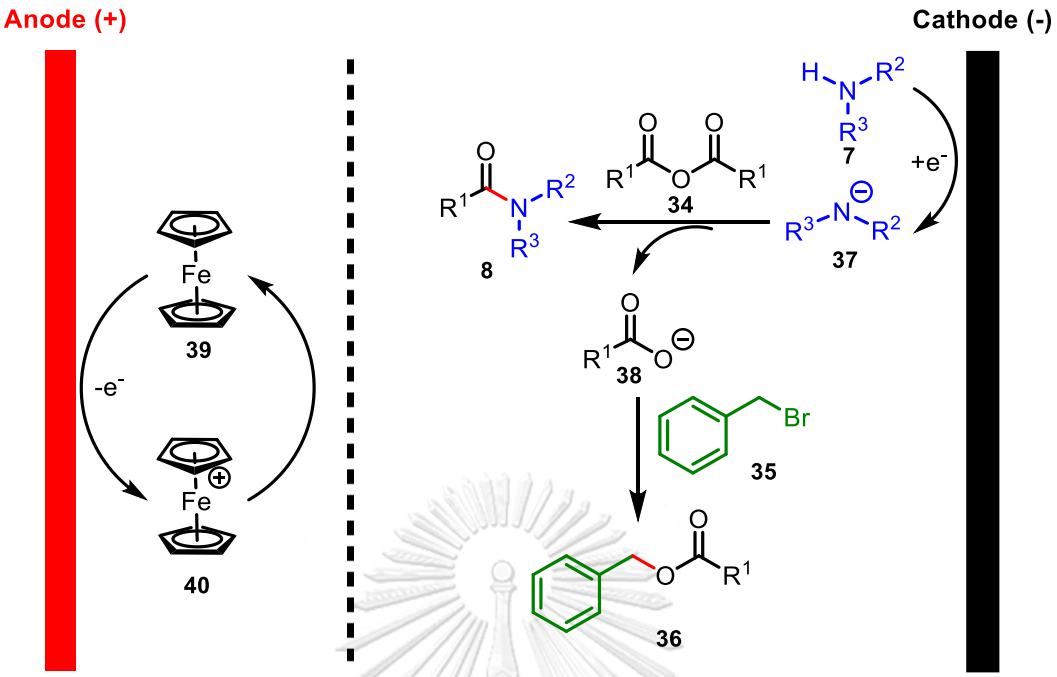

Scheme 1.14 Proposed mechanism for direct electrochemical amidation of acid anhydride, amine and benzyl bromide

Recently, Chen and coworkers published the electrochemical amidation of α-ketoamide **42** from α-ketoaldehyde **41** and amine **7** proceeding under direct electrolysis as shown in Scheme 1.15 [77]. Acetonitrile was used as solvent, graphite rod and platinum plate were used as anode and cathode, respectively. The reaction was setup in undivided cell at room temperature in electrolyte-free condition. Such reaction provided α-ketoamide products **42** in good to excellent yields even no using electrolyte.

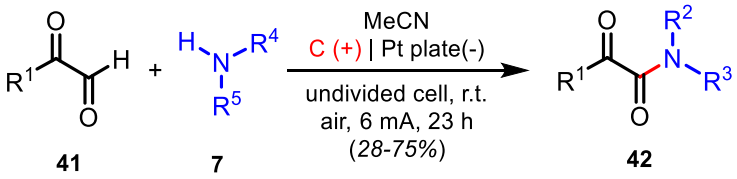

Scheme 1.15 Direct electrochemical amidation of α-ketoaldehyde and amine

To understand how reaction was proceeded, the proposed mechanism shown in Scheme 1.16. α-ketoaldehyde **41** is attacked by amine **7** to form iminium intermediate **43**. Then H_2O react with iminium intermediate **43** to produce hemiaminal intermediate **44**. Eventually, hemiaminal intermediate **44** will be oxidized at anode to generate α-ketoamide product **42**.

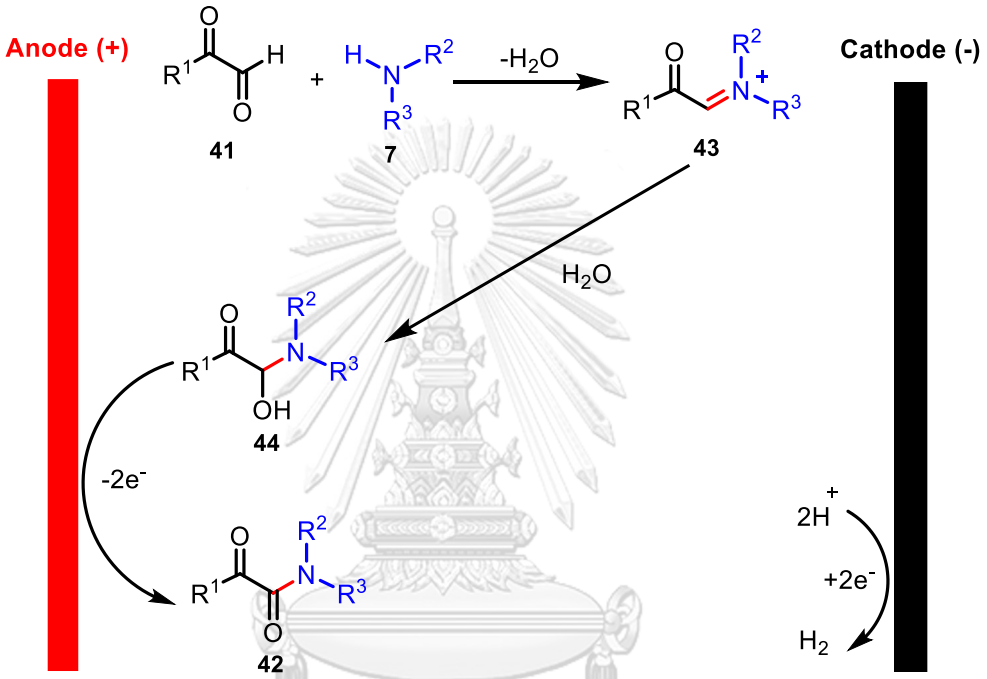

Scheme 1.16 Proposed mechanism for direct electrochemical amidation of α-ketoaldehyde and amine

1.6.2 Examples for electrochemical reactions for C-N bond formation via indirect electrolysis

In 2013, Zhang and coworkers reported the iodine-mediated electrochemical amidation process from acetophenone **25** and amine **7** to α-ketoamide **42** in ethanol under oxygen atmosphere (Scheme 1.17) [78]. This work used tetrabutylammonium iodide as mediator and electrolyte providing 52-90% yields of products **42**.

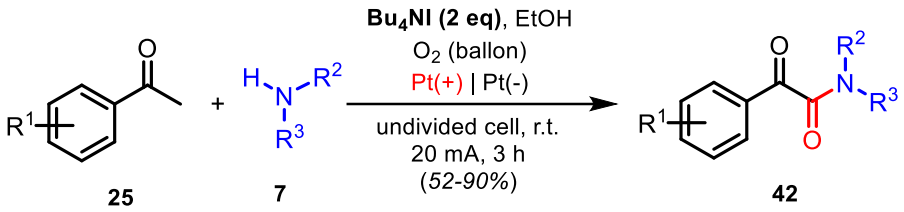

Scheme 1.17 α-Ketoamide synthesis via iodine-mediated electrochemical reaction

The mechanism of this electrochemical process was proposed as shown in Scheme 1.18. Iodide was oxidized at anode to iodide radical. Acetophenone **25** is oxidized by iodide radical to generate α-carbon radical **45** then couples with oxygen molecule to provide α-ketoaldehyde **41**. Then it reacts with amine to provide hemiaminal intermediate **44** which is further oxidized at anode providing α-ketoamide product **42** along with hydrogen evolution at cathode.

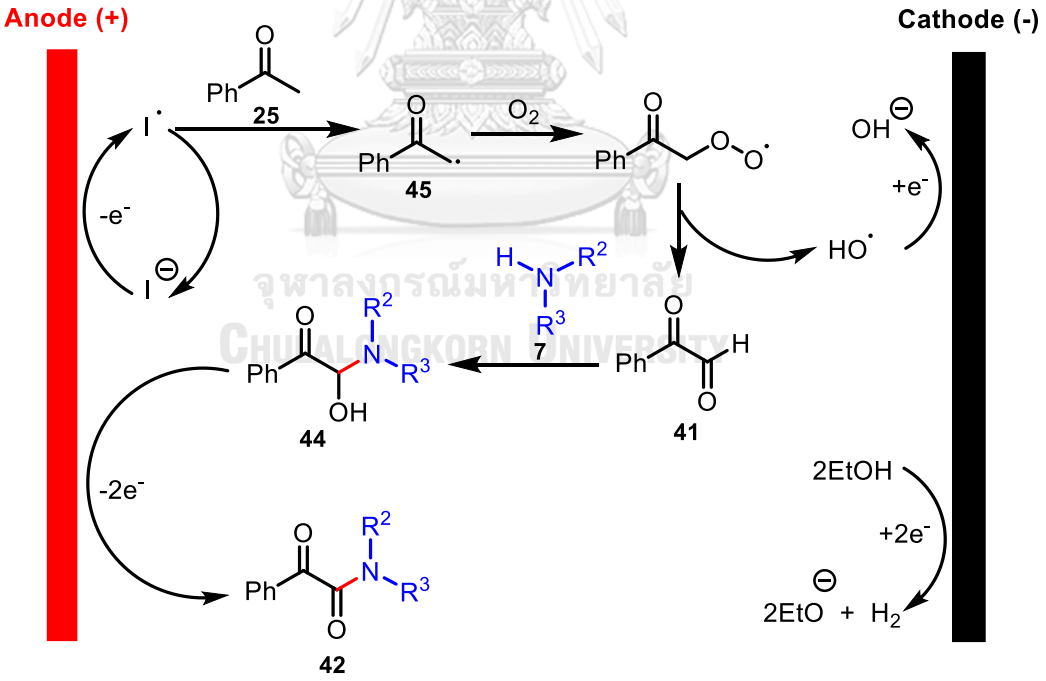

Scheme 1.18 Proposed mechanism for α-ketoamide synthesis via iodine-mediated electrochemical reaction

In 2015, Chen and coworkers synthesized aziridine via electrochemical reaction mediated by iodide from *N*-aminophthalimide **46** and alkene **19** as shown in Scheme 1.19 [79]. This reaction used tetrabutylammonium iodide as mediator and lithium perchlorate as electrolyte in CF_3CH_2OH solvent in undivided cell at room temperature. Aziridine products **47** were produced in 23-71% yields.

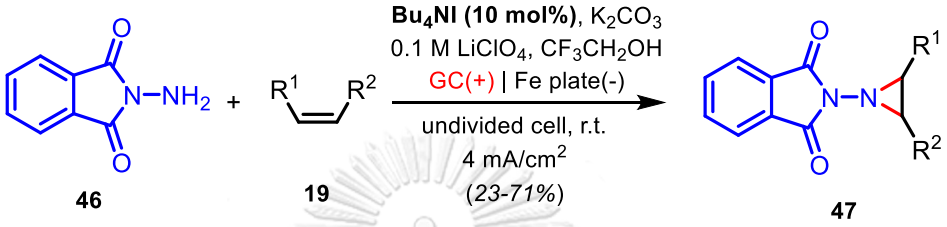

Scheme 1.19 Aziridine synthesis via iodine-mediated electrochemical reaction

The mechanism of this electrochemical process was depicted in Scheme 1.20. Iodide will be oxidized to molecular iodine. The reaction between *N*-aminophthalimide **46** and molecular iodine generates amine radical **48** which will react with alkene **19** via radical process to form aziridine product **47**.

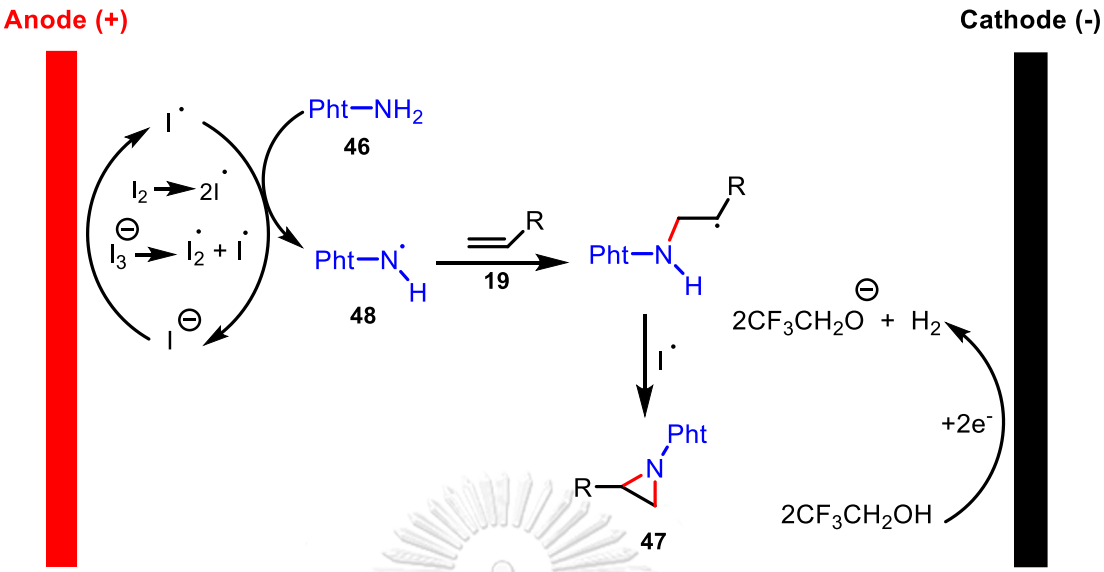

Scheme 1.20 Proposed mechanism for aziridine synthesis via iodine-mediated electrochemical reaction

In 2014, Gao and coworkers published iodine-mediated electrochemical reaction to synthesize 2-aminobenzoxazole **50** from benzoxazole **49** and amine **7** as shown in Scheme 1.21 [80]. This reaction used tetrabutylammonium iodide as mediator and acetic acid as electrolyte in undivided cell using glassy carbon as anode and iron plate as cathode. This reaction provided products **50** in fair to excellent yields.

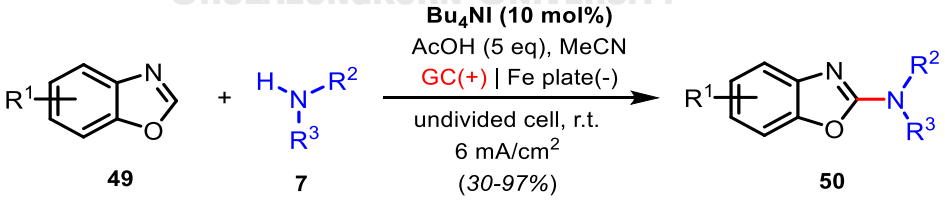

Scheme 1.21 2-Aminobenzoxazole synthesis via iodine-mediated electrochemical reaction

The mechanism of this electrochemical reaction was shown in Scheme 1.22. Benzoxazole starting material **49** will react with acetic acid obtaining imine intermediate **51** which undergoes ring closure to generate intermediate **52**. At the anode, iodide is oxidized into iodide cation species which further reacts with intermediate **52** to form N-I bond in intermediate **53**. Finally, the deprotonation is occurred to obtain 2-aminobenzoxazole product **50**.

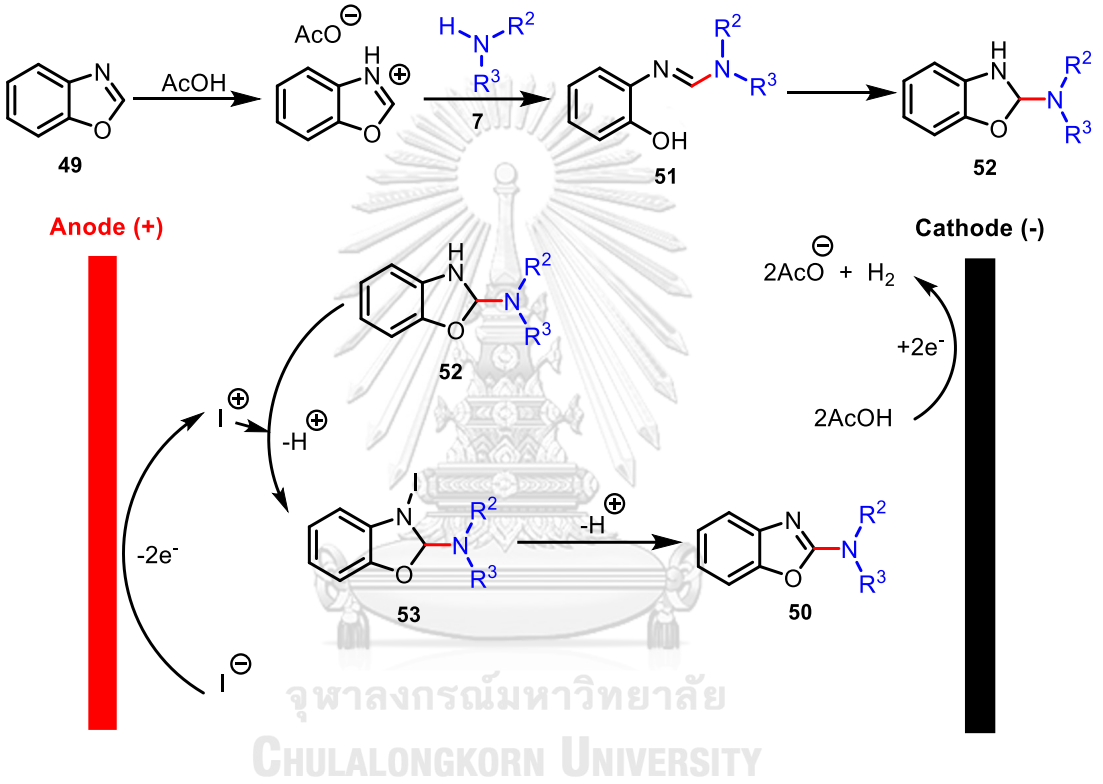

Scheme 1.22 Proposed mechanism for 2-aminobenzoxazole synthesis via iodine-mediated electrochemical reaction

In 2016, Liang and coworkers performed an iodine-mediated electrochemical reaction to synthesize indoline **55** from *N*-(2-vinylphenyl)toluenesulfonamide **54** as shown in Scheme 1.23 [81]. The electrochemical reaction was performed using tetrabutylammonium iodide as mediator in alcohol solvent under undivided cell at room temperature. Graphite plates were used as both anode and cathode. The products **55** were obtained in 29-78% yields.

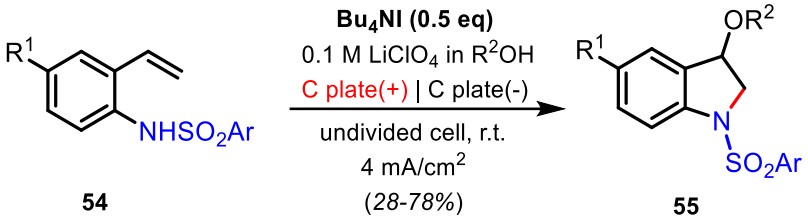

Scheme 1.23 Indoline synthesis via iodine-mediated electrochemical reaction

The mechanism of electrochemical reaction was shown in Scheme 1.24. At the anode, iodide is oxidized to molecular iodine. The reaction between iodine and *N*-(2-vinylphenyl)toluenesulfonamide **54** generates iodonium ion intermediate **56** following the intramolecular nucleophilic attack on cyclic iodonium ion intermediate **56**. Then 3-iodo-1-arylsuldonylindoline **57** is formed to further react with alkoxide ion which produces by reduction of alcohol solvent providing indoline **55** product.

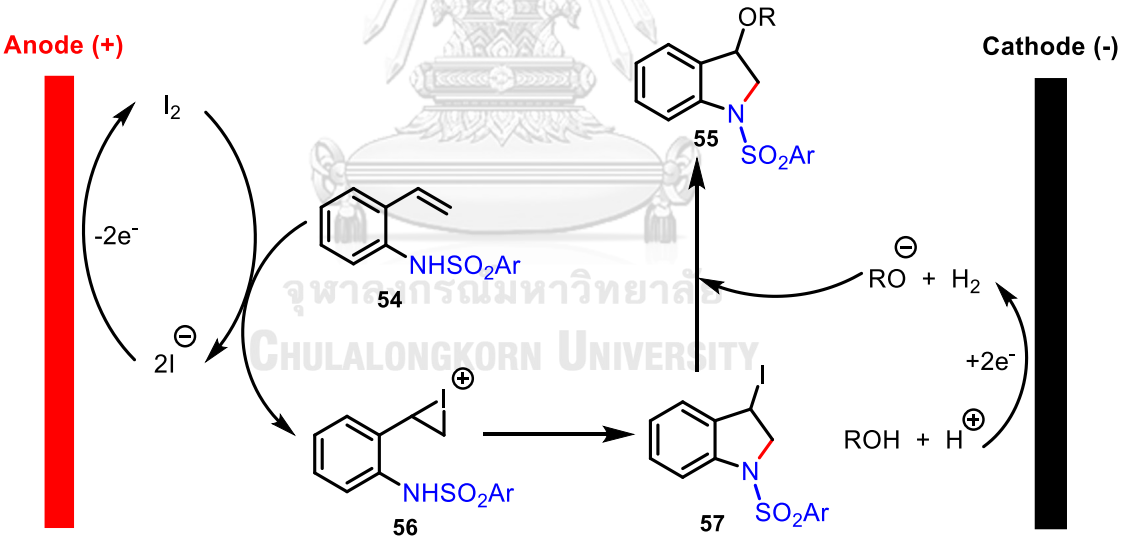

Scheme 1.24 Proposed mechanism for indoline synthesis via iodine-mediated electrochemical reaction

In 2016, Liang and coworkers reported iodine-mediated electrochemical reaction for α-amino ketone synthesis from ketone **25** and amine **7** as shown in Scheme 1.25 [82]. The electrochemical reaction was proceeded by the use of

ammonium iodide as mediator and lithium perchlorate as electrolyte in acetonitrile solvent in undivided cell at room temperature. This reaction provided products **58** from 28 to 75% yields

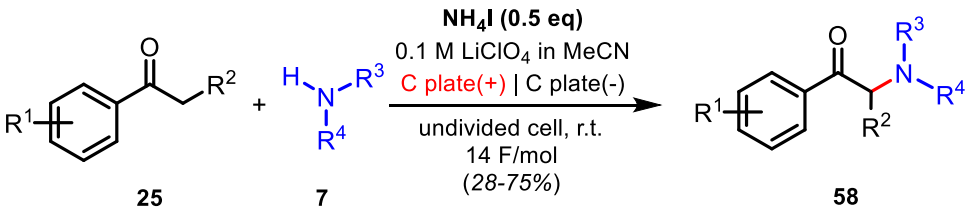

Scheme 1.25 α-Amino ketone synthesis via iodine-mediated electrochemical reaction

The mechanism of this electrochemical process was shown in Scheme 1.26. The reaction begins with oxidation of iodide to molecular iodine at anode. Molecular iodine reacts with ketone **25** at α-carbon position to form α-iodo ketone intermediate **59**. After that, intermediate **59** reacts with amine **7** providing α-amino ketone **58**.

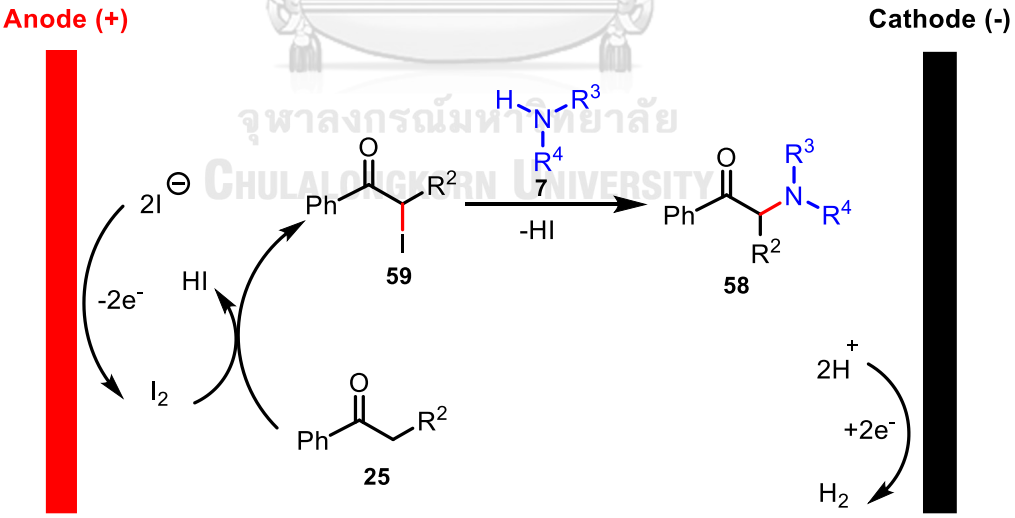

Scheme 1.26 Proposed mechanism for α-amino ketone synthesis via iodine-mediated electrochemical reaction

Based on above literature reviews on oxidative amidation from benzyl alcohol or aldehyde, most of them require stoichiometric amount of strong oxidizing agents. To avoid the direct use of such oxidizing agents, we intend to replace the process with electro-organic synthesis mediated by molecular iodine as a choice of mediator due to their low cost and less toxicity which has never been reported before.

1.7 Objective of this research

In the research, we aim to develop iodine-mediated electrochemical oxidative amidation using aldehyde or benzyl alcohol as starting materials to react with amine as depicted in Scheme 1.27. The reaction parameters of electrochemical oxidative amidation will be investigated including electrolyte, solvent, electrode, current intensity and reaction time to determine the optimized condition. The substrate scope of benzyl alcohols, aldehydes and amines will be examined to grade reaction generality. Finally, the mechanistic studies will be conducted to prove the mechanism of electrochemical oxidative amidation process via conducting control experiments, NMR monitoring and cyclic voltammetry experiment.

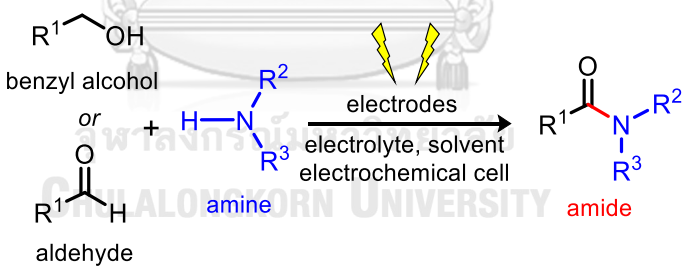

Scheme 1.27 Electrochemical oxidative amdation from benzyl alcohol and aldehyde in our study

CHAPTER II

EXPERIMENTAL

2.1 Chemical reagents, equipment and instrument for synthesis and characterization

All chemicals and solvents were obtained from commercially available suppliers such as Sigma-Aldrich and TCI (Japan) and were used without further purification, unless otherwise stated. Starting material aldehydes **1v**, **1w** and **1x** and alcohols **4f**, **4j** and **4n** were synthesized according to section 2.2 and 2.5. Pyrex reactor (Ø = 2.0 cm, height = 6.2 cm) was used for electrochemical reaction. Power supply (KORAD, KA3005D) was purchased from Shenzhen Korad Technology CO., LTD. Portable power charger (10000 mAh, 5 V) was purchased from HRAY HOLDINGS (ASIA) CO., LTD. All electrodes such as graphite rod (Ø = 5 mm, height = 10 cm) and platinum plate (5x5x0.1 mm) were purchased from Minihua Store, China. Analytical thin layer chromatography (TLC) was performed with precoated Merck silica gel 60 F254 plates (0.25 mm for thick layer) and visualized at 254 nm using an ultraviolet lamp. Column chromatography was performed with Silicycle silica gel 60-200 μm (70-230 mesh). ^{1}H-NMR, ^{13}C-NMR and ^{19}F spectra were obtained with JEOL JNM-ECZ500R/S1 NMR spectrometers operating at 500 MHz for ^{1}H or 125 MHz for ^{13}C or 470 MHz for ^{19}F nuclei. High-resolution mass spectra (HRMS) were recorded using electron spray ionization (ESI) with a MicroTOF Bruker mass spectrometer. Fourier transform infrared spectra were acquired from Nicolet 6700 FT-IR spectrometer equipped with a mercury-cadmium telluride (MCT) detector (Nicolet, USA).

2.2 Preparation of benzaldehydes (1v, 1w and 1x)

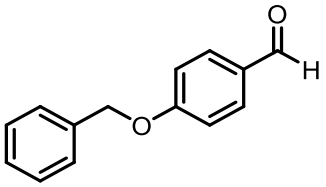

4-(benzyloxy)benzaldehyde [83] (**1v**): A mixture of 4-hydroxybenzaldehyde **1u** [CAS NO. 123-08-0] (1.0 eq, 2.46 mmol), benzyl bromide [CAS NO. 100-39-0] (2.0 eq, 4.92 mmol) and cesium carbonate [CAS NO. 534-17-8] (2.5 eq, 6.15 mmol) was dissolved by

acetonitrile (20 mL) in a 50 mL round bottom flask. The mixture was stirred at room temperature for 1 hour. The reaction mixture was washed with water (3x20 mL) and the organic portion was extracted with EtOAc (3x20 mL). The organic layer was eliminated water by Na_2SO_4. After filtration and removal of the solvent under reduced pressure, the crude product was purified by silica gel column chromatography (3:1 of Hexane:EtOAc) to afford **1v** in 514.4 mg, 2.62 mmol, quantitative yield as a white solid: ^{1}H-NMR (500 MHz, $CDCl_3$): δ (ppm) 9.88 (s, 1H), 7.83 (d, *J* = 8.77 Hz, 2H), 7.43-7.33 (m, 5H), 7.07 (d, *J* = 8.75 Hz, 2H), 5.14 (s, 2H). ^{13}C-NMR (125 MHz, $CDCl_3$): δ (ppm) 191.0, 163.9, 136.1, 132.2, 130.3, 128.9, 128.5, 127.6, 115.3, 70.4. FT-IR (cm^{-1}): 3057, 3035, 2829, 2802, 2742, 1684, 1600, 1571, 1507, 1452, 1250, 1168, 1013.

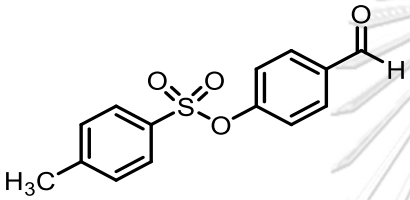

4-formylphenyl 4-methylbenzenesulfonate [84] (**1w**): A mixture of 4-hydroxybenzaldehyde **1u** (1.0 eq, 2.46 mmol), *p*-toluenesulfonyl chloride [CAS NO. 98-59-9] (2.0 eq, 4.92 mmol) and triethylamine [CAS NO. 121-44-8] (2.5 eq, 6.15 mmol) was dissolved by CH_2Cl_2, (20 mL) in a 50 mL round bottom flask. The mixture was stirred at room temperature for 1 hour. The reaction mixture was washed with water (3x20 mL) and the organic portion was extracted with EtOAc (3x20 mL). The organic layer was eliminated water by Na_2SO_4. After filtration and removal of the solvent under reduced pressure, the crude product was purified by silica gel column chromatography (3:1 of Hexane:EtOAc) to afford **1w** in 684.6 mg, 2.48 mmol, quantitative yield as a white solid: ^{1}H-NMR (500 MHz, $CDCl_3$): δ (ppm) 9.97 (s, 1H), 7.83 (d, *J* = 8.69 Hz, 2H), 7.71 (d, *J* = 8.38 Hz, 2H), 7.33 (d, *J* = 8.00 Hz, 2H), 7.17 (d, *J* = 8.61 Hz, 2H), 2.46 (s, 1H). ^{13}C-NMR (125 MHz, $CDCl_3$): δ (ppm) 190.8, 154.0, 146.1, 135.0, 132.2, 131.4, 130.1, 128.6, 123.2, 21.9. FT-IR (cm^{-1}): 3101, 3065, 2923, 2824, 2732, 1705, 1596, 1500, 1368, 1297, 1198, 1175, 1145, 1092.

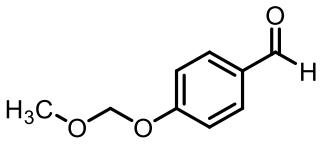

4-(methoxymethoxy)benzaldehyde [85] (**1x**): A mixture of 4-hydroxybenzaldehyde **1u** (1.0 eq, 2.46 mmol), bromomethyl methyl ether [CAS NO. 592-55-2] (2.0 eq, 4.92 mmol) and potassium carbonate [CAS NO. 584-08-7] (2.5 eq, 6.15 mmol) was dissolved by acetonitrile (20 mL) in a 50 mL round bottom flask. The mixture was stirred at room temperature for 3 hours. The reaction mixture was washed with water (3x20 mL) and the organic portion was extracted with EtOAc (3x20 mL). The organic layer was eliminated water by Na_2SO_4. After filtration and removal of the solvent under reduced pressure, the crude product was purified by silica gel column chromatography (3:1 of Hexane:EtOAc) to afford **1x** in 264.4 mg, 1.59 mmol, 65% yield as a colorless oil: ^{1}H-NMR (500 MHz, $CDCl_3$): δ (ppm) 9.87 (s, 1H), 7.81 (d, *J* = 8.84 Hz, 2H), 7.12 (d, *J* = 8.75 Hz, 2H), 5.23 (s, 2H), 3.47 (s, 3H).^{13}C-NMR (125 MHz, $CDCl_3$): δ (ppm) 191.0, 162.3, 132.0, 130.8, 116.4, 94.2, 56.5. FT-IR (cm^{-1}): 3080, 2960, 2900, 2832, 2740, 1697, 1603, 1512, 1322, 1245, 1160, 1086, 983.

2.3 Optimzation

2.3.1 Electrolyte screening

A mixture of 4-bromobenzaldehyde **1a** (1.0 eq, 0.30 mmol), morpholine **2a** (5.0 eq, 1.50 mmol) and electrolytes (5.0 eq of LiI, NaI, KI, TBAI, NaBr, KBr, TBAB, NaCl or $TBABF_4$) was dissolved by co-solvent 3:1 of CH_3CN:H_2O (4 mL) in undivided cell. The reaction was applied constant current at 100 mA via graphite rod as anode and cathode from power supply. Then, the reaction was stirred at room temperature for 3 hours. The reaction mixture was washed with $Na_2S_2O_8$ (1x10 mL) following water (2x10 mL) and the organic portion was extracted with EtOAc (3x10 mL). The organic layer was eliminated water by Na_2SO_4. After filtration and removal of the solvent under reduced pressure, the crude product was purified by silica gel column chromatography to afford **3aa** and the results were shown in Table 3.1.

2.3.2 Solvent screening

A mixture of 4-bromobenzaldehyde **1a** (1.0 eq, 0.30 mmol), morpholine **2a** (5.0 eq, 1.50 mmol) and sodium iodide (5.0 eq, 1.50 mmol) was dissolved by various solvents (100% CH_3CN, 3:1 of DMSO:H_2O, 3:1 of THF:H_2O, 3:1 of EtOH:H_2O, 3:1 of CH_3CN:EtOH or 1:1 of CH_3CN:H_2O) in undivided cell. The reaction was applied constant current at 100 mA via graphite rod as anode and cathode from power supply. Then, the reaction was stirred at room temperature for 3 hours. The reaction mixture was washed with $Na_2S_2O_8$ (1x10 mL) following water (2x10 mL) and the organic portion was extracted with EtOAc (3x10 mL). The organic layer was eliminated water by Na_2SO_4. After filtration and removal of the solvent under reduced pressure, the crude product was purified by silica gel column chromatography to afford **3aa** and the results were shown in Table 3.2.

2.3.3 The amount of amine screening

A mixture of 4-bromobenzaldehyde **1a** (1.0 eq, 0.30 mmol), morpholine **2a** (3.0 eq, 5.0 eq or 10.0 eq) and sodium iodide (5.0 eq, 1.50 mmol) was dissolved by co-solvent 3:1 of CH_3CN:H_2O (4 mL) in undivided cell. The reaction was applied constant current at 100 mA via graphite rod as anode and cathode from power supply. Then, the reaction was stirred at room temperature for 3 hours. The reaction mixture was washed with $Na_2S_2O_8$ (1x10 mL) following water (2x10 mL) and the organic portion was extracted with EtOAc (3x10 mL). The organic layer was eliminated water by Na_2SO_4. After filtration and removal of the solvent under reduced pressure, the crude product was purified by silica gel column chromatography to afford **3aa** and the results were shown in Table 3.3.

2.3.4 Electrodes screening

A mixture of 4-bromobenzaldehyde **1a** (1.0 eq, 0.30 mmol), morpholine **2a** (5.0 eq, 1.50 mmol) and sodium iodide (5.0 eq, 1.50 mmol) was dissolved by co-solvent 3:1 of CH_3CN:H_2O (4 mL) in undivided cell. The reaction was applied constant current at 100 mA via graphite rod or platinum plate electrode from power supply. Then, the reaction was stirred at room temperature for 3 hours. The reaction mixture was washed with $Na_2S_2O_8$ (1x10 mL) following water (2x10 mL) and the organic portion was extracted with EtOAc (3x10 mL). The organic layer was eliminated water by Na_2SO_4.

After filtration and removal of the solvent under reduced pressure, the crude product was purified by silica gel column chromatography to afford **3bc** and the results were shown in Table 3.4.

2.3.5 Current intensity and reaction times screening

A mixture of 4-bromobenzaldehyde **1a** (1.0 eq, 0.30 mmol), morpholine **2a** (3.0 5.0 eq, 1.50 mmol) and sodium iodide (5.0 eq, 1.50 mmol) was dissolved by co-solvent 3:1 of CH_3CN:H_2O (4 mL) in undivided cell. The reaction was applied constant current (80 mA, 100 mA or 150 mA) via graphite rod as anode and platinum plate as cathode. The reaction was stirred at room temperature for 2 or 3 hours. The reaction mixture was washed with $Na_2S_2O_8$ (1x10 mL) following water (2x10 mL) and the organic portion was extracted with EtOAc (3x10 mL). The organic layer was eliminated water by Na_2SO_4. After filtration and removal of the solvent under reduced pressure, the crude product was purified by silica gel column chromatography to afford **3aa** and the results were shown in Table 3.5.

2.3.6 The amount of NaI screening

A mixture of 4-bromobenzaldehyde **1a** (1.0 eq, 0.30 mmol), morpholine **2a** (5.0 eq, 1.50 mmol) and sodium iodide (5.0, 2.5 or 0.8 eq) was dissolved by co-solvent 3:1 of CH_3CN:H_2O (4 mL) in undivided cell. The reaction was applied constant current at 100 mA via graphite rod as anode and platinum plate as cathode from power supply. The reaction was stirred at room temperature for 3 hours. The reaction mixture was washed with $Na_2S_2O_8$ (1x10 mL) following water (2x10 mL) and the organic portion was extracted with EtOAc (3x10 mL). The organic layer was eliminated water by Na_2SO_4. After filtration and removal of the solvent under reduced pressure, the crude product was purified by silica gel column chromatography to afford **3aa** and the results were shown in Table 3.6.

2.4 General procedure for electrochemical oxidative amidation from aromatic aldehydes and secondary amines

General procedure: a mixture of aromatic aldehydes (1.0 eq, 0.30 mmol), secondary amines (5.0 eq, 1.50 mmol) and sodium iodide (2.5 eq, 0.75 mmol) was dissolved by co-solvent 3:1 of CH_3CN:H_2O (4 mL) in undivided cell. The reaction was

applied constant current at 100 mA via graphite rod as anode and platinum plate as cathode from power supply. The reaction was stirred at room temperature for 3 hours. The reaction mixture was washed with $Na_2S_2O_8$ (1x10 mL) following water (2x10 mL) and the organic portion was extracted with EtOAc (3x10 mL). The organic layer was eliminated water by Na_2SO_4. After filtration and removal of the solvent under reduced pressure, the crude product was purified by silica gel column chromatography (3:2 of EtOAc:Hexane) to afford amide products **3aa**-**3ta**, **3va**-**3xa** and **3ab**-**3ag**.

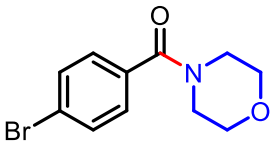

(4-Bromophenyl)(morpholino)methanone [86] (**3aa**): According to the general procedure, the reaction was performed by using 4-bromobenzaldehyde **1a** [CAS NO. 1122-91-4] (1.0 eq, 0.30 mmol), morpholine **2a** [CAS NO. 110-91-8] (5.0 eq, 1.50 mmol) and sodium iodide [CAS NO. 76811-82-5] (2.5 eq, 0.75 mmol) in co-solvent between acetonitrile (3.00 mL) and water (1.00 mL) to afford **3aa** (63.5 mg, 0.235 mmol, 78% yield) as a pale yellow solid: ^{1}H-NMR (500 MHz, $CDCl_3$): δ (ppm) 7.56 (d, *J* = 8.43 Hz, 2H), 7.29 (d, *J* = 8.43 Hz, 2H), 3.75-3.64 (m, 6H), 3.43 (br, 2H). ^{13}C-NMR (125 MHz, $CDCl_3$): δ (ppm) 169.5, 134.1, 131.9, 128.9, 124.3, 66.9, 48.3, 42.7. FT-IR (cm^{-1}): 3055, 2966, 2926, 2858, 1636, 1591, 1428, 1286, 1257, 1119, 1068, 1008. ESI-HRMS: m/z: 291.9934 $[M+Na]^+$ (calcd for $[C_{11}H_{12}BrNO_2Na]^+$ 291.9949).

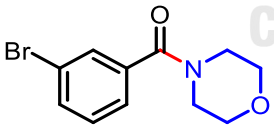

(3-Bromophenyl)(morpholino)methanone [87] (**3ba**): According to the general procedure, the reaction was performed by using 3-bromobenzaldehyde **1b** [CAS NO. 3132-99-8] (1.0 eq, 0.30 mmol), morpholine **2a** (5.0 eq, 1.50 mmol) and sodium iodide (2.5 eq, 0.75 mmol) in co-solvent between acetonitrile (3.00 mL) and water (1.00 mL) to afford **3ba** (60.7 mg, 0.225 mmol, 75% yield) as a pale yellow liquid: ^{1}H-NMR (500 MHz, $CDCl_3$): δ (ppm) 7.54-7.52 (m, 2H), 7.30-7.24 (m, 2H), 3.73-3.60 (m, 6H), 3.39 (br, 2H). ^{13}C-NMR (125 MHz, $CDCl_3$): δ (ppm) 168.8, 137.3, 133.0, 130.3, 130.2, 125.7, 122.8, 66.9, 48.2, 42.7. FT-IR (cm^{-1}): 3061, 2963, 2921, 2851, 1637, 1562, 1438, 1281, 1260,

1114, 1067, 1024. ESI-HRMS: m/z: 291.9943 $[M+Na]^+$ (calcd for $[C_{11}H_{12}BrNO_2Na]^+$ 291.9949).

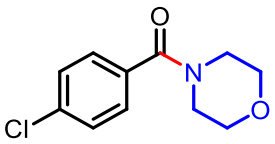

(4-chlorophenyl)(morpholino)methanone [86] (**3ca**): According to the general procedure, the reaction was performed by using 4-chlorobenzaldehyde **1c** [CAS NO. 104-88-1] (1.0 eq, 0.30 mmol), morpholine **2a** (5.0 eq, 1.50 mmol) and sodium iodide (2.5 eq, 0.75 mmol) in co-solvent between acetonitrile (3.00 mL) and water (1.00 mL) to afford **3ca** (45.9 mg, 0.203 mmol, 68% yield) as a white solid: ^{1}H-NMR (500 MHz, $CDCl_3$): δ (ppm) 7.38 (d, J = 8.54 Hz, 2H), 7.34 (d, J = 8.59 Hz, 2H), 3.74-3.43 (m, 8H). ^{13}C-NMR (125 MHz, $CDCl_3$): δ (ppm) 169.5, 136.1, 133.7, 129.0, 128.8, 66.9, 48.3, 42.8. FT-IR (cm^{-1}): 3080, 3052, 2963, 2923, 2862, 1705, 1621, 1594, 1458, 1431, 1366, 1282, 1155, 1111. ESI-HRMS: m/z: 248.0452 $[M+Na]^+$ (calcd for $[C_{11}H_{12}ClNO_2Na]^+$ 248.0454).

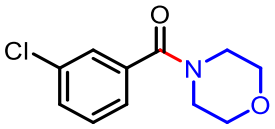

(3-chlorophenyl)(morpholino)methanone [88] (**3da**): According to the general procedure, the reaction was performed by using 3-chlorobenzaldehyde **1d** [CAS NO. 587-04-2] (1.0 eq, 0.30 mmol), morpholine **2a** (5.0 eq, 1.50 mmol) and sodium iodide (2.5 eq, 0.75 mmol) in co-solvent between acetonitrile (3.00 mL) and water (1.00 mL) to afford **3da** (49.7 mg, 0.220 mmol, 73% yield) as a pale yellow liquid: ^{1}H-NMR (500 MHz, $CDCl_3$): δ (ppm) 7.39-7.32 (m, 3H), 7.27-7.25 (m, 1H), 3.75-3.61 (m, 6H), 3.41 (br, 2H). ^{13}C-NMR (125 MHz, $CDCl_3$): δ (ppm) 169.0, 137.1, 134.8, 130.1, 130.0, 127.4, 125.2, 66.9, 48.2, 42.7. FT-IR (cm^{-1}): 3067, 2970, 2924, 2858, 1635, 1571, 1482, 1429, 1277, 1256, 1111, 1024. ESI-HRMS: m/z: 248.0455 $[M+Na]^+$ (calcd for $[C_{11}H_{12}ClNO_2Na]^+$ 248.0454).

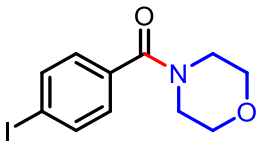

(4-Iodophenyl)(morpholino)methanone [89] (**3ea**): According to the general procedure, the reaction was performed by using 4-iodobenzaldehyde **1e** [CAS NO. 15164-44-0] (1.0 eq, 0.30 mmol), morpholine **2a** (5.0 eq, 1.50 mmol) and sodium iodide (2.5 eq, 0.75 mmol) in co-solvent between acetonitrile (3.00 mL) and water (1.00 mL) to afford **3ea** (54.8 mg, 0.173 mmol, 58% yield) as a white solid: ^{1}H-NMR (500 MHz, $CDCl_3$): δ (ppm) 7.76 (d, *J* = 8.12 Hz, 2H), 7.14 (d, *J* = 8.22 Hz, 2H), 3.75-3.62 (m, 6H), 3.42 (br, 2H). ^{13}C-NMR (125 MHz, $CDCl_3$): δ (ppm) 169.6, 137.9, 134.8, 129.0, 96.3, 66.9, 48.3, 42.8. FT-IR (cm^{-1}): 3061, 2985, 2960, 2914, 2852, 1621, 1588, 1427, 1267, 1253, 1113, 1006. ESI-HRMS: m/z: 339.9814 $[M+Na]^+$ (calcd for $[C_{11}H_{12}INO_2Na]^+$ 339.9810).

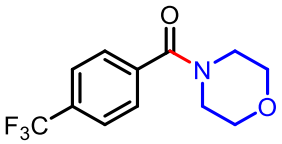

Morpholino(4-(trifluoromethyl)phenyl)methanone [88] (**3fa**): According to the general procedure, the reaction was performed by using 4-(trifluoromethyl)benzaldehyde **1f** (1.0 eq, 0.30 mmol), morpholine **2a** (5.0 eq, 1.50 mmol) and sodium iodide (2.5 eq, 0.75 mmol) in co-solvent between acetonitrile (3.00 mL) and water (1.00 mL) to afford **3fa** (57.9 mg, 0.223 mmol, 74% yield) as a white solid: ^{1}H-NMR (500 MHz, $CDCl_3$): δ (ppm) 7.68 (d, *J* = 7.97 Hz, 2H), 7.52 (d, *J* = 7.91 Hz, 2H), 3.79-3.62 (m, 6H), 3.39 (br, 2H). ^{13}C-NMR (125 MHz, $CDCl_3$): δ (ppm) 169.0, 139.0, 132.4, 132.1, 131.8, 131.6, 127.6, 127.0, 125.8, 124.9, 122.7, 120.5, 66.9, 48.2, 42.7. ^{19}F-NMR (470 MHz, $CDCl_3$): δ (ppm) -62.8. FT-IR (cm^{-1}): 3061, 2983, 2916, 2862, 1638, 1437, 1324, 1272, 1259, 1175, 1104, 1065, 1016. ESI-HRMS: m/z: 282.0718 $[M+Na]^+$ (calcd for $[C_{12}H_{12}F_3NO_2Na]^+$ 282.0717).

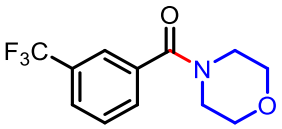

Morpholino(4-(trifluoromethyl)phenyl)methanone [56] (**3ga**): According to the general procedure, the reaction was performed by using 3-(trifluoromethyl)benzaldehyde **1g** [CAS NO. 454-89-7] (1.0 eq, 0.30 mmol), morpholine **2a** (5.0 eq, 1.50 mmol) and sodium iodide (2.5 eq, 0.75 mmol) in co-solvent between acetonitrile (3.00 mL) and water (1.00 mL) to afford **3ga** (61.6 mg, 0.238 mmol, 79%) as a white solid: ^{1}H-NMR (500 MHz, $CDCl_3$): δ (ppm) 7.70-7.68 (m, 2H), 7.60-7.54 (m, 2H), 3.79-3.64 (m, 6H), 3.42 (br, 2H). ^{13}C-NMR (125 MHz, $CDCl_3$): δ (ppm) 168.9, 136.2, 131.7, 131.4, 131.2, 130.9, 130.5, 129.3, 127.0, 126.8, 126.7, 124.8, 124.3, 124.2, 122.6, 120.5, 66.9, 48.3, 42.8. ^{19}F-NMR (470 MHz, $CDCl_3$): δ (ppm) -62.7. FT-IR (cm^{-1}): 3002, 2979, 2927, 2866, 1646, 1634, 1611, 1447, 1426, 1334, 1272, 1253, 1152, 1109, 1075. ESI-HRMS: m/z: 282.0704 $[M+Na]^+$ (calcd for $[C_{12}H_{12}F_3NO_2Na]^+$ 282.0717).

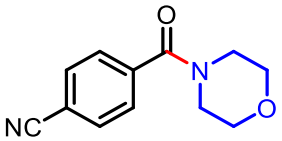

4-(morpholine-4-carbonyl)benzonitrile [90] (**3ha**): According to the general procedure, the reaction was performed by using 4-formylbenzonitrile **1h** [CAS NO.105-07-7] (1.0 eq, 0.30 mmol), morpholine **2a** (5.0 eq, 1.50 mmol) and sodium iodide (2.5 eq, 0.75 mmol) in co-solvent between acetonitrile (3.00 mL) and water (1.00 mL) to afford **3ha** (37.6 mg, 0.174 mmol, 58% yield) as a white solid: ^{1}H-NMR (500 MHz, $CDCl_3$): δ (ppm) 7.72 (d, J = 8.06 Hz, 2H), 7.51 (d, J = 8.09 Hz, 2H), 3.78-3.62 (m, 6H), 3.37 (br, 2H). ^{13}C-NMR (125 MHz, $CDCl_3$): δ (ppm) 1698.4, 139.8, 132.6, 127.9, 118.1, 113.9, 66.9, 48.2, 42.7. FT-IR (cm^{-1}): 3084, 3036, 2973, 2931, 2868, 2226, 1617, 1606, 1468, 1437, 1278, 1263, 1108, 1014. ESI-HRMS: m/z: 239.0800 $[M+Na]^+$ (calcd for $[C_{12}H_{12}N_2O_2Na]^+$ 239.0796).

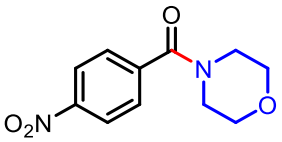

Morpholino(4-nitrophenyl)methanone [86] (**3ia**): According to the general procedure, the reaction was performed by using 4-nitrobenzaldehyde **1i** [CAS NO. 555-16-8] (1.0 eq, 0.30 mmol), morpholine **2a** (5.0 eq, 1.50 mmol) and sodium iodide (5.0 eq, 1.50 mmol) in co-solvent between acetonitrile (3.00 mL) and water (1.00 mL) to afford **3ia** (37.7 mg, 0.160 mmol, 53% yield) as a yellow solid: ^{1}H-NMR (500 MHz, $CDCl_3$): δ (ppm) 8.28 (d, *J* = 8.56 Hz, 2H), 7.58 (d, *J* = 8.56 Hz, 2H), 3.79-3.62 (m, 6H), 3.38 (br, 2H). ^{13}C-NMR (125 MHz, $CDCl_3$): δ (ppm) 168.2, 148.6, 141.6, 128.3, 124.1, 66.9, 48.2, 42.7. FT-IR (cm^{-1}): 3109, 3071, 2981, 2929, 2868, 1623, 11596, 1511, 1443, 1353, 1282, 1259, 1111, 1012. ESI-HRMS: m/z: 237.0841 $[M+H]^+$ (calcd for $[C_{11}H_{13}N_2O_4]^+$ 237.0875).

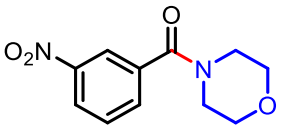

Morpholino(3-nitrophenyl)methanone [91] (**3ja**): According to the general procedure, the reaction was performed by using 3-nitrobenzaldehyde **1j** (1.0 eq, 0.30 mmol), morpholine **2a** (5.0 eq, 1.50 mmol) and sodium iodide (5.0 eq, 1.50 mmol) in co-solvent between acetonitrile (3.00 mL) and water (1.00 mL) to afford **3ja** (53.5 mg, 0.227 mmol. 76% yield) as a yellow solid: ^{1}H-NMR (500 MHz, $CDCl_3$): δ (ppm) 8.26-8.24 (m, 2H), 7.73 (d, *J* = 7.49 Hz, 1H), 7.61 (t, *J* = 7.76 Hz, 1H), 3.77-3.41 (m, 8H). ^{13}C-NMR (125 MHz, $CDCl_3$): δ (ppm) 167.8, 148.2, 137.0, 133.2, 130.0, 124.8, 122.4, 66.8, 48.3, 42.8. FT-IR (cm^{-1}): 3099, 3067, 2986, 2971, 2921, 2868, 1629, 1617, 1540, 1477, 1441, 1349, 1259, 1113. ESI-HRMS: m/z: 259.0690 $[M+Na]^+$ (calcd for $[C_{11}H_{12}N_2O_4Na]^+$ 259.0694).

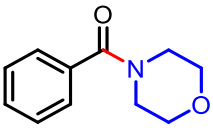

Morpholino(phenyl)methanone [88] (**3ka**): According to the general procedure, the reaction was performed by using benzaldehyde **1k** [CAS NO. 100-52-7] (1.0 eq, 0.30 mmol), morpholine **2a** (5.0 eq, 1.50 mmol) and sodium iodide (2.5 eq, 0.75 mmol) in co-solvent between acetonitrile (3.00 mL) and water (1.00 mL) to afford **3ka** (37.3 mg,

0.195 mmol, 65% yield) as a white solid: ^{1}H-NMR (500 MHz, $CDCl_3$): δ (ppm) 7.40 (m, 5H), 3.76-3.61 (m, 6H), 3.43 (br, 2H). ^{13}C-NMR (125 MHz, $CDCl_3$): δ (ppm) 170.6, 135.4, 130.0, 128.7, 127.2, 67.0, 48.3, 42.6. FT-IR (cm^{-1}): 3008, 2975, 2917, 2864, 1621, 1602, 1579, 1425, 1272, 1251, 1108. ESI-HRMS: m/z: 214.0840 $[M+Na]^+$ (calcd for $[C_{11}H_{13}NO_2Na]^+$ 214.0843).

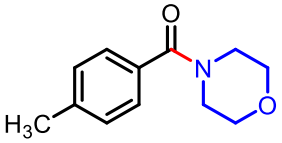

Morpholino(*p*-tolyl)methanone [86] (**3la**): According to the general procedure, the reaction was performed by using *p*-tolualdehyde **1l** [CAS NO. 104-87-0] (1.0 eq, 0.30 mmol), morpholine **2a** (5.0 eq, 1.50 mmol) and sodium iodide (2.5 eq, 0.75 mmol) in co-solvent between acetonitrile (3.00 mL) and water (1.00 mL) to afford **3la** (29.6 mg, 0.144 mmol, 48% yield) as a colorless liquid: ^{1}H-NMR (500 MHz, $CDCl_3$): δ (ppm) 7.30 (d, *J* = 8.07 Hz, 2H), 7.20 (d, *J* = 7.81 Hz, 2H), 3.69-3.48 (m, 8H), 2.37 (s, 3H). ^{13}C-NMR (125 MHz, $CDCl_3$): δ (ppm) 170.7, 140.2, 132.4, 129.3, 127.3, 67.0, 48.4, 42.8, 21.5. FT-IR (cm^{-1}): 3025, 2967, 2920, 2850, 1632, 1512, 1432, 1280, 1257, 1107, 1013. ESI-HRMS: m/z: 228.1010 $[M+Na]^+$ (calcd for $[C_{12}H_{15}NO_2Na]^+$ 228.1000).

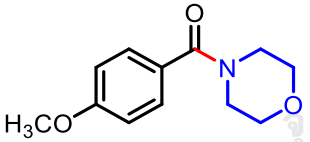

(4-Methoxyphenyl)(morpholino)methanone [86] (**3ma**): According to the general procedure, the reaction was performed by using *p*-anisaldehyde **1m** [CAS NO. 123-11-5] (1.0 eq, 0.30 mmol), morpholine **2a** (5.0 eq, 1.50 mmol) and sodium iodide (2.5 eq, 0.75 mmol) in co-solvent between acetonitrile (3.00 mL) and water (1.00 mL) to afford **3ma** (27.3 mg, 0.071 mmol, 41% yield) as a colorless liquid: ^{1}H-NMR (500 MHz, $CDCl_3$): δ (ppm) 7.38 (d, *J* = 8.73 Hz, 2H), 6.91 (d, *J* = 8.71 Hz, 2H), 3.82 (s, 3H), 3.68-3.63 (br, 8H). ^{13}C-NMR (125 MHz, $CDCl_3$): δ (ppm) 170.6, 161.0, 129.3, 127.3, 113.9, 67.1, 55.5. FT-IR (cm^{-1}): 3065, 2967, 2916, 2856, 1617, 1514, 1455, 1423, 1304, 1244, 1173, 1109. ESI-HRMS: m/z: 244.0959 $[M+Na]^+$ (calcd for $[C_{12}H_{15}NO_3Na]^+$ 244.0949).

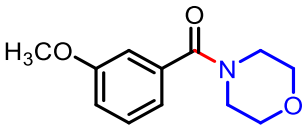

(3-Methoxyphenyl)(morpholino)methanone [88] (**3na**): According to the general procedure, the reaction was performed by using *m*-anisaldehyde **1n** (1.0 eq, 0.30 mmol), morpholine **2a** (5.0 eq, 1.50 mmol) and sodium iodide (2.5 eq, 0.75 mmol) in co-solvent between acetonitrile (3.00 mL) and water (1.00 mL) to afford **3na** (39.8 mg, 0.180 mmol, 60% yield) as a colorless liquid: ^{1}H-NMR (500 MHz, $CDCl_3$): δ (ppm) 7.33-7.30 (m, 1H), 6.96-6.94 (m, 3H), 3.82-3.45 (m, 11H). ^{13}C-NMR (125 MHz, $CDCl_3$): δ (ppm) 170.3, 159.8, 136.7, 129.8, 119.2, 115.8, 112.6, 67.0, 55.5, 48.2, 42.6. FT-IR (cm^{-1}): 3060, 2966, 2921, 2852, 1637, 1461, 1433, 1289, 1237, 1114. ESI-HRMS: m/z: 244.0950 $[M+Na]^+$ (calcd for $[C_{12}H_{15}NO_3Na]^+$ 244.0949).

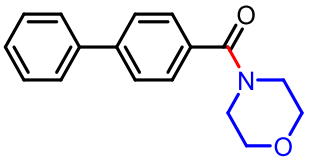

[1,1'-biphenyl]-4-yl(morpholino)methanone [92] (**3oa**): According to the general procedure, the reaction was performed by using biphenyl-4-carboxaldehyde **1o** [CAS NO. 3218-36-8] (1.0 eq, 0.30 mmol), morpholine **2a** (5.0 eq, 1.50 mmol) and sodium iodide (2.5 eq, 0.75 mmol) in co-solvent between acetonitrile (3.00 mL) and water (1.00 mL) to afford **3oa** (62.5 mg, 0.234 mmol, 78% yield) as a white solid: ^{1}H-NMR (500 MHz, $CDCl_3$): δ (ppm) 7.64 (d, J = 8.14 Hz, 2H), 7.59 (d, J = 7.28 Hz, 2H), 7.50-7.44 (m, 4H), 7.38 (t, J = 7.34 Hz, 1H), 3.72-3.54 (m, 8H). ^{13}C-NMR (125 MHz, $CDCl_3$): δ (ppm) 170.4, 142.9, 140.2, 134.1, 129.0, 128.0, 127.8, 127.4, 127.2, 67.0, 48.4, 42.7. FT-IR (cm^{-1}): 3023, 2983, 2962, 2900, 2856, 1625, 1604, 1456, 1431, 1274, 1259, 1113. ESI-HRMS: m/z: 290.1157 $[M+Na]^+$ (calcd for $[C_{17}H_{17}NO_2Na]^+$ 290.1156).

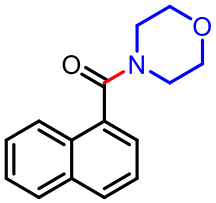

Morpholino(naphthalen-1-yl)methanone [90] (**3pa**): According to the general procedure, the reaction was performed by using 1-naphthaldehyde **1p** [CAS NO.66-77-3] (1.0 eq, 0.30 mmol), morpholine **2a** (5.0 eq, 1.50 mmol) and sodium iodide (2.5 eq, 0.75 mmol) in co-solvent between acetonitrile (3.00 mL) and water (1.00 mL) to afford **3pa** (47.2 mg, 0.196 mmol, 65% yield) as a white liquid: ^{1}H-NMR (500 MHz, $CDCl_3$): δ (ppm) 7.89-7.84 (m, 3H), 7.56-7.47 (m, 3H), 7.42 (d, *J* = 6.89 Hz, 1H), 4.03-3.83 (m, 4H), 3.55-3.48 (m, 2H), 3.23-3.16 (m, 2H). ^{13}C-NMR (125 MHz, $CDCl_3$): δ (ppm) 169.6, 133.8, 133.6, 129.6, 129.5, 128.6, 127.3, 126.7, 125.3, 124.7, 124.0, 67.2, 67.1, 47.7, 42.3. FT-IR (cm^{-1}): 3059, 2968, 2919, 2852, 1623, 1508, 1464, 1385, 1279, 1207, 1114. ESI-HRMS: m/z: 264.0997 $[M+Na]^+$ (calcd for $[C_{15}H_{15}NO_2Na]^+$ 264.1000).

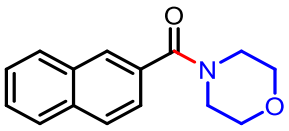

Morpholino(naphthalen-2-yl)methanone [93] (**3qa**): According to the general procedure, the reaction was performed by using 2-naphthaldehyde **1q** [CAS NO. 66-99-9] (1.0 eq, 0.30 mmol), morpholine **2a** (5.0 eq, 1.50 mmol) and sodium iodide (2.5 eq, 0.75 mmol) in co-solvent between acetonitrile (3.00 mL) and water (1.00 mL) to afford **3qa** (58.0 mg, 0.240 mmol, 80% yield) as a pale yellow solid: ^{1}H-NMR (500 MHz, $CDCl_3$): δ (ppm) 7.91-7.85 (m, 4H), 7.56-7.48 (m, 3H), 3.80-3.52 (m, 8H). ^{13}C-NMR (125 MHz, $CDCl_3$): δ (ppm) 170.6, 133.9, 132.8, 132.7, 128.6, 128.5, 127.9, 127.3, 127.2, 126.9, 124.3, 67.0, 48.3, 42.8. FT-IR (cm^{-1}): 3051, 3008, 2985, 2964, 2915, 2853, 1618, 1600, 1470, 1425, 1259, 1115. ESI-HRMS: m/z: 264.1004 $[M+Na]^+$ (calcd for $[C_{15}H_{15}NO_2Na]^+$ 264.1000).

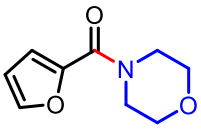

Furan-2-yl(morpholino)methanone [86] (**3ra**): According to the general procedure, the reaction was performed by using furfural **1r** [CAS NO. 98-01-1] (1.0 eq, 0.30 mmol), morpholine **2a** (5.0 eq, 1.50 mmol) and sodium iodide (2.5 eq, 0.75 mmol) in co-solvent between acetonitrile (3.00 mL) and water (1.00 mL) to afford **3ra** (13.3 mg, 0.074 mmol, 24% yield) as a yellow liquid: ^{1}H-NMR (500 MHz, $CDCl_3$): δ (ppm) 7.48-7.47 (m, 1H), 7.03 (d, *J* = 3.49 Hz, 1H), 6.48 (dd, *J* = 1.74, 3.44 Hz, 1H), 3.82 (br, 4H), 3.75-3.74 (m, 4H). ^{13}C-NMR (125 MHz, $CDCl_3$): δ (ppm) 159.3, 147.9, 143.9, 117.0, 111.5, 67.1. FT-IR (cm^{-1}): 3116, 2965, 2861, 1620, 1490, 1425, 1368, 1279, 1114, 1029. ESI-HRMS: m/z: 204.0627 $[M+Na]^+$ (calcd for $[C_9H_{11}NO_3Na]^+$ 204.0636).

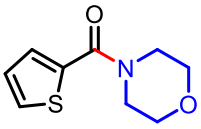

Morpholino(thiophen-2-yl)methanone [86] (**3sa**): According to the general procedure, the reaction was performed by using 2-thiophenecarboxaldehyde **1s** [CAS NO. 98-03-3] (1.0 eq, 0.30 mmol), morpholine **2a** (5.0 eq, 1.50 mmol) and sodium iodide (2.5 eq, 0.75 mmol) in co-solvent between acetonitrile (3.00 mL) and water (1.00 mL) to afford **3sa** (27.9 mg, 0.141 mmol, 47% yield) as a yellow liquid: ^{1}H-NMR (500 MHz, $CDCl_3$): δ (ppm) 7.46 (d, *J* = 4.93 Hz, 1H), 7.28 (d, *J* = 3.68 Hz, 1H), 7.05 (dd, *J* = 3.84, 4.69 Hz, 1H), 3.77-3.75 (m, 4H), 3.73-3.71 (m, 4H). ^{13}C-NMR (125 MHz, $CDCl_3$): δ (ppm) 163.8, 136.7, 129.1, 129.0, 126.9, 67.0, 45.9. FT-IR (cm^{-1}): 3088, 2963, 2921, 2856, 1614, 1525, 1436, 1274, 1254, 1113, 999. ESI-HRMS: m/z: 220.0406 $[M+Na]^+$ (calcd for $[C_9H_{11}NO_2SNa]^+$ 220.0408).

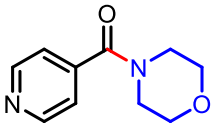

Morpholino(pyridine-4-yl)methanone [94] (**3ta**): According to the general procedure, the reaction was performed by using 4-pyridinecarboxaldehyde **1t** [CAS NO. 872-85-5] (1.0 eq, 0.30 mmol), morpholine **2a** (5.0 eq, 1.50 mmol) and sodium iodide (5.0 eq, 1.50 mmol) in co-solvent between acetonitrile (3.00 mL) and water (1.00 mL) to afford

3tc (4.2 mg, 0.022 mmol, 7% yield) as a yellow liquid: ^{1}H-NMR (500 MHz, $CDCl_3$): δ (ppm) 7.24 (d, *J* = 6.00 Hz, 2H), 8.64 (d, *J* = 5.94 Hz, 2H), 3.73 (br, 2H), 3.56 (br, 2H), 3.32 (br, 2H). ^{13}C-NMR (125 MHz, $CDCl_3$): δ (ppm) 167.7, 150.3, 143.1, 121.3, 66.7, 47.9, 42.4. FT-IR (cm^{-1}): 3046, 2968, 2919, 2862, 1638, 1551, 1499, 1452, 1279, 1118. ESI-HRMS: m/z: 193.0967 $[M+H]^+$ (calcd for $[C_{10}H_{13}N_2O_2]^+$ 193.0977).

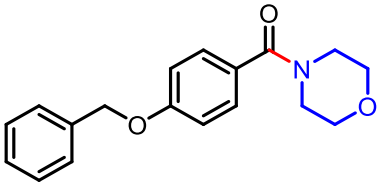

(4-(benzyloxy)phenyl)(morpholino)methanone[18] (**3va**): According to the general procedure, the reaction was performed by using 4-(benzyloxy)benzaldehyde **1v** (1.0 eq, 0.30 mmol), morpholine **2a** (5.0 eq, 1.50 mmol) and sodium iodide (2.5 eq, 0.75 mmol) in co-solvent between acetonitrile (3.00 mL) and water (1.00 mL) to afford **3va** (46.3 mg, 0.156 mmol, 52% yield) as a colorless liquid: ^{1}H-NMR (500 MHz, $CDCl_3$): δ (ppm) 7.43-7.37 (m, 6H), 7.35-7.32 (m, 1H), 6.98 (d, *J* = 8.61 Hz, 2H), 5.09 (s, 2H), 3.69 (br, 8H). ^{13}C-NMR (125 MHz, $CDCl_3$): δ (ppm) 170.5, 160.2, 136.5, 129.3, 128.8, 128.2, 127.6, 127.5, 114.8, 70.2, 67.0, 48.0, 43.3. FT-IR (cm^{-1}): 3066, 3031, 2963, 2921, 2856, 1615, 1514, 1454, 1426,1304, 1173, 1115. ESI-HRMS: m/z: 298.1448 $[M+H]^+$ (calcd for $[C_{18}H_{20}NO_3]^+$ 298.1443).

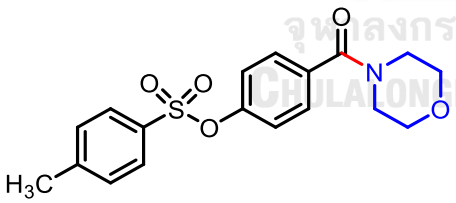

4-(morpholine-4-carbonyl)phenyl 4-methylbenzenesulfonate (**3wa**): According to the general procedure, the reaction was performed by using 4-formylphenyl 4-methylbenzenesulfonate **1w** (1.0 eq, 0.30 mmol), morpholine **2a** (5.0 eq, 1.50 mmol) and sodium iodide (2.5 eq, 0.75 mmol) in co-solvent between acetonitrile (3.00 mL) and water (1.00 mL) to afford **3wa** (70.4 mg, 0.195 mmol, 65% yield) as a white solid: ^{1}H-NMR (500 MHz, $CDCl_3$): δ (ppm) 7.71 (d, *J* = 8.32 Hz, 2H), 7.34 (d, *J* = 8.54 Hz, 2H), 7.32 (d, *J* = 8.11 Hz, 2H), 7.04 (d, *J* = 8.51 Hz, 2H), 3.74-3.62 (m, 6H), 3.41 (br, 2H), 2.44 (s, 3H). ^{13}C-NMR (125 MHz, $CDCl_3$): δ (ppm) 169.3, 150.6, 145.8, 134.1, 132.2, 130.0,

128.9, 128.6, 122.7, 66.9, 48.3, 42.8, 21.8. FT-IR (cm^{-1}): 3015, 2996, 2965, 2916, 2854, 1625, 1594, 1458, 1435, 1378, 1284, 1175, 1150, 1103, 1092. ESI-HRMS: m/z: 362.1060 $[M+H]^+$ (calcd for $[C_{18}H_{20}NO_5SNa]^+$ 362.1062).

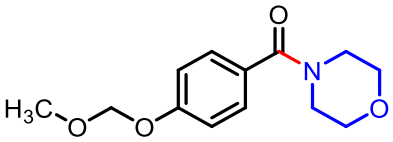

(4-(methoxymethoxy)phenyl)(morpholino)methanone (**3xa**): According to the general procedure, the reaction was performed by using 4-(methoxymethoxy)benzaldehyde **1x** (1.0 eq, 0.30 mmol), morpholine **2a** (5.0 eq, 1.50 mmol) and sodium iodide (2.5 eq, 0.75 mmol) in co-solvent between acetonitrile (3.00 mL) and water (1.00 mL) to afford **3xa** (39.7 mg, 0.158 mmol, 53% yield) as a colorless liquid: ^{1}H-NMR (500 MHz, $CDCl_3$): δ (ppm) 7.36 (d, *J* = 8.69 Hz, 2H), 7.05 (d, *J* = 8.72 Hz, 2H), 5.19 (s, 2H), 3.68-3.47 (br, 11H). ^{13}C-NMR (125 MHz, $CDCl_3$): δ (ppm) 170.4, 158.6, 129.2, 128.6, 116.1, 94.3, 67.1, 56.3. FT-IR (cm^{-1}): 3045, 2957, 2898, 2851, 1628, 1510, 1426, 1302, 1237, 1158, 1074, 994. ESI-HRMS: m/z: 274.1057 $[M+H]^+$ (calcd for $[C_{13}H_{17}NO_4Na]^+$ 274.1055).

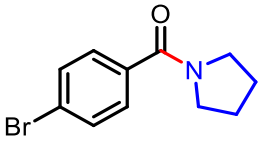

(4-Bromophenyl)(pyrrolidin-1-yl)methanone [52] (**3ab**) According to the general procedure, the reaction was performed by using 4-bromobenzaldehyde **1a** (1.0 eq, 0.30 mmol), pyrrolidine **2b** [CAS NO. 123-75-1] (5.0 eq, 1.50 mmol) and sodium iodide (2.5 eq, 0.75 mmol) in co-solvent between acetonitrile (3.00 mL) and water (1.00 mL) to afford **3ab** (54.1 mg, 0.213 mmol, 71% yield) as a pale yellow solid: ^{1}H-NMR (500 MHz, $CDCl_3$): δ (ppm) 7.52 (d, *J* = 8.46 Hz, 2H), 7.39 (d, *J* = 8.49 Hz, 2H), 3.62 (s, 2H), 3.39 (s, 2H), 1.94 (br, 2H), 1.87 (br, 2H).^{13}C-NMR (125 MHz, $CDCl_3$): δ (ppm) 168.7, 136.1, 131.6, 129.0, 124.2, 49.7, 46.4, 26.5, 24.5. FT-IR (cm^{-1}): 3061, 2972, 2878, 1629, 1562, 1426,1340, 1068, 1017. ESI-HRMS: m/z: 276.0063 $[M+Na]^+$ (calcd for $[C_{11}H_{12}BrNONa]^+$ 275.9999).

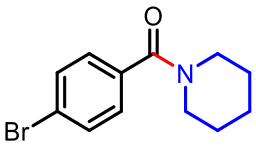

(4-Bromophenyl)(piperidin-1-yl)methanone [95] (**3ac**): According to the general procedure, the reaction was performed by using 4-bromobenzaldehyde **1a** (1.0 eq, 0.30 mmol), piperidine **2c** [CAS NO. 110-89-4] (5.0 eq, 1.50 mmol) and sodium iodide (2.5 eq, 0.75 mmol) in co-solvent between acetonitrile (3.00 mL) and water (1.00 mL) to afford **3ac** (55.8 mg, 0.208 mmol, 69% yield) as a white solid: ^{1}H-NMR (500 MHz, $CDCl_3$): δ (ppm) 7.53 (d, *J* = 8.31 Hz, 2H), 7.27 (d, *J* = 8.29 Hz, 2H), 3.67 (br, 2H), 3.33 (br, 2H), 1.68-1.56 (m, 6H). ^{13}C-NMR (125 MHz, $CDCl_3$): δ (ppm) 169.4, 135.4, 131.8, 128.7, 123.7, 48.9, 43.3, 26.6, 25.7, 24.6. FT-IR (cm^{-1}): 3021, 2992, 2952, 2939, 2917, 2854, 1617, 1586, 1441, 1274, 996. ESI-HRMS: m/z: 290.0153 $[M+Na]^+$ (calcd for $[C_{12}H_{14}BrNONa]^+$ 290.0156).

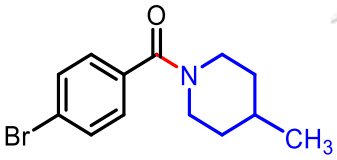

(4-Bromophenyl)(4-methylpiperidin-1-yl)methanone [96] (**3ad**): According to the general procedure, the reaction was performed by using 4-bromobenzaldehyde **1a** (1.0 eq, 0.30 mmol), 4-methylpiperidine **2d** [CAS NO. 626-58-4] (5.0 eq, 1.50 mmol) and sodium iodide (2.5 eq, 0.75 mmol) in co-solvent between acetonitrile (3.00 mL) and water (1.00 mL) to afford **3ad** (53.1 mg, 0.188 mmol, 63% yield) as a white solid: ^{1}H-NMR (500 MHz, $CDCl_3$): δ (ppm) 7.52 (d, *J* = 8.31 Hz, 2H), 7.26 (d, *J* = 8.36 Hz, 2H), 4.62 (br, 1H), 3.67 (br, 1H), 2.94-2.77 (m, 2H), 1.93-1.61 (m, 3H), 1.15 (br, 2H), 0.97 (d, *J* = 6.39 Hz, 3H). ^{13}C-NMR (125 MHz, $CDCl_3$): δ (ppm) 169.4, 135.4, 131.8, 128.7, 123.8, 48.3, 42.7, 34.7, 33.9, 31.3, 21.8. FT-IR (cm^{-1}): 3086, 3059, 3008, 2954, 2927,2858, 1625, 1583, 1441, 1370, 1305, 1278, 1247. ESI-HRMS: m/z: 304.0314 $[M+Na]^+$ (calcd for $[C_{13}H_{16}BrNONa]^+$ 304.0312).

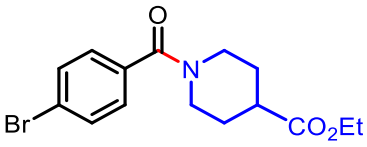

Ethyl 1-(4-bromonemzoyl)piperidine-4-catboxylate (**3ae**): According to the general procedure, the reaction was performed by using 4-bromobenzaldehyde **1a** (1.0 eq, 0.30 mmol), ethyl 4-piperidinecarboxylate **2e** [CAS NO. 1126-09-6] (5.0 eq, 1.50 mmol) and sodium iodide (2.5 eq, 0.75 mmol) in co-solvent between acetonitrile (3.00 mL) and water (1.00 mL) to afford **3ae** (54.1 mg, 0.159 mmol, 53%) as a yellow liquid: ^{1}H-NMR (500 MHz, $CDCl_3$): δ (ppm) 7.53 (d, *J* = 8.30 Hz, 2H), 7.26 (d, *J* = 8.30 Hz, 2H), 4.48 (br, 1H), 4.15 (q, *J* = 7.12 Hz, 2H), 3.69 (br, 1H), 3.03 (br, 2H), 2.59-2.53 (m, 1H), 1.97-1.69 (m, 4H), 1.25 (t, *J* = 7.14 Hz, 3H). ^{13}C-NMR (125 MHz, $CDCl_3$): δ (ppm) 174.2, 169.5, 134.9, 131.9, 128.7, 124.1, 60.8, 47.1, 41.8, 41.1, 28.5, 28.0, 14.3. FT-IR (cm^{-1}): 3050, 2977, 2933, 2863, 1727, 1643, 1447, 1316, 1188, 1043, 1005. ESI-HRMS: m/z: 362.0362 $[M+Na]^+$ (calcd for $[C_{15}H_{18}BrNO_3Na]^+$ 362.0367).

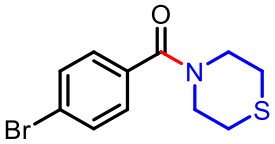

(4-Bromophenyl)(thiomorpholino)methanone [97] (**3af**): According to the general procedure, the reaction was performed by using 4-bromobenzaldehyde **1a** (1.0 eq, 0.30 mmol), thiomorpholine **2f** [CAS NO. 123-90-0] (5.0 eq, 1.50 mmol) and sodium iodide (2.5 eq, 0.75 mmol) in co-solvent between acetonitrile (3.00 mL) and water (1.00 mL) to afford **3af** (21.6 mg, 0.076 mmol, 25% yield) as a pale yellow solid: ^{1}H-NMR (500 MHz, $CDCl_3$): δ (ppm) 7.53 (d, *J* = 7.90 Hz, 2H), 7.24 (d, *J* = 8.02 Hz, 2H), 3.97 (br, 2H), 3.63 (br, 2H), 2.69-2.54 (m, 4H). ^{13}C-NMR (125 MHz, $CDCl_3$): δ (ppm) 196.8, 134.6, 131.9, 128.6, 124.2, 50.2, 44.7, 28.0, 27.5. FT-IR (cm^{-1}): 3057, 2960, 2898, 1617, 1588, 1458, 1429, 1309, 1293, 1259, 1136. ESI-HRMS: m/z: 307.9713 $[M+Na]^+$ (calcd for $[C_{11}H_{12}BrNOSNa]^+$ 307.9720).

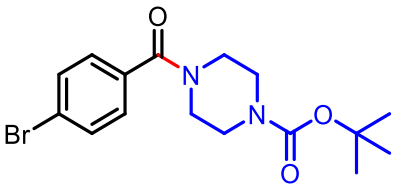

***tert*-Butyl-4-(4-bromobenzoyl)piperazine-1-carboxylate** [98] (**3ag**) According to the general procedure, the reaction was performed by using 4-bromobenzaldehyde **1a** (1.0 eq, 0.30 mmol), 1-(*tert*-butoxycarbonyl)piperazine **2g** [CAS NO. 57260-71-6] (5.0 eq, 1.50 mmol) and sodium iodide (2.5 eq, 0.75 mmol) in co-solvent between acetonitrile (3.00 mL) and water (1.00 mL) to afford **3ag** (92.1 mg, 0.249 mmol, 83% yield) as a white solid: ^{1}H-NMR (500 MHz, $CDCl_3$): δ (ppm) 7.56 (d, *J* = 8.34 Hz, 2H), 7.28 (d, *J* = 8.35 Hz, 2H), 3.71-3.39 (m, 8H), 1.46 (s, 9H). ^{13}C-NMR (125 MHz, $CDCl_3$): δ (ppm) 169.7, 154.6, 134.3, 132.0, 128.9, 124.4, 80.6, 47.7, 43.8, 42.3, 28.4. FT-IR (cm^{-1}): 3004, 2979, 2963, 2931, 2864, 1682, 1621, 1596, 1460, 1427, 1364, 1242, 1169, 1008. ESI-HRMS: m/z: 391.0628 $[M+Na]^+$ (calcd for $[C_{16}H_{121}BrN_2O_3Na]^+$ 391.0633).

2.5 Preparation of benzyl alcohols (4f, 4j and 4n)

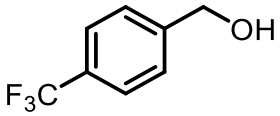

4-(trifluoromethyl)benzyl alcohol (**4f**) [CAS NO. 349-95-1]: A solution of 4-(trifluoromethyl)benzaldehyde **1f** [CAS NO. 455-19-6] (1.0 eq, 1.50 mmol) in methanol (5 mL) was added sodium borohydride [CAS NO. 16940-66-2] (2.0 eq, 3.00 mmol) slowly over 10 minutes at 0°C. The solution was stirred at room temperature for 1 hour. The reaction mixture was quenched with 1M HCl and extracted with CH_2Cl_2 (10 mL). The organic layer was eliminated water by Na_2SO_4. After filtration and removal of the solvent under reduced pressure, the crude product was purified by silica gel column chromatography (3:2 of EtOAc:Hexane) to afford **4f** in 131.8 mg, 0.75 mmol, 50% yield as a colorless liquid. The spectroscopic data are identical to commercial source.

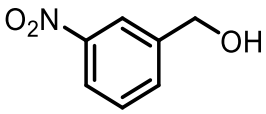

3-nitrobenzyl alcohol (**4j**) [CAS NO. 619-25-0]: A solution of 3-nitrobenzaldehyde **1j** [CAS NO. 99-61-6] (1.0 eq, 1.50 mmol) in methanol (5 mL) was added sodium borohydride (2.0 eq, 3.00 mmol) slowly over 10 minutes at 0°C. The solution was stirred at room temperature for 1 hour. The reaction mixture was quenched with 1M HCl and extracted with CH_2Cl_2 (10 mL). The organic layer was eliminated water by Na_2SO_4. After filtration and removal of the solvent under reduced pressure, the crude product was purified by silica gel column chromatography to afford **4j** in 173.9 mg, 0.85 mmol, 48% yield as a yellow gum. The spectroscopic data are identical to commercial source.

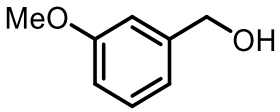

3-methoxybenzyl alcohol (**4n**) [CAS NO. 6971-51-3]: A solution of *m*-anisaldehyde **1n** [CAS NO. 591-31-1] (1.0 eq, 1.50 mmol) in methanol (5 mL) was added sodium borohydride (2.0 eq, 3.00 mmol) slowly over 10 minutes at 0°C. The solution was stirred at room temperature for 1 hour. The reaction mixture was quenched with 1M HCl and extracted with CH_2Cl_2 (10 mL). The organic layer was eliminated water by Na_2SO_4. After filtration and removal of the solvent under reduced pressure, the crude product was purified by silica gel column chromatography to **4n** in 191.4 mg, 0.71 mmol, 57% yield as a colorless liquid. The spectroscopic data are identical to commercial source.

2.6 General procedure for electrochemical oxidative amidation of benzyl alcohols and morpholine

General procedure: a mixture of benzyl alcohols (1.0 eq, 0.30 mmol), morpholine (5.0 eq, 1.50 mmol) and sodium iodide (5.0 eq, 1.50 mmol) was dissolved by co-solvent 3:1 of CH_3CN:H_2O (4 mL) in undivided cell. The reaction was applied constant current at 100 mA via graphite rod as anode and platinum plate as cathode from power supply. The reaction was stirred at room temperature for 3 hours. The

reaction mixture was washed with $Na_2S_2O_8$ (1x10 mL) following water (2x10 mL) and the organic portion was extracted with EtOAc (3x10 mL). The organic layer was eliminated water by Na_2SO_4. After filtration and removal of the solvent under reduced pressure, the crude product was purified by silica gel column chromatography to afford amide products **3aa**, **3ca**, **3fa** and **3ia**-**3na**.

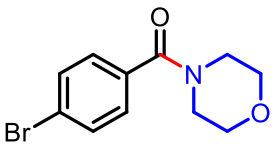

(4-Bromophenyl)(morpholino)methanone (**3aa**): According to the general procedure, the reaction was performed by using 4-bromobenzyl alcohol **4a** [CAS NO. 873-75-6] (1.0 eq, 0.30 mmol), morpholine **2a** (5.0 eq, 1.50 mmol) and sodium iodide (5.0 eq, 1.50 mmol) in co-solvent between acetonitrile (3.00 mL) and water (1.00 mL) to afford **3aa** (43.9 mg, 0.163 mmol, 54% yield) as a pale yellow solid. The ^{1}H and ^{13}C-NMR data are identical to above experiment.

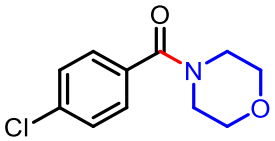

(4-chlorophenyl)(morpholino)methanone (**3ca**): According to the general procedure, the reaction was performed by using 4-chlorobenzyl alcohol **4c** [CAS NO. 873-76-7] (1.0 eq, 0.30 mmol), morpholine **2a** (5.0 eq, 1.50 mmol) and sodium iodide (5.0 eq, 1.50 mmol) in co-solvent between acetonitrile (3.00 mL) and water (1.00 mL) to afford **3ca** (43.8 mg, 0.194 mmol, 65% yield) as a white solid. The ^{1}H and ^{13}C-NMR data are identical to above experiment.

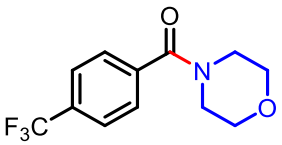

Morpholino(4-(trifluoromethyl)phenyl)methanone (**3fa**): According to the general procedure, the reaction was performed by using 4-(trifluoromethyl)benzyl alcohol **4f** (1.0 eq, 0.30 mmol), morpholine **2a** (5.0 eq, 1.50 mmol) and sodium iodide (5.0 eq, 1.50 mmol) in co-solvent between acetonitrile (3.00 mL) and water (1.00 mL) to afford **3fa** (46.8 mg, 0.180 mmol, 60% yield) as a white solid. The ^{1}H and ^{13}C-NMR data are identical to above experiment.

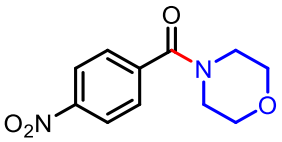

Morpholino(4-nitrophenyl)methanone (**3ia**): According to the general procedure, the reaction was performed by using 4-nitrobenzyl alcohol **4i** [CAS NO. 619-73-8] (1.0 eq, 0.30 mmol), morpholine **2a** (5.0 eq, 1.50 mmol) and sodium iodide (5.0 eq, 1.50 mmol) in co-solvent between acetonitrile (3.00 mL) and water (1.00 mL) to afford **3ia** (6.3 mg, 0.027 mmol, 9% yield) as a yellow solid. The ^{1}H and ^{13}C-NMR data are identical to above experiment.

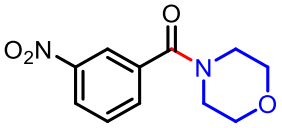

Morpholino(3-nitrophenyl)methanone (**3ja**): According to the general procedure, the reaction was performed by using 3-nitrobenzyl alcohol **4j** (1.0 eq, 0.30 mmol), morpholine **2a** (5.0 eq, 1.50 mmol) and sodium iodide (5.0 eq, 1.50 mmol) in co-solvent between acetonitrile (3.00 mL) and water (1.00 mL) to afford **3ja** (21.7 mg, 0.092 mmol. 31% yield) as a yellow solid. The ^{1}H and ^{13}C-NMR data are identical to above experiment.

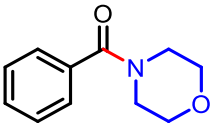

Morpholino(phenyl)methanone (**3ka**): According to the general procedure, the reaction was performed by using benzyl alcohol **4k** [CAS NO. 100-51-6] (1.0 eq, 0.30 mmol), morpholine **2a** (5.0 eq, 1.50 mmol) and sodium iodide (5.0 eq, 1.50 mmol) in co-solvent between acetonitrile (3.00 mL) and water (1.00 mL) to afford **3ka** (24.4 mg, 0.129 mmol, 43% yield) as a white solid. The ^{1}H and ^{13}C-NMR data are identical to above experiment.

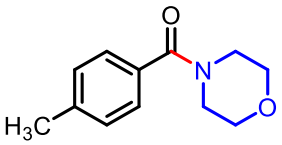

Morpholino(*p*-tolyl)methanone (**3la**): According to the general procedure, the reaction was performed by using 4-methylbenzyl alcohol **4l** [CAS NO. 589-18-4] (1.0 eq, 0.30 mmol), morpholine **2a** (5.0 eq, 1.50 mmol) and sodium iodide (5.0 eq, 1.50 mmol) in co-solvent between acetonitrile (3.00 mL) and water (1.00 mL) to afford **3la** (25.3 mg, 0.123 mmol, 41% yield) as a colorless liquid. The ^{1}H and ^{13}C-NMR data are identical to above experiment.

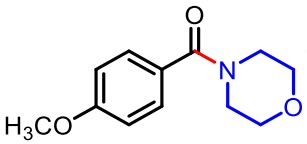

(4-Methoxyphenyl)(morpholino)methanone (**3ma**): According to the general procedure, the reaction was performed by using 4-methoxybenzyl alcohol **4m** [CAS NO. 105-13-5] (1.0 eq, 0.30 mmol), morpholine **2a** (5.0 eq, 1.50 mmol) and sodium iodide (5.0 eq, 1.50 mmol) in co-solvent between acetonitrile (3.00 mL) and water (1.00 mL) to afford **3ma** (21.2 mg, 0.096 mmol, 32% yield) as a colorless liquid. The ^{1}H and ^{13}C-NMR data are identical to above experiment.

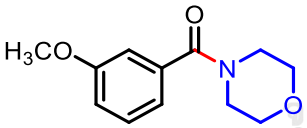

(3-Methoxyphenyl)(morpholino)methanone (**3na**): According to the general procedure, the reaction was performed by using 3-methoxylbenzyl alcohol **4n** (1.0 eq, 0.30 mmol), morpholine **2a** (5.0 eq, 1.50 mmol) and sodium iodide (5.0 eq, 1.50 mmol) in co-solvent between acetonitrile (3.00 mL) and water (1.00 mL) to afford **3na** (25.1 mg, 0.113 mmol, 38% yield) as a colorless liquid. The ^{1}H and ^{13}C-NMR data are identical to above experiment.

2.7 Gram-scale synthesis

A mixture of 4-bromobenzaldehyde **1a** (1.0 eq, 5.41 mmol), morpholine **2a** (5.0 eq, 27.03 mmol) and sodium iodide (2.5 eq, 13.51) mmol was dissolved by co-solvent 3:1 of CH_3CN:H_2O (60 mL) in 100 mL of three-neck round bottom flask. The reaction

was applied constant current at 100 mA via graphite rod as anode and cathode from power supply. The reaction was stirred at room temperature for 24 hours. The reaction mixture was washed with $Na_2S_2O_8$ (1x10 mL) following water (2x10 mL) and the organic portion was extracted with EtOAc (3x10 mL). The organic layer was eliminated water by Na_2SO_4. After filtration and removal of the solvent under reduced pressure, the crude product was purified by silica gel column chromatography (3:2 of EtOAc:Hexane) to afford **3aa** in 1.302 g, 4.82 mmol, 89% yield. The ^{1}H and ^{13}C-NMR data are identical to above experiment.

2.8 Electrochemical oxidative amidation using portable power charger

A mixture of 4-bromobenzaldehydes **1a** (1.0 eq, 0.3 mmol), morpholine **2a** (5.0 eq, 1.5 mmol) and sodium iodide (2.5 eq, 0.75 mmol) was dissolved by co-solvent 3:1 of CH_3CN:H_2O (4 mL) in undivided cell. The reaction was applied with portable power charger having 10,000 mAh capacity and 5 V via graphite rod as anode and platinum plate as cathode. The reaction was stirred at room temperature for 3 hours. The reaction mixture was washed with $Na_2S_2O_8$ (1x10 mL) following water (2x10 mL) and the organic portion was extracted with EtOAc (3x10 mL). The organic layer was eliminated water by Na_2SO_4. After filtration and removal of the solvent under reduced pressure, the crude product was purified by silica gel column chromatography (3:2 of EtOAc:Hexane) to afford **3aa** in 59.9 g, 0.222 mmol, 74% yield. The ^{1}H and ^{13}C-NMR data are identical to above experiment.

2.9 Mechanistic investigations

2.9.1 Control experiment: part 1

A solution of 4-bromobenzyl alcohol **4a** (1.0 eq, 0.30 mmol), morpholine **2a** (5.0 eq, 1.50 mmol) and sodium iodide (5.0 eq, 1.50 mmol) was prepared under optimized condition without electrical current. The reaction mixture was washed with $Na_2S_2O_8$ (1x10 mL) following water (2x10 mL) and the organic portion was extracted with EtOAc (3x10 mL). The organic layer was eliminated water by Na_2SO_4. The crude reaction mixture was spotted on TLC comparing with starting material **4a** and amide product **3aa**. The visualization on TLC shown no amide product **3aa** was obtained.

A solution of 4-bromobenzaldehyde **1a** (1.0 eq, 0.30 mmol), morpholine **2a** (5.0 eq, 1.50 mmol) and sodium iodide (2.5 eq, 0.75 mmol) was prepared under optimized condition without electrical current. The reaction mixture was washed with $Na_2S_2O_8$ (1x10 mL) following water (2x10 mL) and the organic portion was extracted with EtOAc (3x10 mL). The organic layer was eliminated water by Na_2SO_4. The crude reaction mixture was spotted on TLC comparing with starting material **1a** and amide product **3aa**. The visualization on TLC shown no amide product **3aa** was obtained.

2.9.2 Control experiment: part 2

A solution of 4-bromobenzyl alcohol **4a** (1.0 eq, 0.30 mmol), morpholine **2a** (5.0 eq, 1.50 mmol) and molecular iodine (5.0 eq, 1.50 mmol) was prepared under optimized condition without electrical current. The reaction mixture was washed with $Na_2S_2O_8$ (1x10 mL) following water (2x10 mL) and the organic portion was extracted with EtOAc (3x10 mL). The organic layer was eliminated water by Na_2SO_4. After filtration and removal of the solvent under reduced pressure, the crude product was purified by silica gel column chromatography (3:2 of EtOAc:Hexane) to afford **1a** in less than 5% yield.

A solution of 4-bromobenzaldehyde **1a** (1.0 eq, 0.30 mmol), morpholine **2a** (5.0 eq, 1.50 mmol) and molecular iodine (2.5 eq, 0.75 mmol) was prepared under optimized condition without electrical current. The reaction mixture was washed with $Na_2S_2O_8$ (1x10 mL) following water (2x10 mL) and the organic portion was extracted with EtOAc (3x10 mL). The organic layer was eliminated water by Na_2SO_4. After filtration and removal of the solvent under reduced pressure, the crude product was purified by silica gel column chromatography (3:2 of EtOAc:Hexane) to afford **3aa** in 17.0 mg, 0.063 mmol, 21% yield.

2.9.3 Control experiment: part 3

A solution of 4-bromobenzaldehyde **1a** (1.0 eq, 0.30 mmol), morpholine **2a** (5.0 eq, 1.50 mmol) and potassium iodate (2.5 eq, 0.75 mmol) and a solution of 4-bromobenzaldehyde **1a** (1.0 eq, 0.30 mmol), morpholine **2a** (5.0 eq, 1.50 mmol) and sodium periodate (2.5 eq, 0.75 mmol) were prepared under optimized condition without electrical current. The reaction mixture was washed with $Na_2S_2O_8$ (1x10 mL) following water (2x10 mL) and the organic portion was extracted with EtOAc (3x10 mL).

The organic layer was eliminated water by Na_2SO_4. The crude reaction mixture was spotted on TLC comparing with starting material **1a** and amide product **3aa**. The visualization on TLC shown no amide product **3aa** was obtained.

2.9.4 Control experiment: part 4

A solution of 4-bromobenzaldehyde **1a** (1.0 eq, 0.30 mmol), morpholine **2a** (5.0 eq, 1.50 mmol) and sodium iodide (2.5 eq, 0.75 mmol) was prepared under nitrogen atmosphere using optimized condition. The reaction mixture was washed with $Na_2S_2O_8$ (1x10 mL) following water (2x10 mL) and the organic portion was extracted with EtOAc (3x10 mL). The organic layer was eliminated water by Na_2SO_4. After filtration and removal of the solvent under reduced pressure, the crude product was purified by silica gel column chromatography (3:2 of EtOAc:Hexane) to afford **3aa** in 64.0 mg, 0.237 mmol, 79% yield.

A solution of 4-bromobenzaldehyde **1a** (1.0 eq, 0.30 mmol), morpholine **2a** (5.0 eq, 1.50 mmol), sodium iodide (2.5 eq, 0.75 mmol) and TEMPO (1.0 eq, 0.30 mmol) was prepared under optimized condition. The reaction mixture was washed with $Na_2S_2O_8$ (1x10 mL) following water (2x10 mL) and the organic portion was extracted with EtOAc (3x10 mL). The organic layer was eliminated water by Na_2SO_4. After filtration and removal of the solvent under reduced pressure, the crude product was purified by silica gel column chromatography (3:2 of EtOAc:Hexane) to afford **3aa** in 63.2 mg, 0.234 mmol, 78% yield.

2.9.5 NMR monitoring

The ^{1}H-NMR spectra of 4-cyanobenzaldehyde **1h** and morpholine **2a** under CD_3CN solvent were collected as standard spectra. The solution of 4-cyanobenzaldehyde **1h** with morpholine **2a** in ratio 1:1 under CD_3CN was characterized by ^{1}H-NMR after ten minutes mixing. Those three ^{1}H-NMR spectra were stacked together to interpret chemical structure of intermediate.

2.9.6 Cyclic voltammetry

Each starting material was prepared at 10 mM under 0.1 M tetrabutylammonium tetrafluoroborate dissolving in acetonitrile. In this experiment, the three-electrode configuration such as glassy carbon, platinum plate and 0.4 M Ag/AgCl were used as working electrode (WE), counter electrode (CE) and quasi-

reference electrode (QRE), respectively as shown in Figure 2.1. All cyclic voltammograms were collect by using scan rate at 50 mV/S in the potential range from 0.0 to 1.8 V under nitrogen atmosphere.

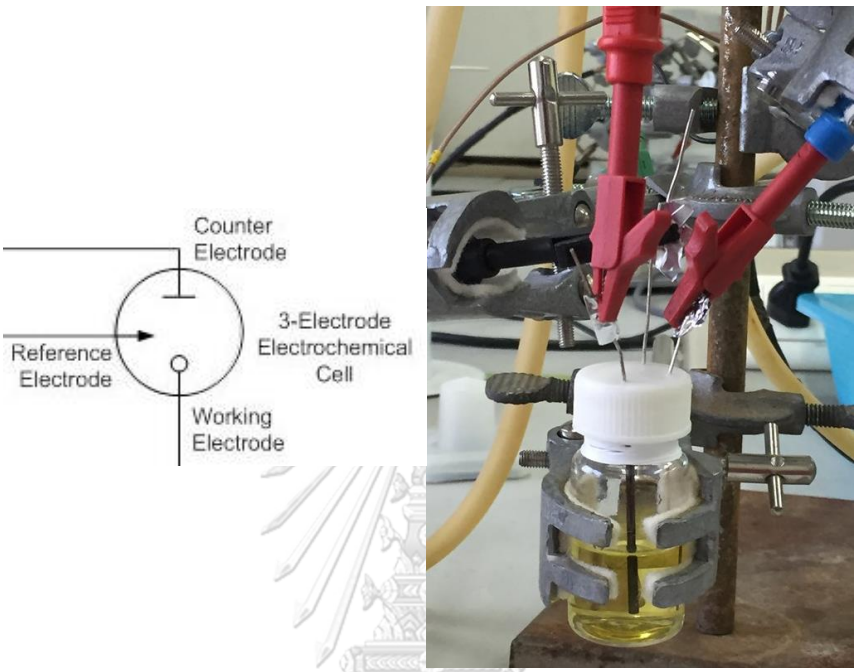

Figure 2.1 Three-electrode configuration setup for cyclic voltammetry

CHAPTER III

RESULTS & DISCUSSION

3.1 Reaction setup

Our electrolytic cell in this work for electrochemical oxidative amidation composes of three parts as shown in Figure 3.1. The first part is a power supply which can adjust into two modes, constant voltage and constant current with the voltage limit at 0-30 V and current limit at 0-5 A (Figure 3.1a). The second part is electrochemical reactor (Figure 3.1b). Herein, we used undivided cell to perform the electrochemical oxidative amidation because of less complicate operation. The third part is electrodes which require both anodic and cathodic electrode (Figure 3.1c). Notably, the non-sacrificial electrodes were recommended to use in order to avoid corrosion and to provide high reusability. Therefore, graphite rode and platinum plate were mainly used in this work. To complete the circuit, anodic and cathodic electrodes were put in electrochemical reaction which clipped with electrical wires before turning on the magnetic stirrer and power supply. The electrodes were reused by cleaning with acetone and soaking in 3M HCl solution.

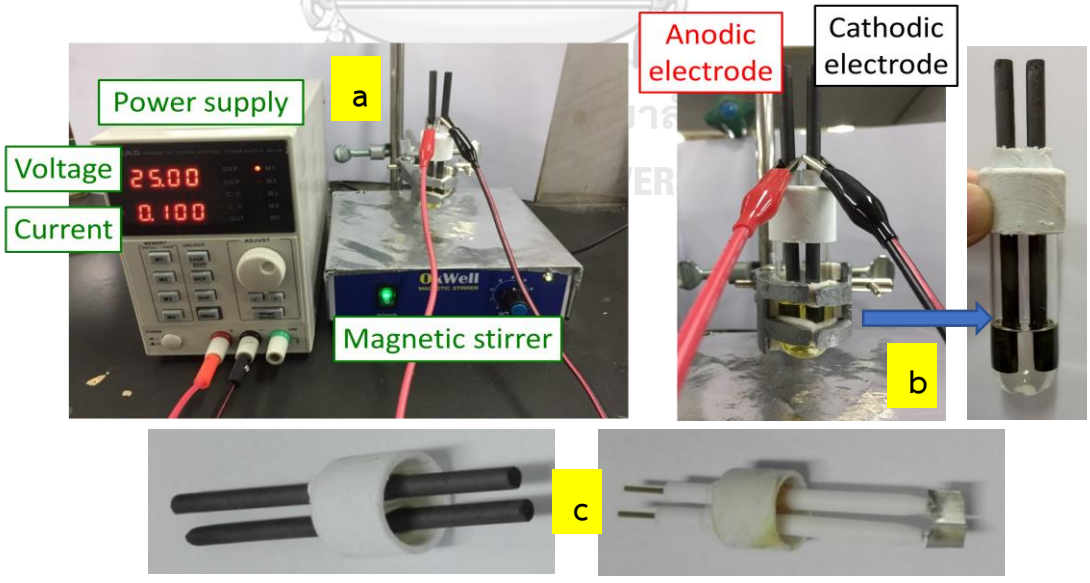

Figure 3.1 Reaction setup for electrochemical oxidative amidation

3.2 Optimization of electrochemical oxidative amidation

For our optimization, we used 4-bromobenzaldehyde **1a** and morpholine **2a** as model substrates for studying various factors about oxidative amidation. 4-bromobenzaldehyde **1a** was chosen due to bromo substituent group which provides suitable electronic effect. Moreover, NMR splitting pattern of aromatic ring on amide product **3aa** is clearly separable as seen in Appendix, Figure A7.

3.2.1 Electrolyte screening

We conducted the reaction by using co-solvent 3:1 of CH_3CN:H_2O, graphite rods as anode and cathode with a current intensity 100 mA for 3 hours at room temperature in an undivided cell as standard condition. The screening of electrolytes was shown in Table 3.1. The use of iodide salts such as LiI, NaI, KI and TBAI as redox electrolyte provided amide product **3aa** from 70 to 22% yields, respectively with remaining starting material **1a** (Table 3.1, entries 1-4). The high amide yields from LiI and NaI over KI and TBAI resulted from the high conductivity of cation. Switching from iodide salts to bromide salts such as NaBr, KBr and TBAB (Table 3.1, entries 5-7) and chloride salt, NaCl (Table 3.1, entry 8) resulted in no reaction. These observations suggested that iodide anion plays a crucial role in this electrochemical reaction. To confirm the necessity of iodide in our reaction, $TBABF_4$ was used as non-redox electrolyte (Table 3.1, entry 9). However, the oxidative amidation of **1a** and **2a** cannot take place. This result confirmed that our reaction proceeds by indirect electrolysis rather than direct electrolysis. Among those iodide sources, we selected NaI as electroyte for further screening due to its cheaper price and providing amide **3aa** in good yields.

Table 3.1 Electrolyte screening[a]

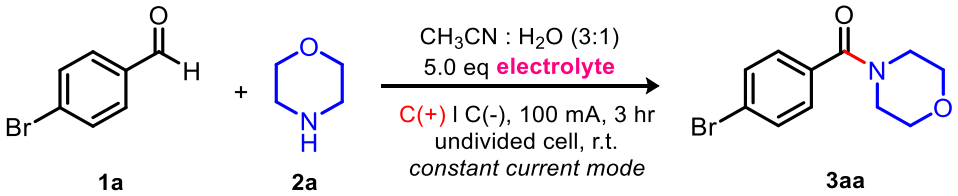

1a **2a** **3aa**

Entry	Electrolytes	% Yields[b]
1	LiI	70
2	NaI	67
3	KI	42
4	TBAI	22
5	NaBr	no reaction
6	KBr	no reaction
7	TBAB	no reaction
8	NaCl	no reaction
9	$TBABF_4$	no reaction

[a] Unless otherwise noted, the reaction conditions were as followed: 4-bromobenzaldehyde (1.0 eq, 0.30 mmol), morpholine (5.0 eq, 1.50 mmol), electrolyte (5.0 eq, 1.50 mmol), CH_3CN:H_2O (3 mL:1 mL), graphite rod (Ø = 5 mm, immersed 1.0 cm) as anode and cathode, 100 mA for 3 hours at room temperature in undivided cell. [b] Isolated yield.

3.2.2 Solvent screening

To screen solvent, we performed the reaction in various organic solvent such as CH_3CN, EtOH, DMSO and THF as shown in Table 3.2. Using pure CH_3CN solvent, the reaction provided amide **3aa** in 70% yield (Table 3.2, entry 1). We observed the high resistance showing more than 10 volts. Therefore, we planned to add water as a co-solvent to reduce such high voltage. We used 3:1 ratio of five organic solvents and water (Table 3.2, entries 2-5). Among them, acetonitrile still provided the best condition yielding amide product **3aa** in 67% yield. Switching from water to ethanol resulted in no reaction (Table 3.3, entry 6) while increase of water content provided

amide product **3aa** in much lower yield (Table 3.2, entry 7). Hence, co-solvent 3:1 of CH_3CN:H_2O was a suitable solvent for further study.

Table 3.2 Solvent screening[a]

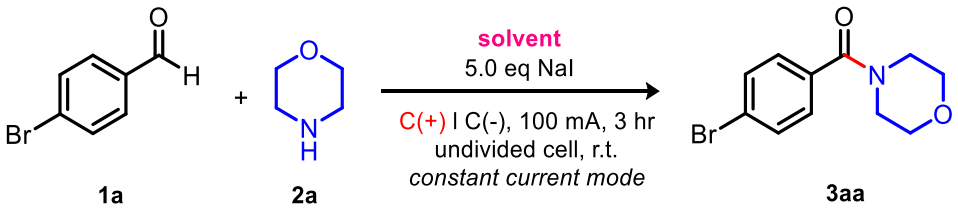

1a **2a** **3aa**

Entry	Ratio of solvent	Solvent	% Yields[b]
1	100%	CH_3CN	70
2	3 : 1	CH_3CN : H_2O	67
3	3 : 1	DMSO : H_2O	50
4	3 : 1	THF : H_2O	40
5	3 : 1	EtOH : H_2O	33
6	3 : 1	CH_3CN : EtOH	no reaction
7	1 : 1	CH_3CN : H_2O	8

[a] Unless otherwise noted, the reaction conditions were as followed: 4-bromobenzaldehyde (1.0 eq, 0.30 mmol), morpholine (5.0 eq, 1.50 mmol), NaI (5.0 eq, 1.50 mmol), solvent, graphite rod (Ø = 5 mm, immersed 1.0 cm) as anode and cathode, 100 mA for 3 hours at room temperature in undivided cell. [b] Isolated yield.

3.2.3 The amount of amine screening

Next, we studied the amount of amine in our electrochemical oxidative amidation and the data were summarized in Table 3.3. The amount of amine **2a** was varied from 3.0, 5.0 and 10.0 equivalent (Table 3.3, entries 1-3). Amide product **3aa** was isolated in high yield when 5.0 equivalent of amine were added. At low amount of amine, we believed that the reaction adding amine **2a** into aldehyde **1a** to generate the corresponding hemiaminal is relatively slow. Therefore, it requires high amount of amine to drive the reaction forward. However, at high concentration of amine (10.0 equivalent), we hypothesized that the reaction viscosity increased causing poor

electron transfer process. Therefore, 5.0 equivalent of amines will be used to further study.

Table 3.3 The amount of amine screening[a]

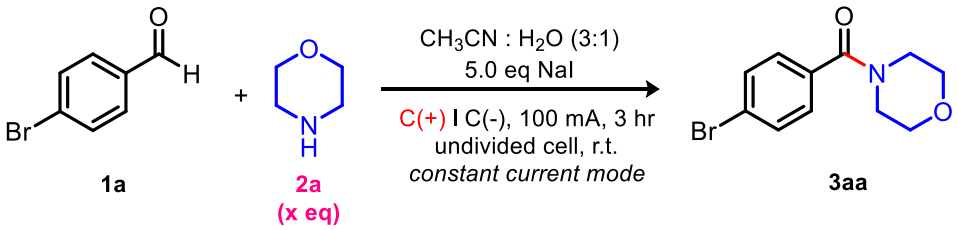

Entry	Equivalent of amine	% Yields[b]
1	5.0	67
2	3.0	49
3	10.0	33

[a] Unless otherwise noted, the reaction conditions were as followed: 4-bromobenzaldehyde (1.0 eq, 0.30 mmol), morpholine, NaI (5.0 eq, 1.50 mmol), CH_3CN:H_2O (3 mL:1 mL), graphite rod (Ø = 5 mm, immersed 1.0 cm) as anode and cathode, 100 mA for 3 hours at room temperature in undivided cell. [b] Isolated yield.

3.2.4 Electrode screening

In this section, the electrodes were examined as shown in Table 3.4. We changed the anode and cathode from both graphite rods (Table 3.4, entry 1) into platinum plates (Table 3.4, entry 2). The yield of **3aa** was dramatically decreased and we observed that starting material **1a** was largely remained in the reaction. Then we used graphite rod as anode and platinum plate as cathode (Table 3.4, entry 3). Fortunately, the yield of amide product **3aa** was increased from 67 to 83% yields because of the suitable energy between two electrodes. Therefore, graphite rod and platinum plate will be selected as anode and cathode for further study.

Table 3.4 Electrode screening[a]

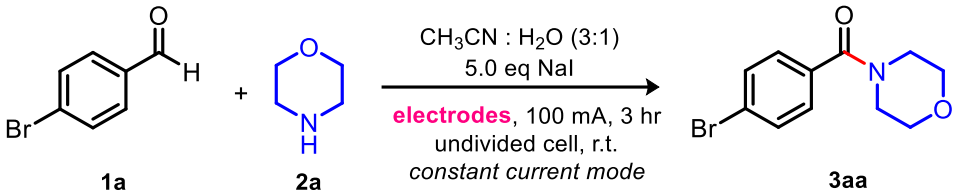

1a **2a** **3aa**

Entry	Type of electrodes	% Yields[b]
1	Graphite rod (+)/(-)	67
2	Platinum plate (+)/(-)	24
3	Graphite rode (+)/Platinum plate (-)	83

[a] Unless otherwise noted, the reaction conditions were as followed: 4-bromobenzaldehyde (1.0 eq, 0.30 mmol), morpholine (5.0 eq, 1.50 mmol), NaI (5.0 eq, 1.50 mmol), CH_3CN:H_2O (3 mL:1 mL), graphite rod (Ø = 5 mm, immersed 1.0 cm) or platinum plate (5x5x0.1 mm) for anode or cathode, 100 mA for 3 hours at room temperature in undivided cell. [b] Isolated yield.

3.2.5 Current intensity and reaction time screening

The effect of current intensity and reaction time were optimized as shown in Table 3.5. First, we fixed the reaction time at 3 hours and varied the current intensity from 80 to 150 mA (Table 3.5, entries 1-3). When we decreased the current intensity to 80 mA, the reaction provided amide product **3aa** in much lower yield along with aldehyde starting material **1a**. Moreover, the use of current intensity at 150 mA provided similar yield of amide product **3aa** at 100 mA for 3 hours while reducing reaction time into 2 hours provided amide product **3aa** in poor yield (Table 3.5, entry 4). Based on these results, we decided to use the current intensity at 100 mA and reaction time for 3 hours for further study.

Table 3.5 Current intensity and reaction time screening[a]

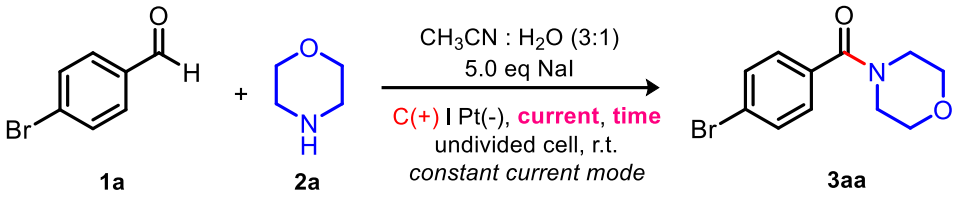

Entry	Current (mA)	Time (hour)	% Yields[b]
1	100	3	83
2	80	3	58
3	150	3	79
4	150	2	49

[a] Unless otherwise noted, the reaction conditions were as followed: 4-bromobenzaldehyde (1.0 eq, 0.30 mmol), morpholine (5.0 eq, 1.50 mmol), NaI (5.0 eq, 1.50 mmol), CH_3CN:H_2O (3 mL:1 mL), graphite rod (Ø = 5 mm, immersed 1.0 cm) as anode platinum plate (5x5x0.1 mm) as cathode, current intensity and reaction time at room temperature in undivided cell. [b] Isolated yield.

3.2.6 The amount of NaI screening

With suitable electrolyte, solvent, the amount of amine, electrodes, current intensity and reaction time in our hands, we next studied the amount of NaI (Table 3.6). In the previous studies, we used 5.0 equivalent of NaI for electrochemical oxidative amidation. To make greener reaction, we aim to reduce the amout of NaI. At 0.8 equivalent of NaI, we obtained amide product **3aa** only in 50% yield (Table 3.6, entry 2). On the other hand, at 2.5 equivalent of NaI, the amide product **3aa** was obtained in similar yield as the use of NaI at 5.0 equivalent (Table 3.6, entry 3). Eventually, we decided to use the reaction condition in Table 3.6, entry 2 as our optimized condition for electrochemical oxidative amidation.

Table 3.6 The amount of NaI screening[a]

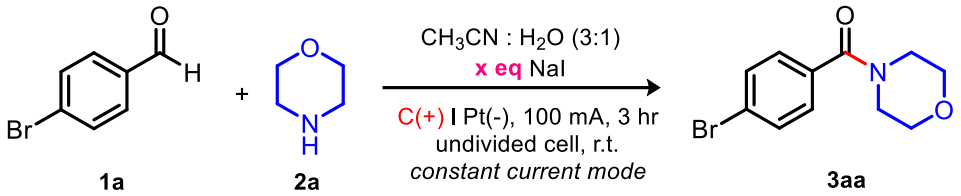

1a **2a** **3aa**

Entry	Equivalent of NaI	% Yields[b]
1	5.0	83
2	0.8	50
3	2.5	78

[a] Unless otherwise noted, the reaction conditions were as followed: 4-bromobenzaldehyde (1.0 eq, 0.30 mmol), morpholine (5.0 eq, 1.50 mmol), NaI, CH_3CN:H_2O (3 mL:1 mL), graphite rod (Ø = 5 mm, immersed 1.0 cm) as anode platinum plate (5x5x0.1 mm) as cathode, 100 mA for 3 hours at room temperature in an undivided cell. [b] Isolated yield.

3.3 Substrate scope of electrochemical oxidative amidation

With an optimized condition in our hands. We would like to expand the scope of our reaction. Various aldehydes and amine nucleophiles will be examined to demonstrate the reaction efficiency.

3.3.1 Scope of aldehydes

To study the scope of aldehyde, Various benzaldehydes carrying electron withdrawing substituent were tested with morpholine under our optimized condition as shown Scheme 3.1. Benzaldehydes carrying halogen substituent such as bromo (**1a** and **1b**), chloro (**1c** and **1d)** and iodo **1e** provided amide products, **3aa**-**3ea** from moderate to good yields. Moreover, benzaldehydes possessed trifluoromethyl (**1f** and **1g)** and cyano **1h** can be tolerated under optimized condition and afford **3fa**, **3ga** and **3ha** in 74, 79 and 46% yields, respectively. However, nitro substituent (**1i** and **1j**) provided the amide product **3ia** and **3ja** in 37 and 31% yields. Upon the increase amount of NaI to 5.0 equivalent the amide product **3ia** and **3ja** were obtained in better yields (53 and 76%). We hypothesized that nitro substituents on benzaldehyde are

reduced under our electrochemical reaction. To avoid the production of byproduct, the amount of NaI was increased from 2.5 equivalent to 5.0 equivalent. Therefore, the amide product **3ia** and **3ja** were obtained in higher yields.

Scheme 3.1 Electron withdrawing substituent on aromatic aldehyde scope[a, b]

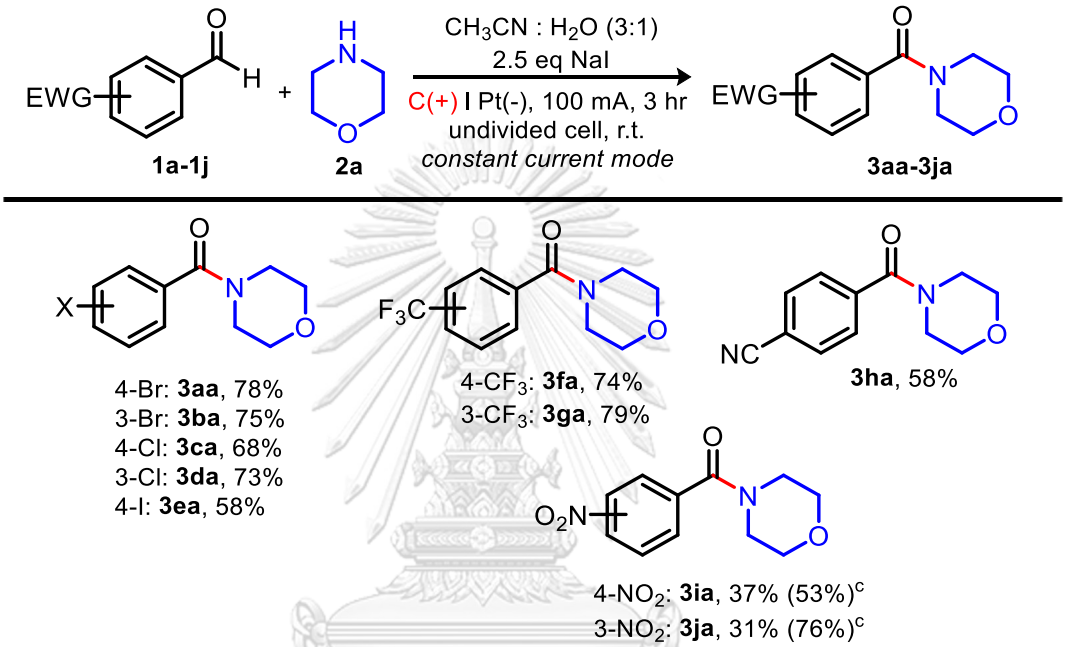

[a] Unless otherwise noted, the reaction conditions were as followed: aromatic aldehyde (1.0 eq, 0.30 mmol), morpholine (5.0 eq, 1.50 mmol), NaI (5.0 eq, 1.50 mmol), CH_3CN:H_2O (3 mL:1 mL), graphite rod (Ø = 5 mm, immersed 1.0 cm) as anode, platinum plate (5x5x0.1 mm) as cathode, 100 mA for 3 hours at room temperature in an undivided cell. [b] Isolated yield. [c] 5.0 eq NaI were used.

We then tested our electrochemical process to benzaldehydes carrying non-substituent and electron donating substituent with morpholine under our optimized condition as reported in Scheme 3.2. Benzaldehyde **1k** and benzaldehydes carrying electron donating substituent such as methyl **1l**, methoxy (**1m** and **1n)** and phenyl **1o** were transformed to amide **3ka**-**3oa** in satisfactory yield. Besides, naphthyl aldehydes (**1p** and **1q**) were converted into amide **3pa** and **3qa** in good yields.

Scheme 3.2 Electron donating substituent on aromatic aldehyde scope[a, b]

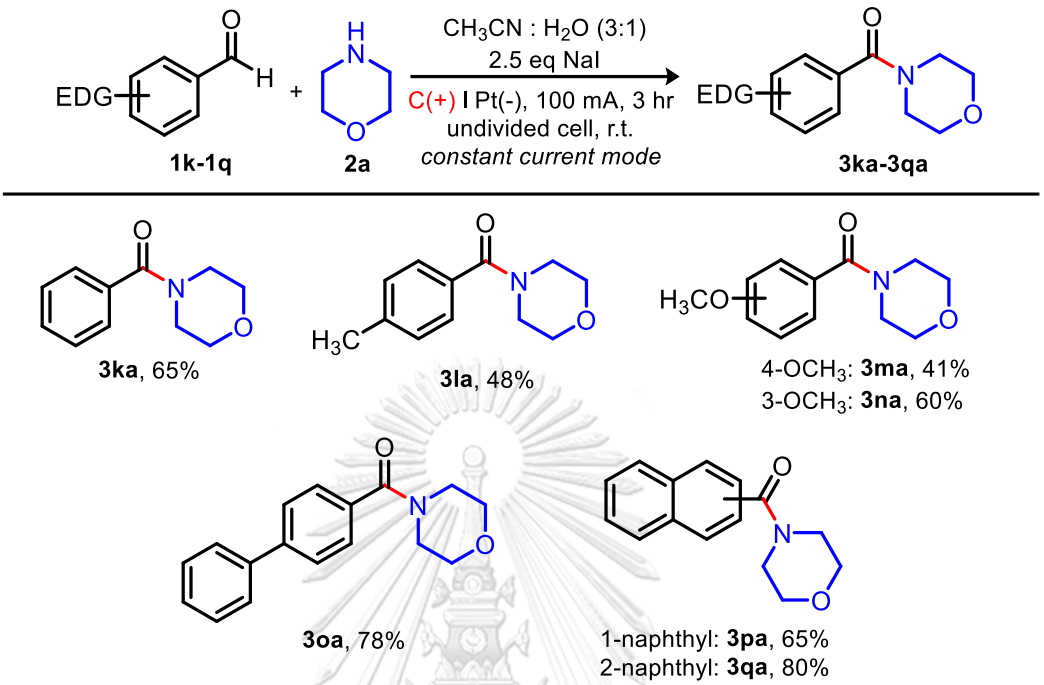

[a] Unless otherwise noted, the reaction conditions were as followed: aromatic aldehyde (1.0 eq, 0.30 mmol), morpholine (5.0 eq, 1.50 mmol), NaI (5.0 eq, 1.50 mmol), CH_3CN:H_2O (3 mL:1 mL), graphite rod (Ø = 5 mm, immersed 1.0 cm) as anode, platinum plate (5x5x0.1 mm) as cathode, 100 mA for 3 hours at room temperature in an undivided cell. [b] Isolated yield.

Next, heterocyclic aldehyde such as furfuraldehyde **1r**, 2-thiophenecarboxaldehyde **1s** and 4-pyridinecarboxyaldehyde **1t** were subjected to our electrolysis process as shown in Scheme 3.3. We were able to isolate amide **3ra**, **3sa** and **3ta** in 24, 47 and 7% yields, respectively. We hypothesized that low yields from this series resulted from the poor addition of amine to aldehyde caused by heteroatom in aromatic aldehyde.

Scheme 3.3 Heteroaromatic aldehyde scope[a, b]

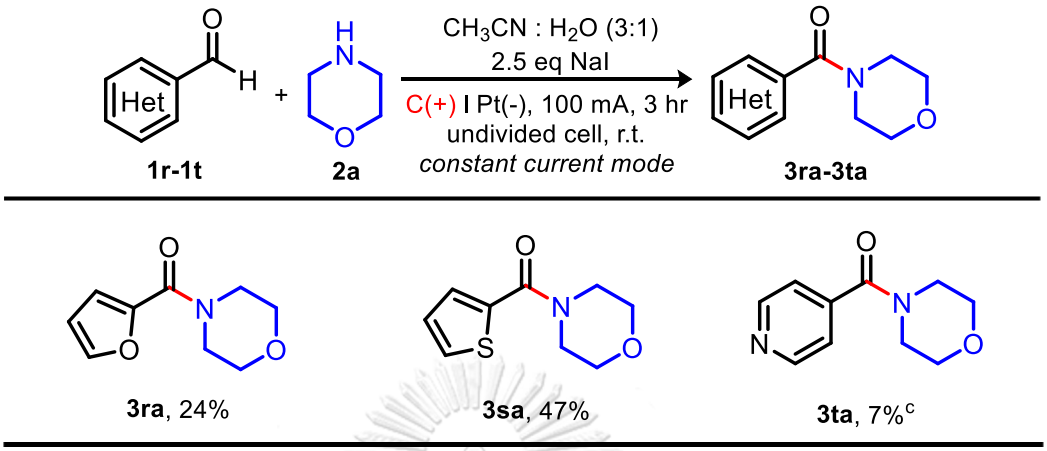

[a] Unless otherwise noted, the reaction conditions were as followed: aromatic aldehyde (1.0 eq, 0.30 mmol), morpholine (5.0 eq, 1.50 mmol), NaI (5.0 eq, 1.50 mmol), CH_3CN:H_2O (3 mL:1 mL), graphite rod (Ø = 5 mm, immersed 1.0 cm) as anode, platinum plate (5x5x0.1 mm) as cathode, 100 mA for 3 hours at room temperature in an undivided cell. [b] Isolated yield. [c] 5.0 eq NaI were used.

Next, we tried to use sensitive substrate, 4-hydroxybenzaldehyde **1u** to react with morpholine under our optimized condition as shown in Scheme 3.4. However, there was no product **3ua** and no starting material **1u** remained. We hypothesized that phenol was oxidized during the reaction. Therefore, we decided to protect hydroxy group in benzaldehyde **1u** into **1v**, **1w** and **1x** using benzyl bromide, *p*-toluenesulfonyl chloride and bromomethyl methyl ether, respectively. The details for synthesis of compounds were described in section 2.2. With those protecting groups, we successfully synthesized amide **3va**, **3wa** and **3xa** in 52, 65 and 53% yields, respectively. Therefore, such protecting groups can tolerate under electrochemical oxidative amidation.

Scheme 3.4 Protection of OH group on 4-hydroxybenzaldehyde scope[a, b]

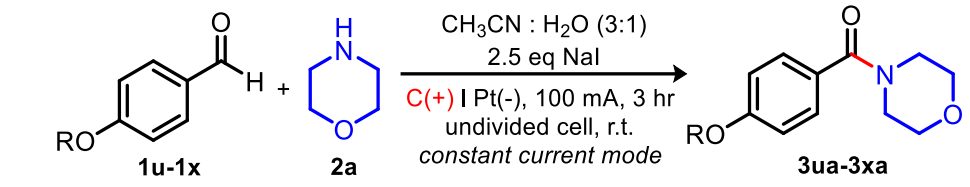

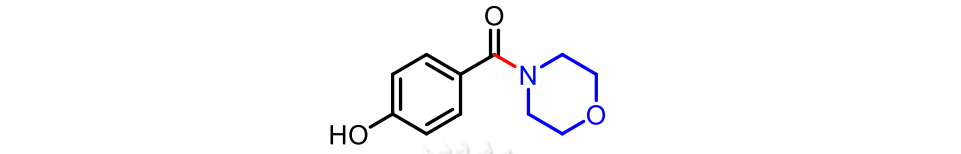

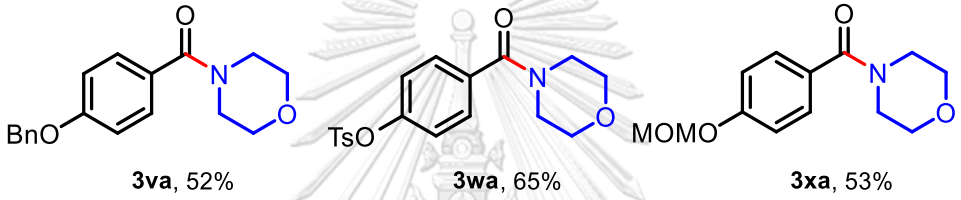

[a] Unless otherwise noted, the reaction conditions were as followed: aromatic aldehyde (1.0 eq, 0.30 mmol), morpholine (5.0 eq, 1.50 mmol), NaI (5.0 eq, 1.50 mmol), CH_3CN:H_2O (3 mL:1 mL), graphite rod (Ø = 5 mm, immersed 1.0 cm) as anode, platinum plate (5x5x0.1 mm) as cathode, 100 mA for 3 hours at room temperature in an undivided cell. [b] Isolated yield.

With the successful in electrochemical oxidative amidation of aromatic aldehyde substrates, we turned our attention to alkyl and vinyl aldehyde substrates. The results were shown in Scheme 3.5. Unfortunately, alkyl aldehyde substrates such as formaldehyde **1aa**, butylaldehyde **1ab**, cyclopropanealdehyde **1ac** and diphenylacetaldehyde **1ad** were failed to undergo electrochemical oxidative amination resulting in no reaction as we detected mostly starting materials. This results perhaps caused by low reactivity of the corresponding aldehyde and failed to react with morpholine to generate the corresponding hemiaminal. Similarly, cinnamaldehyde **1ae** gave decomposition during the electro-oxidation process.

Scheme 3.5 Unsuccessful aldehyde scope

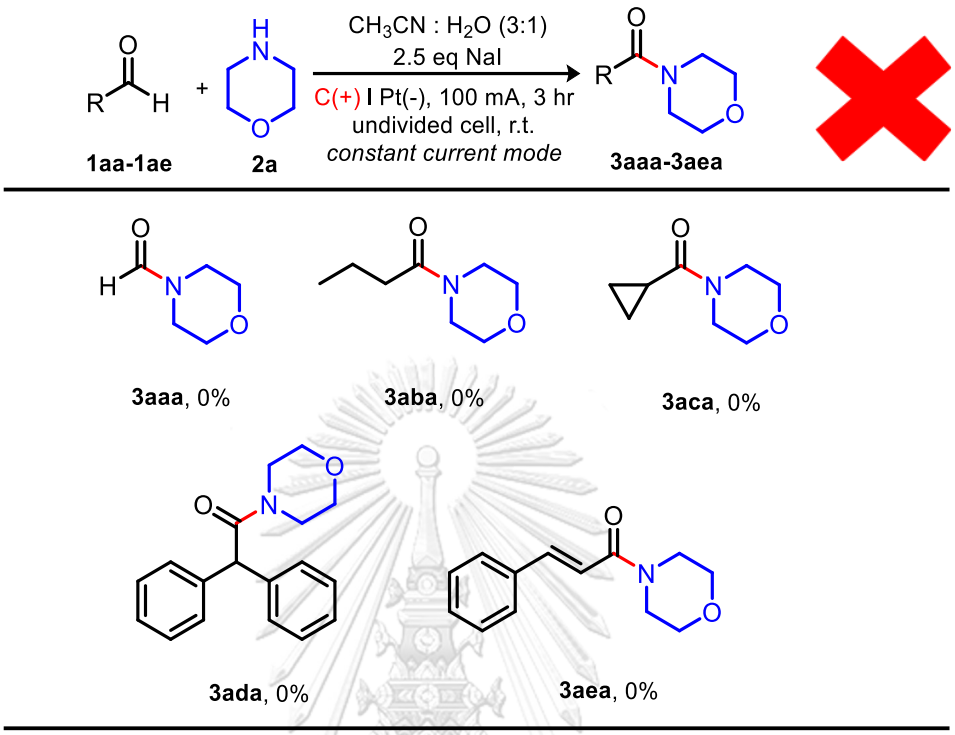

3.3.2 Scope of amines

Besides morpholine, various cyclic amines were tested under our optimized condition as depicted in Scheme 3.6. The secondary cyclic amines such as pyrrolidine **2b**, piperidine **2c**, 4-methylpiperidine **2d** and ethyl piperidine-4-carboxylate **2e** underwent our electrochemical reaction smoothly to provide target amides **3ab**-**3ae** from 53 to 71% yields. We would like to note that the ester functional group tolerates under our electrochemical reaction.

Scheme 3.6 Secondary cyclic amine scope: part 1[a, b]

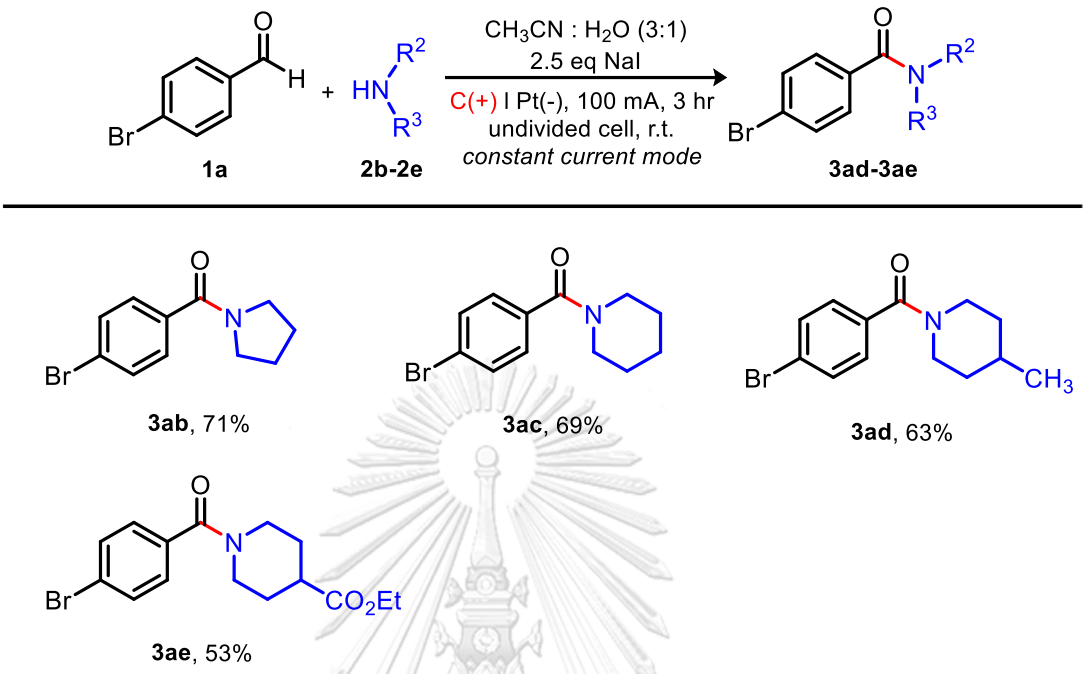

[a] Unless otherwise noted, the reaction conditions were as followed: 4-bromobenzaldehyde (1.0 eq, 0.30 mmol), secondary cyclic amine (5.0 eq, 1.50 mmol), NaI (5.0 eq, 1.50 mmol), CH_3CN:H_2O (3 mL:1 mL), graphite rod (Ø = 5 mm, immersed 1.0 cm) as anode, platinum plate (5x5x0.1 mm) as cathode, 100 mA for 3 hours at room temperature in an undivided cell. [b] Isolated yield.

Then, we tested our electrochemical reaction to amines carrying sensitive heteroatom such as thiomorpholine **2f** and *tert*-butyl piperazine-1-carboxylate **2g** reacting with 4-bromobenzaldehyde as shown in Scheme 3.7. We were able to isolate amide product **3af** in 25% yield with the remaining of starting material **1a** in large amount. This result indicated that thiomorpholine may be oxidized under our electrochemical reaction preventing them to react with aldehyde starting material **1a**. In addition, we obtained amide product **3ag** in 83% yield. Therefore, the *N*-Boc protecting group on amine survives under our electrochemical reaction.

Scheme 3.7 Secondary cyclic amine scope: part 2[a, b]

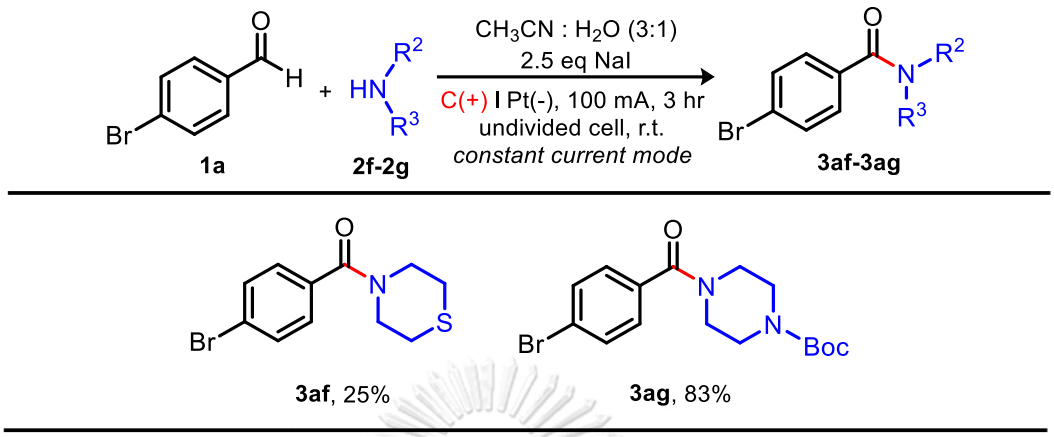

[a] Unless otherwise noted, the reaction conditions were as followed: 4-bromobenzaldehyde (1.0 eq, 0.30 mmol), secondary cyclic amine (5.0 eq, 1.50 mmol), NaI (5.0 eq, 1.50 mmol), CH_3CN:H_2O (3 mL:1 mL), graphite rod (Ø = 5 mm, immersed 1.0 cm) as anode, platinum plate (5x5x0.1 mm) as cathode, 100 mA for 3 hours at room temperature in an undivided cell. [b] Isolated yield.

Furthermore, we expanded the scope of amine into aliphatic amines such as butylamine **2aa** and benzylamine **2ab**, secondary aliphatic amine such as diethylamine **2ac**, secondary cyclic amines such as azepane **2ad**, 4-methylpiperazine **2ae** and tetraisohydroquinoline **2af**, aromatic amines such as aniline **2ag**, imidazole **2ah** and indole **2ai** reacted with 4-bromobenzaldehyde **1a** as shown in Scheme 3.8. Unfortunately, all mentioned amines above were failed to proceed the electrochemical oxidative amidation obtaining no reaction of amide product **3aaa**-**3aai**. We hypothesized that amine starting materials such as **2aa**-**2af** were less reactive nucleophile to undergo the addition on 4-bromobenzaldehyde **1a** as we are able to detect mostly starting material **1a** remaining in the reaction. For other aromatic amine substrates **2ag**-**2ai**, a complex mixture was observed and we hypothesized that they may undergo over-oxidation during the electrochemical oxidative amidation.

Scheme 3.8 Unsuccessful amine scope

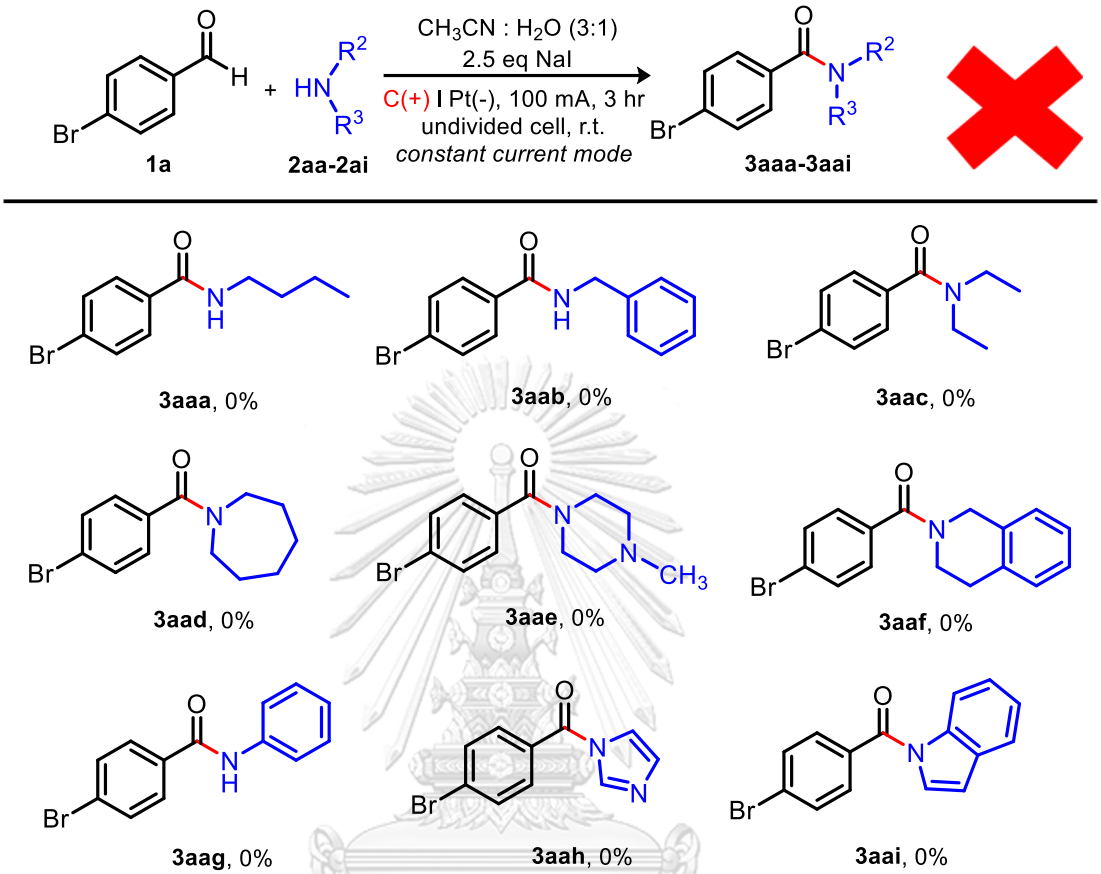

3.4 Electrochemical oxidative amidation between benzyl alcohols and morpholine

With the successful oxidative amidation of aldehyde above, we expanded the scope of electrochemical reaction into benzyl alcohol as starting material (Scheme 3.9). Using benzyl alcohol as starting material offered several benefits such as low cost and higher stability of starting material. Therefore, benzyl alcohol can carry sensitive functional groups over than aldehyde starting material. Following our previous optimization, 4-bromobenzyl alcohol **4a** was reacted with morpholine **2a** in the presence of 2.5 equivalent of NaI. Only 21% yield of amide product **3aa** was obtained. The is perhaps caused by loss the NaI mediator to undergo double oxidation from alcohol substrate comparing with the aldehyde substrate. To improve the yield of amide **3aa**, we therefore increased the amount of NaI from 2.5 equivalent to 5.0

equivalent. Fortunately, we were able to prepare amide **3aa** in 54% yield which will be used for further study for oxidative amidation of benzyl alcohol substrate. Various benzyl alcohols such as chloro substituent **4c**, trifluoromethyl **4f**, benzyl alcohol **4k**, methyl **4l** and methoxy (**4m** and **4n**) can be converted into corresponding amide **3ca**, **3fa** and **3ka**-**3na** in fair to good yields via electrochemical process. Notably, benzyl alcohols carrying nitro substituent such as (**4i** and **4j**) provided amide product **3ia** and **3ja** in 9% and 31% yields. We believed that the low yield from **3ia** case governs by the electronic effect generated from 4-nitro substituent which prohibits the elimination step. The full mechanism will be explained in last section.

Scheme 3.9 Electrochemical oxidative amidation between benzyl alcohols and morpholine[a, b]

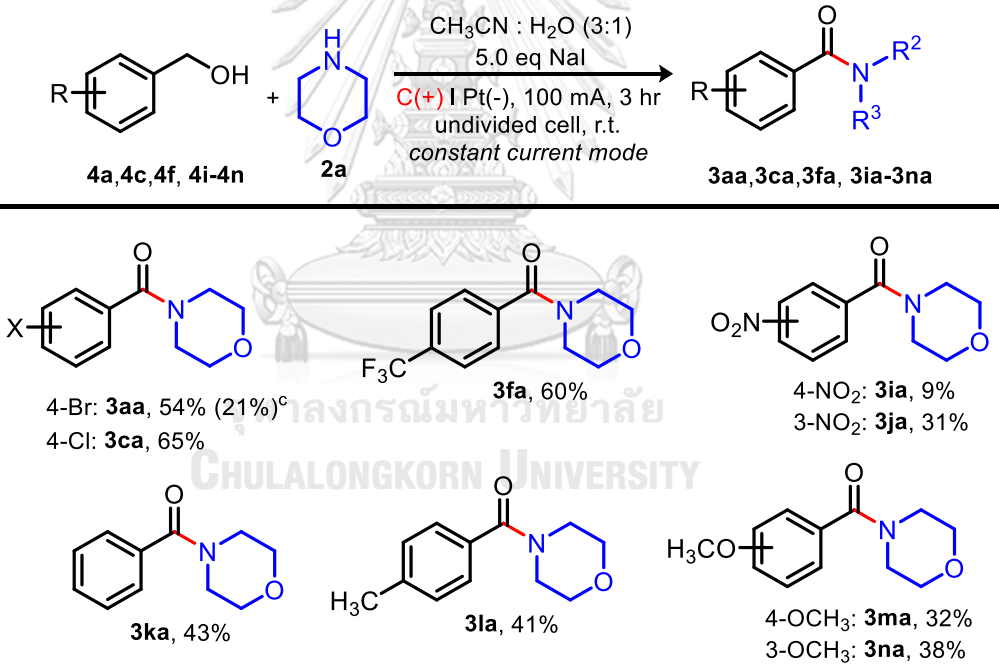

[a] Unless otherwise noted, the reaction conditions were as followed: benzyl alcohols (1.0 eq, 0.30 mmol), morpholine (5.0 eq, 1.50 mmol), NaI (5.0 eq, 1.50 mmol), CH_3CN:H_2O (3 mL:1 mL), graphite rod (Ø = 5 mm, immersed 1.0 cm) as anode, platinum plate (5x5x0.1 mm) as cathode, 100 mA for 3 hours at room temperature in an undivided cell. [b] Isolated yield. [c] 2.5 eq of NaI were used.

3.5 Gram-scale synthesis of electrochemical oxidative amidation between aldehyde and amine

With the success to perform electrochemical amidation in small-scale (ca. 30-80 mg), we would like to test our reaction in gram-scale level. Therefore, the gram-scale synthesis between 1.0 gram of 4-bromobenzaldehyde **1a** and morpholine **2a** was performed as shown in Scheme 3.10. We changed the reactor from 10 mL-test tube into 100 mL-three-necked round bottom flask. Moreover, the reaction time needed to be increased from 3 to 8 and 24 hours in order to completely consume starting material. With those condition, we were able to isolate the target product **3aa** in satisfactory yields (74% and 89%), respectively.

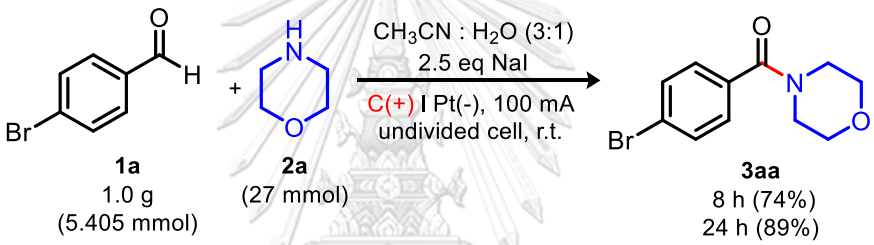

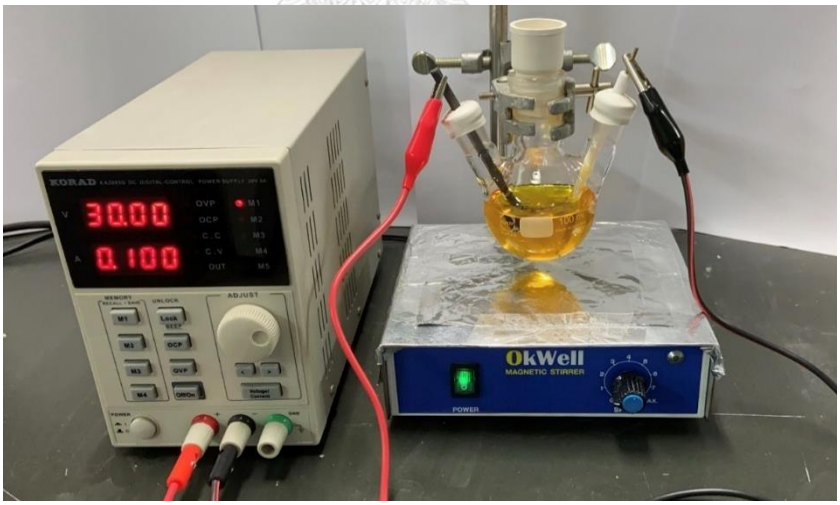

Scheme 3.10 Gram-scale synthesis setup

3.6 Mediated-electrochemical oxidative amidation using portable power charger

To simplify our electrochemical oxidative amidation, we would like to replace electrical source from power supply into power charger as shown in Scheme 3.11. This offered several benefits such as low cost, portability and safeness which would be able to adapt in academic laboratory. Therefore, we used USB type portable power charger having 10,000 mAh capacity and 5 V as electrical source to perform electrochemical oxidative amidation of **1a** and **2a** under our optimization. The amide product **3aa** was isolated in 74% yield within 3 hours.

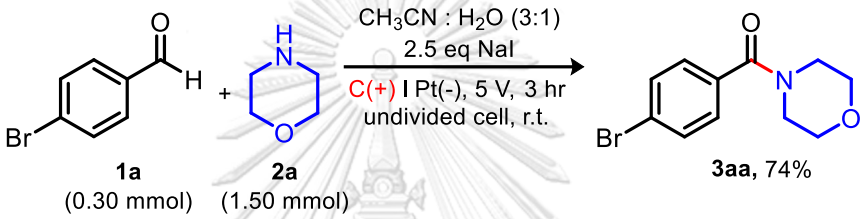

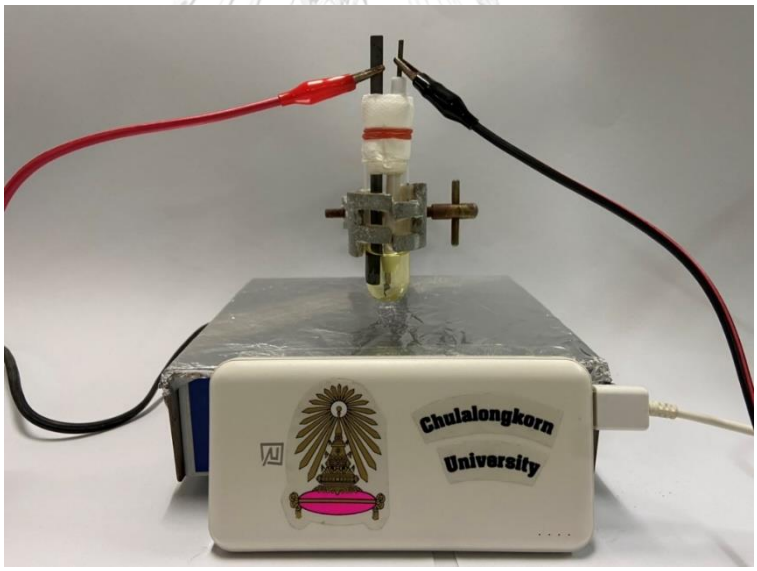

Scheme 3.11 Mediated-electrochemical oxidative amidation using portable power charger setup

3.7 Mechanistic investigations

3.7.1 Control experiments

Various control experiments were performed in this section. First, the role of electricity was investigated. 4-bromobenzyl alcohol **4a** and 4-bromobenzaldehyde **1a** were reacted with morpholine **2a** in the presence of NaI under optimized condition without electricity as depicted in Scheme 3.12. No amide product was observed in both reaction conditions (Scheme 3.12, eq. 1-2). Therefore, our oxidative amidations were mediated by electricity.

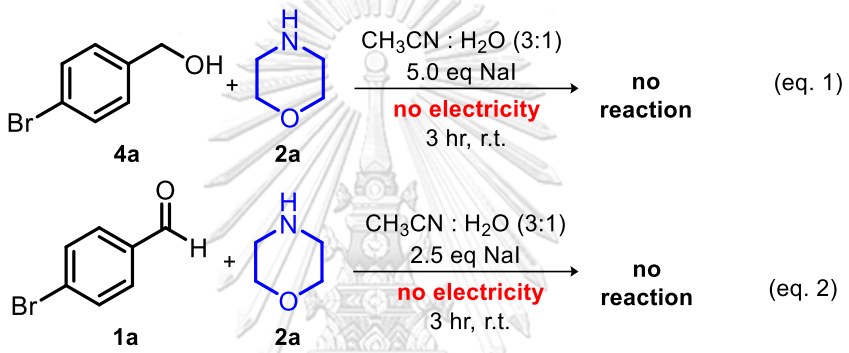

Scheme 3.12 Control experiment: part 1

We suspected that our reaction was mediated by molecular iodine which generated *in situ* from iodide via electro-oxidation. To confirm the existence of molecular iodine, the reactions of morpholine **2a** with 4-bromobenzyl alcohol **4a** (Scheme 3.13, eq. 3) or 4-bromobenzaldehyde **1a** (Scheme 3.13, eq. 4) were carried in the presence of molecular iodine without applying the electricity. We obtained a small amount of 4-bromobenzaldehyde **1a** from the oxidation of **4a** (5% yield) without amide **3aa** product. Moreover, the oxidation of **1a** with molecular iodine generated 21% yield of amide product **3aa**. Hence, these observations proved that molecular iodine may be served as an oxidizing agent in our reactions. However, the low yield of amide product **3aa** could result from high concentration of molecular iodine that could generate quaternary ammonium salt which can prohibit our process providing low yield of amide. This observation indicated that the slow generation of molecular

iodine via electro-oxidation from iodide provides more reaction efficiency than the direct use of molecular iodine in classical oxidation reaction.

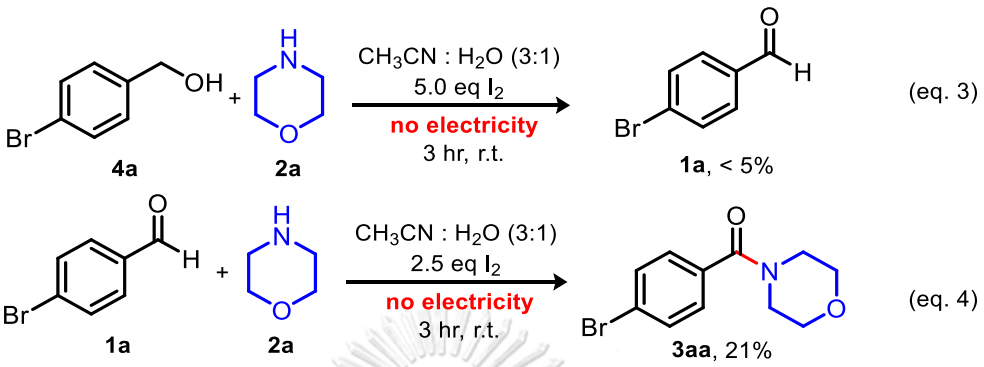

Scheme 3.13 Control experiment: part 2

It is also possible that other oxidizing agents from ioiode may involve in this reaction including hypervalent species (IO_x) such as IO_3^- and IO_4^-. We therefore performed the oxidation of 4-bromobenzaldehyde **1a** with either KIO_3 (Scheme 3.14, eq. 5) or $NaIO_4$ (Scheme 3.14, eq. 6) under no electricity. Surprisingly, there are no reaction in both cases. We hypothesized that such strong oxidizing agents could oxidizied amine **2a** before it can react with **1a** as large amount of starting material remains.

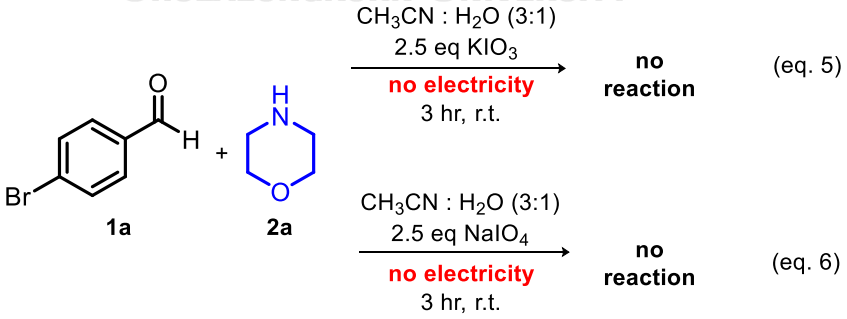

Scheme 3.14 Control experiment: part 3

As mentioned in the literature reviews, several works demonstrated the use of oxygen as source for electro-oxidation via radical process [78, 99, 100]. First, we would like to investigate the role of oxygen in our electrochemical process. We performed the electrochemical reaction of **1a** and **2a** under our optimized condition in nitrogen atmosphere (Scheme 3.15, eq. 7). The amide product **3aa** was isolated in 79% yield which is similar to the optimized condition under open air. The results indicated that the oxygen may not involve in our electrochemical oxidative amidation. To confirm that our reaction pathway is not involved a radical species, we then performed the trapping experiment. Radical scavenger, TEMPO was added into our electrochemical oxidative amidation of **1a** (Scheme 3.15, eq. 8). We were able to isolate the amide product **3aa** in 78% which is similar to our optimized condition. Therefore, this electrochemical oxidative amidation is not involved with radical pathway mechanism.

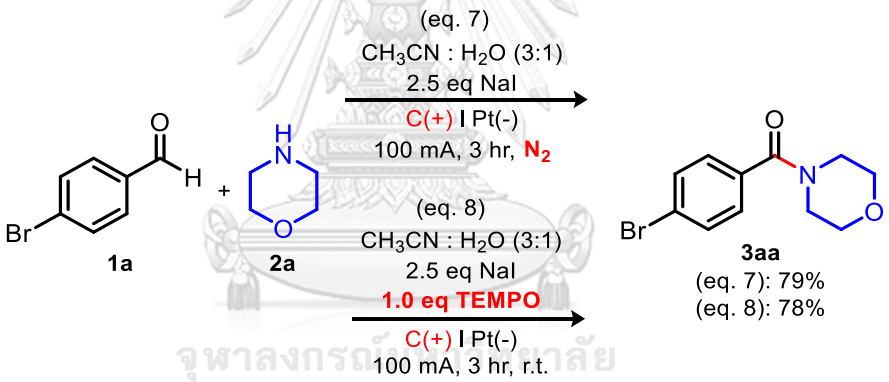

Scheme 3.15 Control experiment: part 4

3.7.2 NMR monitoring

To catch the intermediate of our electrochemical oxidative amidaiton, we performed NMR monitoring of the reaction between 4-cyanobenzaldehyde **1h** and morpholine **2a** without the electricity. The proton signals of crude product were collected as shown in Figure 3.2 using CD_3CN as solvent comparing with starting material **1h** and **2a**. For starting material, proton signals of 4-cyanobenzaldehyde **1h** appeared at 10.0 ppm from CHO group, 7.98 ppm and 7.89 ppm from CH on aromatic ring (Figure 3.2a) while morpholine **2a** shown proton signals at 3.51 ppm and 2.69 ppm

which belong to CH_2-O and CH_2-N (Figure 3.2b), respectively. On the other hand, the crude reaction from 4-cyanobenzaldehyde **1h** and morpholine **2a** after ten minutes mixing displayed new proton signal was obtained at 7.69 ppm, 7.34 ppm (CH on aromatic ring), 5.26 ppm (OH) and 3.73 ppm (benzylic proton) (Figure 3.2c). All those new proton signals correspond to hemiaminal intermediate **6ha** which was also reported in literature [97].

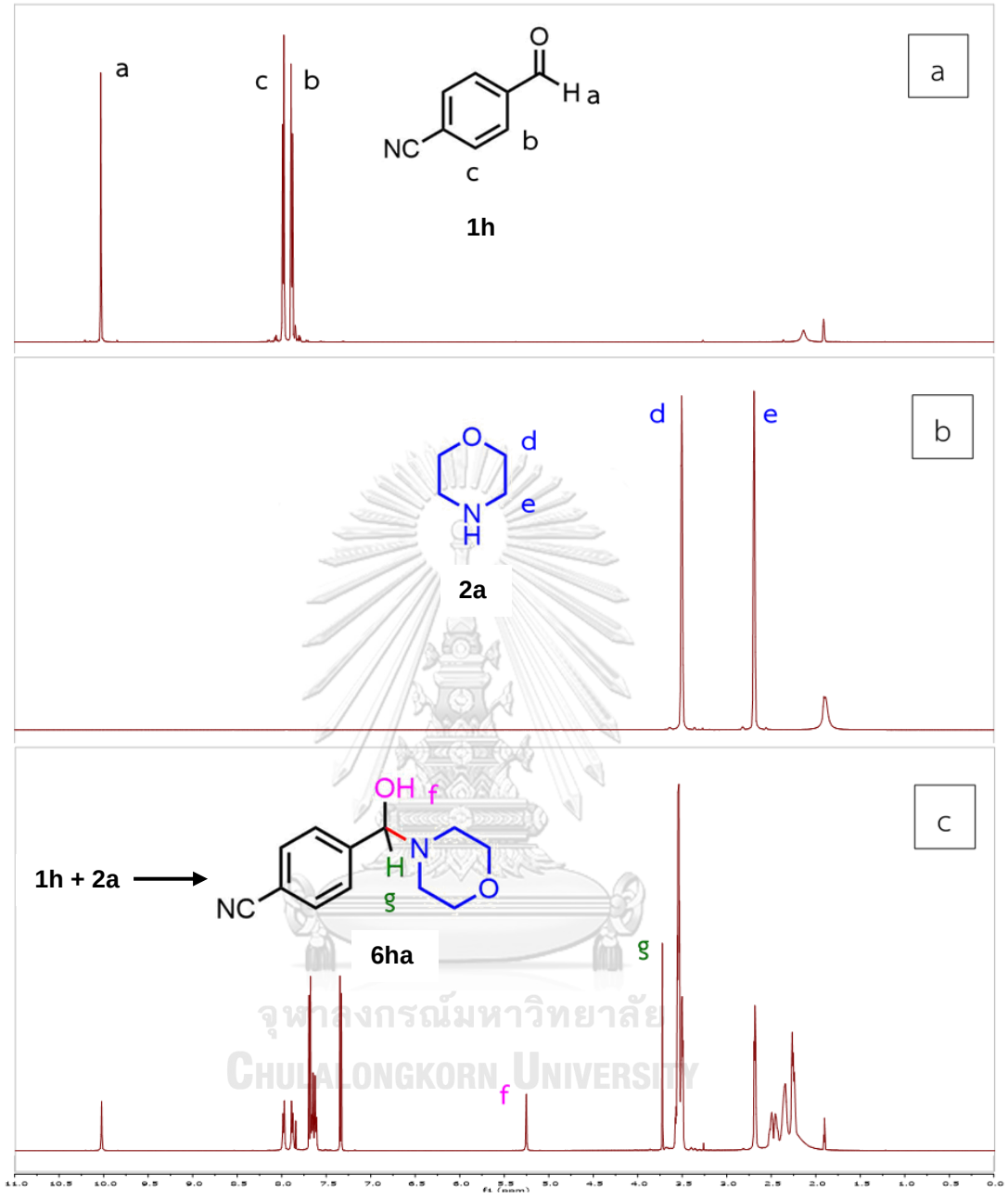

Figure 3.2 ^{1}H-NMR spectrum a) 4-cyanobenzaldehyde **1h**, b) morpholine **2a** and c) mixture between **1h** and **2a** in CD_3CN

3.7.3 Cyclic voltammetry

In order to gain more information for our electrochemical oxidative amidation, cyclic voltammetry was performed as shown in Figure 3.2. We performed each experiments in 0.1 $TBABF_4$ as electrolyte in MeCN. The background signal from 0.1 $TBABF_4$ in MeCN shown smooth signal (black curve) indicating there is no oxidation process in this experiment. Next, we performed the cyclic voltammetry measurement of 4-bromobenzaldehyde **1a** and morpholine **2a** under above condition. **1a** shown no oxidation peak (red curve) whereas morpholine **2a** shown oxidation peak at 1.34 V (blue curve). For the oxidation of NaI, two oxidation processes were observed at 0.86 V and 1.16 V (green curve). These two peaks belonged to the I^-/I_2 and I_3^-/I^-, respectively [101-103]. In addition, the mixture of 4-bromobenzaldehyde **1a**, morpholine **2a** and NaI shown a new oxidation peak at 1.14 V (pink curve) which we hypothesized that it belongs to hemiaminal intermediate. Based on NaI oxidation profile, this reactive intermediate should be able to oxidize via I_2 which generated from the oxidation of NaI. These results corresponded to the control experiment that only I_2 (Scheme 3.13, eq. 4) is able to use as oxidizing agent but no IO_3^- and IO_4^- (Scheme 3.13, eq. 5-6).

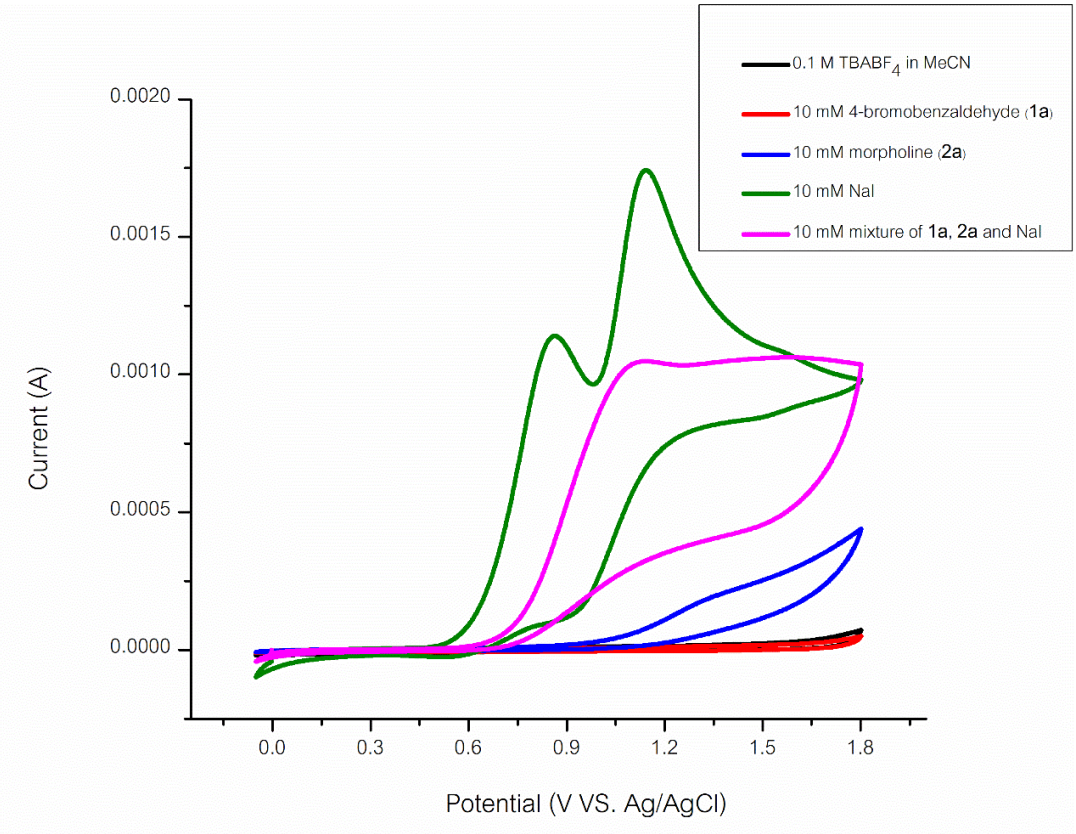

Figure 3.3 Cyclic voltammograms

3.7.4 Proposed mechanism

With all experiments we carried above, we therefore proposed the mechanism of electrochemical oxidation amidation. The reaction involves four main steps as depicted in Scheme 3.16. Initially, iodide will be oxidized to form molecular iodine as true mediator at anode. Consequently, starting material benzyl alcohol **4** was oxidized by molecular iodine to the corresponding aldehyde **1** through alkoxide-iodide intermediate **5** [104]. Next, the addition of amine nucleophile **2** into aldehyde **1** took place forming hemiaminal intermediate **6**. Finally, hemiaminal intermediate **6** was further oxidized by another molecular iodine to provide amide product **3**. In addition, the hydrogen evolution was occurred at cathode via reduction of water providing hydrogen gas byproduct along with the re-oxidation of iodide to molecular iodine at anode.

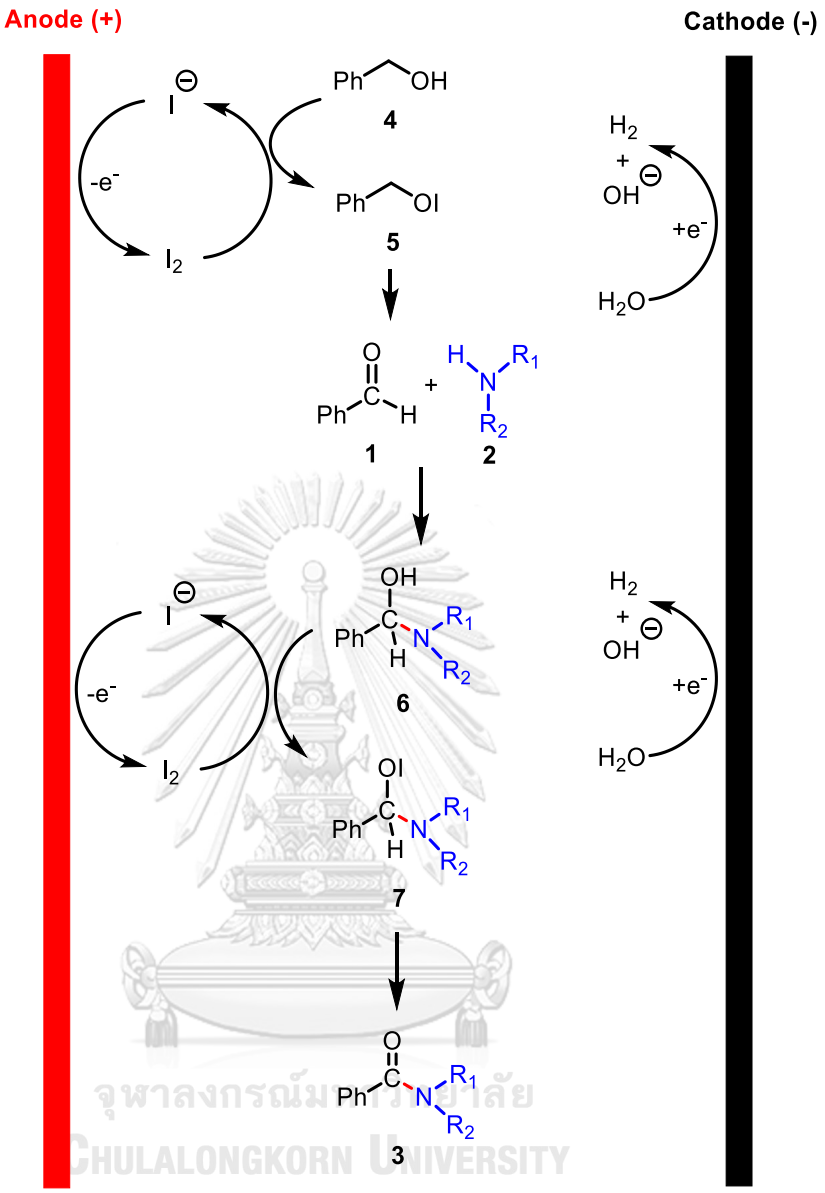

Scheme 3.16 Proposed mechanism for electrochemical oxidative amidation

CHAPTER IV

CONCLUSION

In summary, we develop a novel electrochemical oxidative amidation process from benzyl alcohol and aromatic aldehyde as starting materials providing amide products in moderate to good yields. Various benzyl alcohols/aromatic aldehydes carrying electron withdrawing groups, electron donating groups and heteroatoms are able to tolerate under our electrochemical oxidative reaction and 23 amide examples are prepared in good to excellent yields. 6 various secondary cyclic amines carrying other heteroatoms and sensitive functional group can react with aromatic aldehyde providing amide product in good yields. Gram-scale synthesis is also performed under our optimized condition for providing amide product in good yields. In addition, the replacement of expensive power supply into cheaper portable power charger is accomplished providing a convenience electrolysis setup for academic and teaching laboratory. With the evidences from control experiments, NMR monitoring and cyclic voltammetry, we propose the mechanism involves indirect electrolysis from NaI into molecular iodine to oxidize hemiaminal intermediate. Importantly, our electrochemical oxidative amidation offers many adavantages including the use of low toxic reagent in aqueous solution, easy operation in open-air at room temperature and gram scalability which can be applicable in industry or academic laboratory.

REFERENCES

1. Chirumamilla, R. R.; Marchant, R.; Nigam, P., Captopril and its synthesis from chiral intermediates. *Journal of Chemical Technology & Biotechnology* **2001**, *76* (2), 123-127.

2. Hong Woo, L. E. E.; Young Min, K. I. M.; Choong Leol, Y. O. O.; Sung Kwon, K.; and Soon Kil, A. H. N., An Efficient Method for the Large-Scale Synthesis of Atorvastatin Calcium. *Biomolecules & Therapeutics* **2008,** *16* (1), 28-33.

3. Ananthanarayanan, V. S.; Tetreault, S.; Saint-Jean, A., Interaction of calcium channel antagonists with calcium: spectroscopic and modeling studies on diltiazem and its Ca2+ complex. *Journal of Medicinal Chemistry* **1993,** *36* (10), 1324-1332.

4. Bennett, C.; Mathias, L. J., Synthesis and characterization of polyamides containing octadecanedioic acid: Nylon-2,18, nylon-3,18, nylon-4,18, nylon-6,18, nylon-8,18, nylon-9,18, and nylon-12,18. *Journal of Polymer Science Part A: Polymer Chemistry* **2005,** *43* (5), 936-945.

5. Wang, X. J.; Yang, Q.; Liu, F.; You, Q. D., Microwave-Assisted Synthesis of Amide under Solvent-free Conditions. *Synthetic Communications* **2008,** *38* (7), 1028-1035.

6. Gooßen, L. J.; Ohlmann, D. M.; Lange, P. P., The Thermal Amidation of Carboxylic Acids Revisited. *Synthesis* **2009,** *2009* (01), 160-164.

7. Ojeda-Porras, A.; Hernández-Santana, A.; Gamba-Sánchez, D., Direct amidation of carboxylic acids with amines under microwave irradiation using silica gel as a solid support. *Green Chemistry* **2015,** *17* (5), 3157-3163.

8. El-Faham, A.; Albericio, F., Peptide Coupling Reagents, More than a Letter Soup. *Chemical Reviews* **2011,** *111* (11), 6557-6602.

9. Dunetz, J. R.; Magano, J.; Weisenburger, G. A., Large-Scale Applications of Amide Coupling Reagents for the Synthesis of Pharmaceuticals. *Organic Process Research & Development* **2016,** *20* (2), 140-177.

10. Han, S.-Y.; Kim, Y.-A., Recent development of peptide coupling reagents in organic synthesis. *Tetrahedron* **2004,** *60* (11), 2447-2467.

11. Valeur, E.; Bradley, M., Amide bond formation: beyond the myth of coupling reagents. *Chemical Society Reviews* **2009,** *38* (2), 606-631.

12. de Figueiredo, R. M.; Suppo, J.-S.; Campagne, J.-M., Nonclassical Routes for Amide Bond Formation. *Chemical Reviews* **2016,** *116* (19), 12029-12122.

13. Mohy El Dine, T.; Erb, W.; Berhault, Y.; Rouden, J.; Blanchet, J., Catalytic Chemical Amide Synthesis at Room Temperature: One More Step Toward Peptide Synthesis. *The Journal of Organic Chemistry* **2015,** *80* (9), 4532-4544.

14. Hoang, L. T. M.; Ngo, L. H.; Nguyen, H. L.; Nguyen, H. T. H.; Nguyen, C. K.; Nguyen, B. T.; Ton, Q. T.; Nguyen, H. K. D.; Cordova, K. E.; Truong, T., An azobenzene-containing metal–organic framework as an efficient heterogeneous catalyst for direct amidation of benzoic acids: synthesis of bioactive compounds. *Chemical Communications* **2015,** *51* (96), 17132-17135.

15. Bode, J. W.; Fox, R. M.; Baucom, K. D., Chemoselective Amide Ligations by Decarboxylative Condensations of N-Alkylhydroxylamines and α-Ketoacids. *Angewandte Chemie International Edition* **2006,** *45* (8), 1248-1252.

16. Dumas, A. M.; Molander, G. A.; Bode, J. W., Amide-Forming Ligation of Acyltrifluoroborates and Hydroxylamines in Water. *Angewandte Chemie International Edition* **2012,** *51* (23), 5683-5686.

17. Schuemacher, A. C.; Hoffmann, R. W., Condensation Between Isocyanates and Carboxylic Acids in the Presence of 4-Dimethylaminopyridine (DMAP), a Mild and Efficient Synthesis of Amides. *Synthesis* **2001,** *2001* (02), 0243-0246.

18. Wu, X.; Li, X.; Danishefsky, S. J., Thio-mediated two-component coupling reaction of carboxylic acids and isonitriles under mild conditions. *Tetrahedron Letters* **2009,** *50* (14), 1523-1525.

19. Pourvali, A.; Cochrane, J. R.; Hutton, C. A., A new method for peptide synthesis in the N⟶C direction: amide assembly through silver-promoted reaction of thioamides. *Chemical Communications* **2014,** *50* (100), 15963-15966.

20. Bai, J.; Zambroń, B. K.; Vogel, P., Amides in One Pot from Carboxylic Acids and Amines via Sulfinylamides. *Organic Letters* **2014,** *16* (2), 604-607.

21. Burés, J.; Martín, M.; Urpí, F.; Vilarrasa, J., Catalytic Staudinger—Vilarrasa Reaction for the Direct Ligation of Carboxylic Acids and Azides. *The Journal of Organic Chemistry* **2009,** *74* (5), 2203-2206.

22. Xiong, B.; Zhu, L.; Feng, X.; Lei, J.; Chen, T.; Zhou, Y.; Han, L.-B.; Au, C.-T.; Yin, S.-F., Direct Amidation of Carboxylic Acids with Tertiary Amines: Amide Formation over Copper Catalysts through C–N Bond Cleavage. *European Journal of Organic Chemistry* **2014,** *2014* (20), 4244-4247.

23. Seo, H.-A.; Cho, Y.-H.; Lee, Y.-S.; Cheon, C.-H., Formation of Amides from Imines via Cyanide-Mediated Metal-Free Aerobic Oxidation. *The Journal of Organic Chemistry* **2015,** *80* (24), 11993-11998.

24. Liu, S.; Wang, H.; Dai, X.; Shi, F., Organic ligand-free carbonylation reactions with unsupported bulk Pd as catalyst. *Green Chemistry* **2018,** *20* (15), 3457-3462.

25. Driller, K. M.; Prateeptongkum, S.; Jackstell, R.; Beller, M., A General and Selective Iron-Catalyzed Aminocarbonylation of Alkynes: Synthesis of Acryl- and Cinnamides. *Angewandte Chemie International Edition* **2011,** *50* (2), 537-541.

26. Nanayakkara, P.; Alper, H., Asymmetric synthesis of **α**-aminoamides by Pd-catalyzed double carbohydroamination. *Chemical Communications* **2003,** (18), 2384-2385.

27. Han, C.; Lee, J. P.; Lobkovsky, E.; Porco, J. A., Catalytic Ester–Amide Exchange Using Group (IV) Metal Alkoxide–Activator Complexes. *Journal of the American Chemical Society* **2005,** *127* (28), 10039-10044.

28. Eldred, S. E.; Stone, D. A.; Gellman, S. H.; Stahl, S. S., Catalytic Transamidation under Moderate Conditions. *Journal of the American Chemical Society* **2003,** *125* (12), 3422-3423.

29. Mali, S. M.; Bhaisare, R. D.; Gopi, H. N., Thioacids Mediated Selective and Mild N-Acylation of Amines. *The Journal of Organic Chemistry* **2013,** *78* (11), 5550-5555.

30. Zhu, C.; Wei, W.; Du, P.; Wan, X., Metal free amide synthesis via carbon–carbon bond cleavage. *Tetrahedron* **2014,** *70* (51), 9615-9620.

31. Li, X.; Li, Z.; Deng, H.; Zhou, X., An efficient protocol for the preparation of amides by copper-catalyzed reactions between nitriles and amines in water. *Tetrahedron Letters* **2013,** *54* (18), 2212-2216.

32. Park, S.; Choi, Y.-a.; Han, H.; Ha Yang, S.; Chang, S., Rh-Catalyzed one-pot and practical transformation of aldoximes to amides. *Chemical Communications* **2003,** (15), 1936-1937.

33. Shimizu, K.-i.; Ohshima, K.; Satsuma, A., Direct Dehydrogenative Amide Synthesis from Alcohols and Amines Catalyzed by **γ**-Alumina Supported Silver Cluster. *Chemistry – A European Journal* **2009,** *15* (39), 9977-9980.

34. Soulé, J.-F.; Miyamura, H.; Kobayashi, S., Direct Amidation from Alcohols and Amines through a Tandem Oxidation Process Catalyzed by Heterogeneous-Polymer-Incarcerated Gold Nanoparticles under Aerobic Conditions. *Chemistry – An Asian Journal* **2013,** *8* (11), 2614-2626.

35. Watson, A. J. A.; Wakeham, R. J.; Maxwell, A. C.; Williams, J. M. J., Ruthenium-catalysed oxidation of alcohols to amides using a hydrogen acceptor. *Tetrahedron* **2014,** *70* (23), 3683-3690.

36. Rostamnia, S.; Doustkhah, E.; Golchin-Hosseini, H.; Zeynizadeh, B.; Xin, H.; Luque, R., Efficient tandem aqueous room temperature oxidative amidations catalysed by supported Pd nanoparticles on graphene oxide. *Catalysis Science & Technology* **2016,** *6* (12), 4124-4133.

37. Arefi, M.; Saberi, D.; Karimi, M.; Heydari, A., Superparamagnetic Fe(OH)3@Fe3O4 Nanoparticles: An Efficient and Recoverable Catalyst for Tandem Oxidative Amidation of Alcohols with Amine Hydrochloride Salts. *ACS Combinatorial Science* **2015,** *17* (6), 341-347.

38. Darvishi, A.; Kazemi Miraki, M.; Arefi, M.; Heydari, A., Oxidative amidation by Cu(ii)–guanidine acetic acid immobilized on magnetized sawdust with eggshell as a natural base. *New Journal of Chemistry* **2020,** *44* (27), 11777-11785.

39. Nakagawa, K.; Onoue, H.; Minami, K., Oxidation with nickel peroxide. A new synthesis of amides from aldehydes or alcohols. *Chemical Communications (London)* **1966,** (1), 17-18.

40. Gilman, N. W., The preparation of carboxylic amides from aldehydes by oxidation. *Journal of the Chemical Society D: Chemical Communications* **1971,** (14), 733-734.

41. Tillack, A.; Rudloff, I.; Beller, M., Catalytic Amination of Aldehydes to Amides. *European Journal of Organic Chemistry* **2001,** *2001* (3), 523-528.

42. Li, G.-L.; Kung, K. K.-Y.; Wong, M.-K., Gold-catalyzed amide synthesis from aldehydes and amines in aqueous medium. *Chemical Communications* **2012,** *48* (34), 4112-4114.

43. Singh, A.; Azad, C. S.; Narula, A. K., Oxidative Amidation of Aldehydes with Amines Catalysed by Fe(II) – Hydride Complex and N- Heterocyclic Carbenes (NHC). *ChemistrySelect* **2020,** *5* (30), 9417-9423.

44. Ghosh, S. C.; Ngiam, J. S. Y.; Seayad, A. M.; Tuan, D. T.; Chai, C. L. L.; Chen, A., Copper-Catalyzed Oxidative Amidation of Aldehydes with Amine Salts: Synthesis of Primary, Secondary, and Tertiary Amides. *The Journal of Organic Chemistry* **2012,** *77* (18), 8007-8015.

45. Sutar, Y. B.; Bhagat, S. B.; Telvekar, V. N., General and efficient oxidative amidation of benzyl alcohols with amines using diacetoxyiodobenzene and TBHP. *Tetrahedron Letters* **2015,** *56* (48), 6768-6771.

46. Karimi, M.; Saberi, D.; Azizi, K.; Arefi, M.; Heydari, A., Transition-metal-free oxidative amidation of benzyl alcohols with amines catalyzed by NaI: a new method for the synthesis of benzamides. *Tetrahedron Letters* **2014,** *55* (39), 5351-5353.

47. Ekoue-Kovi, K.; Wolf, C., Metal-Free One-Pot Oxidative Amination of Aldehydes to Amides. *Organic Letters* **2007,** *9* (17), 3429-3432.

48. Liang, J.; Lv, J.; Shang, Z.-c., Metal-free synthesis of amides by oxidative amidation of aldehydes with amines in PEG/oxidant system. *Tetrahedron* **2011,** *67* (44), 8532-8535.

49. Shie, J.-J.; Fang, J.-M., Direct Conversion of Aldehydes to Amides, Tetrazoles, and Triazines in Aqueous Media by One-Pot Tandem Reactions. *The Journal of Organic Chemistry* **2003,** *68* (3), 1158-1160.

50. Reddy, K. R.; Maheswari, C. U.; Venkateshwar, M.; Kantam, M. L., Oxidative Amidation of Aldehydes and Alcohols with Primary Amines Catalyzed by KI-TBHP. *European Journal of Organic Chemistry* **2008,** *2008* (21), 3619-3622.

51. Deshidi, R.; Rizvi, M. A.; Shah, B. A., Highly efficient dehydrogenative cross-coupling of aldehydes with amines and alcohols. *RSC Advances* **2015,** *5* (110), 90521-90524.

52. Kumar, V.; Connon, S. J., Direct, efficient NHC-catalysed aldehyde oxidative amidation: in situ formed benzils as unconventional acylating agents. *Chemical Communications* **2017,** *53* (73), 10212-10215.

53. Tankam, T.; Poochampa, K.; Vilaivan, T.; Sukwattanasinitt, M.; Wacharasindhu, S., Organocatalytic visible light induced S–S bond formation for oxidative coupling of thiols to disulfides. *Tetrahedron* **2016,** *72* (6), 788-793.

54. Rattanangkool, E.; Sukwattanasinitt, M.; Wacharasindhu, S., Organocatalytic Visible Light Enabled SNAr of Heterocyclic Thiols: A Metal-Free Approach to 2-Aminobenzoxazoles and 4-Aminoquinazolines. *The Journal of Organic Chemistry* **2017,** *82* (24), 13256-13262.

55. Saetan, T.; Sukwattanasinitt, M.; Wacharasindhu, S., A Mild Photocatalytic Synthesis of Guanidine from Thiourea under Visible Light. *Organic Letters* **2020,** *22* (20), 7864-7869.

56. Leow, D., Phenazinium Salt-Catalyzed Aerobic Oxidative Amidation of Aromatic Aldehydes. *Organic Letters* **2014,** *16* (21), 5812-5815.

57. Wang, X.-F.; Yu, S.-S.; Wang, C.; Xue, D.; Xiao, J., BODIPY catalyzed amide synthesis promoted by BHT and air under visible light. *Organic & Biomolecular Chemistry* **2016,** *14* (29), 7028-7037.

58. Deng, J.-R.; Chan, W.-C.; Chun-Him Lai, N.; Yang, B.; Tsang, C.-S.; Chi-Bun Ko, B.; Lai-Fung Chan, S.; Wong, M.-K., Photosensitizer-free visible light-mediated gold-catalysed cis-difunctionalization of silyl-substituted alkynes. *Chemical Science* **2017,** *8* (11), 7537-7544.

59. Deol, H.; Kumar, M.; Bhalla, V., Exploring organic photosensitizers based on hemicyanine derivatives: a sustainable approach for preparation of amide linkages. *RSC Advances* **2018,** *8* (54), 31237-31245.

60. Pandey, G.; Koley, S.; Talukdar, R.; Sahani, P. K., Cross-Dehydrogenating Coupling of Aldehydes with Amines/R-OTBS Ethers by Visible-Light Photoredox Catalysis: Synthesis of Amides, Esters, and Ureas. *Organic Letters* **2018,** *20* (18), 5861-5865.

61. Kärkäs, M. D., Electrochemical strategies for C–H functionalization and C–N bond formation. *Chemical Society Reviews* **2018,** *47* (15), 5786-5865.

62. Wiebe, A.; Gieshoff, T.; Möhle, S.; Rodrigo, E.; Zirbes, M.; Waldvogel, S. R., Electrifying Organic Synthesis. *Angewandte Chemie International Edition* **2018,** *57* (20), 5594-5619.

63. Hilt, G., Basic Strategies and Types of Applications in Organic Electrochemistry. *ChemElectroChem* **2020,** *7* (2), 395-405.

64. Kingston, C.; Palkowitz, M. D.; Takahira, Y.; Vantourout, J. C.; Peters, B. K.; Kawamata, Y.; Baran, P. S., A Survival Guide for the "Electro-curious". *Accounts of Chemical Research* **2020,** *53* (1), 72-83.

65. Verschueren, R. H.; De Borggraeve, W. M., Electrochemistry and Photoredox Catalysis: A Comparative Evaluation in Organic Synthesis. *Molecules* **2019,** *24* (11).

66. Wang, D.; Wang, P.; Wang, S.; Chen, Y.-H.; Zhang, H.; Lei, A., Direct electrochemical oxidation of alcohols with hydrogen evolution in continuous-flow reactor. *Nature Communications* **2019,** *10* (1), 2796.

67. Yan, M.; Kawamata, Y.; Baran, P. S., Synthetic Organic Electrochemical Methods Since 2000: On the Verge of a Renaissance. *Chemical Reviews* **2017,** *117* (21), 13230-13319.

68. Liu, K.; Song, C.; Lei, A., Recent advances in iodine mediated electrochemical oxidative cross-coupling. *Organic & Biomolecular Chemistry* **2018,** *16* (14), 2375-2387.

69. Li, W.-C.; Zeng, C.-C.; Hu, L.-M.; Tian, H.-Y.; Little, R. D., Efficient Indirect Electrochemical Synthesis of 2-Substituted Benzoxazoles using Sodium Iodide as Mediator. *Advanced Synthesis & Catalysis* **2013,** *355* (14-15), 2884-2890.

70. Wang, Z.-Q.; Meng, X.-J.; Li, Q.-Y.; Tang, H.-T.; Wang, H.-S.; Pan, Y.-M., Electrochemical Synthesis of 3,5-Disubstituted-1,2,4-thiadiazoles through NH4I-Mediated Dimerization of Thioamides. *Advanced Synthesis & Catalysis* **2018,** *360* (21), 4043-4048.

71. Yang, Z.; Zhang, J.; Hu, L.; Li, L.; Liu, K.; Yang, T.; Zhou, C., Electrochemical Oxidative Intramolecular N–S Bond Formation: Synthesis of 3-Substituted 5-Amino-1,2,4-Thiadiazoles. *The Journal of Organic Chemistry* **2020,** *85* (5), 3358-3363.

72. Wang, F.; Gerken, J. B.; Bates, D. M.; Kim, Y. J.; Stahl, S. S., Electrochemical Strategy for Hydrazine Synthesis: Development and Overpotential Analysis of Methods

for Oxidative N–N Coupling of an Ammonia Surrogate. *Journal of the American Chemical Society* **2020,** *142* (28), 12349-12356.

73. Wu, Y.; Ding, H.; Zhao, M.; Ni, Z.-H.; Cao, J.-P., Electrochemical and direct C–H methylthiolation of electron-rich aromatics. *Green Chemistry* **2020,** *22* (15), 4906-4911.

74. Sun, X.-J.; Yang, S.-F.; Wang, Z.-T.; Liang, S.; Tian, H.-Y.; Yang, S.-X.; Liu, Y.-G.; Sun, B.-G.; Zeng, C.-C., Electrochemically Oxidative Coupling of S-H/S-H for S-S Bond Formation: A Facile Approach to Diacid-disulfides. *ChemistrySelect* **2020,** *5* (15), 4637-4641.

75. Tang, L.; Matuska, J. H.; Huang, Y.-H.; He, Y.-H.; Guan, Z., Amide Synthesis from Thiocarboxylic Acids and Amines by Spontaneous Reaction and Electrosynthesis. *ChemSusChem* **2019,** *12* (12), 2570-2575.

76. Dissanayake, D. M. M. M.; Melville, A. D.; Vannucci, A. K., Electrochemical anion pool synthesis of amides with concurrent benzyl ester synthesis. *Green Chemistry* **2019,** *21* (11), 3165-3171.

77. Chen, J.-Y.; Wu, H.-Y.; Gui, Q.-W.; Han, X.-R.; Wu, Y.; Du, K.; Cao, Z.; Lin, Y.-W.; He, W.-M., Electrochemical Synthesis of α-Ketoamides under Catalyst-, Oxidant-, and Electrolyte-Free Conditions. *Organic Letters* **2020,** *22* (6), 2206-2209.

78. Zhang, Z.; Su, J.; Zha, Z.; Wang, Z., A novel approach for the one-pot preparation of α-ketoamides by anodic oxidation. *Chemical Communications* **2013,** *49* (79), 8982-8984.

79. Chen, J.; Yan, W.-Q.; Lam, C. M.; Zeng, C.-C.; Hu, L.-M.; Little, R. D., Electrocatalytic Aziridination of Alkenes Mediated by n-Bu4NI: A Radical Pathway. *Organic Letters* **2015,** *17* (4), 986-989.

80. Gao, W.-J.; Li, W.-C.; Zeng, C.-C.; Tian, H.-Y.; Hu, L.-M.; Little, R. D., Electrochemically Initiated Oxidative Amination of Benzoxazoles Using Tetraalkylammonium Halides As Redox Catalysts. *The Journal of Organic Chemistry* **2014,** *79* (20), 9613-9618.

81. Liang, S.; Zeng, C.-C.; Luo, X.-G.; Ren, F.-z.; Tian, H.-Y.; Sun, B.-G.; Little, R. D., Electrochemically catalyzed amino-oxygenation of styrenes: n-Bu4NI induced C–N

followed by a C–O bond formation cascade for the synthesis of indolines. *Green Chemistry* **2016,** *18* (7), 2222-2230.

82. Liang, S.; Zeng, C.-C.; Tian, H.-Y.; Sun, B.-G.; Luo, X.-G.; Ren, F.-z., Electrochemically Oxidative α-C–H Functionalization of Ketones: A Cascade Synthesis of α-Amino Ketones Mediated by NH4I. *The Journal of Organic Chemistry* **2016,** *81* (23), 11565-11573.

83. Kurosawa, W.; Kan, T.; Fukuyama, T., Stereocontrolled Total Synthesis of (–)-Ephedradine A (Orantine). *Journal of the American Chemical Society* **2003,** *125* (27), 8112-8113.

84. Shankaraiah, G.; Sateesh Chandra Kumar, R.; Poornima, B.; Babu, K. S., Stereoselective synthesis of (+)-radicamine B. *Tetrahedron Letters* **2011,** *52* (38), 4885-4887.

85. Jacquemet, A.; Rihn, S.; Ulrich, G.; Renard, P.-Y.; Romieu, A.; Ziessel, R., Rational Design of Latent Fluorophores from Water-Soluble Hydroxyphenyltriazine Dyes Suitable for Lipase Sensing. *European Journal of Organic Chemistry* **2015,** *2015* (8), 1664-1669.

86. Gu, J.; Fang, Z.; Liu, C.; Li, X.; Wei, P.; Guo, K., Direct oxidative amination of aromatic aldehydes with amines in a continuous flow system using a metal-free catalyst. *RSC Advances* **2016,** *6* (76), 72121-72126.

87. Goel, B.; Vyas, V.; Tripathi, N.; Kumar Singh, A.; Menezes, P. W.; Indra, A.; Jain, S. K., Amidation of Aldehydes with Amines under Mild Conditions Using Metal-Organic Framework Derived NiO@Ni Mott-Schottky Catalyst. *ChemCatChem* **2020,** *12* (22), 5743-5749.

88. Zhu, J.; Zhang, Y.; Shi, F.; Deng, Y., Dehydrogenative amide synthesis from alcohol and amine catalyzed by hydrotalcite-supported gold nanoparticles. *Tetrahedron Letters* **2012,** *53* (25), 3178-3180.

89. Kainz, Q. M.; Linhardt, R.; Maity, P. K.; Hanson, P. R.; Reiser, O., Ring-Opening Metathesis Polymerization-based Recyclable Magnetic Acylation Reagents. *ChemSusChem* **2013,** *6* (4), 721-729.

90. Liu, X.; Jensen, K. F., Direct oxidative amidation of aromatic aldehydes using aqueous hydrogen peroxide in continuous flow microreactor systems. *Green Chemistry* **2012,** *14* (5), 1471-1474.

91. Papp, M.; Szabó, P.; Srankó, D.; Skoda-Földes, R., Solvent-free aminocarbonylation of iodobenzene in the presence of SILP-palladium catalysts. *RSC Advances* **2016,** *6* (51), 45349-45356.

92. Hua, X.; Masson-Makdissi, J.; Sullivan, R. J.; Newman, S. G., Inherent vs Apparent Chemoselectivity in the Kumada–Corriu Cross-Coupling Reaction. *Organic Letters* **2016,** *18* (20), 5312-5315.

93. Ben Halima, T.; Masson-Makdissi, J.; Newman, S. G., Nickel-Catalyzed Amide Bond Formation from Methyl Esters. *Angewandte Chemie International Edition* **2018,** *57* (39), 12925-12929.

94. Krabbe, S. W.; Chan, V. S.; Franczyk, T. S.; Shekhar, S.; Napolitano, J. G.; Presto, C. A.; Simanis, J. A., Copper-Catalyzed Aerobic Oxidative Amidation of Benzyl Alcohols. *The Journal of Organic Chemistry* **2016,** *81* (22), 10688-10697.

95. Albert-Soriano, M.; Pastor, I. M., Metal–Organic Framework Based on Copper and Carboxylate-Imidazole as Robust and Effective Catalyst in the Oxidative Amidation of Carboxylic Acids and Formamides. *European Journal of Organic Chemistry* **2016,** *2016* (30), 5180-5188.

96. Li, W.; Wu, X.-F., N2 Extrusion and CO Insertion: A Novel Palladium-Catalyzed Carbonylative Transformation of Aryltriazenes. *Organic Letters* **2015,** *17* (8), 1910-1913.

97. Kurose, Y.; Imada, Y.; Okada, Y.; Chiba, K., Electrochemical Amide Bond Formation from Benzaldehydes and Amines: Oxidation by Cathodic-Generated Hydrogen Peroxide. *European Journal of Organic Chemistry* **2020,** *2020* (25), 3844-3846.

98. Palanki, M. S. S.; Akiyama, H.; Campochiaro, P.; Cao, J.; Chow, C. P.; Dellamary, L.; Doukas, J.; Fine, R.; Gritzen, C.; Hood, J. D.; Hu, S.; Kachi, S.; Kang, X.; Klebansky, B.; Kousba, A.; Lohse, D.; Mak, C. C.; Martin, M.; McPherson, A.; Pathak, V. P.; Renick, J.; Soll, R.; Umeda, N.; Yee, S.; Yokoi, K.; Zeng, B.; Zhu, H.; Noronha, G., Development of Prodrug 4-Chloro-3-(5-methyl-3-{[4-(2-pyrrolidin-1-ylethoxy)phenyl]amino}-1,2,4-benzotriazin-7-yl)phenyl Benzoate (TG100801): A Topically Administered Therapeutic

Candidate in Clinical Trials for the Treatment of Age-Related Macular Degeneration. *Journal of Medicinal Chemistry* **2008,** *51* (6), 1546-1559.

99. Qian, P.; Su, J.-H.; Wang, Y.; Bi, M.; Zha, Z.; Wang, Z., Electrocatalytic C–H/N–H Coupling of *2′*-Aminoacetophenones for the Synthesis of Isatins. *The Journal of Organic Chemistry* **2017,** *82* (12), 6434-6440.

100. Zhang, Z.; Su, J.; Zha, Z.; Wang, Z., Electrochemical Synthesis of the Aryl **α**-Ketoesters from Acetophenones Mediated by KI. *Chemistry – A European Journal* **2013,** *19* (52), 17711-17714.

101. Bentley, C. L.; Bond, A. M.; Hollenkamp, A. F.; Mahon, P. J.; Zhang, J., Voltammetric Determination of the Iodide/Iodine Formal Potential and Triiodide Stability Constant in Conventional and Ionic Liquid Media. *The Journal of Physical Chemistry C* **2015,** *119* (39), 22392-22403.

102. Roth, H. G.; Romero, N. A.; Nicewicz, D. A., Experimental and Calculated Electrochemical Potentials of Common Organic Molecules for Applications to Single-Electron Redox Chemistry. *Synlett* **2016,** *27* (05), 714-723.

103. Elgrishi, N.; Rountree, K. J.; McCarthy, B. D.; Rountree, E. S.; Eisenhart, T. T.; Dempsey, J. L., A Practical Beginner's Guide to Cyclic Voltammetry. *Journal of Chemical Education* **2018,** *95* (2), 197-206.

104. Gogoi, P.; Konwar, D., Transition-metal- and organic-solvent-free: a highly efficient anaerobic process for selective oxidation of alcohols to aldehydes and ketones in water. *Organic & Biomolecular Chemistry* **2005,** *3* (19), 3473-3475.

APPENDIX

Calculation of current density in electrochemical oxidative amidation

Herein, we calculated current density from anodic electrode (cylindrical graphite rod) because electrochemical oxidative amidation took place at such electrode.

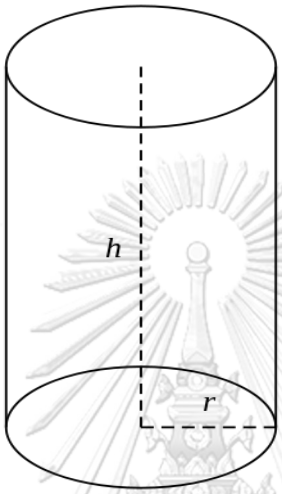

h = 10.0 cm

r = 0.25 cm

$$current\ density = \frac{current\ (mA)}{electrode\ surface\ area\ (cm^2)}$$

$$= \frac{current\ (mA)}{2\pi rh + 2\pi r^2\ (cm^2)}$$

$$= \frac{100\ mA}{2\pi(0.25)(10.0) + 2\pi(0.25)^2\ cm^2}$$

$$= \frac{100\ mA}{15.9\ cm^2}$$

$$= 6.3\ mA/cm^2$$

Calculation of mole of used electron in electrochemical oxidative amidation

Herein, we calculated mole of used electron in electrochemical oxidative amidation from our optimization in Table 3.6, entry 3.

$$mole\ of\ electron = \frac{charge\ (C)}{F\ \left(\frac{c}{mol\ e^-}\right) x\ mole\ of\ limiting\ agent}$$

$$= \frac{i\ x\ t\ (C)}{F\ \left(\frac{c}{mole\ e^-}\right) x\ mole\ of\ limiting\ agent}$$

$$= \frac{100\ x\ 10^{-3} x\ 3\ x\ 3600\ (C)}{96485\ \left(\frac{c}{mol\ e^-}\right) x\ 0.3\ x\ 10^{-3}\ mole\ of\ limiting\ agent}$$

$$= \frac{1080\ mole\ of\ electron}{28.95\ mole\ of\ limiting\ agent}$$

$$= 37.3\ mole\ of\ electron$$

Calculation of Faradaic efficiency in electrochemical oxidative amidation

Herein, we calculated Faradaic efficiency in electrochemical oxidative amidation from our optimization in Table 3.6, entry 3.

$$Faradaic\ efficiency = \frac{Q_{experimental}}{Q_{theoretical}} x\ 100$$

$$Faradaic\ efficiency = \frac{z\ x\ n\ x\ F}{i\ x\ t} x\ 100$$

where Z = number of electron that reaction used

n = mole of product that obtained (mol)

F = Faraday's constant (96485 C/mol e^-)

i = electrical current intensity (A)

t = reaction time (s)

$$Faradaic\ efficiency = \frac{2\ x\ 0.234\ x\ 10^{-3}\ x\ 96485}{0.1\ x\ 3\ x\ 3600} x\ 100$$

$$= 4.2\ \%$$

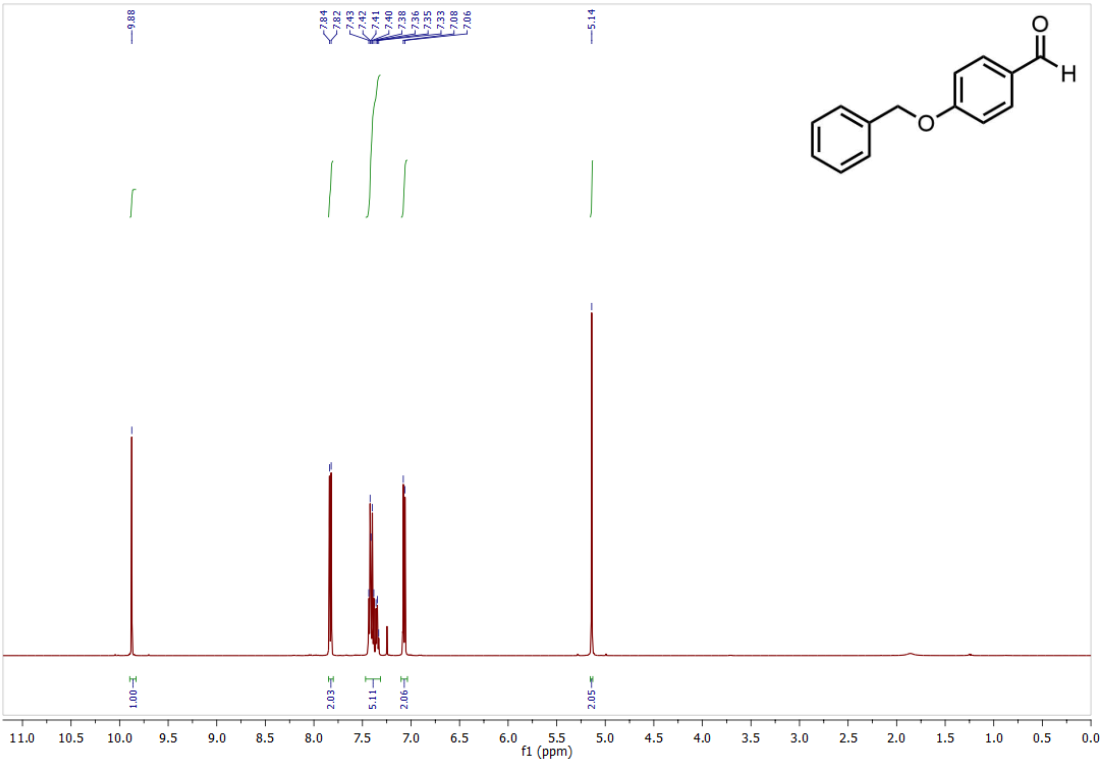

Figure A1 ^{1}H-NMR spectrum of **1v** ($CDCl_3$, 500 MHz)

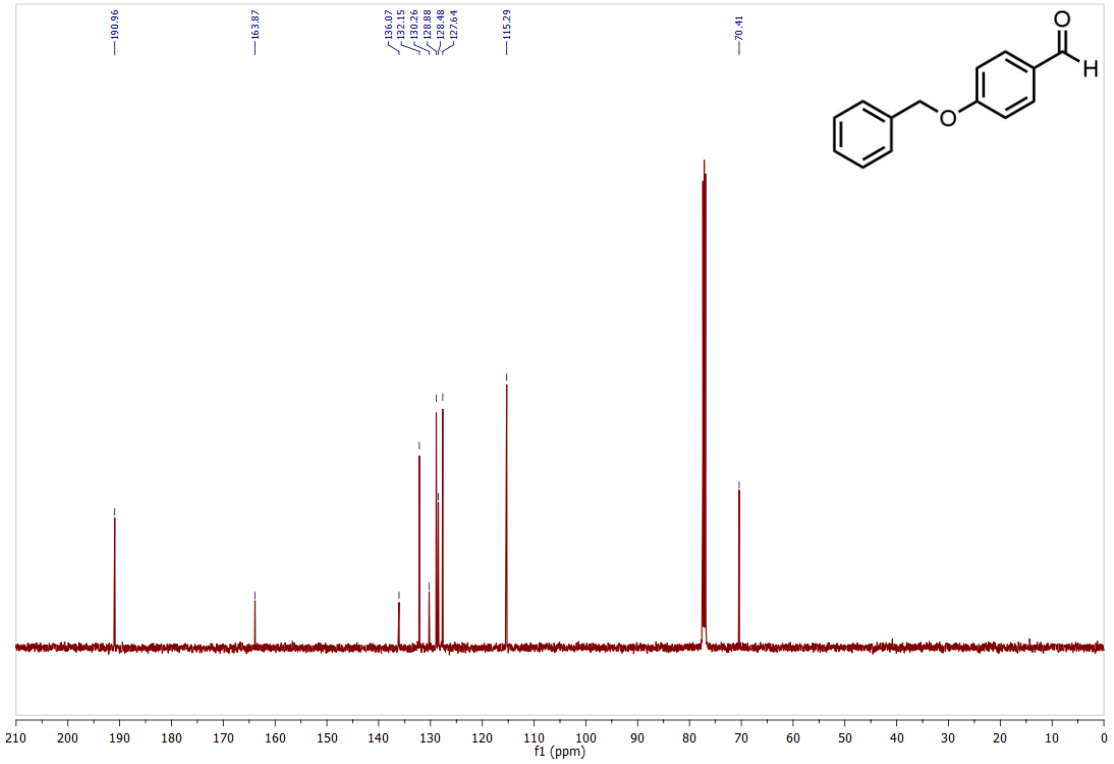

Figure A2 ^{13}C-HMR spectrum of **1v** ($CDCl_3$, 125 MHz)

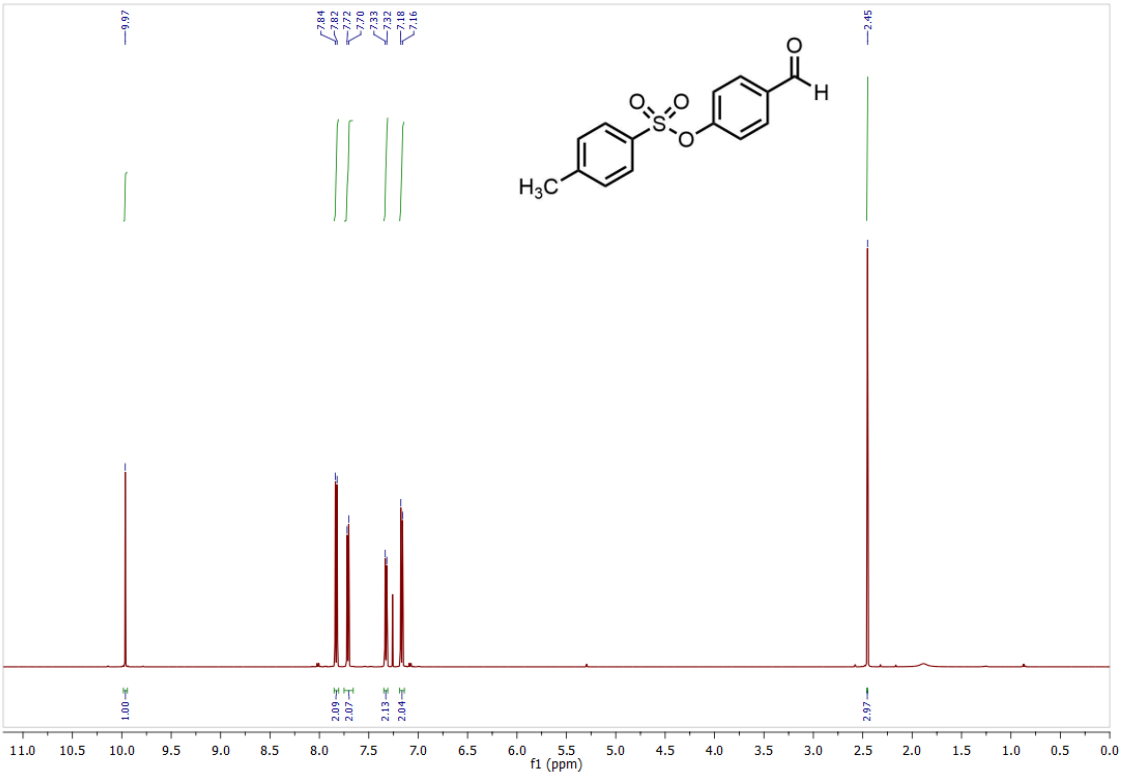

Figure A3 ^{1}H-NMR spectrum of **1w** ($CDCl_3$, 500 MHz)

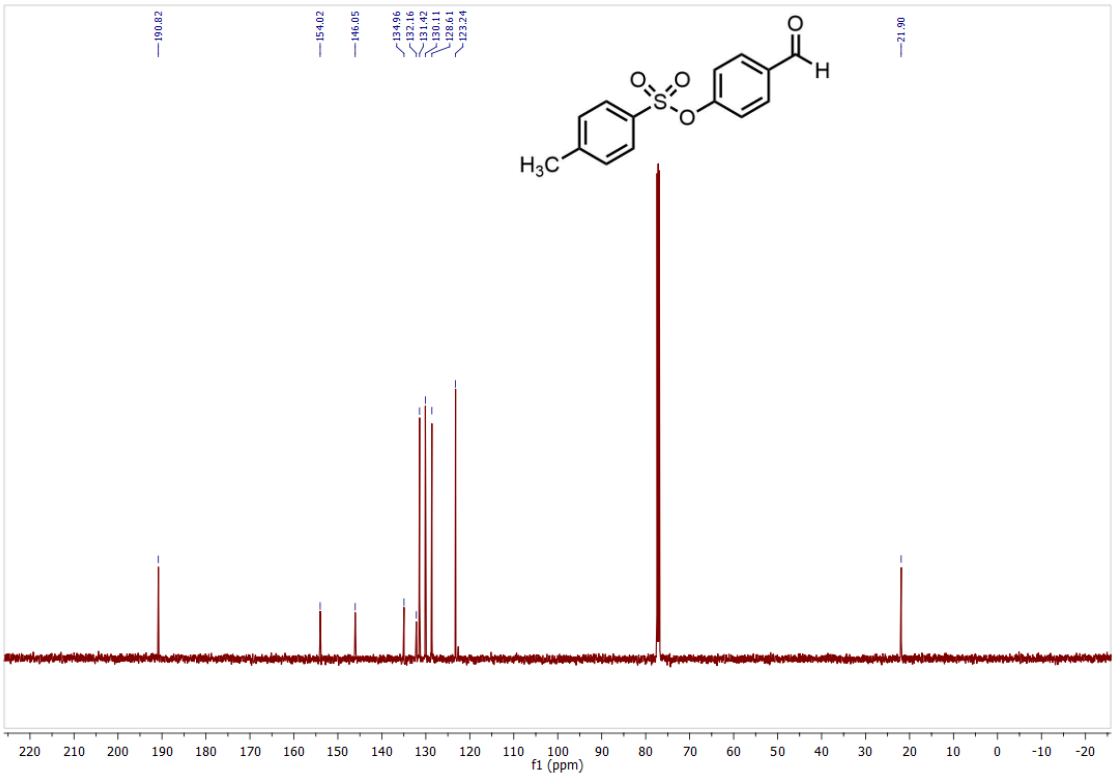

Figure A4 ^{13}C-NMR spectrum of **1w** ($CDCl_3$, 125 MHz)

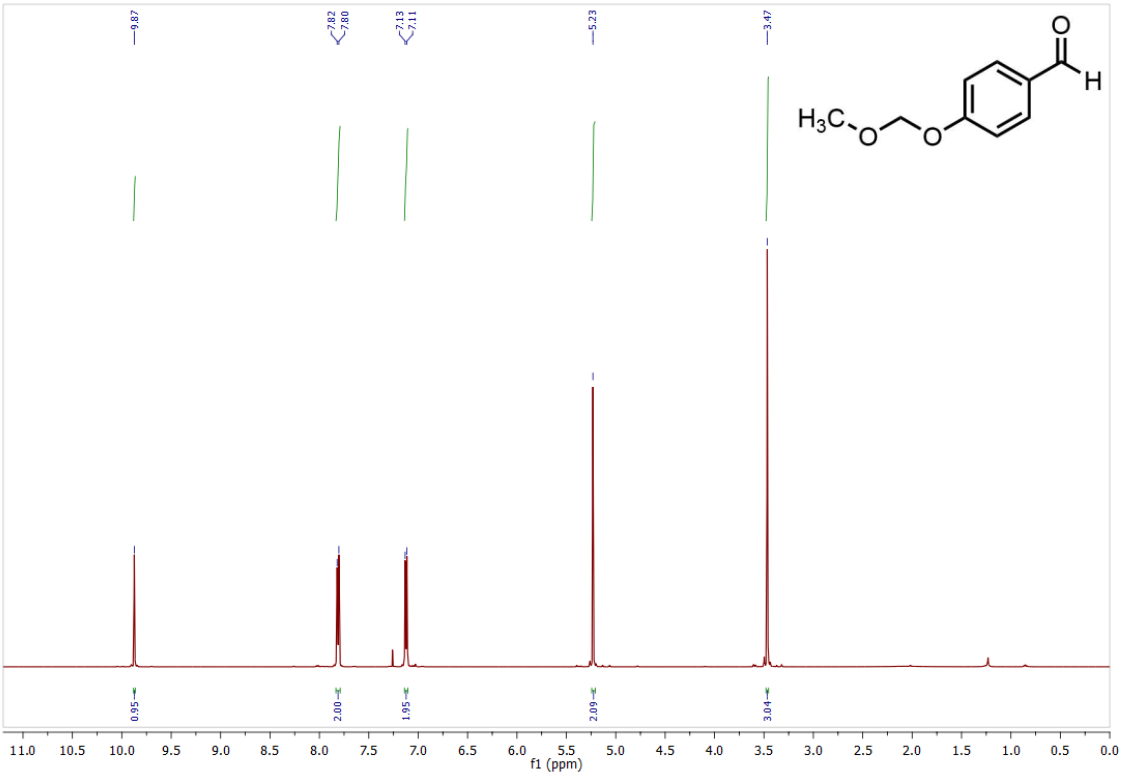

Figure A5 ^{1}H-NMR spectrum of **1x** ($CDCl_3$, 500 MHz)

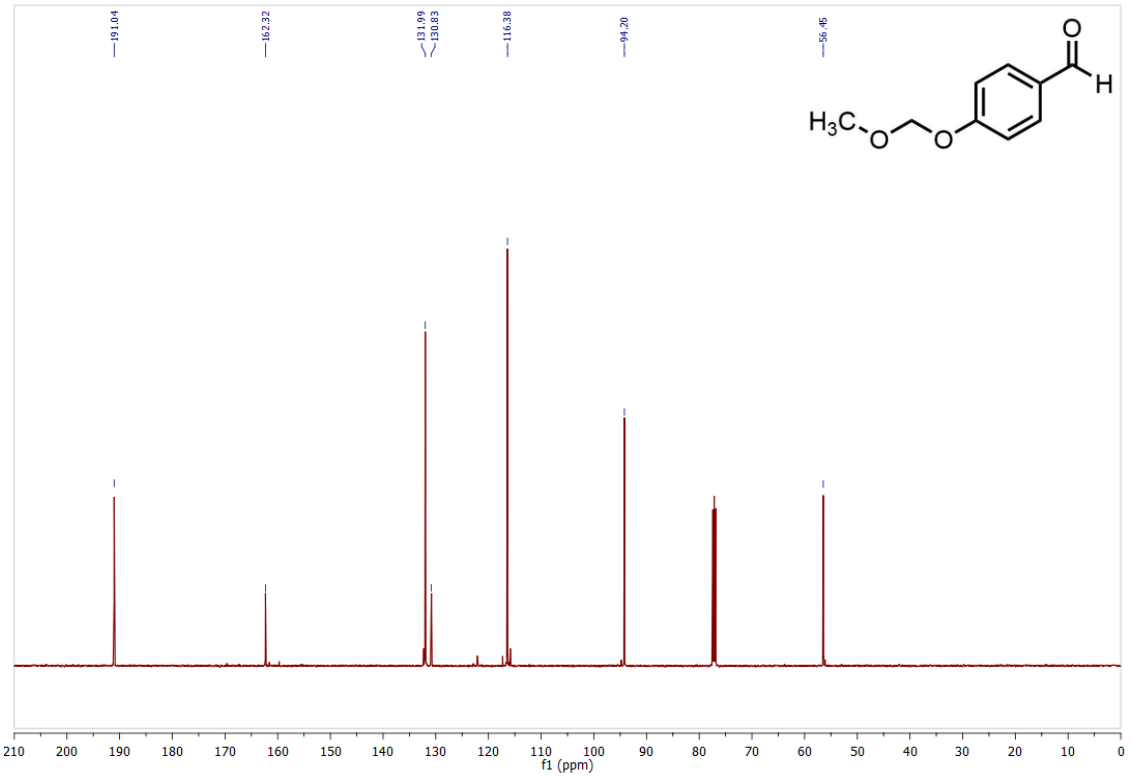

Figure A6 ^{13}C-NMR spectrum of **1x** ($CDCl_3$, 125 MHz)

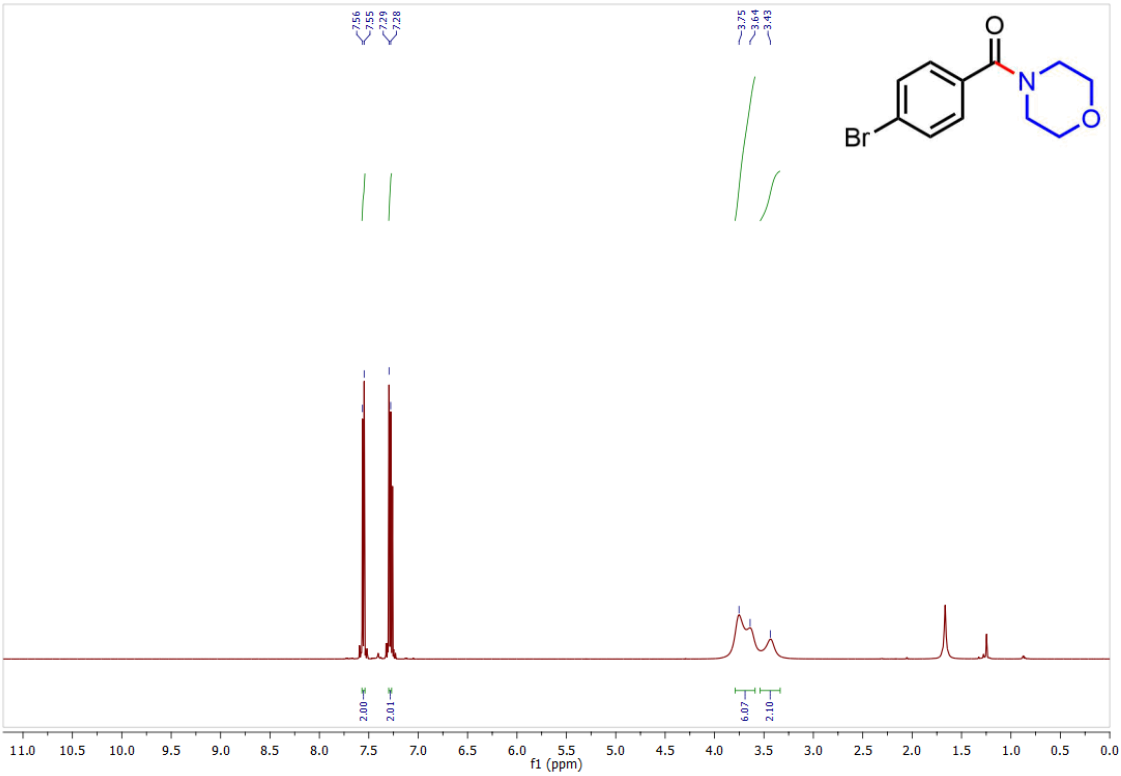

Figure A7 ^{1}H-NMR spectrum of **3aa** ($CDCl_3$, 500 MHz)

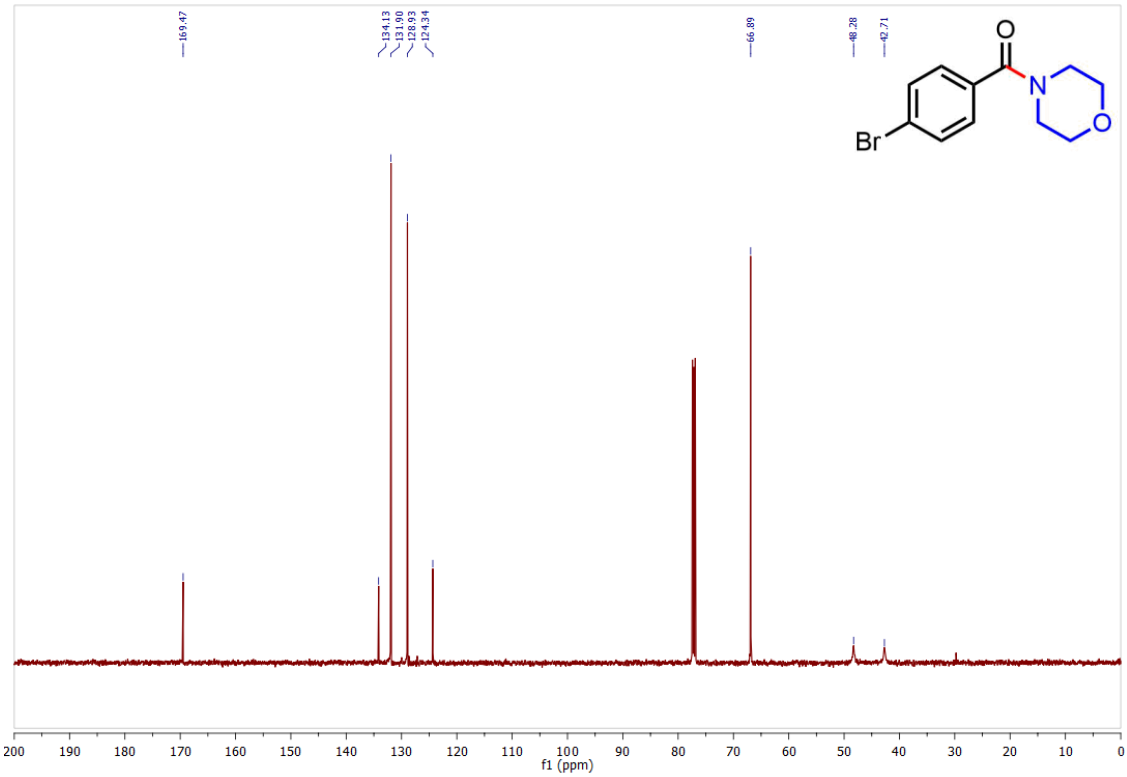

Figure A8 ^{13}C-NMR spectrum of **3aa** ($CDCl_3$, 125 MHz)

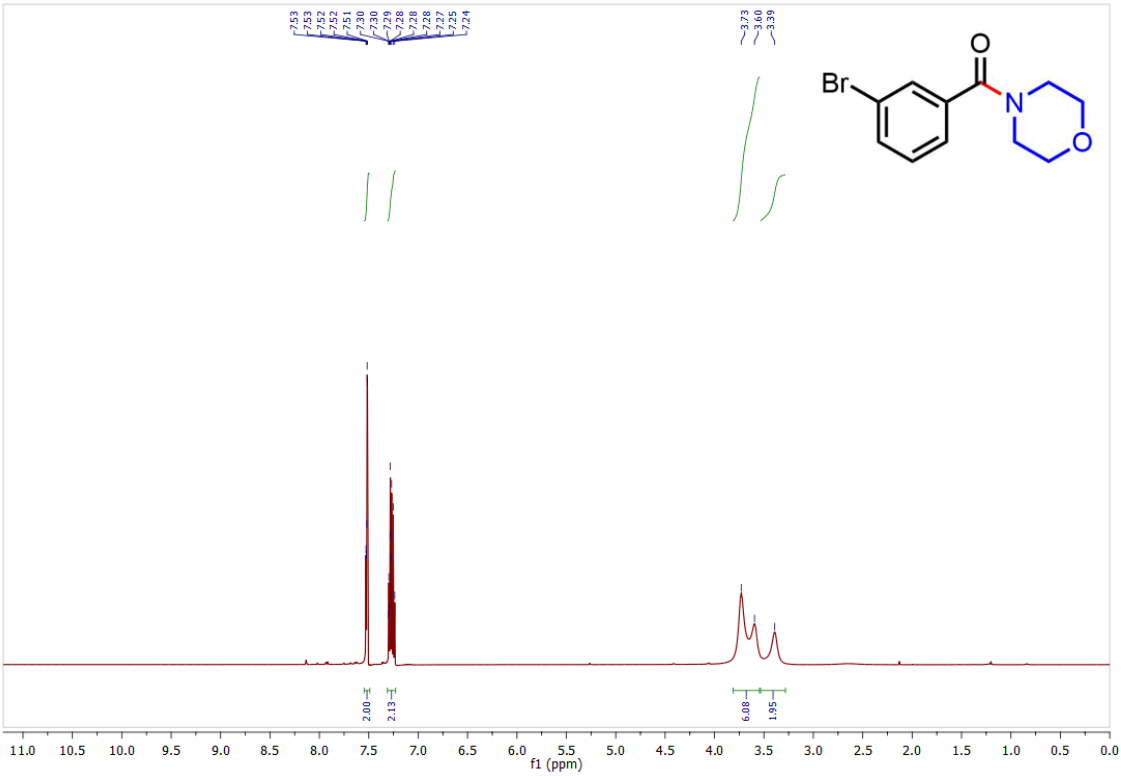

Figure A9 ^{1}H-NMR spectrum of **3ba** ($CDCl_3$, 500 MHz)

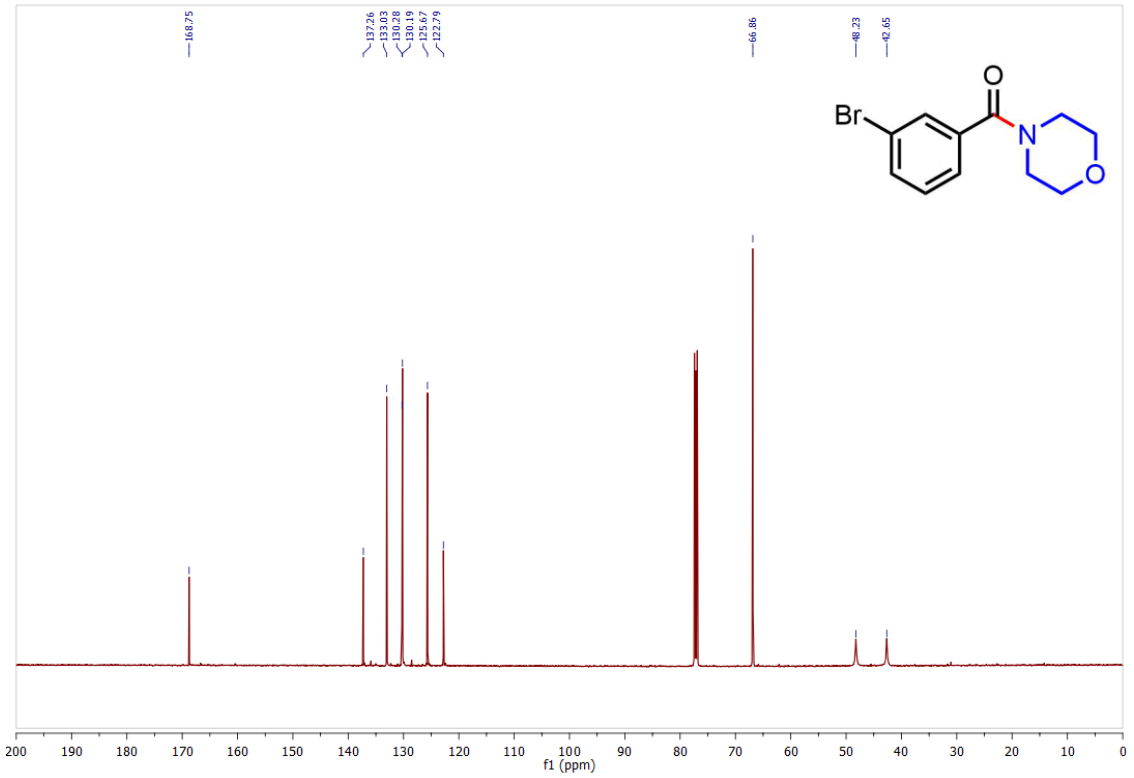

Figure A10 ^{13}C-NMR spectrum of **3ba** ($CDCl_3$, 125 MHz)

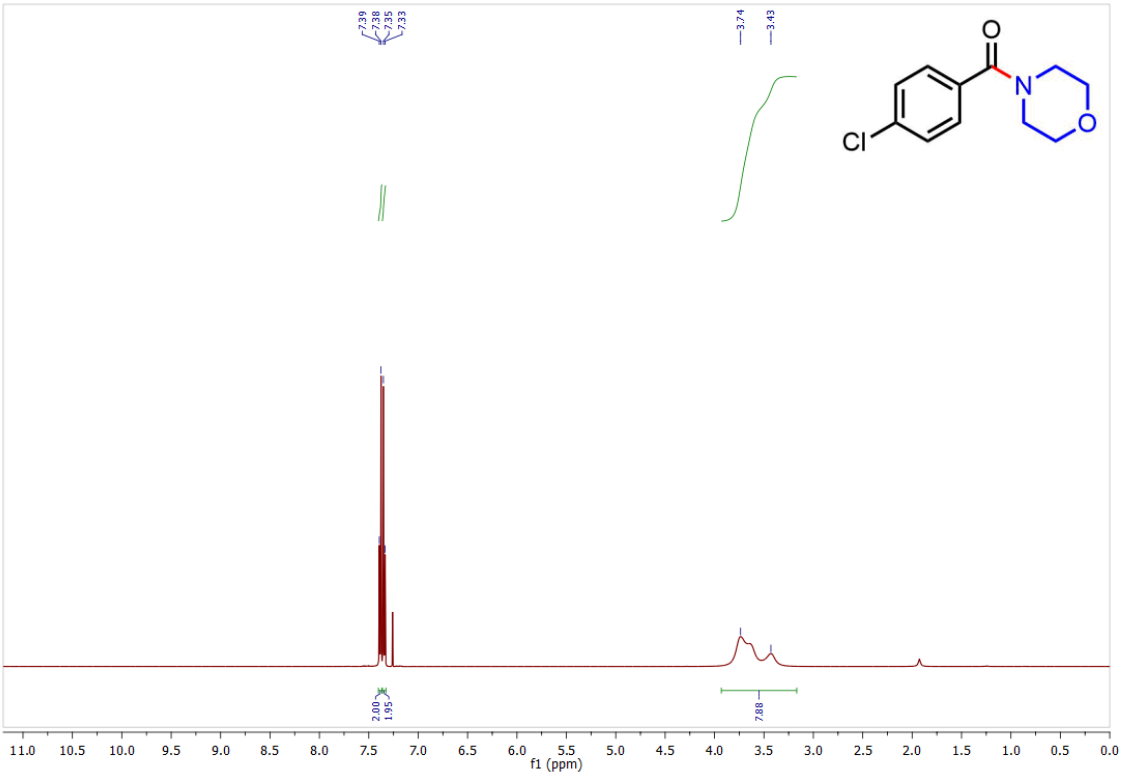

Figure A11 ^{1}H-NMR spectrum of **3ca** ($CDCl_3$, 500 MHz)

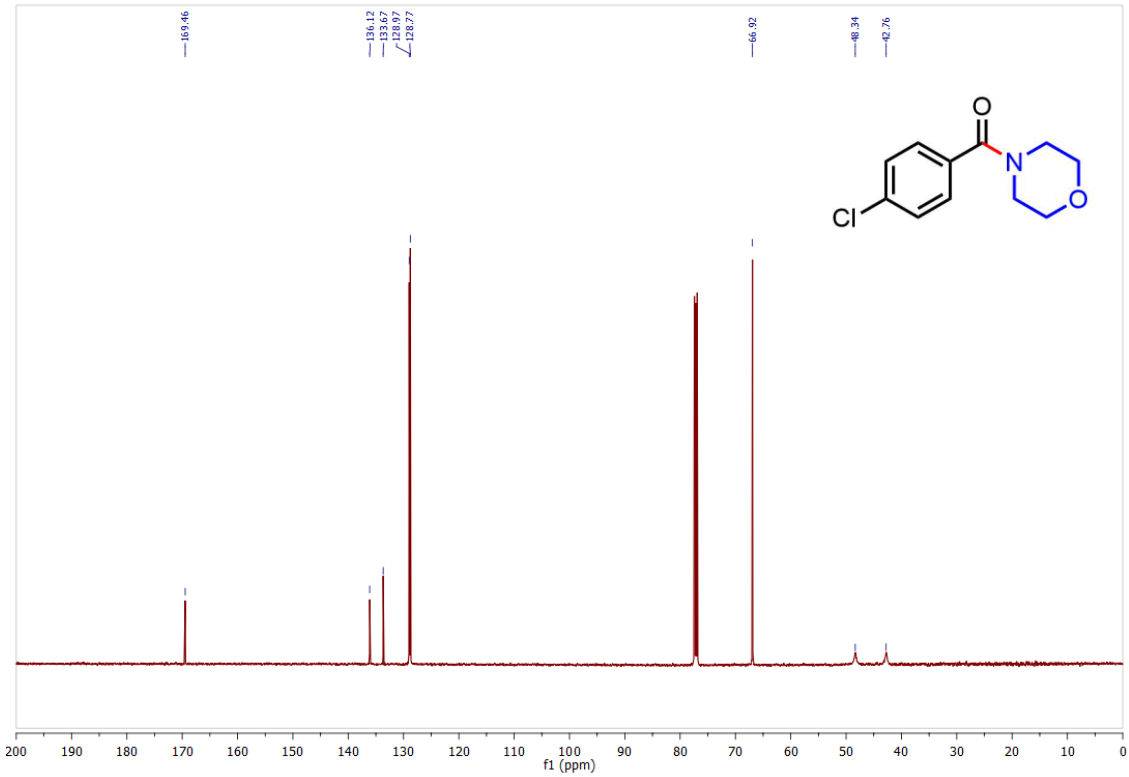

Figure A12 ^{13}C-NMR spectrum of **3ca** ($CDCl_3$, 125 MHz)

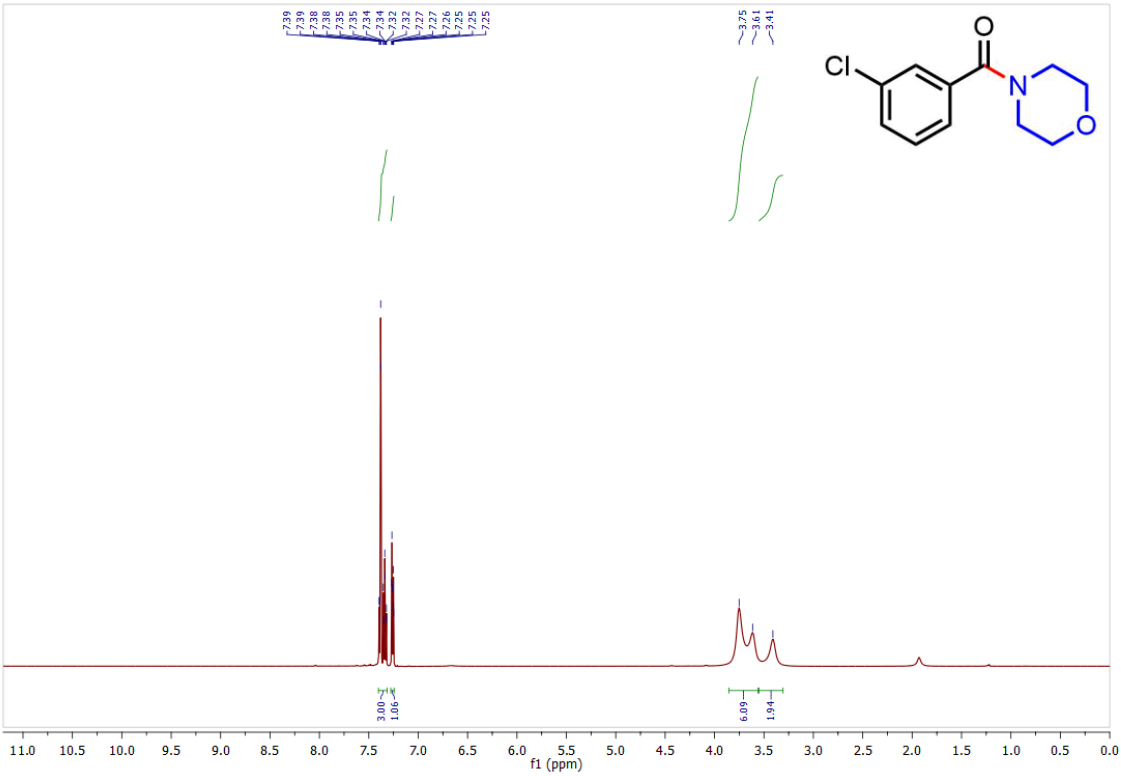

Figure A13 ^{1}H-NMR spectrum of **3da** ($CDCl_3$, 500 MHz)

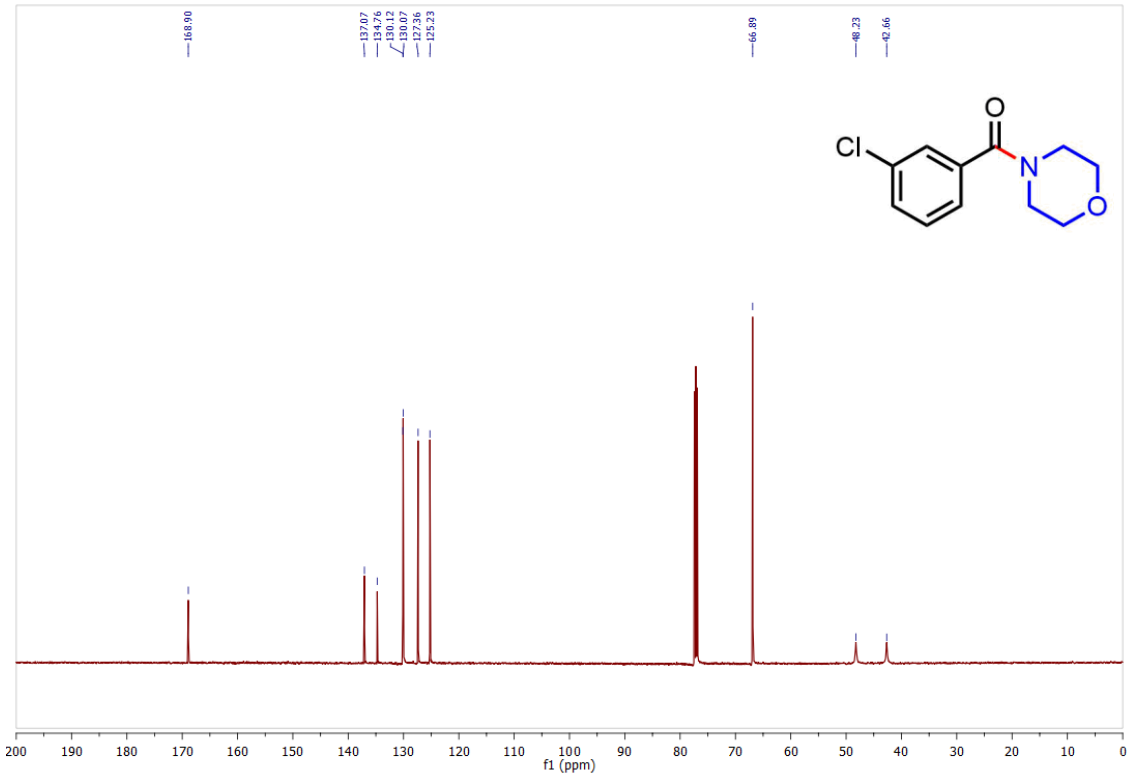

Figure A14 ^{13}C-NMR spectrum of **3da** ($CDCl_3$, 125 MHz)

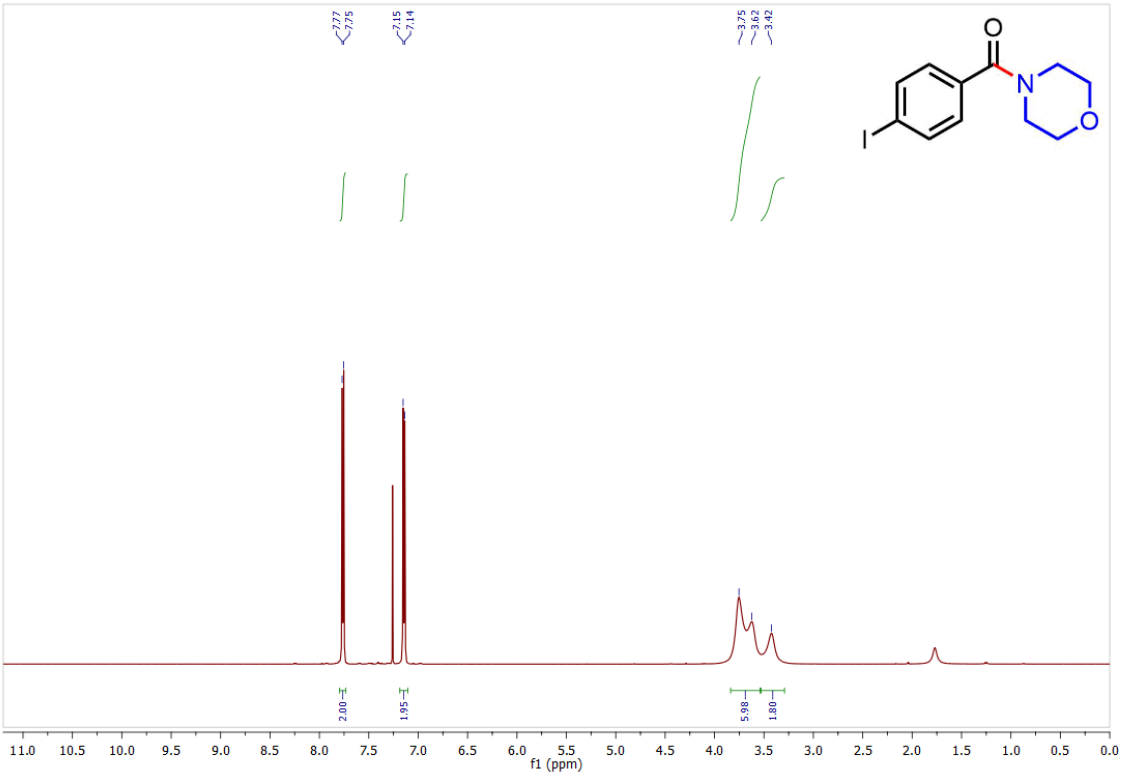

Figure A15 ^{1}H-NMR spectrum of **3ea** ($CDCl_3$, 500 MHz)

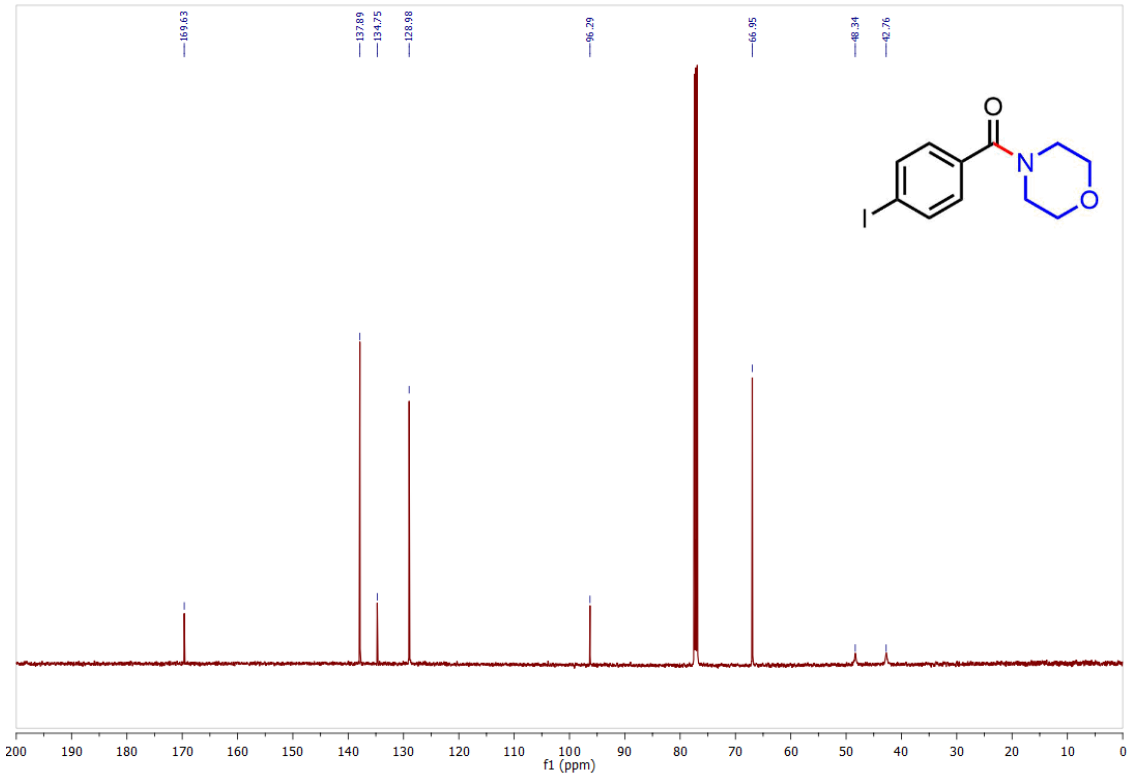

Figure A16 ^{13}C-NMR spectrum of **3ea** ($CDCl_3$, 125 MHz)

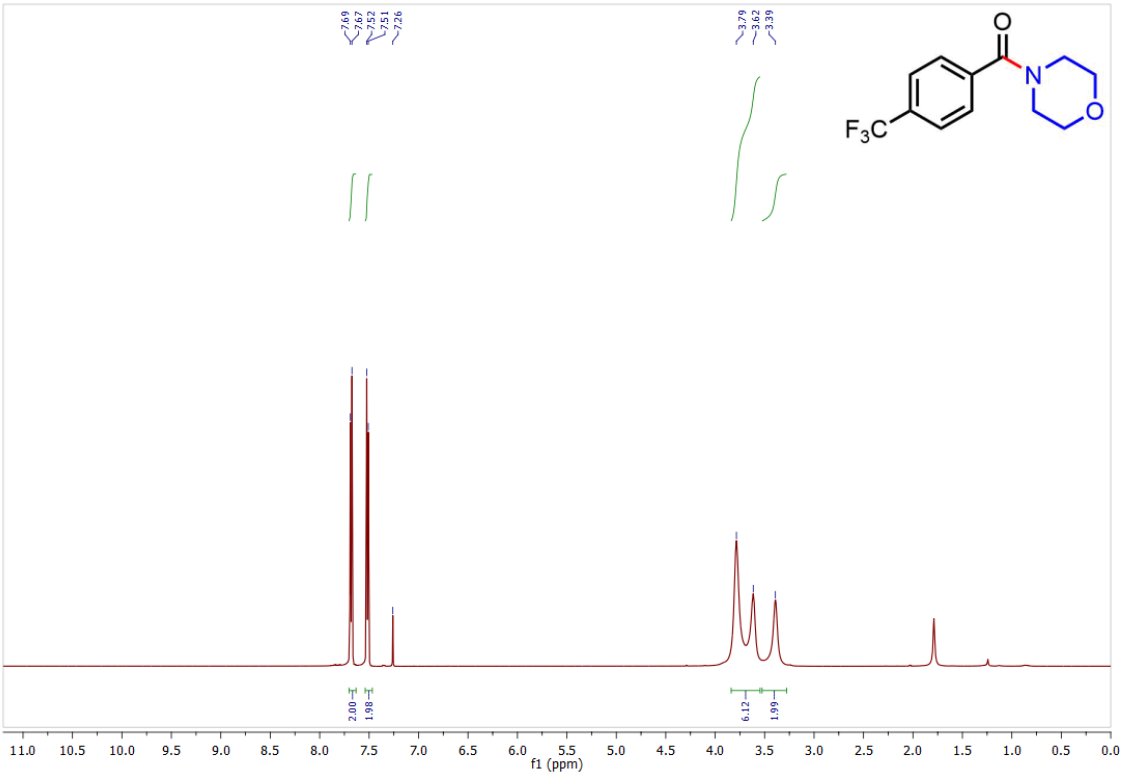

Figure A17 ^{1}H-NMR spectrum of **3fa** ($CDCl_3$, 500 MHz)

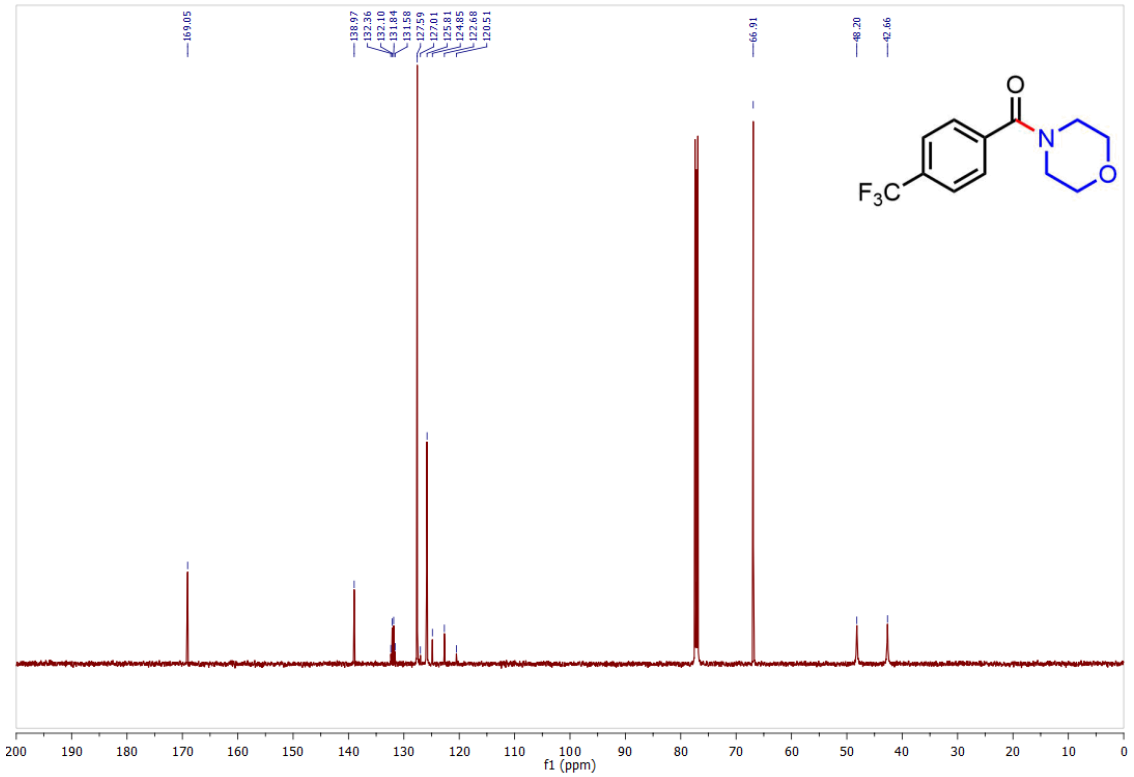

Figure A18 ^{13}C-NMR spectrum of **3fa** ($CDCl_3$, 125 MHz)

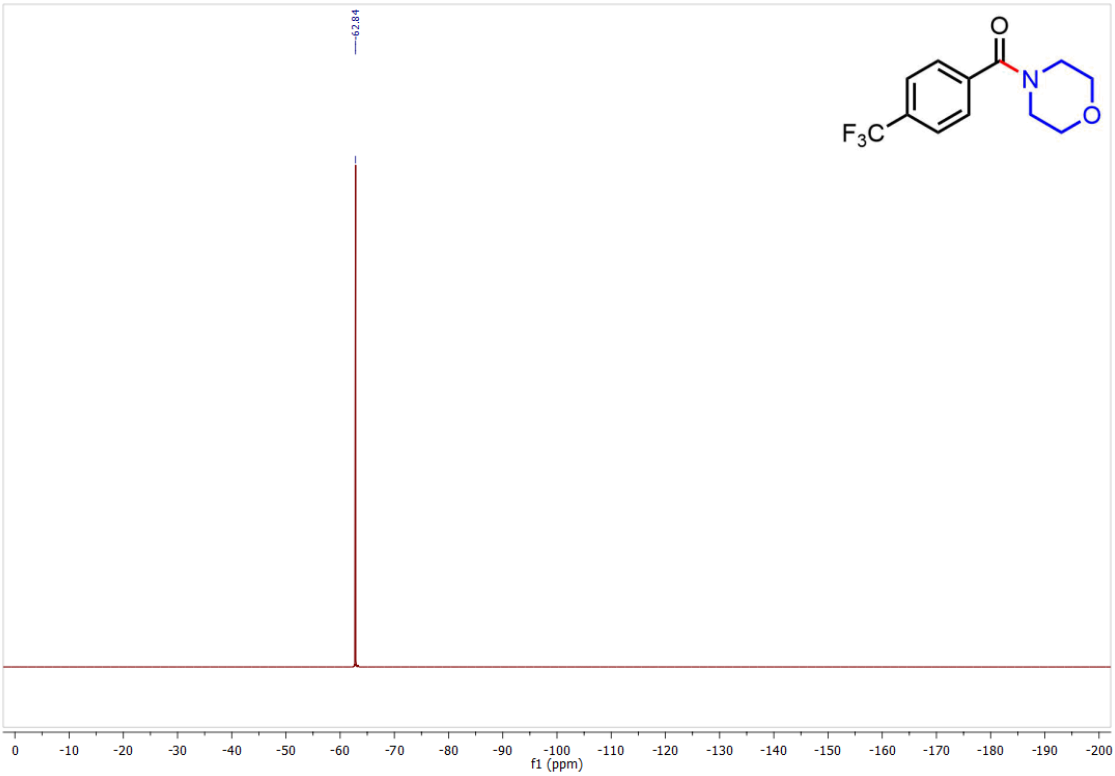

Figure A19 ^{19}F-NMR spectrum of **3fa** ($CDCl_3$, 470 MHz)

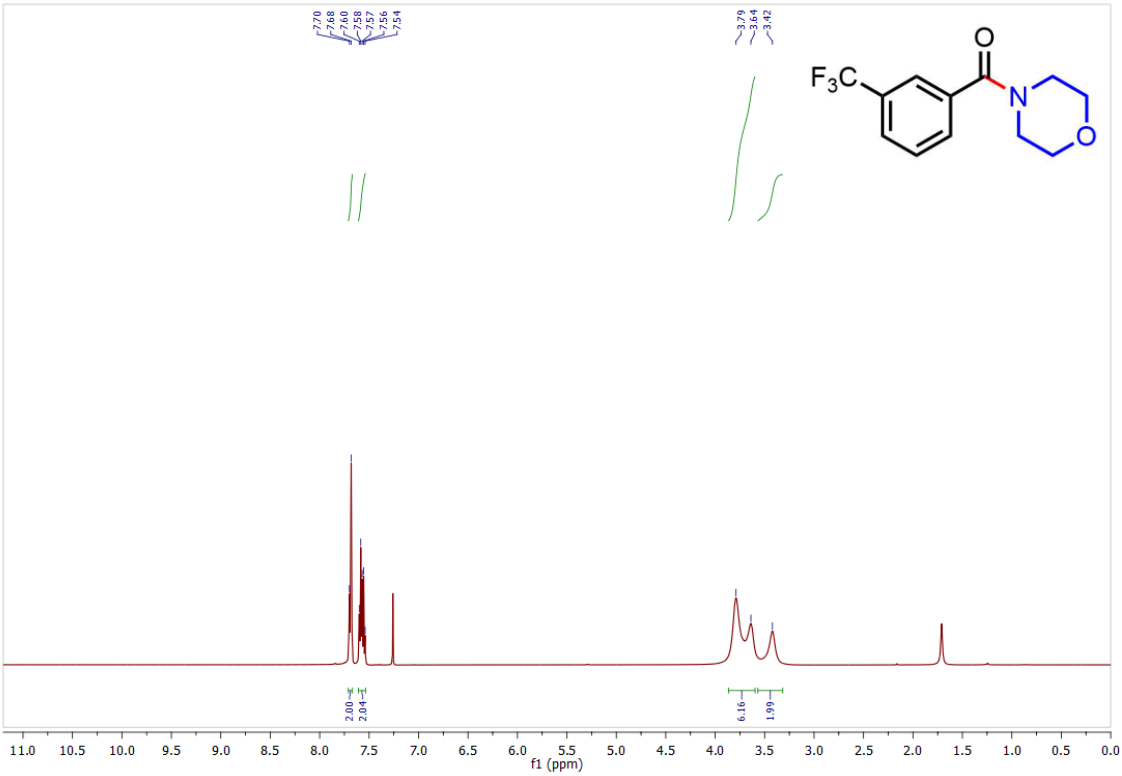

Figure A20 ^{1}H-NMR spectrum of **3ga** ($CDCl_3$, 500 MHz)

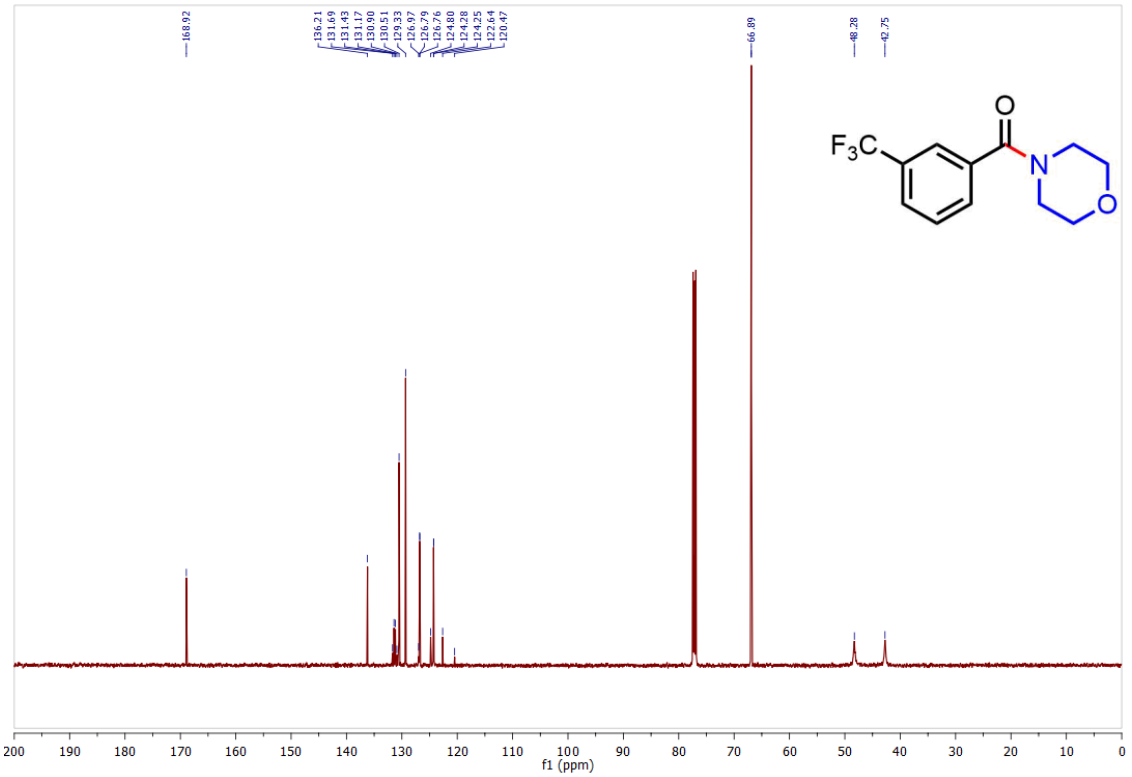

Figure A21 ^{13}C-NMR spectrum of **3ga** ($CDCl_3$, 125 MHz)

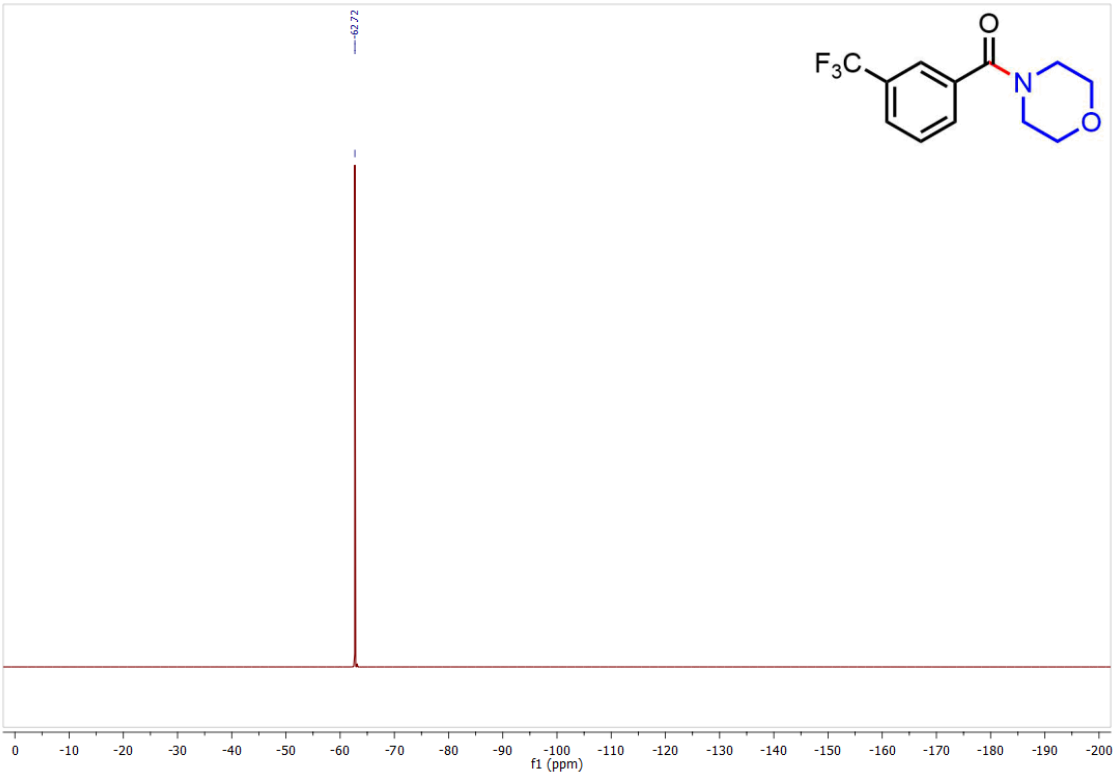

Figure A22 ^{19}F-NMR spectrum of **3ga** ($CDCl_3$, 470 MHz)

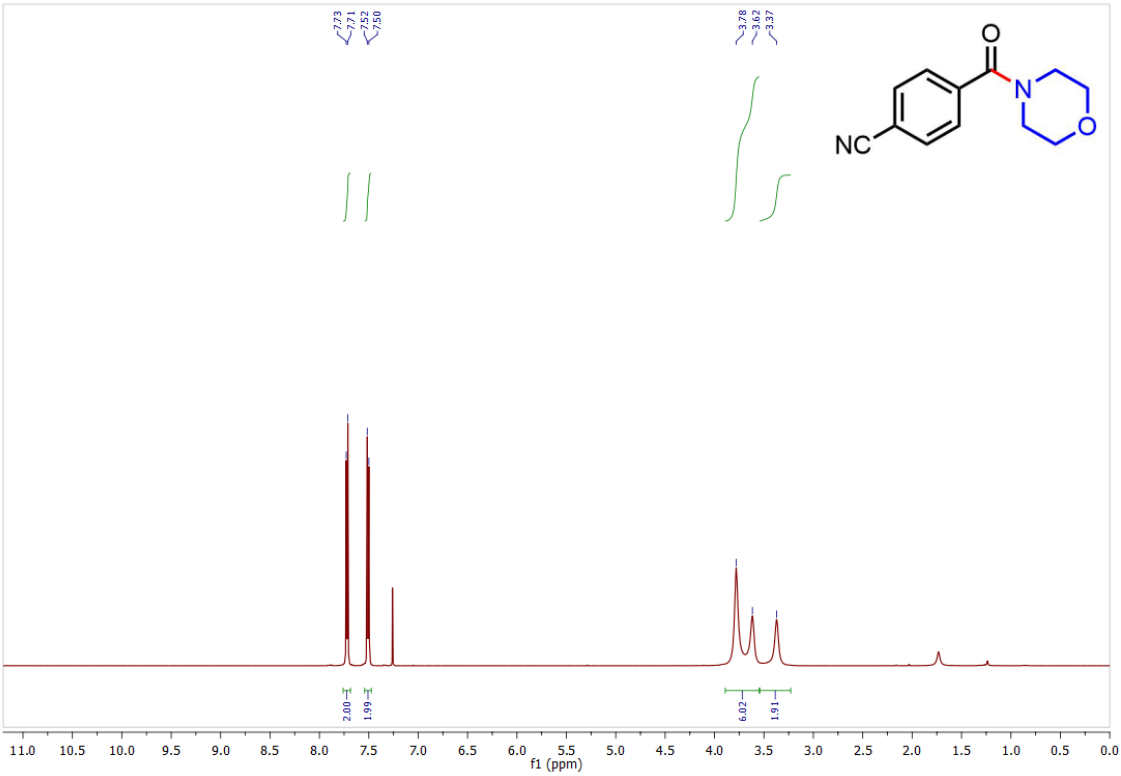

Figure A23 ^{1}H-NMR spectrum of **3ha** ($CDCl_3$, 500 MHz)

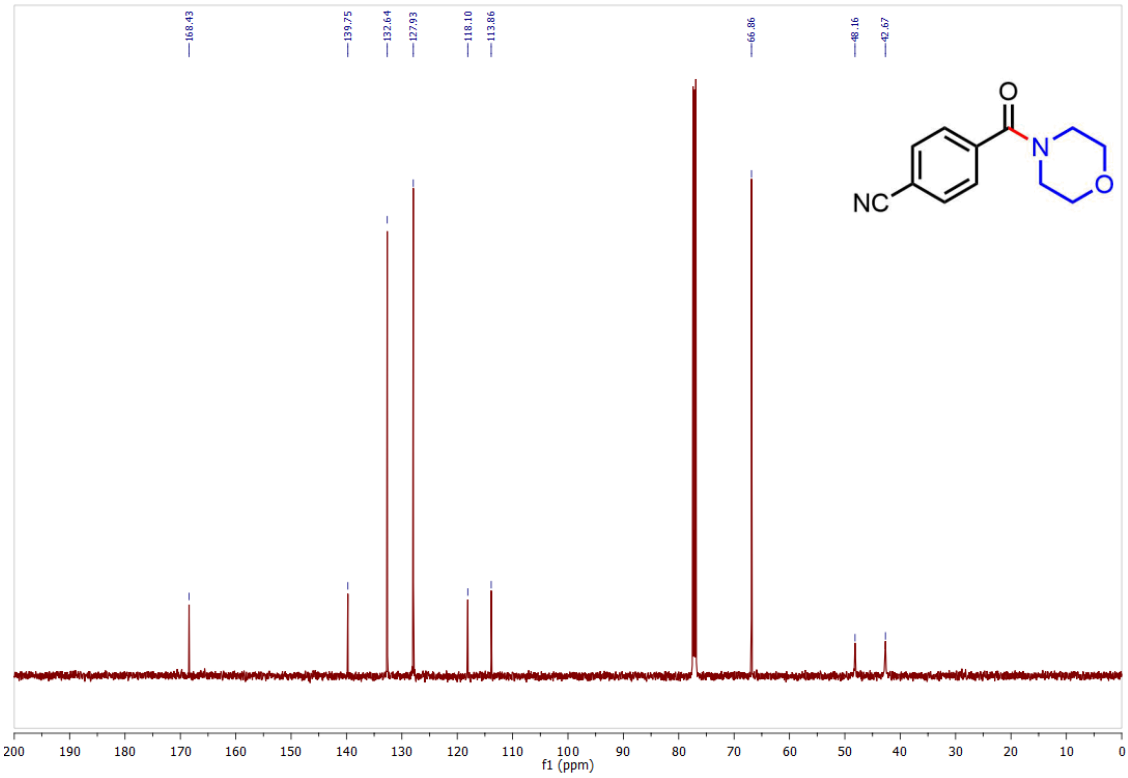

Figure A24 ^{13}C-NMR spectrum of **3ha** ($CDCl_3$, 125 MHz)

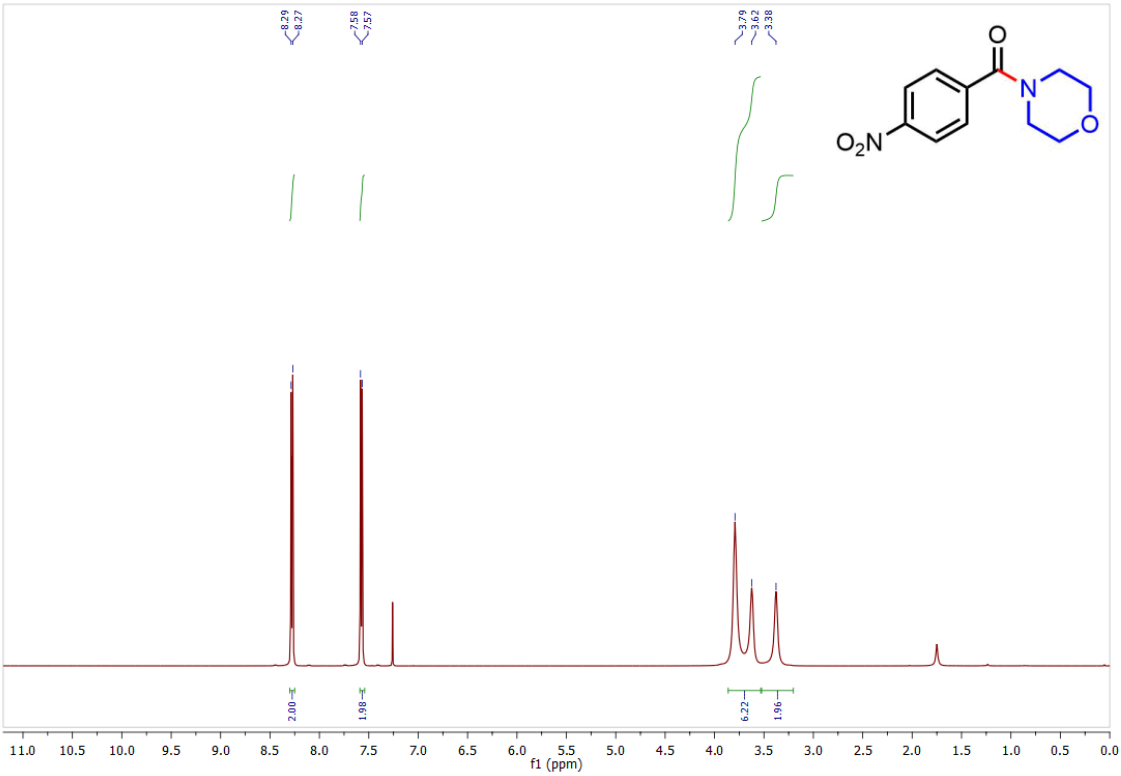

Figure A25 ^{1}H-NMR spectrum of **3ia** ($CDCl_3$, 500 MHz)

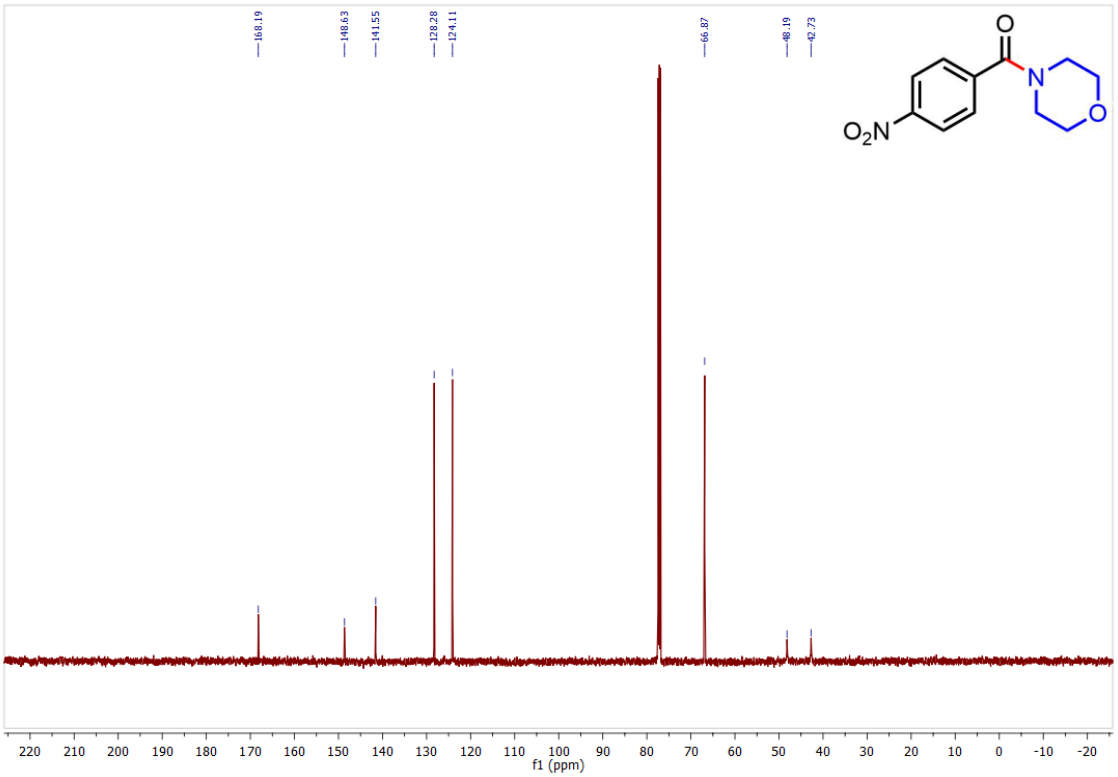

Figure A26 ^{13}C-NMR spectrum of **3ia** ($CDCl_3$, 125 MHz)

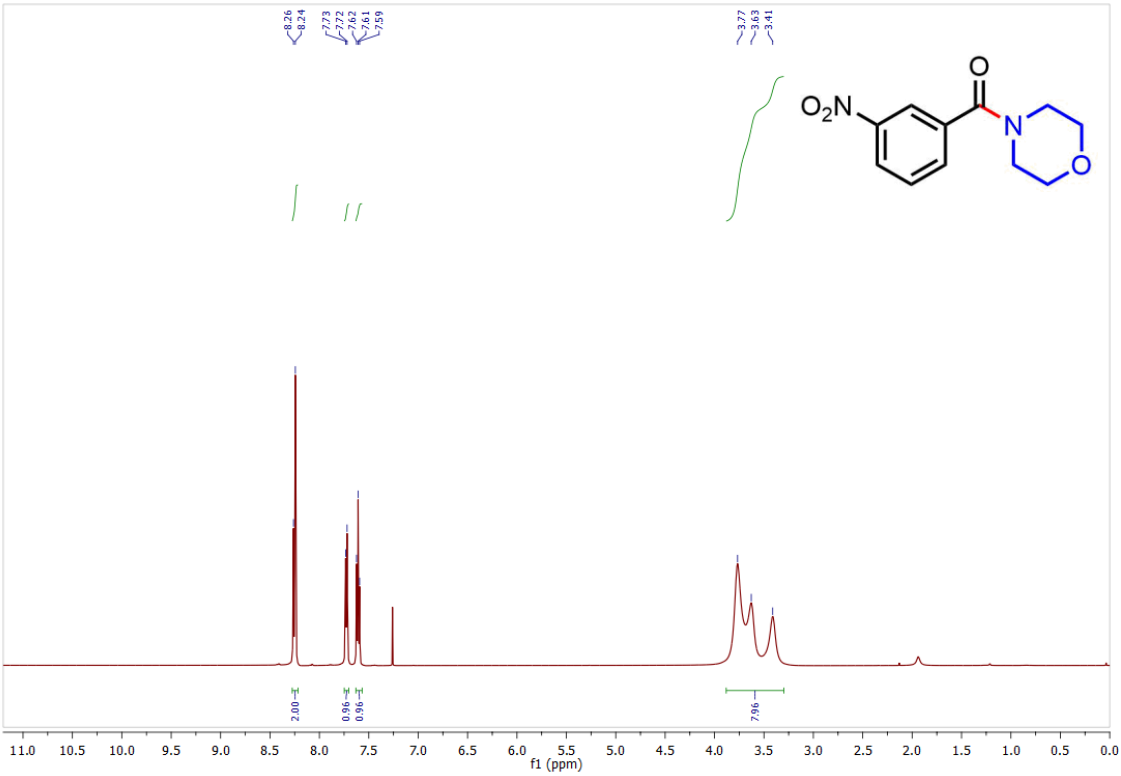

Figure A27 ^{1}H-NMR spectrum of **3ja** ($CDCl_3$, 500 MHz)

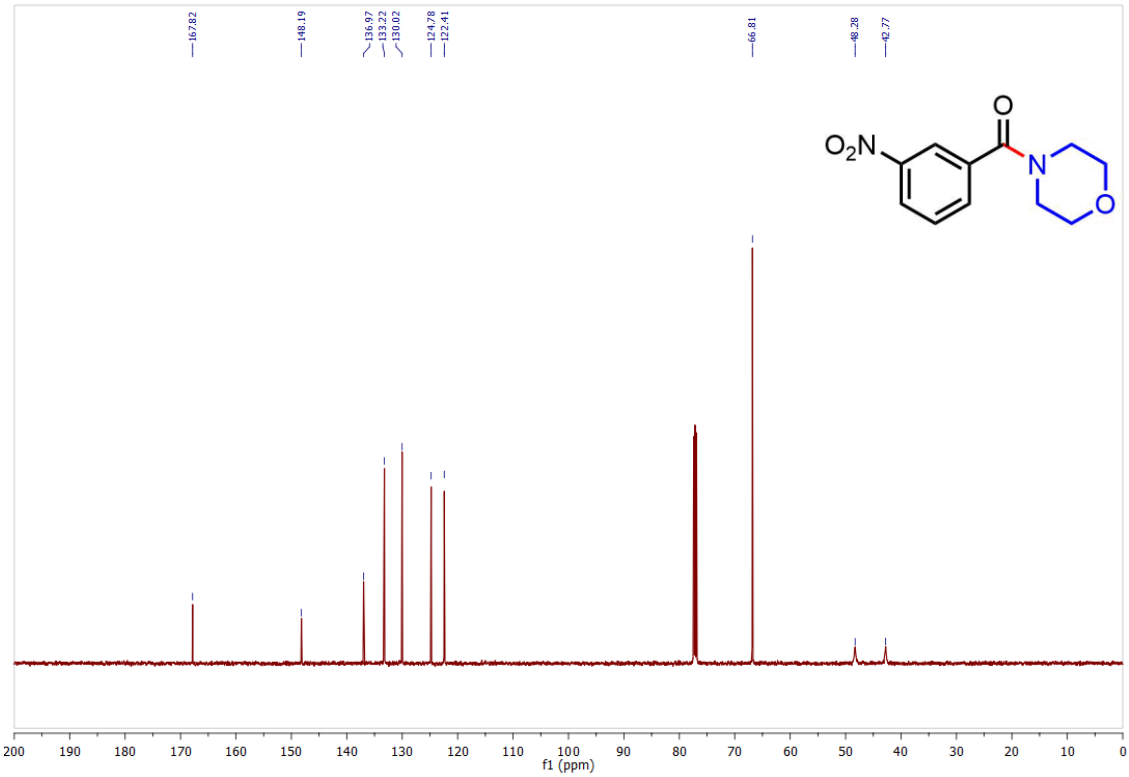

Figure A28 ^{13}C-NMR spectrum of **3ja** ($CDCl_3$, 125 MHz)

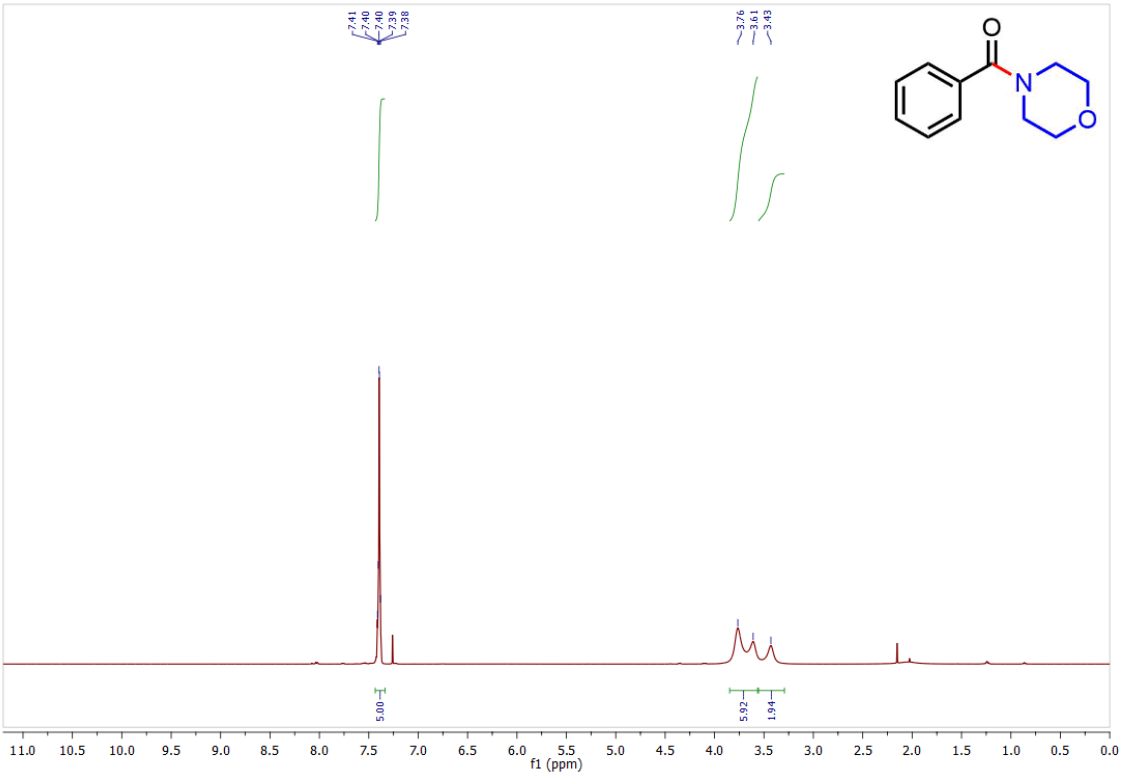

Figure A29 ^{1}H-NMR spectrum of **3ka** ($CDCl_3$, 500 MHz)

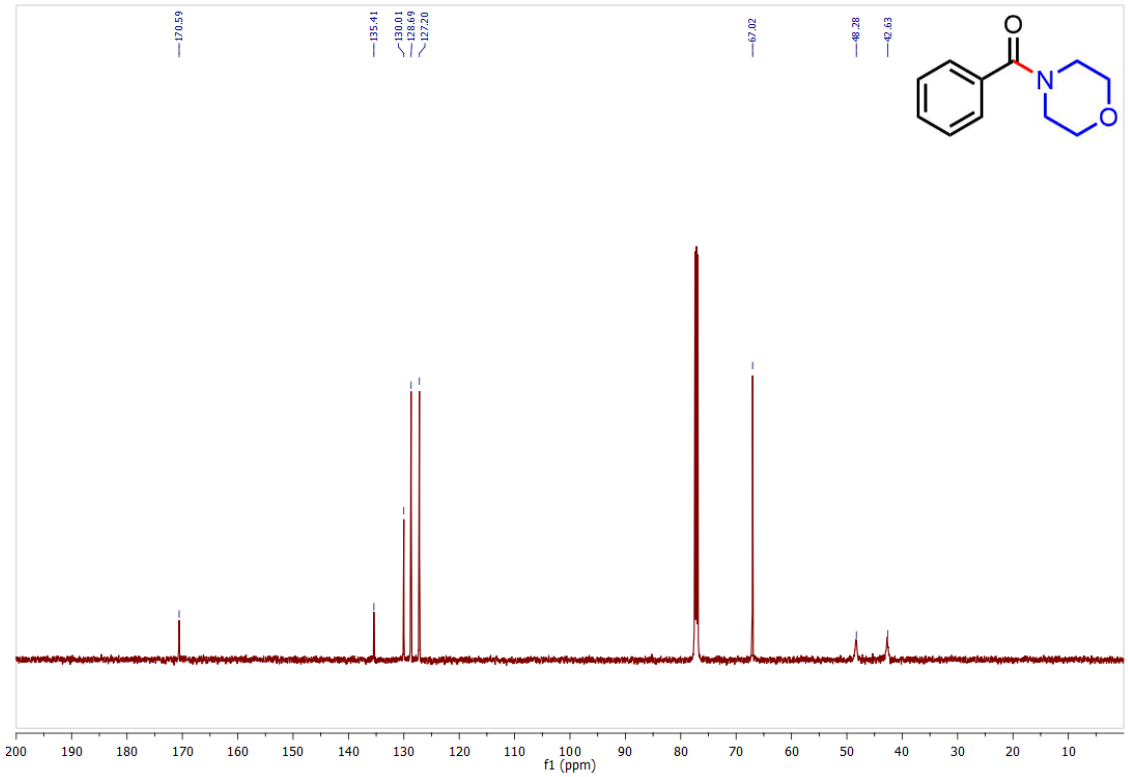

Figure A30 ^{13}C-NMR spectrum of **3ka** ($CDCl_3$, 125 MHz)

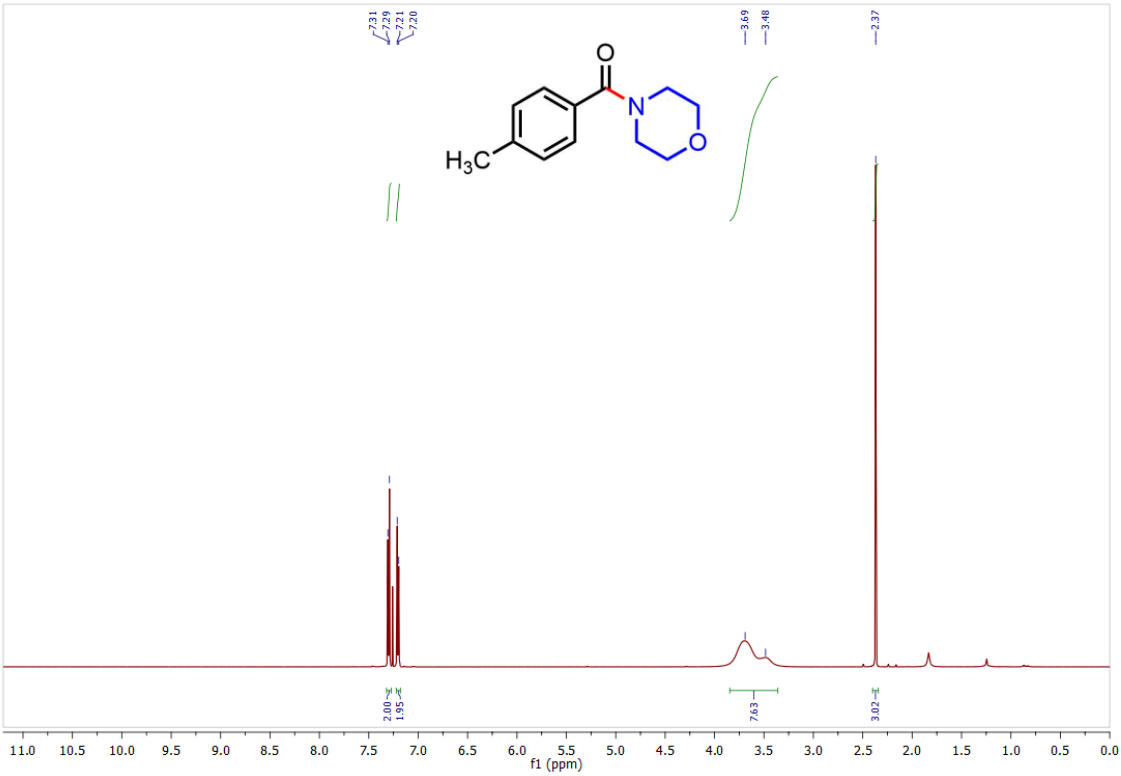

Figure A31 ^{1}H-NMR spectrum of **3la** ($CDCl_3$, 500 MHz)

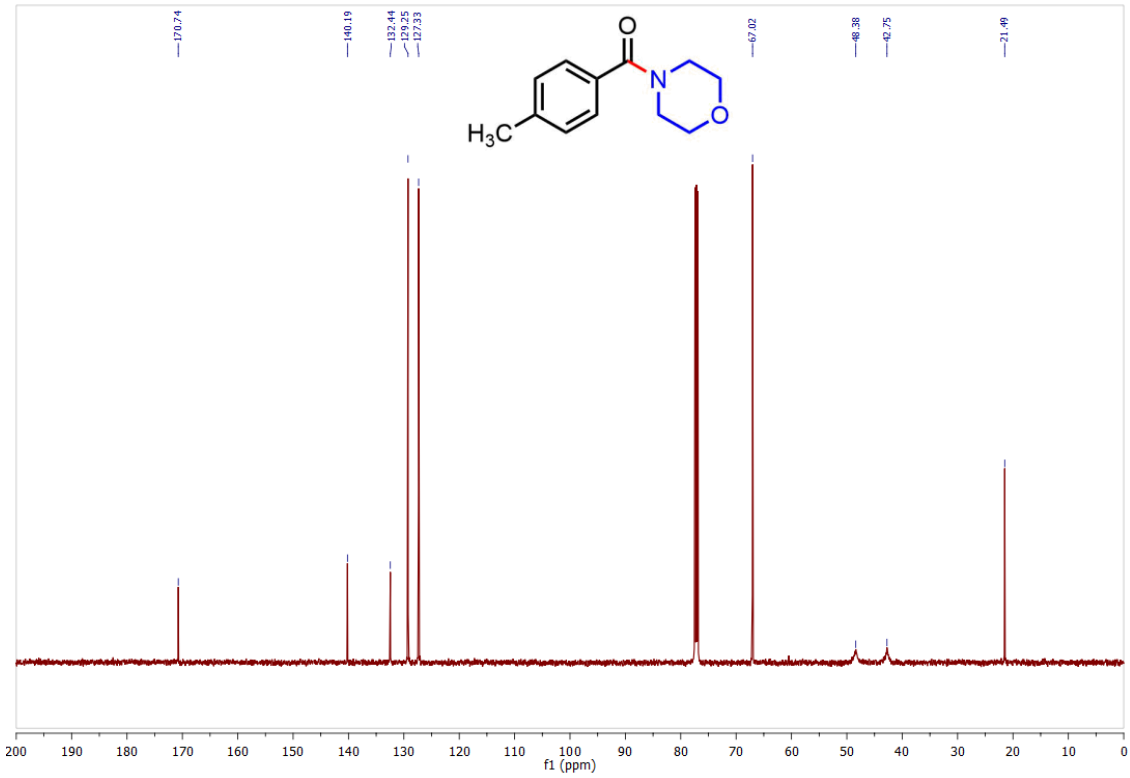

Figure A32 ^{13}C-NMR spectrum of **3la** ($CDCl_3$, 125 MHz)

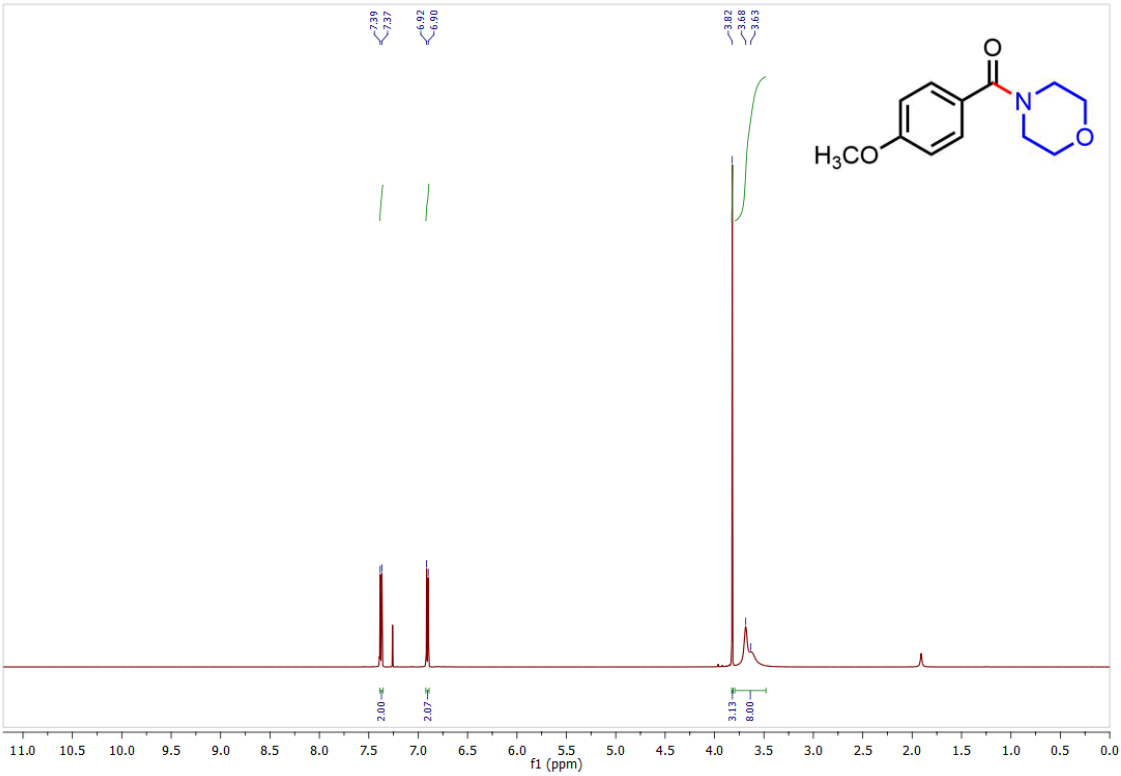

Figure A33 ^{1}H-NMR spectrum of **3ma** ($CDCl_3$, 500 MHz)

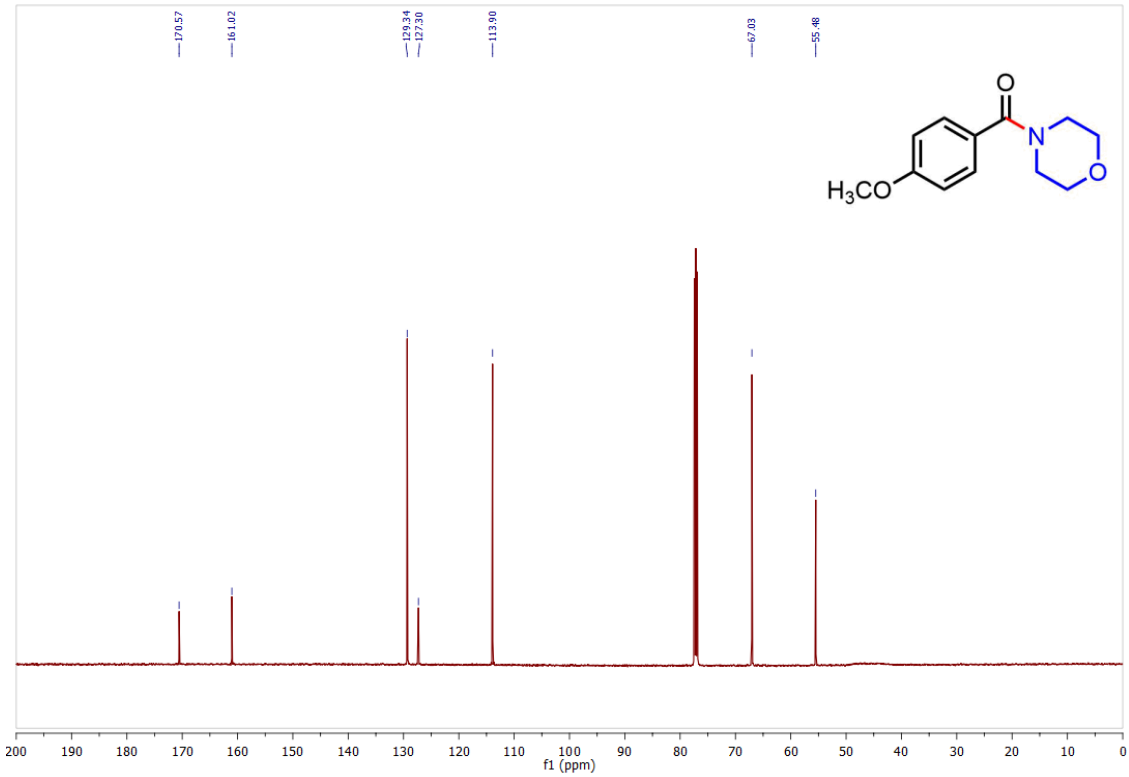

Figure A34 ^{13}C-NMR spectrum of **3ma** ($CDCl_3$, 125 MHz)

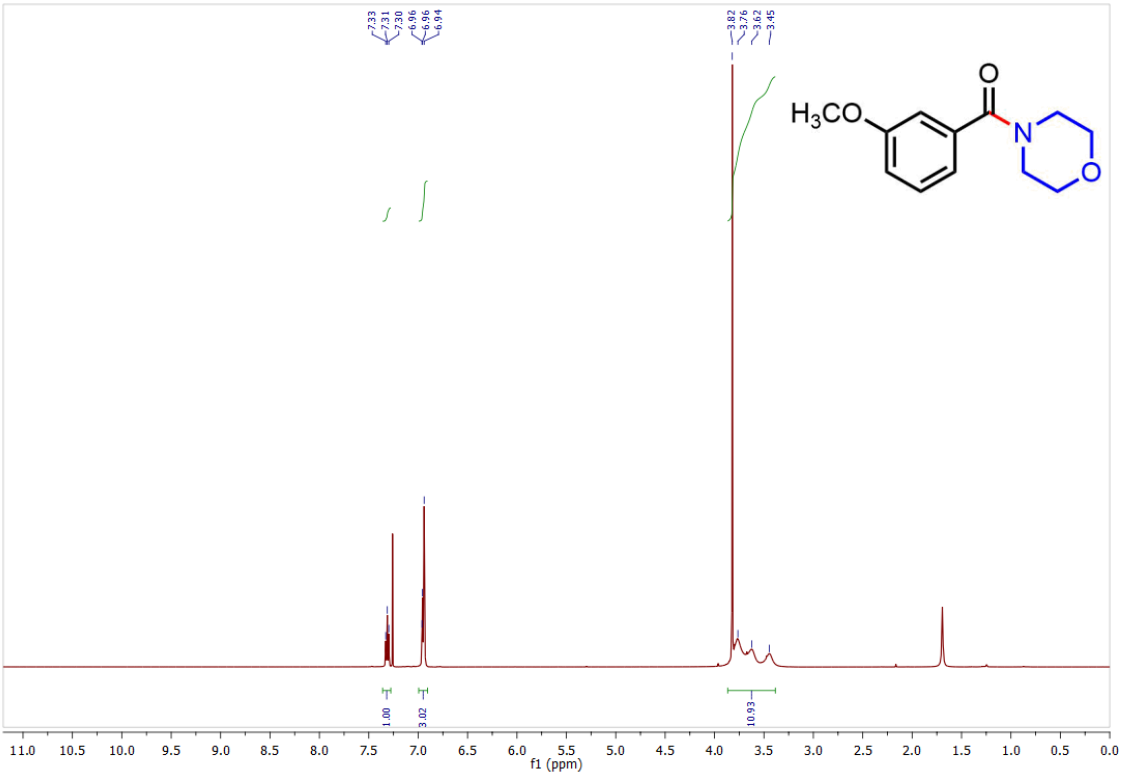

Figure A35 ^{1}H-NMR spectrum of **3na** ($CDCl_3$, 500 MHz)

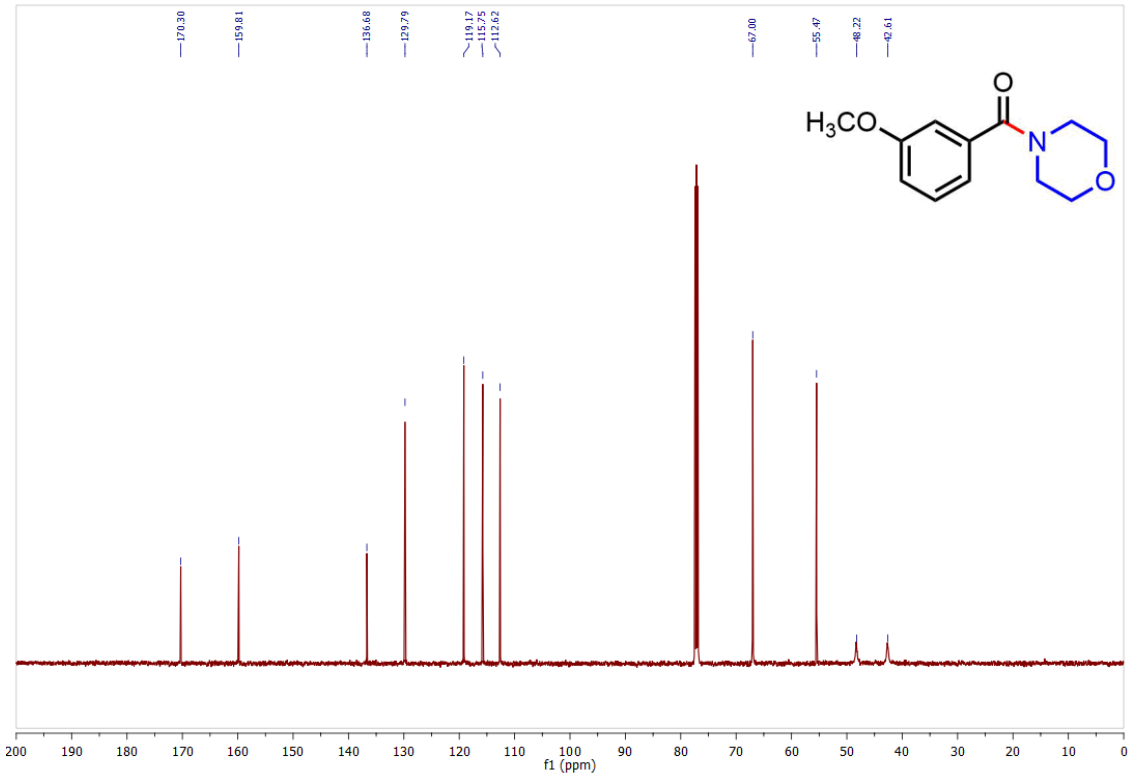

Figure A36 ^{13}C-NMR spectrum of **3na** ($CDCl_3$, 125 MHz)

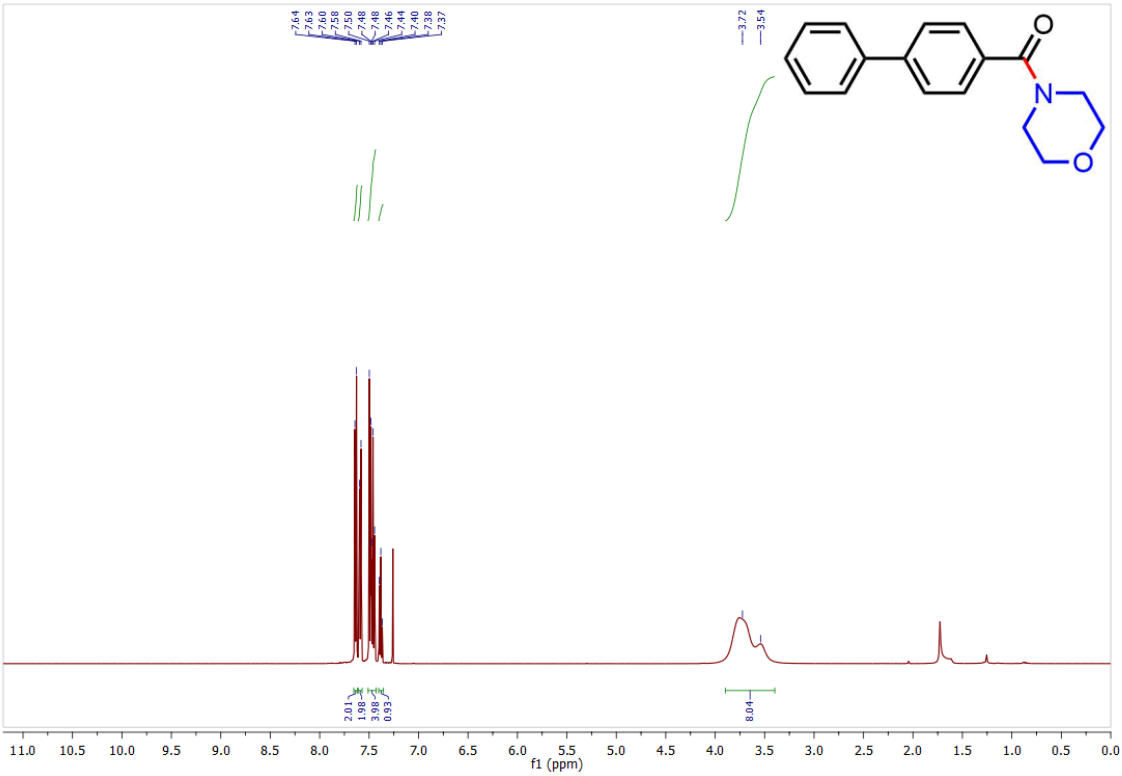

Figure A37 ^{1}H-NMR spectrum of **3oa** ($CDCl_3$, 500 MHz)

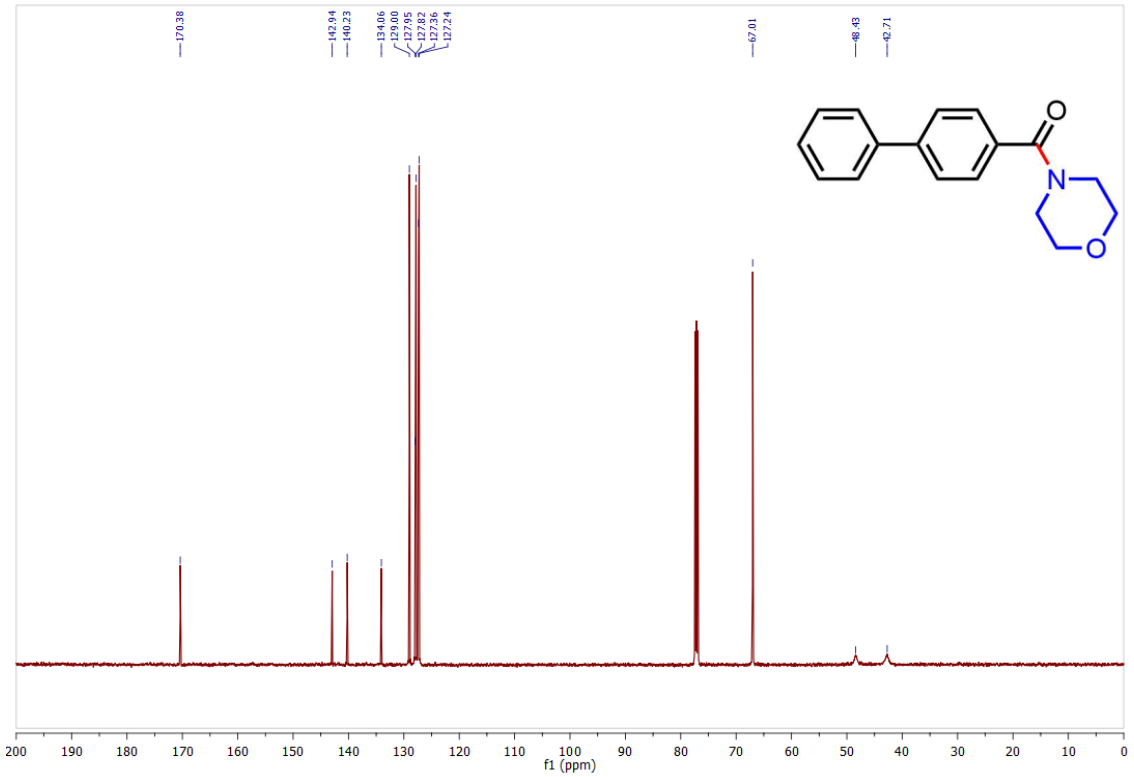

Figure A38 ^{13}C-NMR spectrum of **3oa** ($CDCl_3$, 125 MHz)

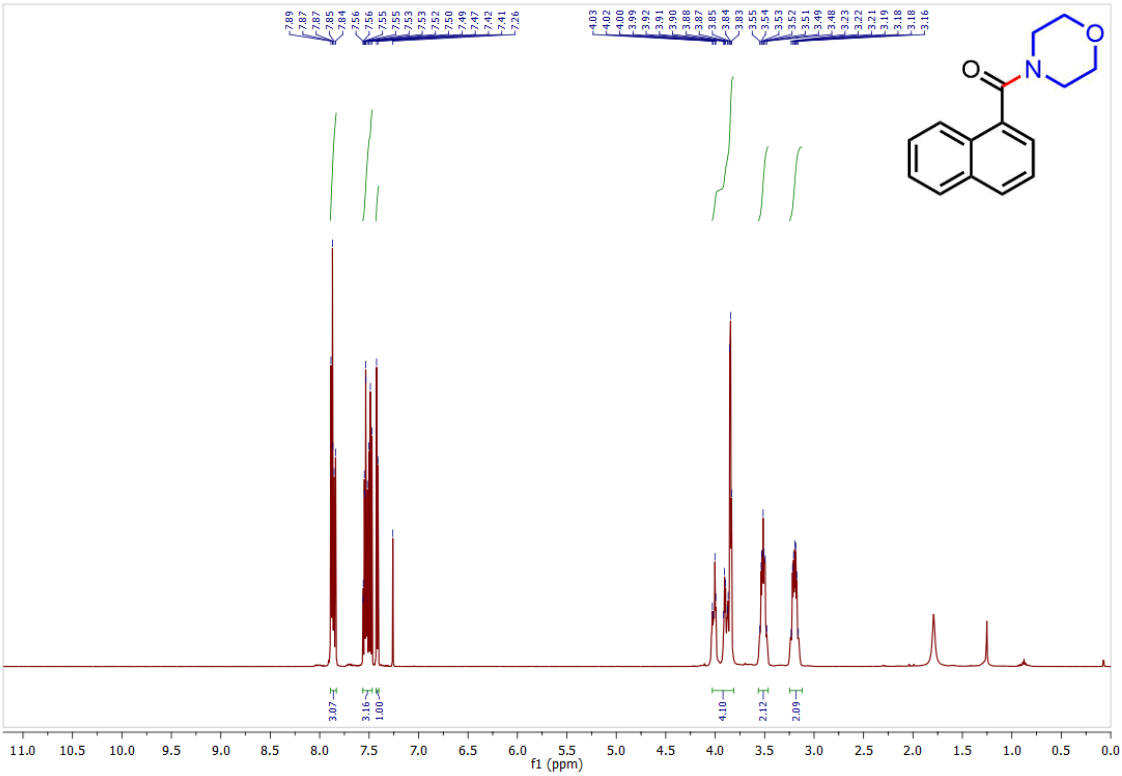

Figure A39 ^{1}H-NMR spectrum of **3pa** ($CDCl_3$, 500 MHz)

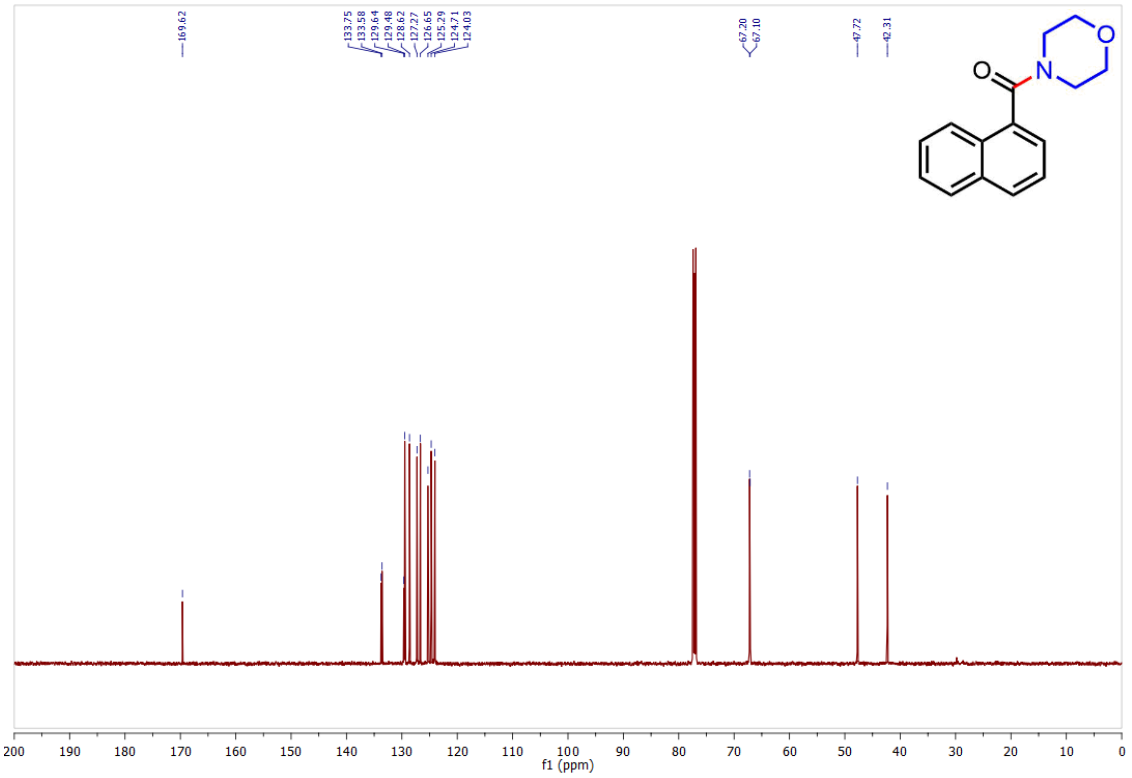

Figure A40 ^{13}C-NMR spectrum of **3pa** ($CDCl_3$, 125 MHz)

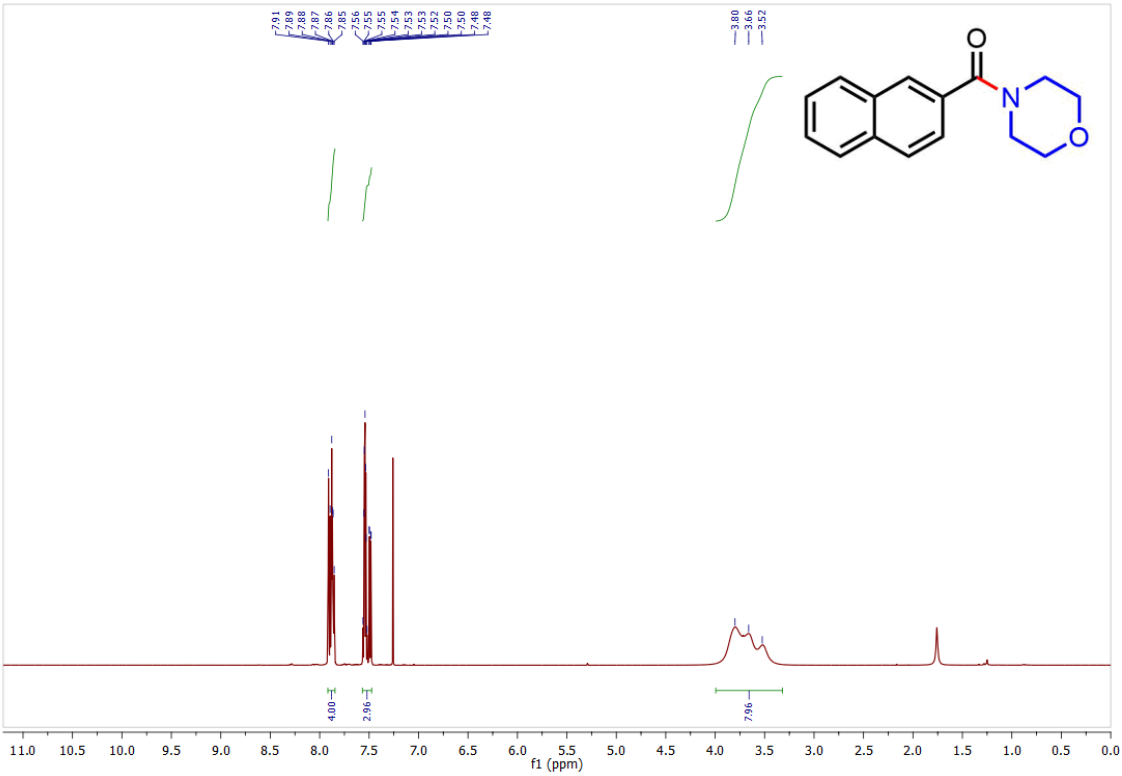

Figure A41 ^{1}H-NMR spectrum of **3qa** ($CDCl_3$, 500 MHz)

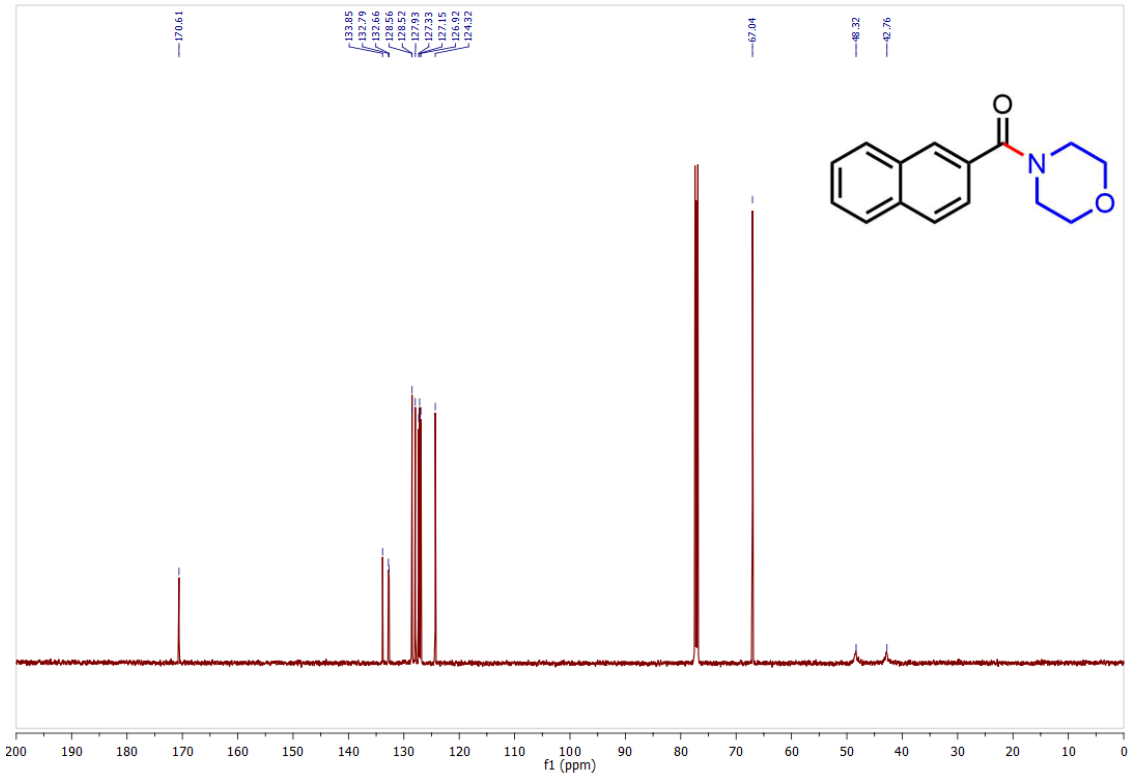

Figure A42 ^{13}C-NMR spectrum of **3qa** ($CDCl_3$, 125 MHz)

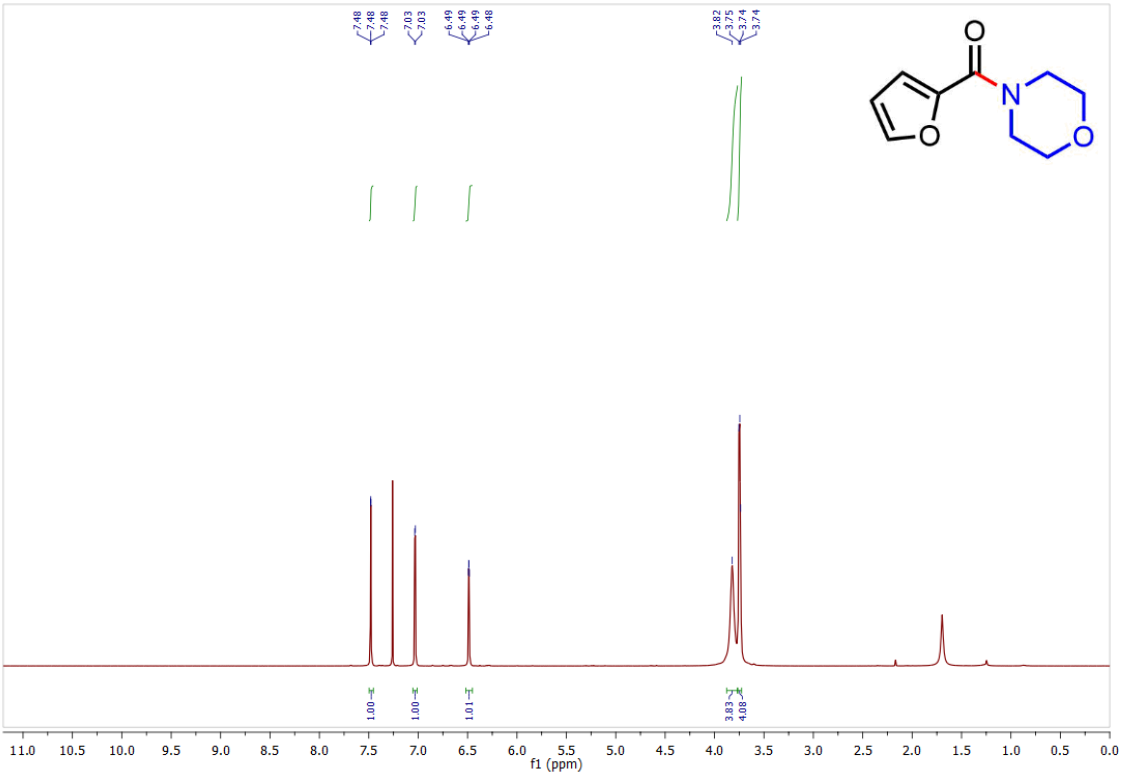

Figure A43 ^{1}H-NMR spectrum of **3ra** ($CDCl_3$, 500 MHz)

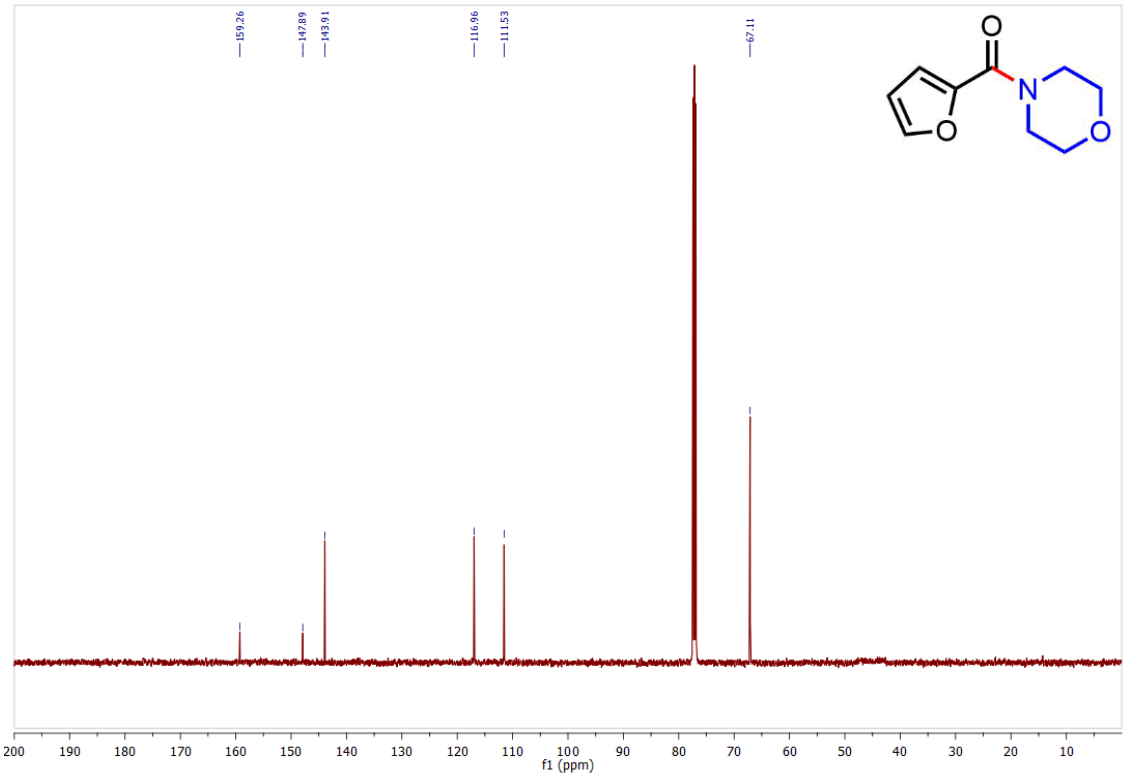

Figure A44 ^{13}C-NMR spectrum of **3ra** ($CDCl_3$, 125 MHz)

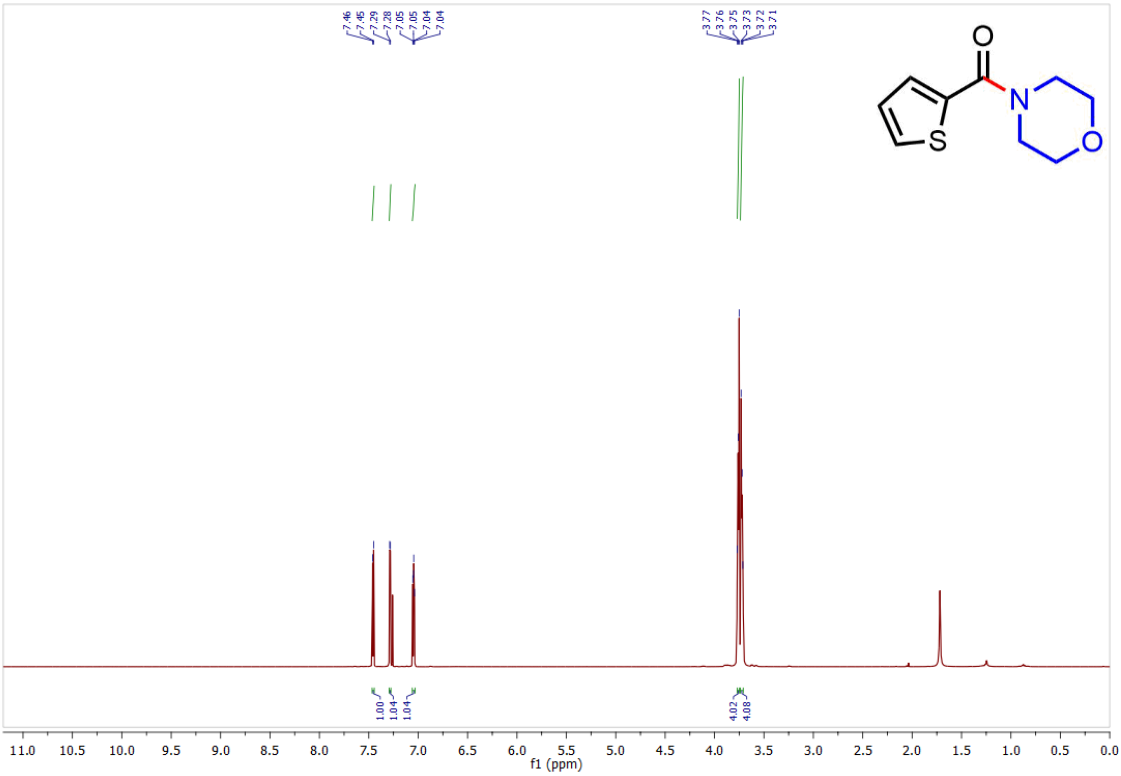

Figure A45 ^{1}H-NMR spectrum of **3sa** ($CDCl_3$, 500 MHz)

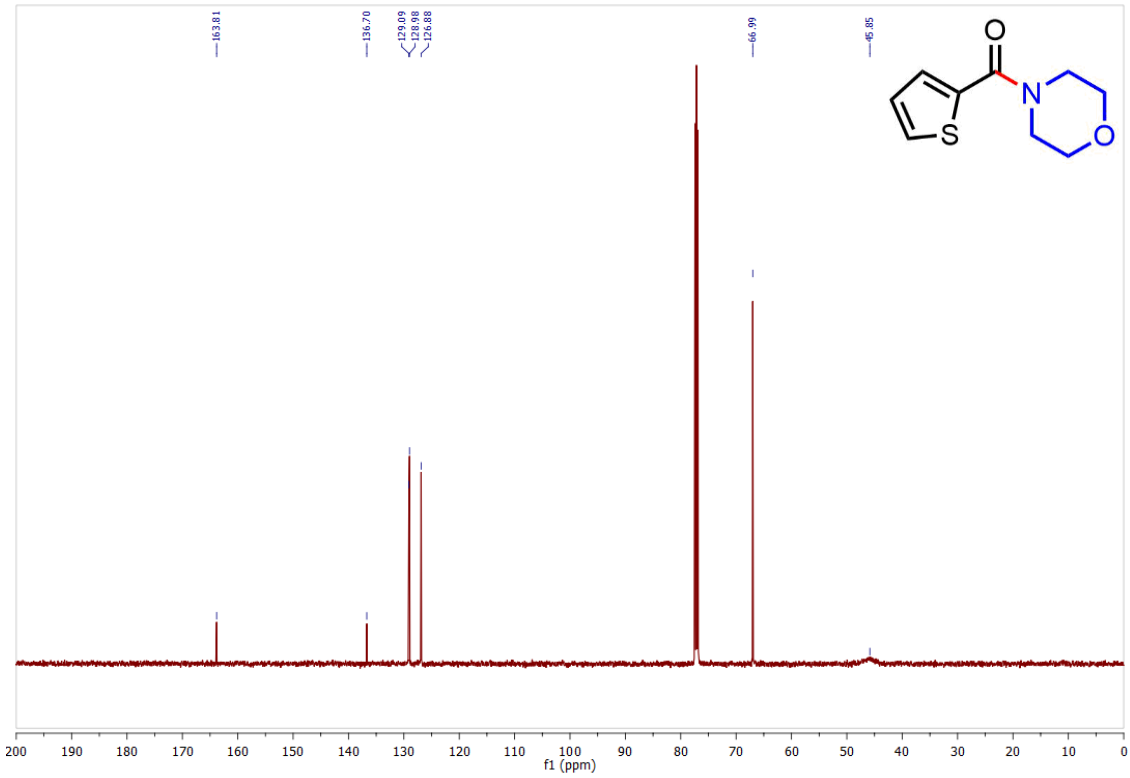

Figure A46 ^{13}C-NMR spectrum of **3sa** ($CDCl_3$, 125 MHz)

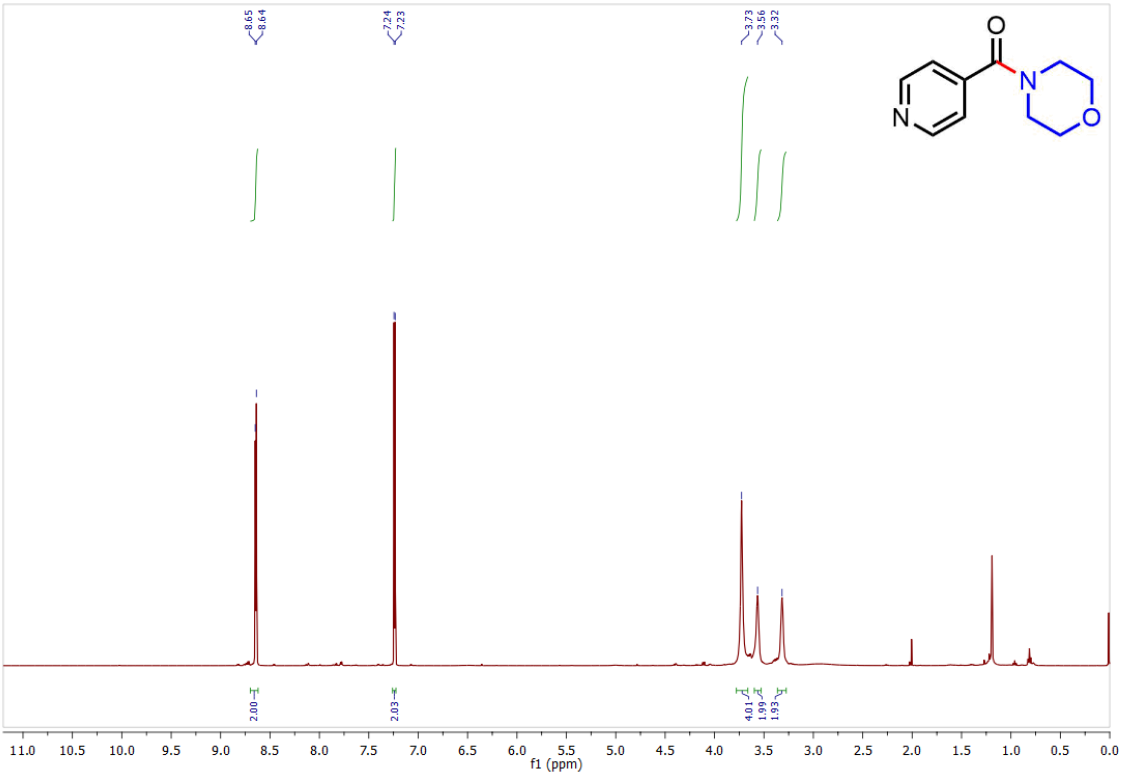

Figure A47 ^{1}H-NMR spectrum of **3ta** ($CDCl_3$, 500 MHz)

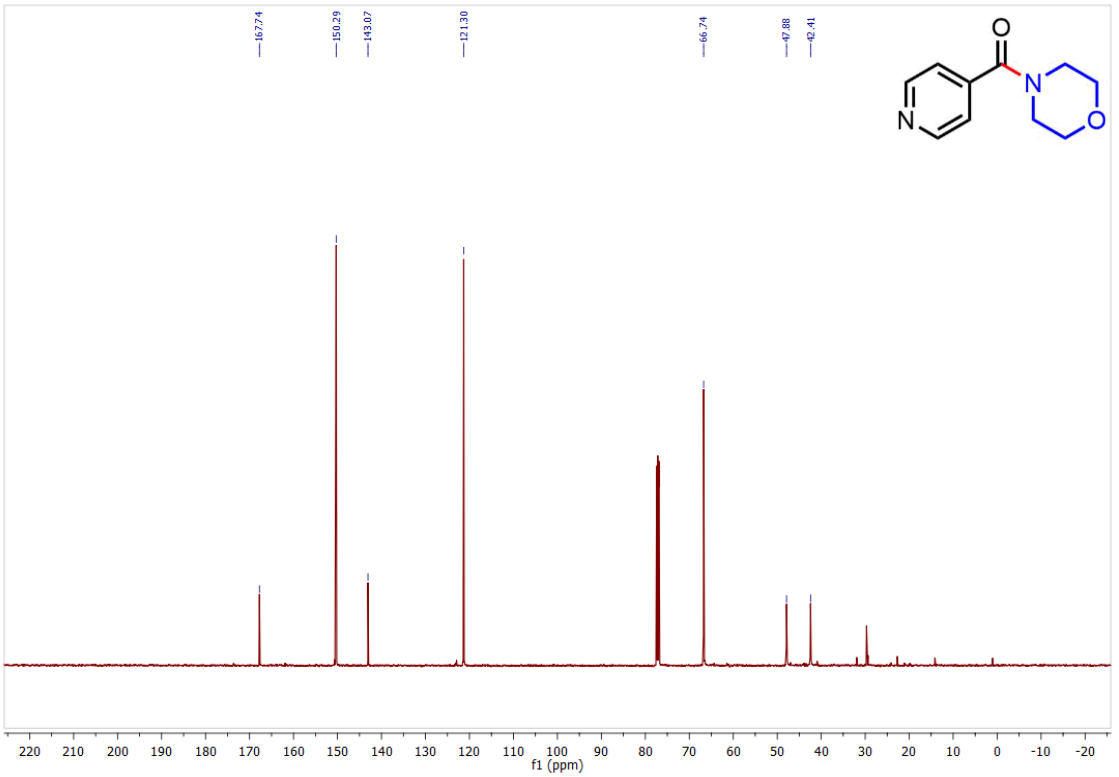

Figure A48 ^{13}C-NMR spectrum of **3ta** ($CDCl_3$, 125 MHz)

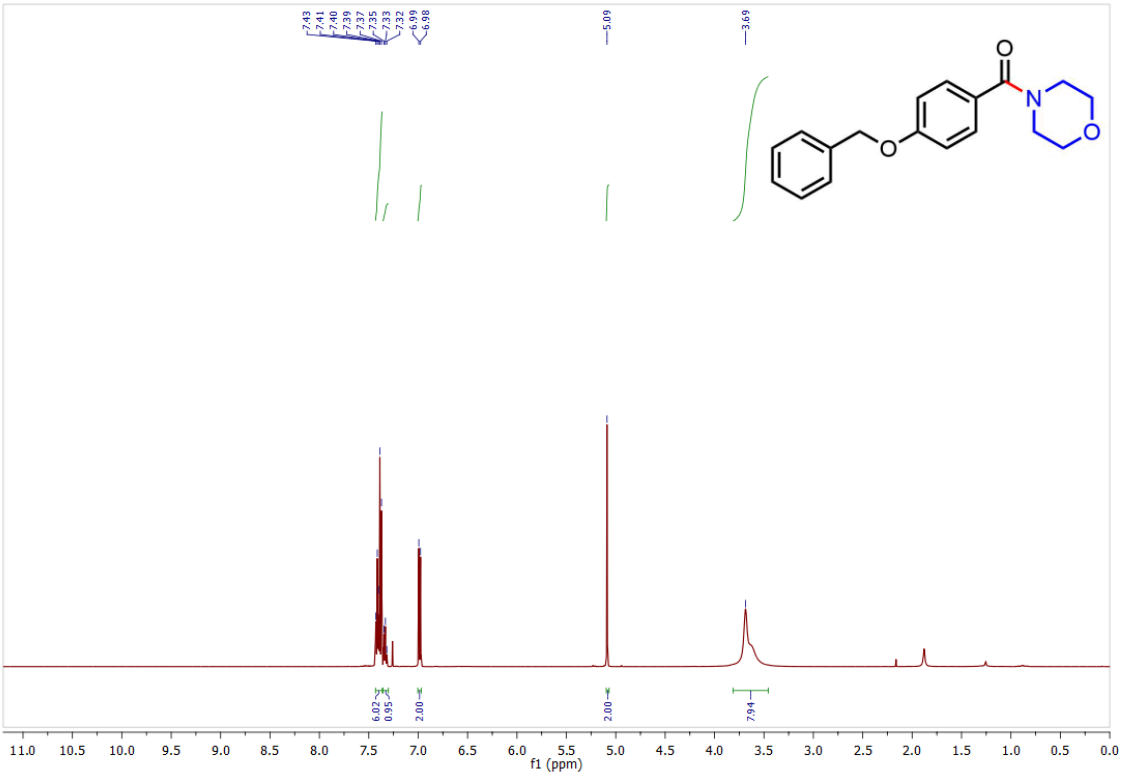

Figure A49 ^{1}H-NMR spectrum of **3va** ($CDCl_3$, 500 MHz)

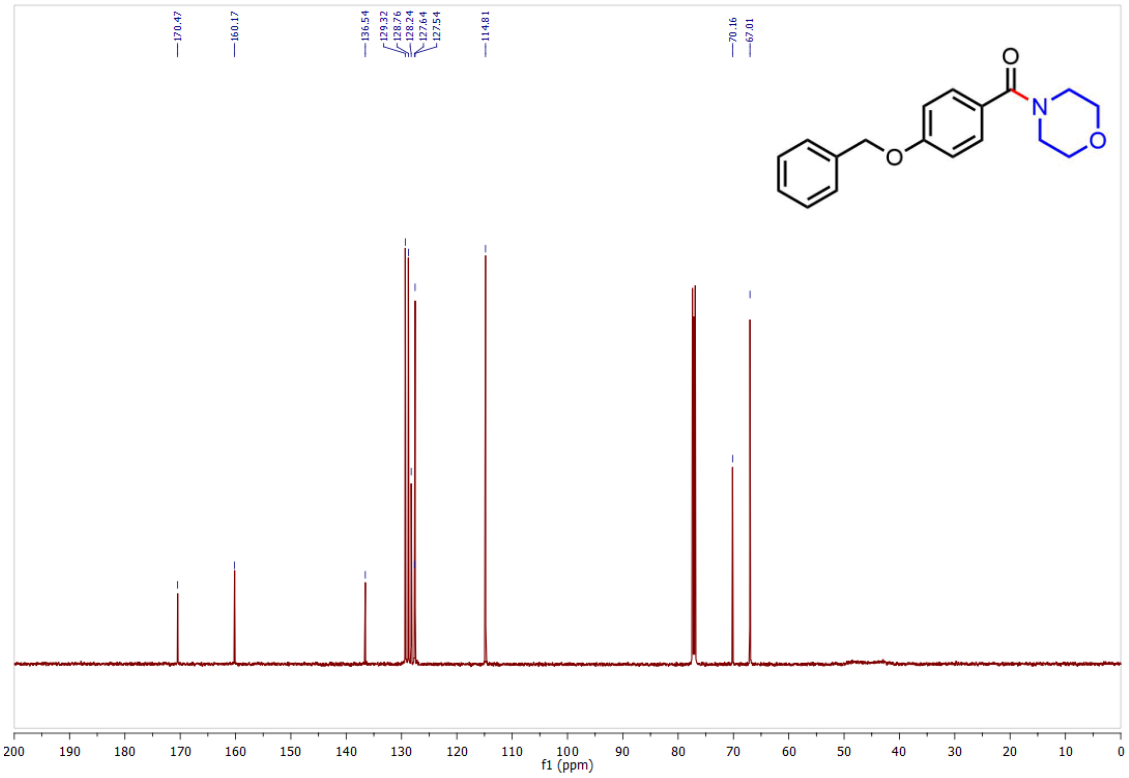

Figure A50 ^{13}C-NMR spectrum of **3va** ($CDCl_3$, 125 MHz)

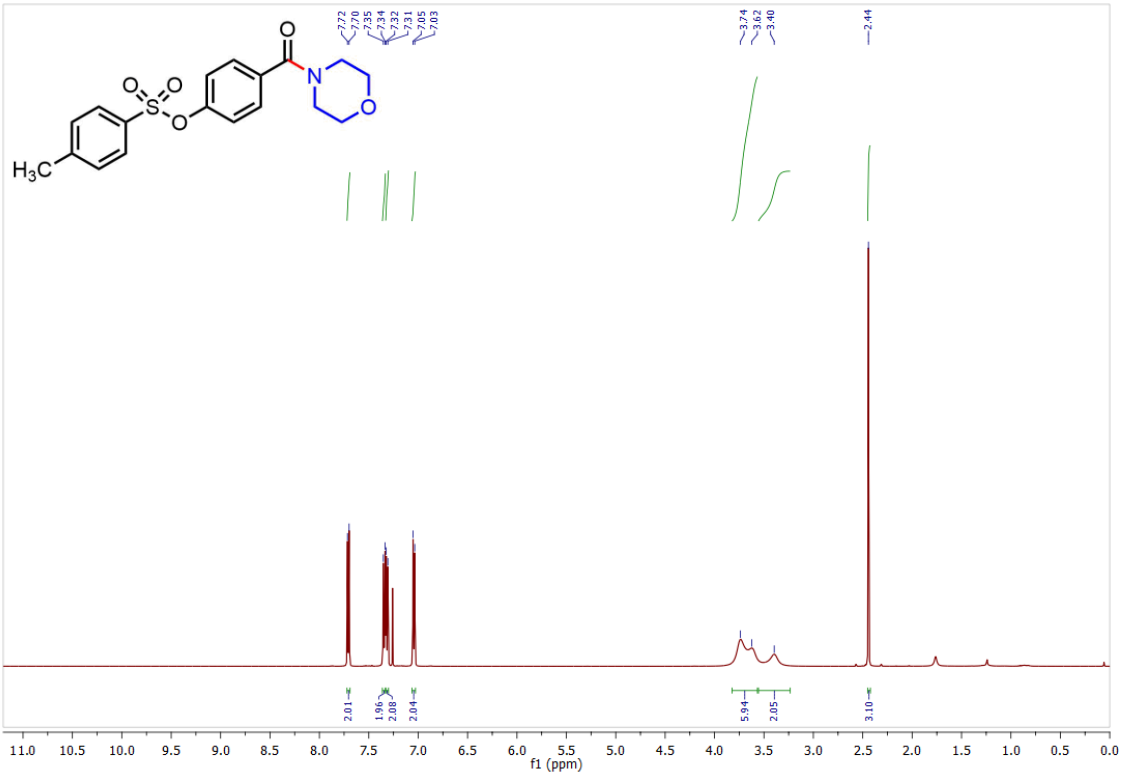

Figure A51 ^{1}H-NMR spectrum of **3wa** ($CDCl_3$, 500 MHz)

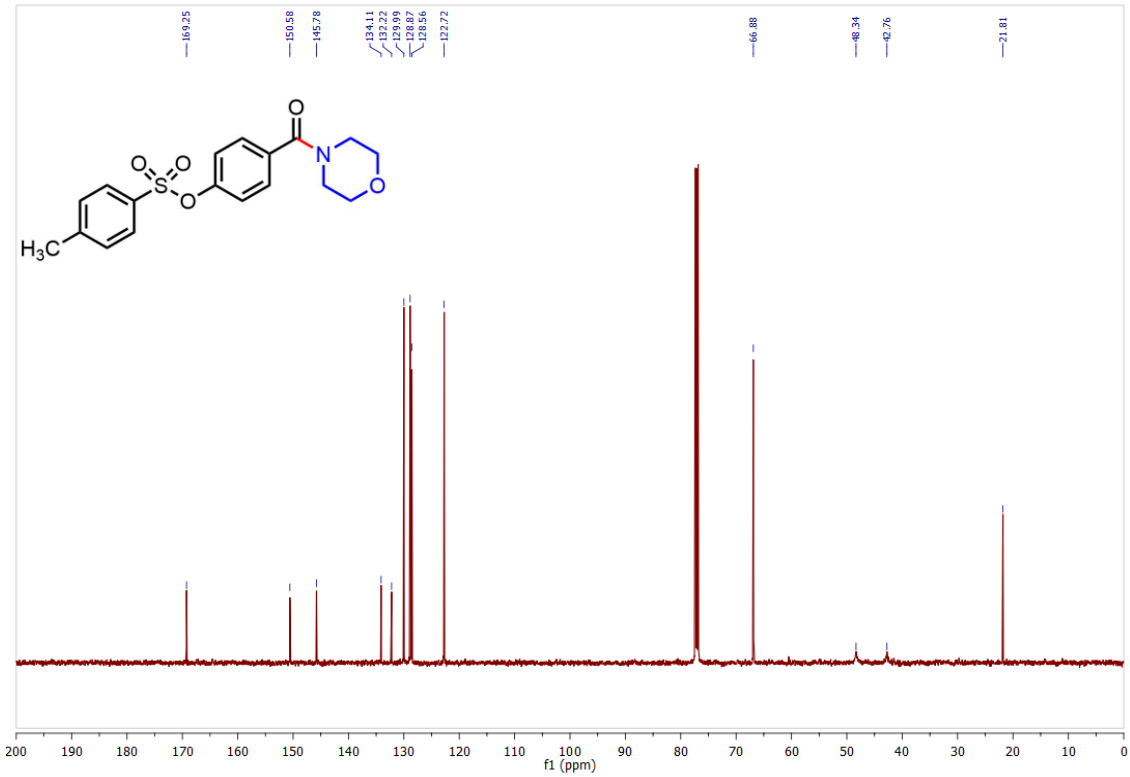

Figure A52 ^{13}C-NMR spectrum of **3wa** ($CDCl_3$, 125 MHz)

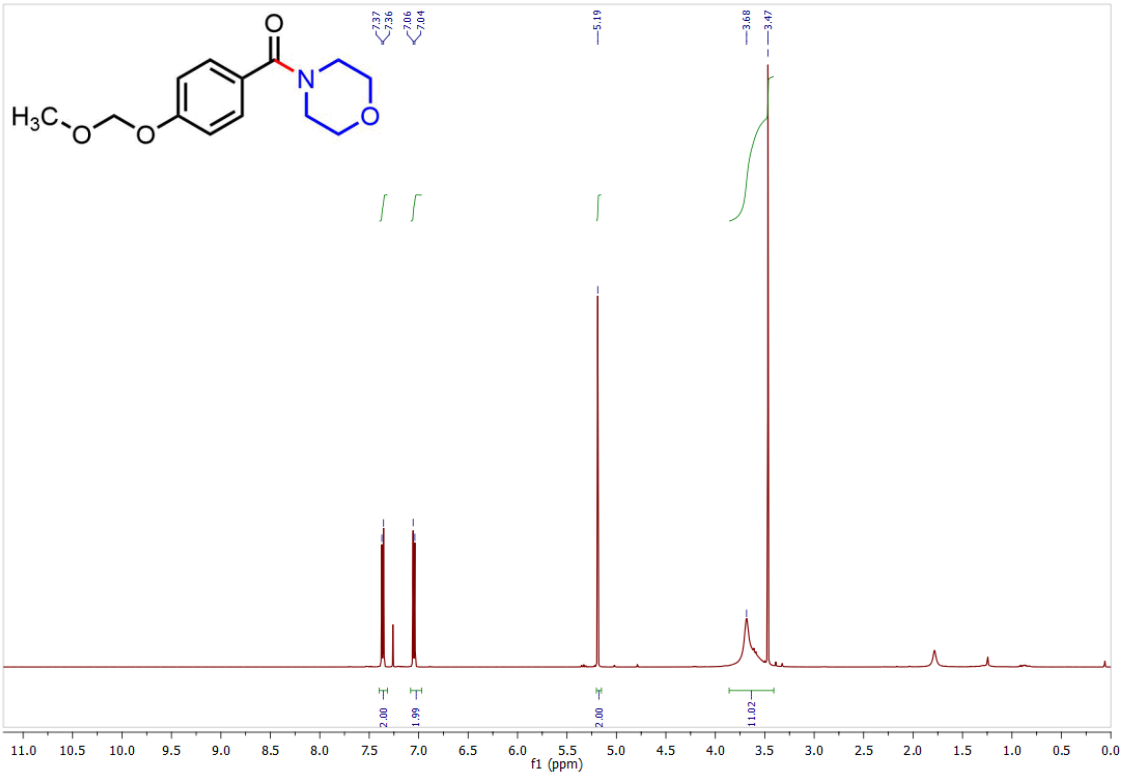

Figure A53 ^{1}H-NMR spectrum of **3xa** ($CDCl_3$, 500 MHz)

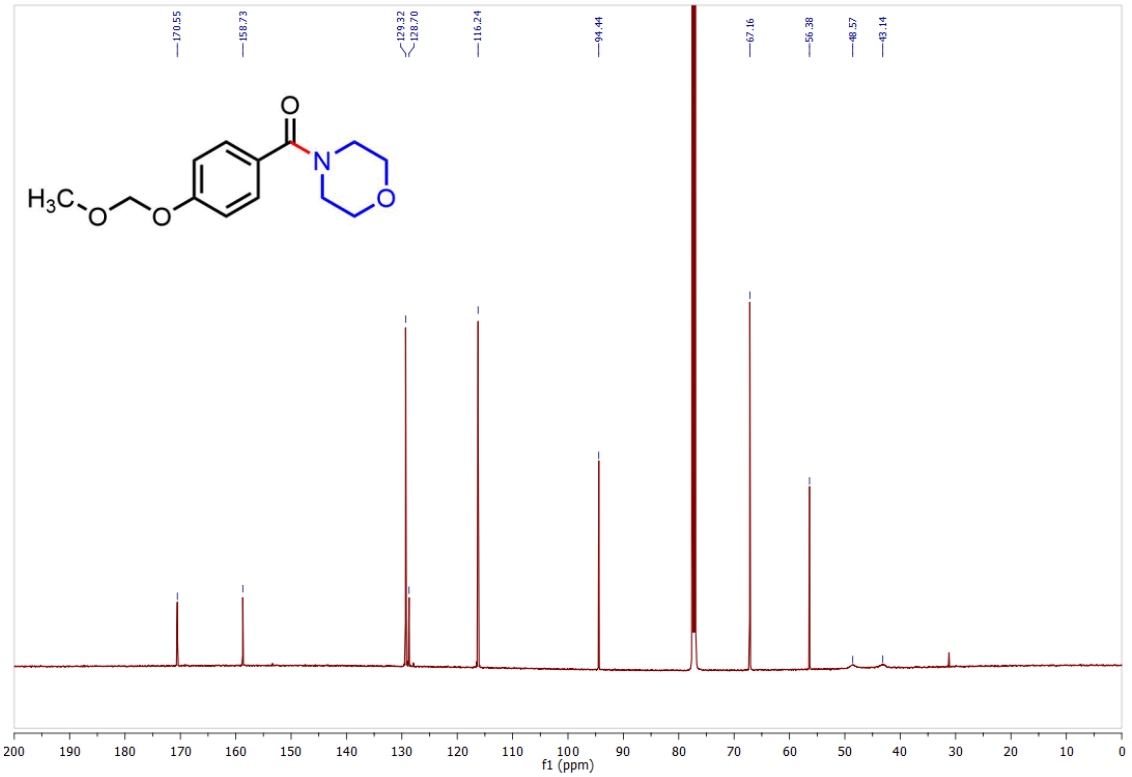

Figure A54 ^{13}C-NMR spectrum of **3xa** ($CDCl_3$, 125 MHz)

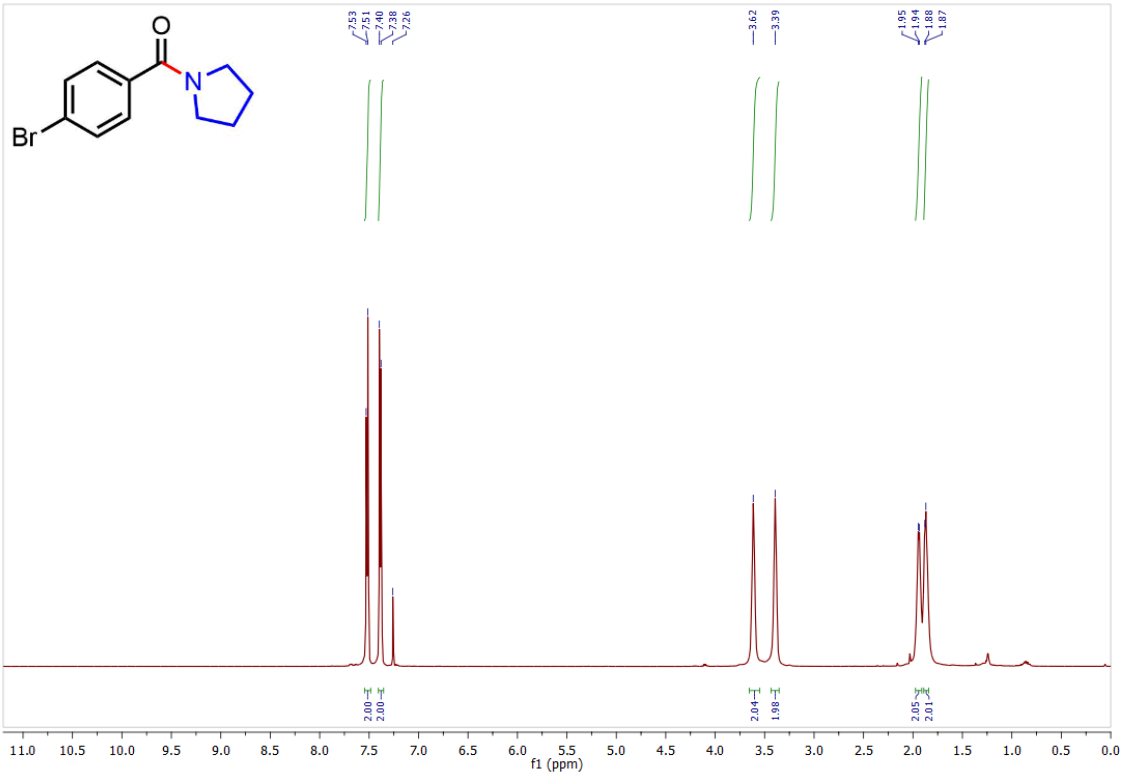

Figure A55 ^{1}H-NMR spectrum of **3ab** ($CDCl_3$, 500 MHz)

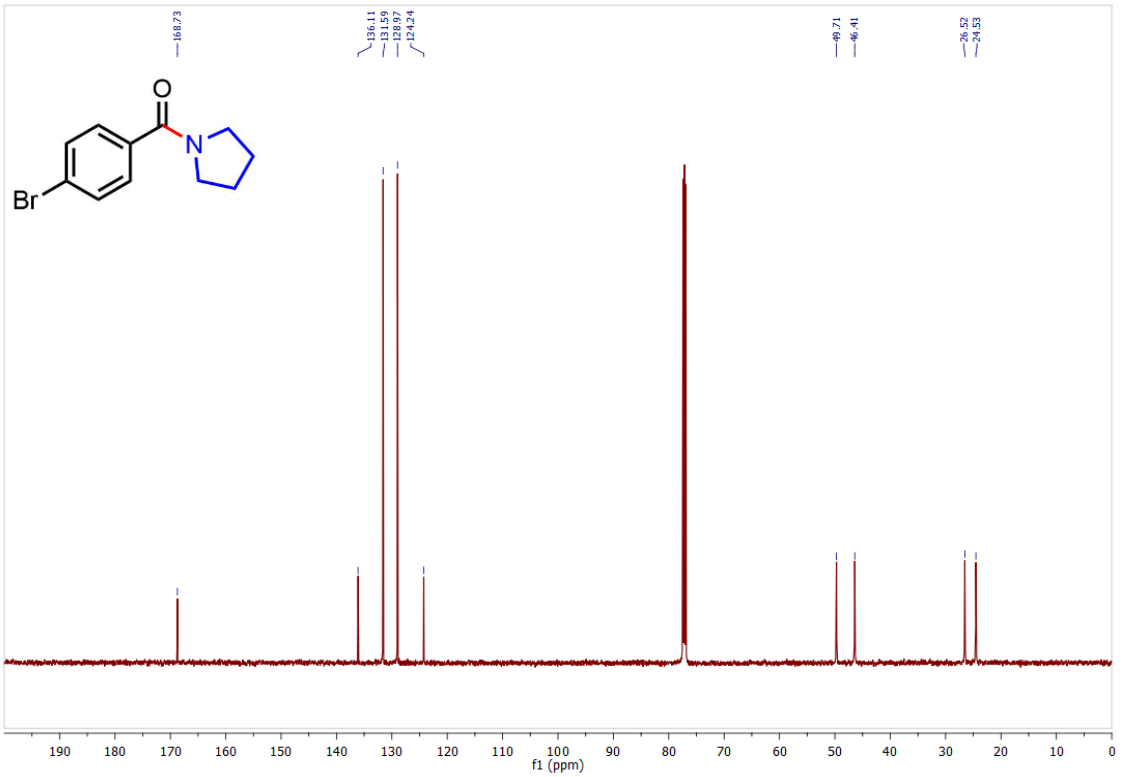

Figure A56 ^{13}C-NMR spectrum of **3ab** ($CDCl_3$, 125 MHz)

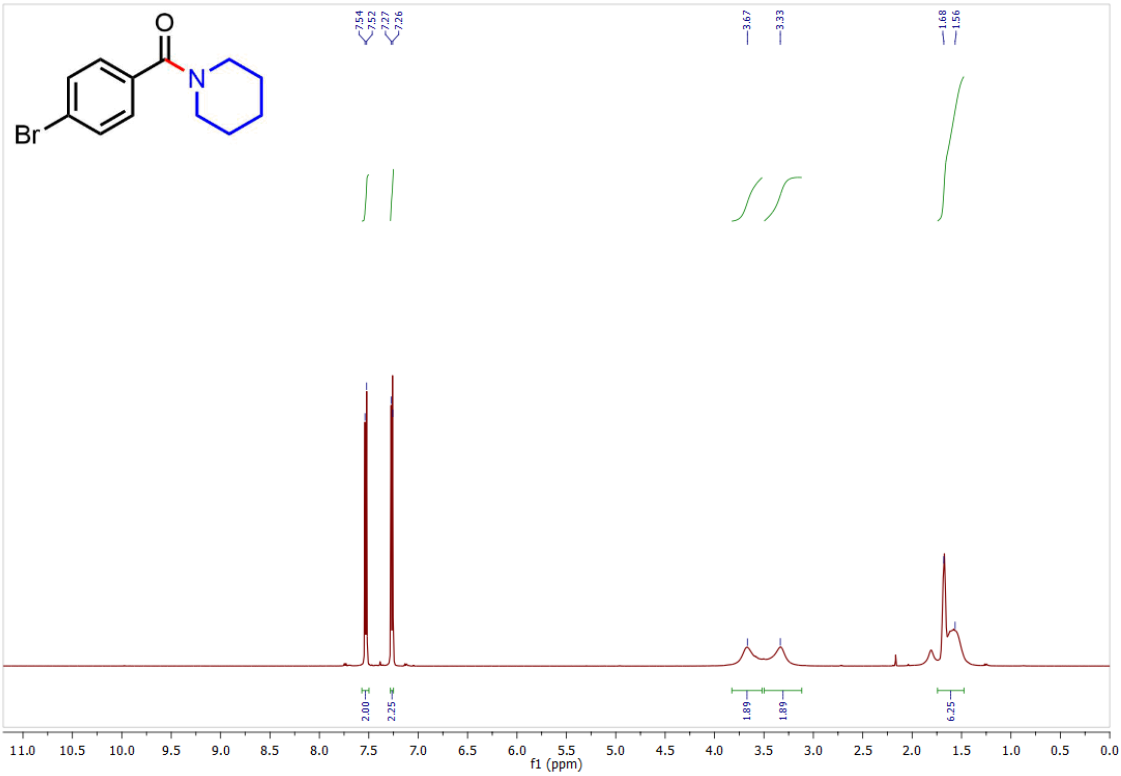

Figure A57 ^{1}H-NMR spectrum of **3ac** ($CDCl_3$, 500 MHz)

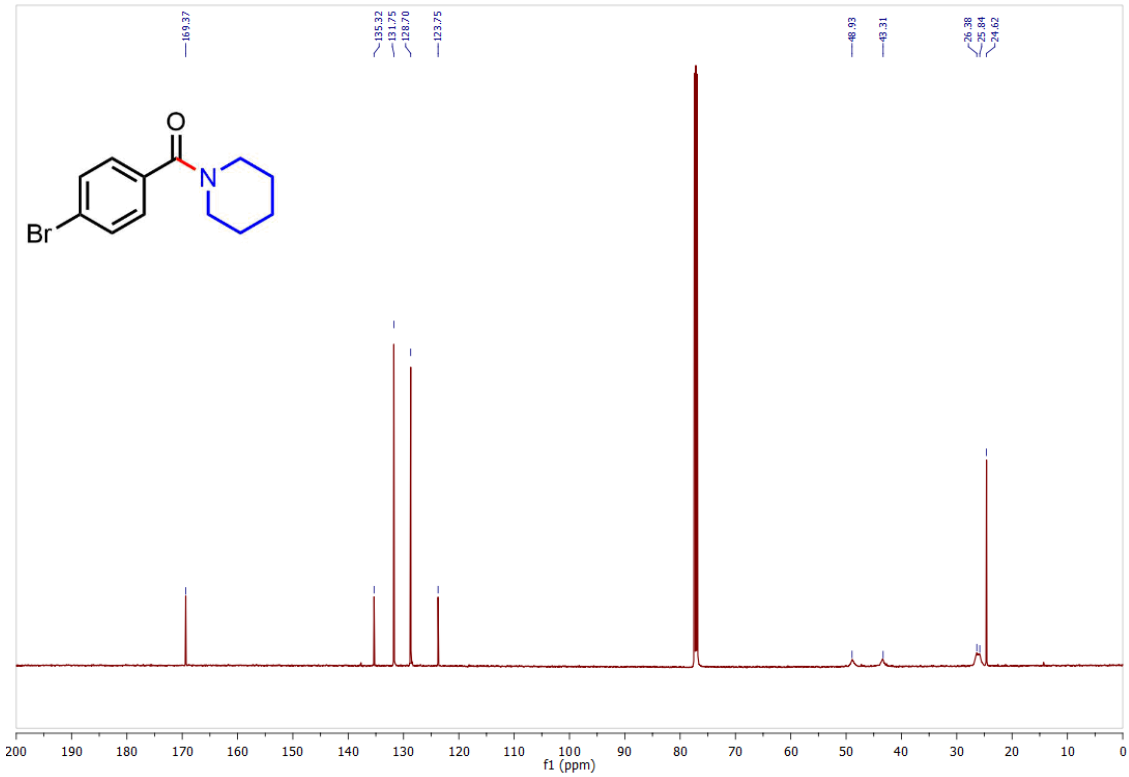

Figure A58 ^{13}C-NMR spectrum of **3ac** ($CDCl_3$, 125 MHz)

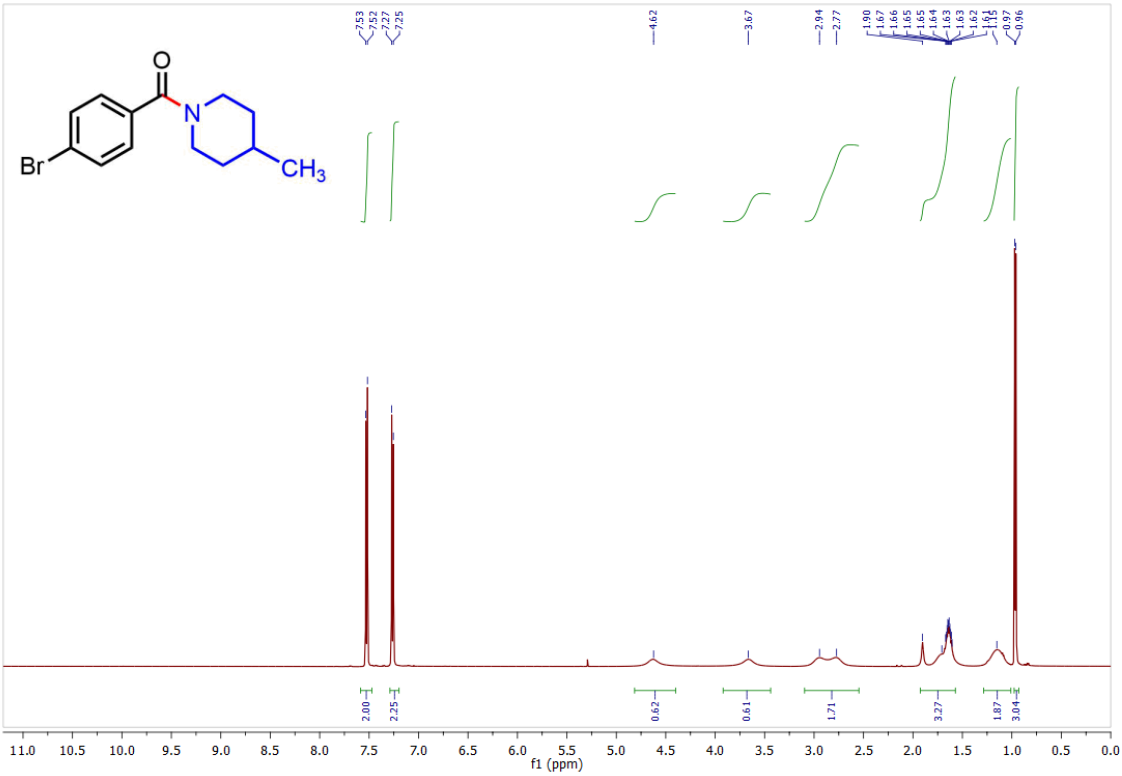

Figure A59 ^{1}H-NMR spectrum of **3ad** ($CDCl_3$, 500 MHz)

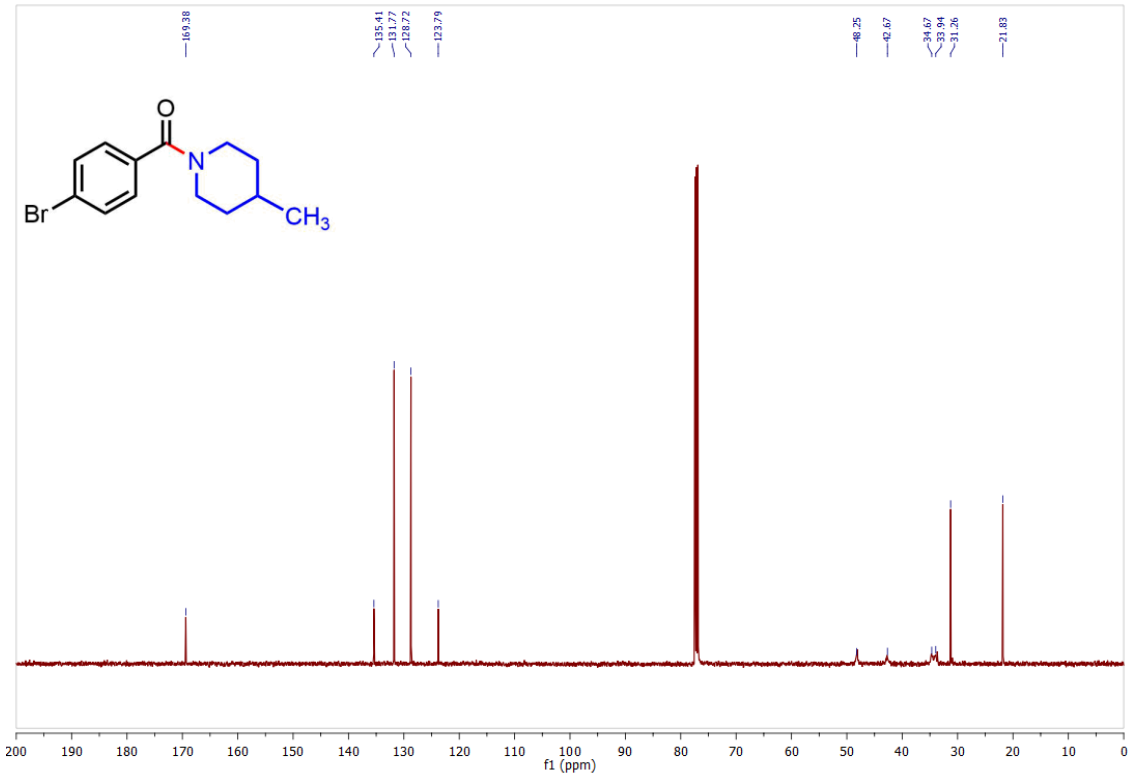

Figure A60 ^{13}C-NMR spectrum of **3ad** ($CDCl_3$, 125 MHz)

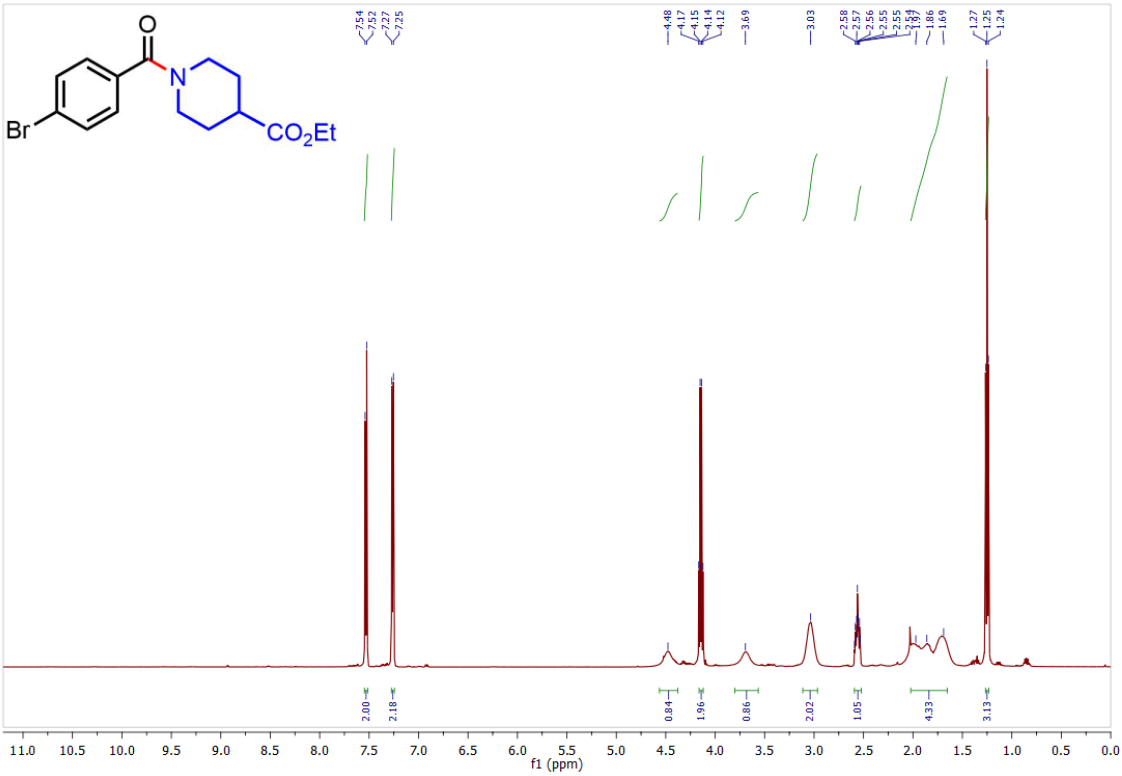

Figure A61 ^{1}H-NMR spectrum of **3ae** ($CDCl_3$, 500 MHz)

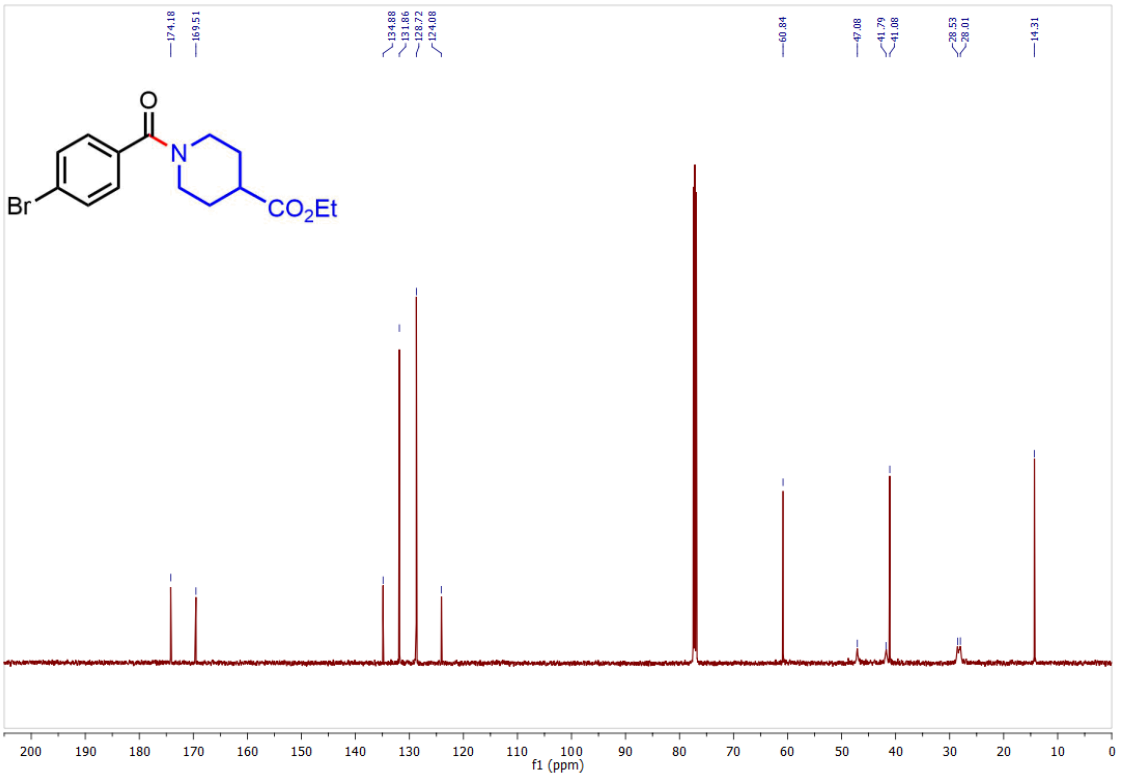

Figure A62 ^{13}C-NMR spectrum of **3ae** ($CDCl_3$, 125 MHz)

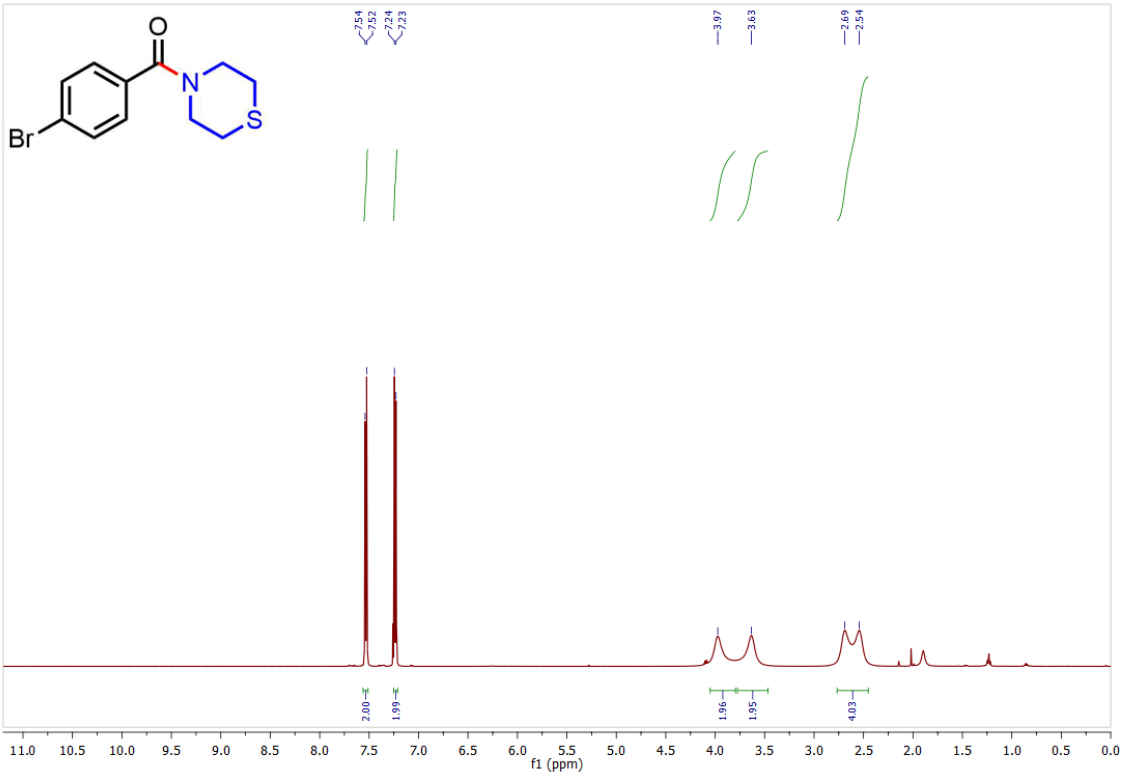

Figure A63 ^{1}H-NMR spectrum of **3af** ($CDCl_3$, 500 MHz)

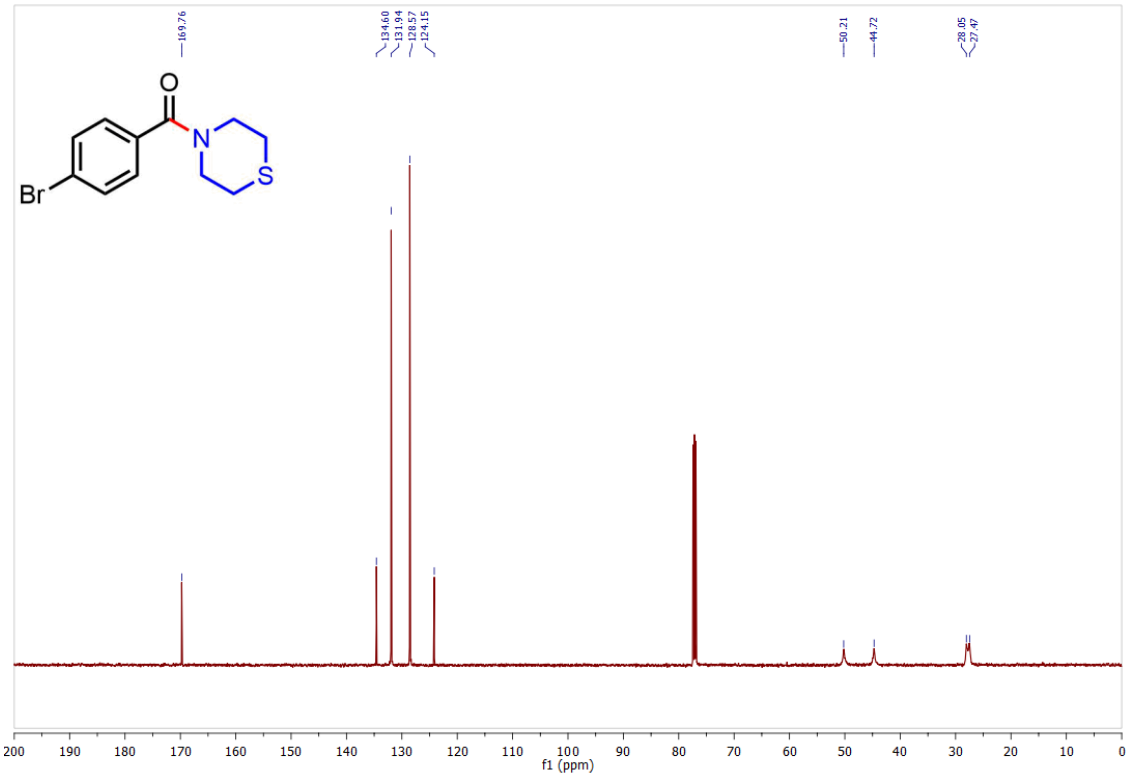

Figure A64 ^{13}C-NMR spectrum of **3af** ($CDCl_3$, 125 MHz)

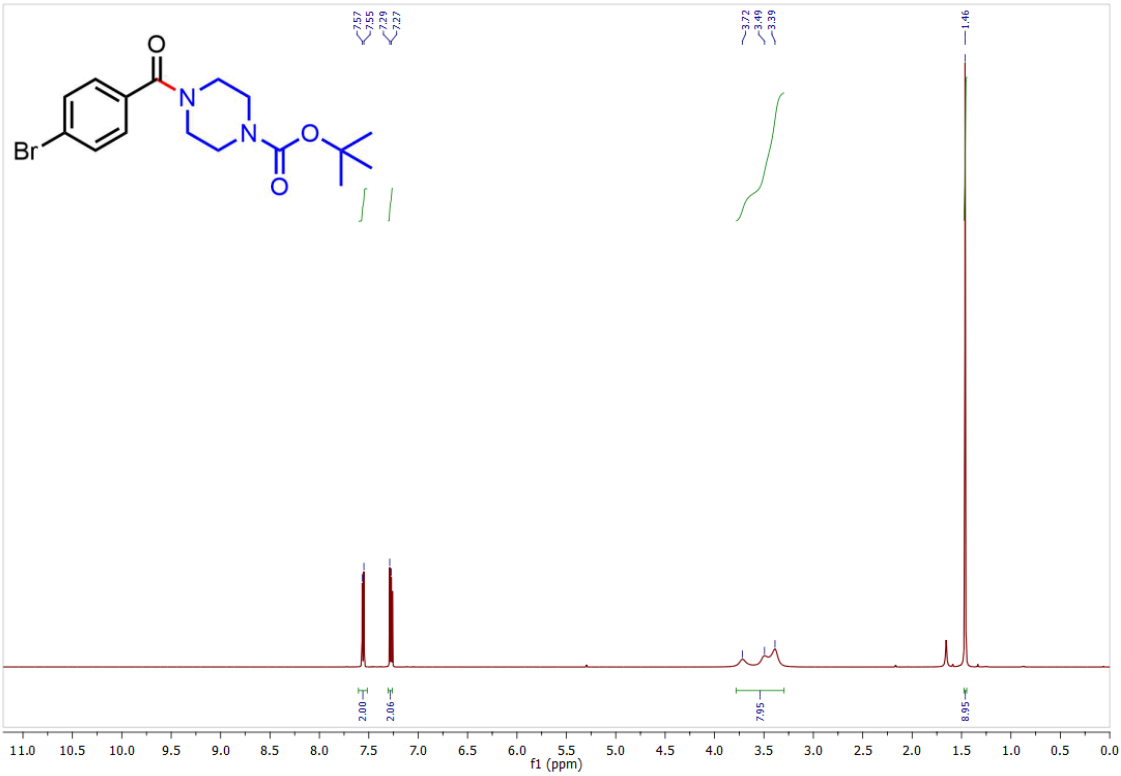

Figure A65 ^{1}H-NMR spectrum of **3ag** ($CDCl_3$, 500 MHz)

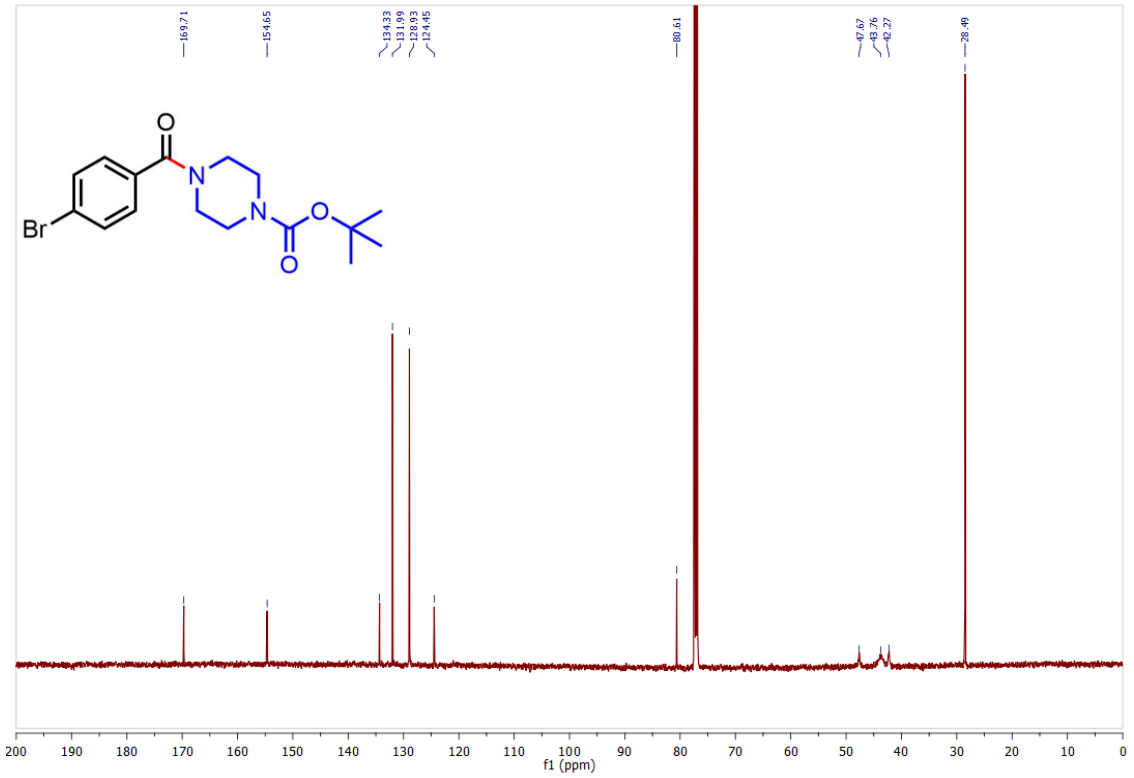

Figure A66 ^{13}C-NMR spectrum of **3ag** ($CDCl_3$, 125 MHz)

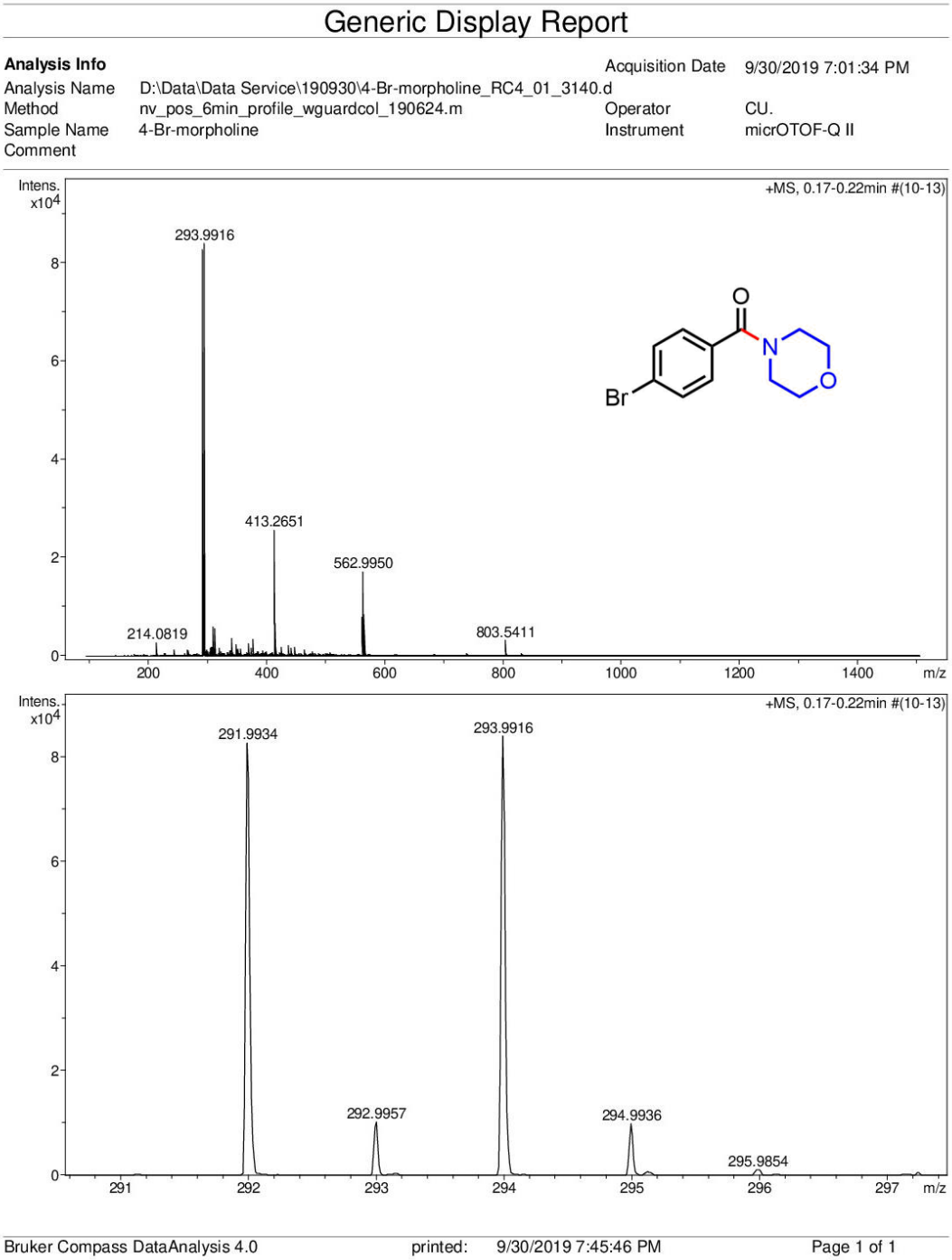

Figure A67 ESI-HRMS spectrum of **3aa**

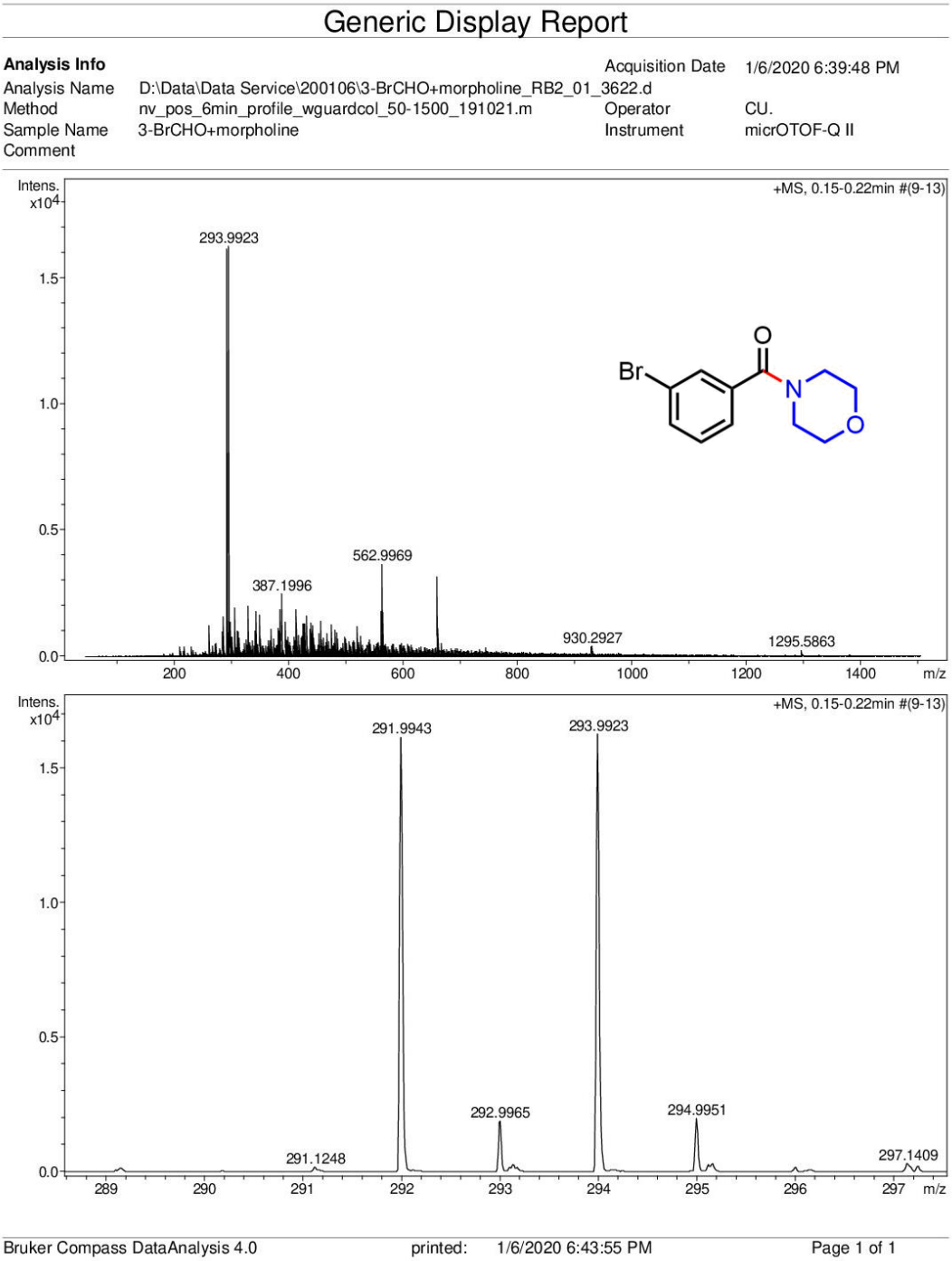

Figure A68 ESI-HRMS spectrum of **3ba**

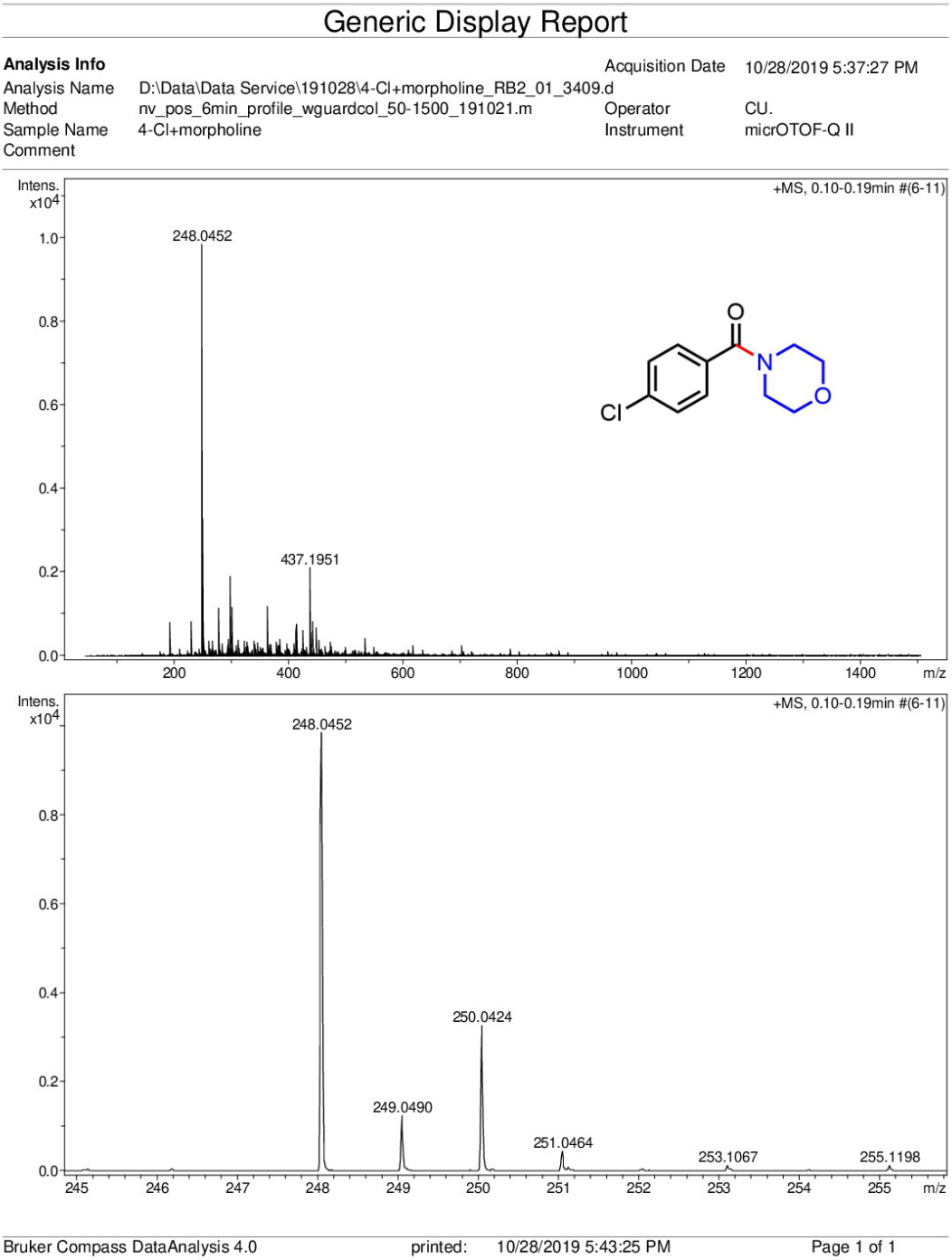

Figure A69 ESI-HRMS spectrum of **3ca**

Generic Display Report

Analysis Info

Analysis Name	D:\Data\Data Service\200309\3-Cl-CHO+morpholine_RA7_01_3805.d	Acquisition Date	3/9/2020 3:34:06 PM
Method	nv_pos_6min_profile_wguardcol_50-1500_191021.m	Operator	CU.
Sample Name	3-Cl-CHO+morpholine	Instrument	micrOTOF-Q II
Comment			

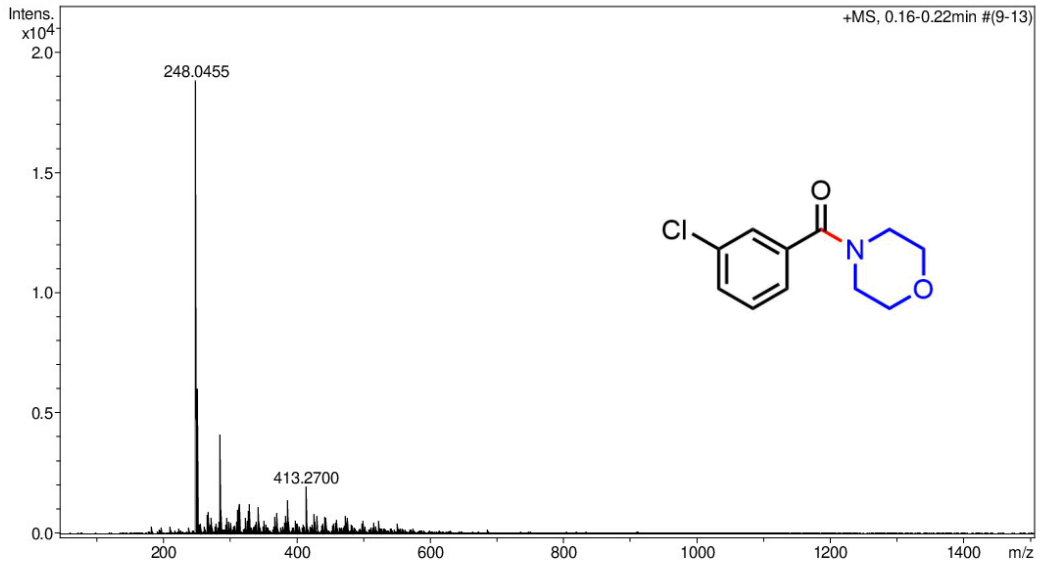

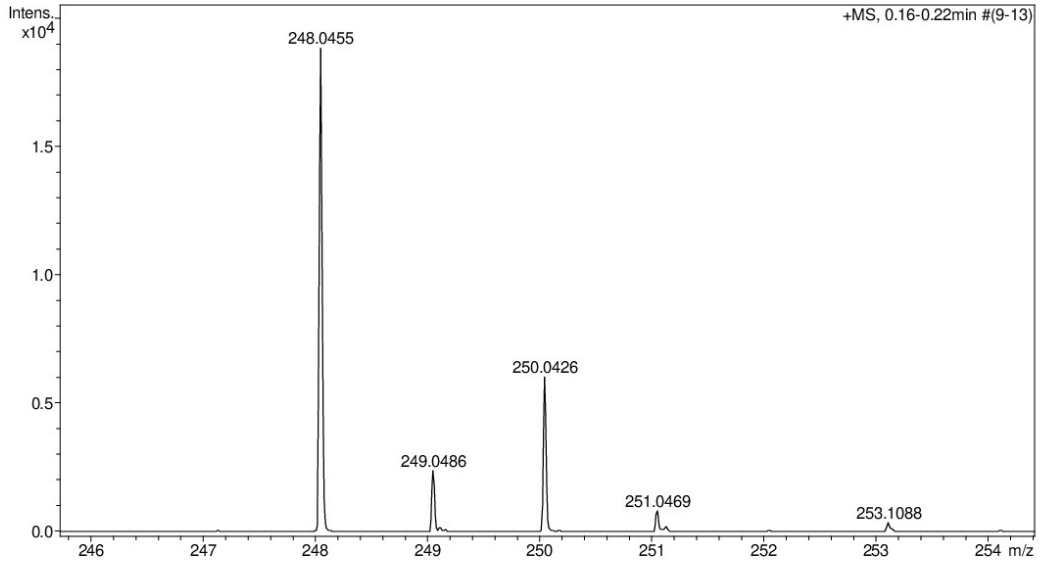

Bruker Compass DataAnalysis 4.0 printed: 3/9/2020 4:25:01 PM Page 1 of 1

Figure A70 ESI-HRMS spectrum of **3da**

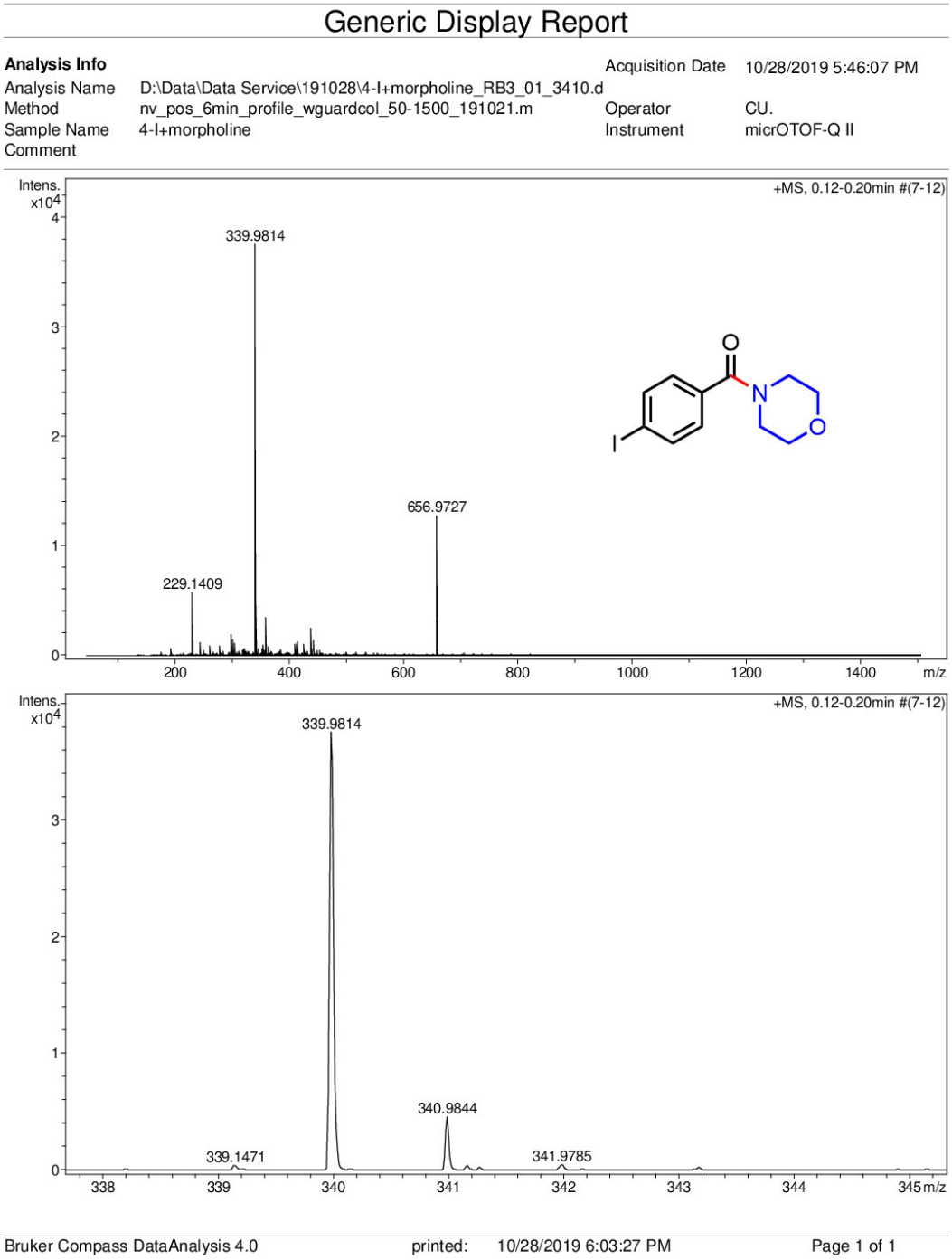

Figure A71 ESI-HRMS spectrum of **3ea**

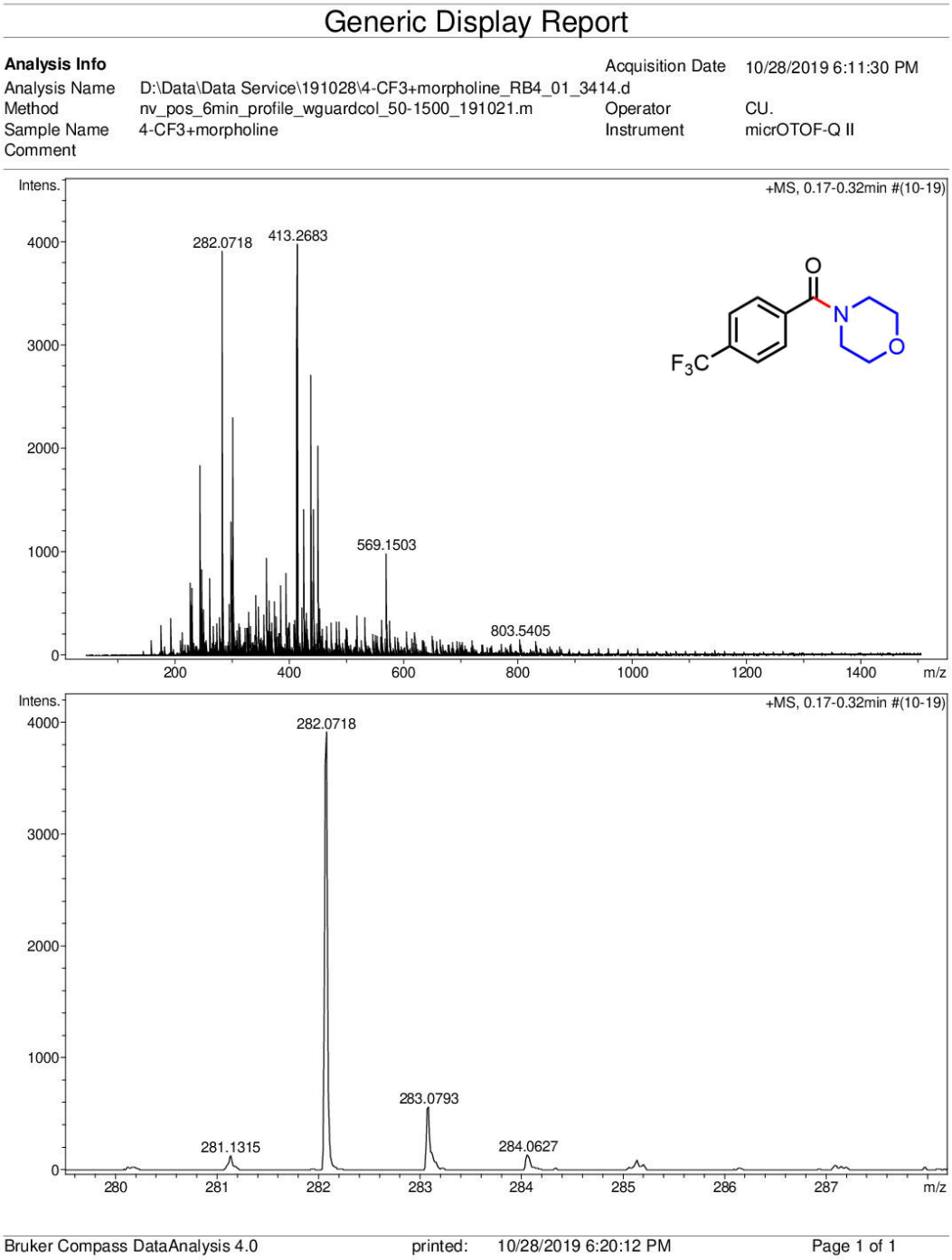

Figure A72 ESI-HRMS spectrum of **3fa**

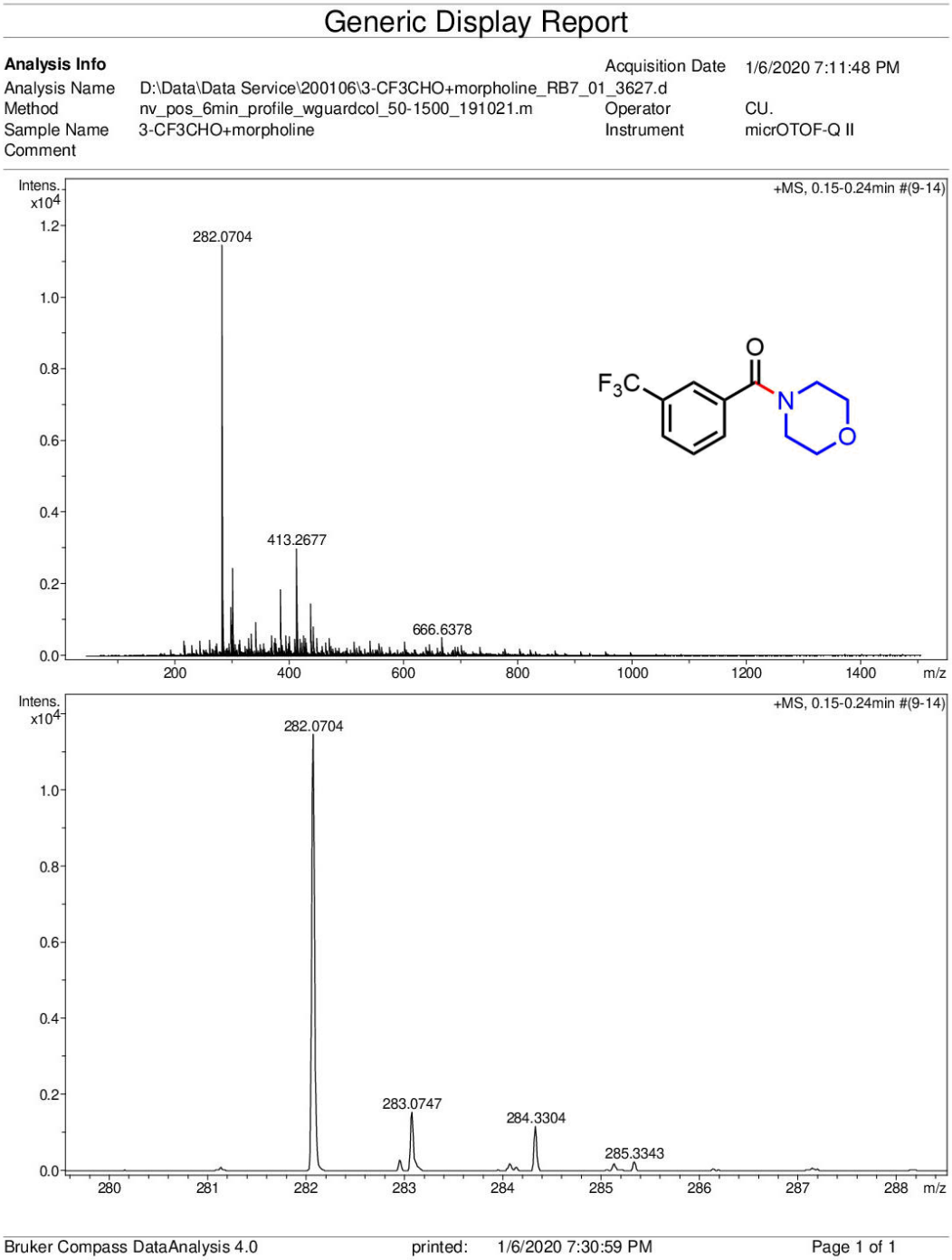

Figure A73 ESI-HRMS spectrum of **3ga**

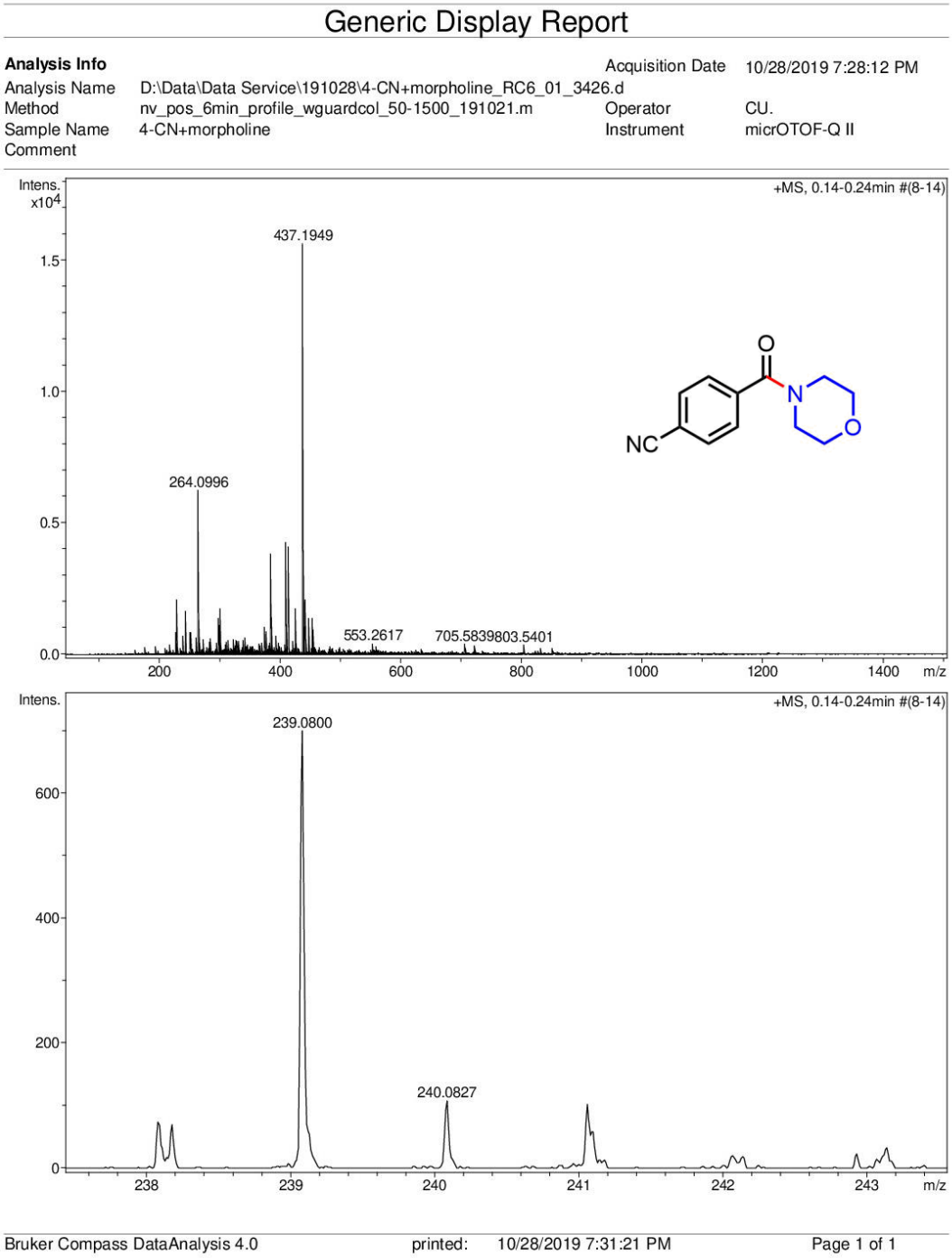

Figure A74 ESI-HRMS spectrum of **3ha**

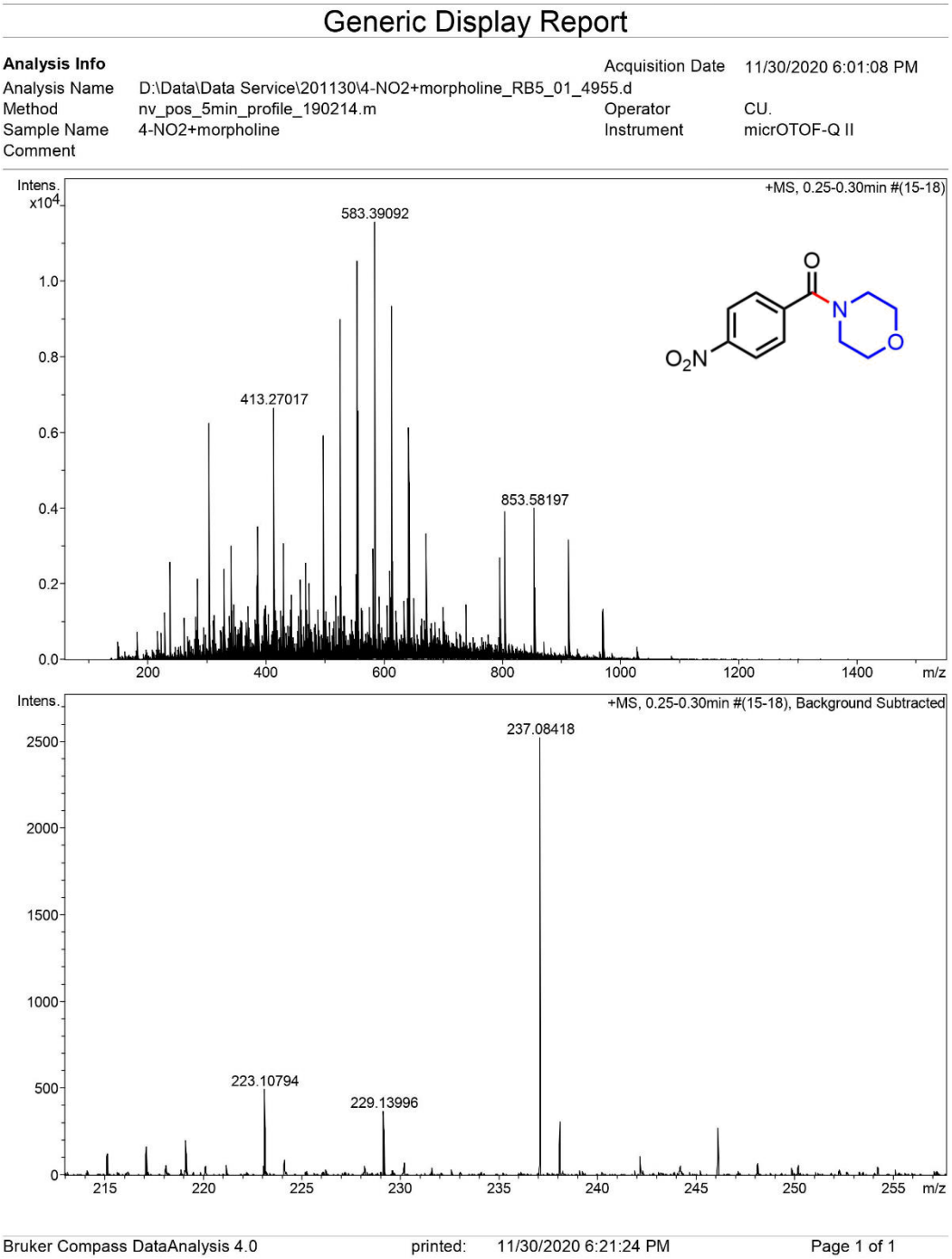

Figure A75 ESI-HRMS spectrum of **3ia**

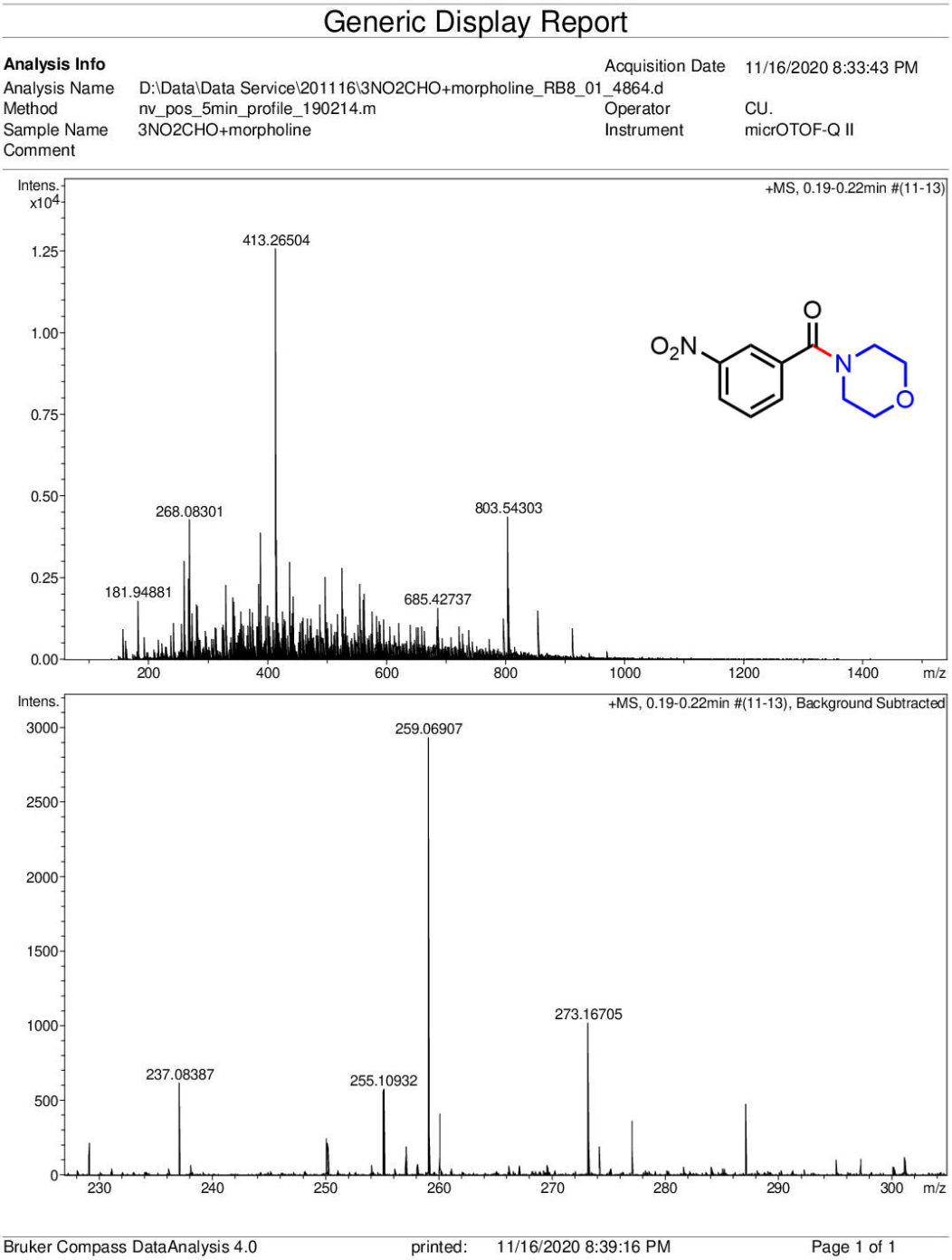

Figure A76 ESI-HRMS spectrum of **3ja**

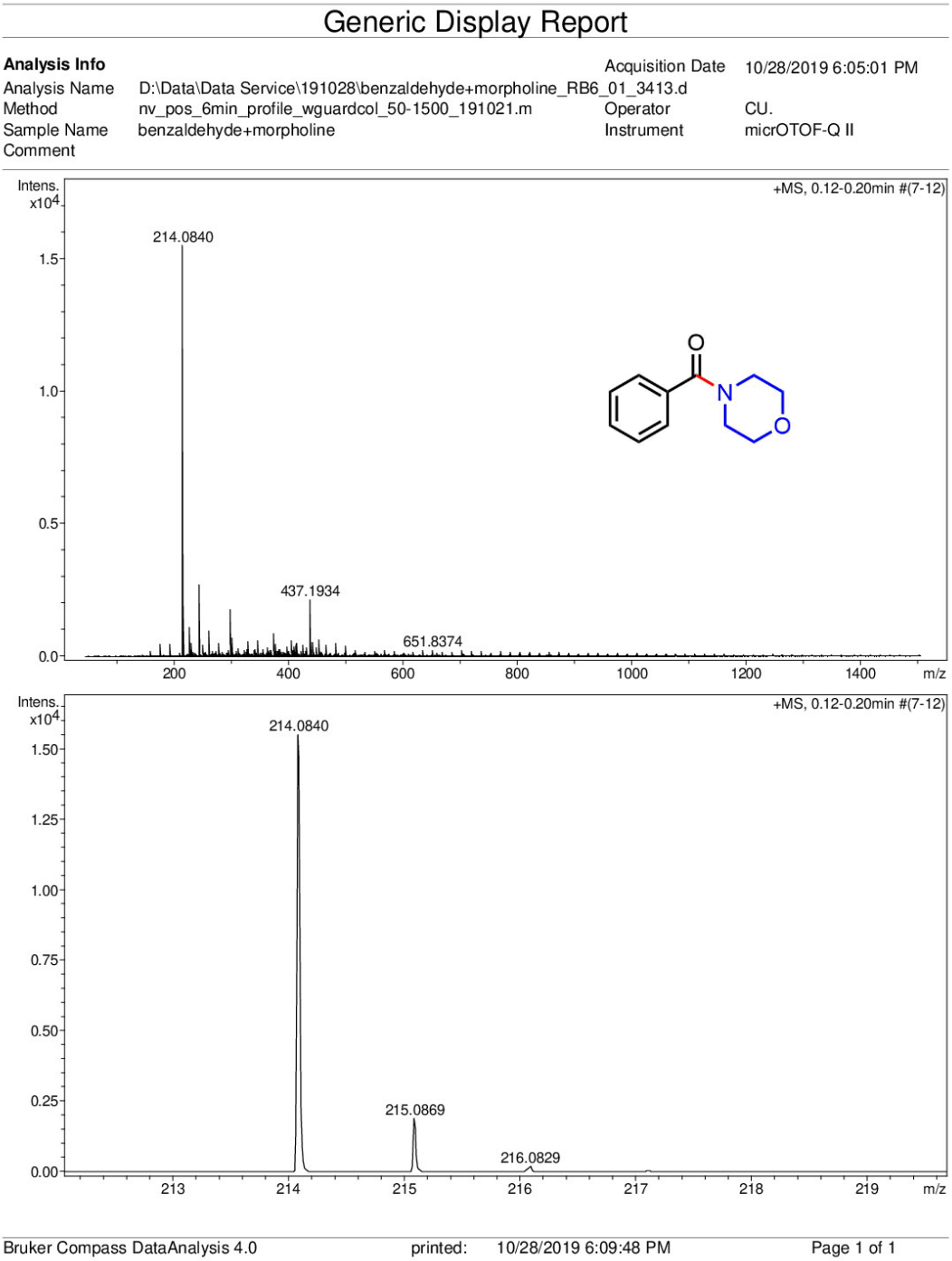

Figure A77 ESI-HRMS spectrum of **3ka**

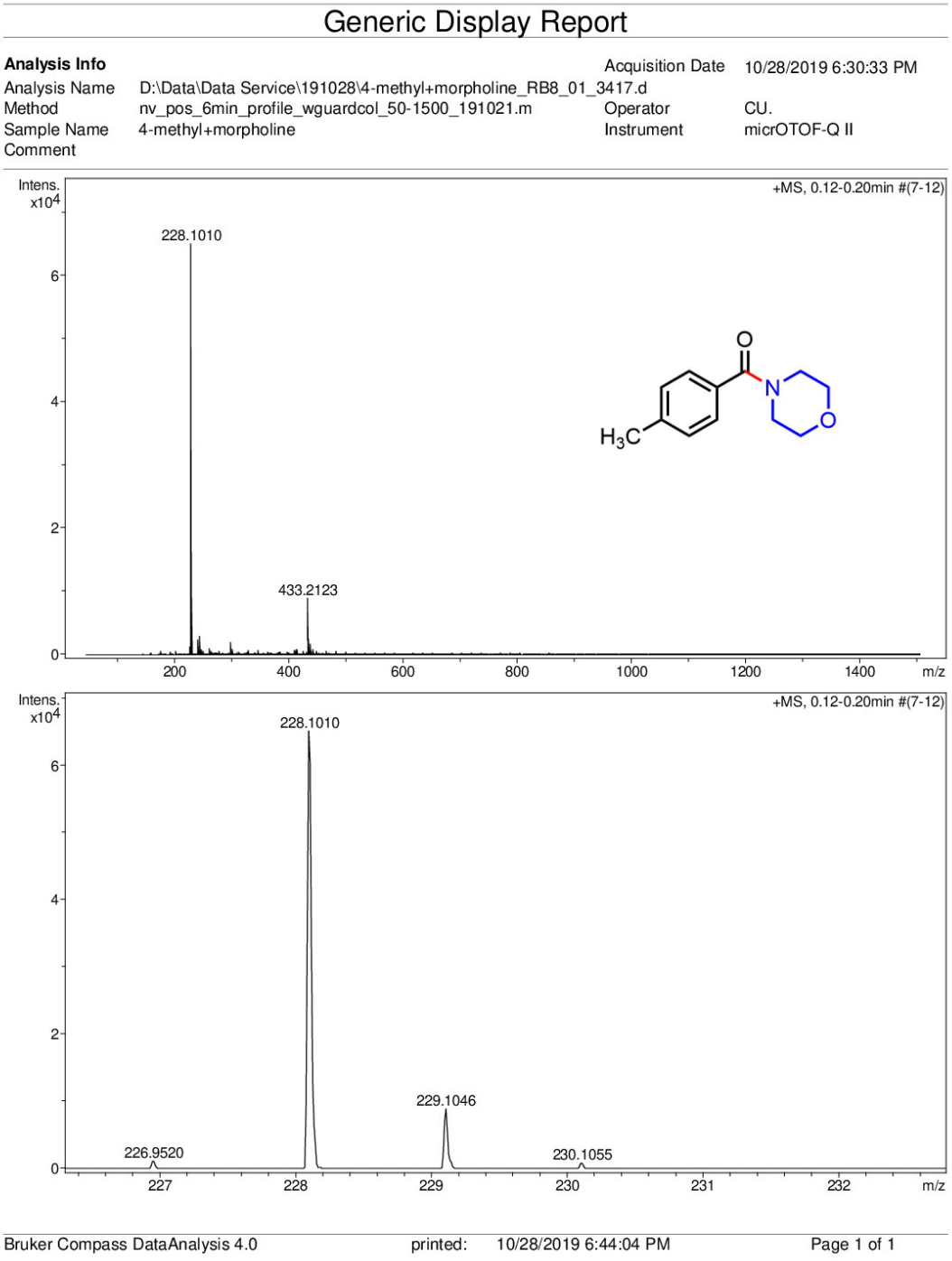

Figure A78 ESI-HRMS spectrum of **3la**

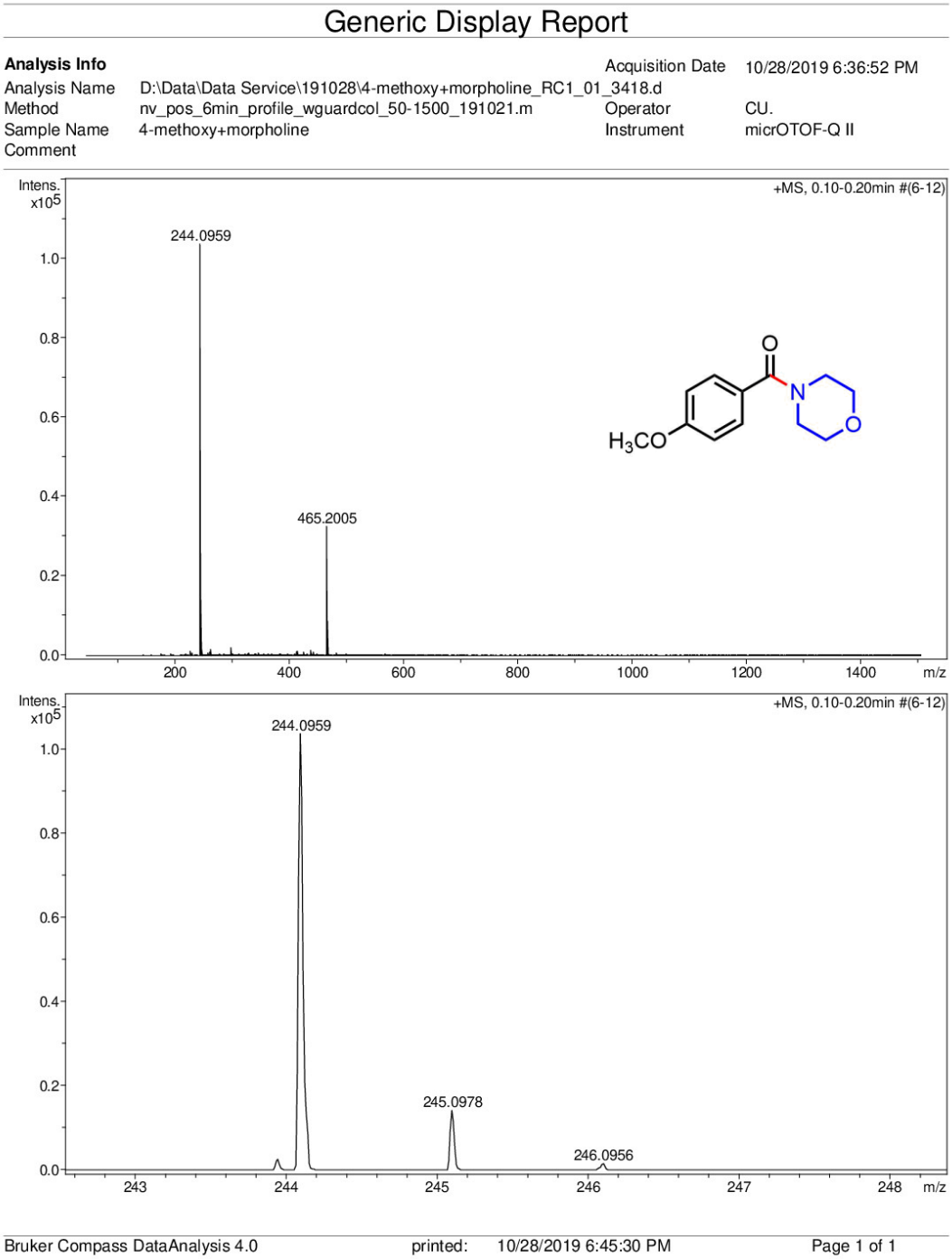

Figure A79 ESI-HRMS spectrum of **3ma**

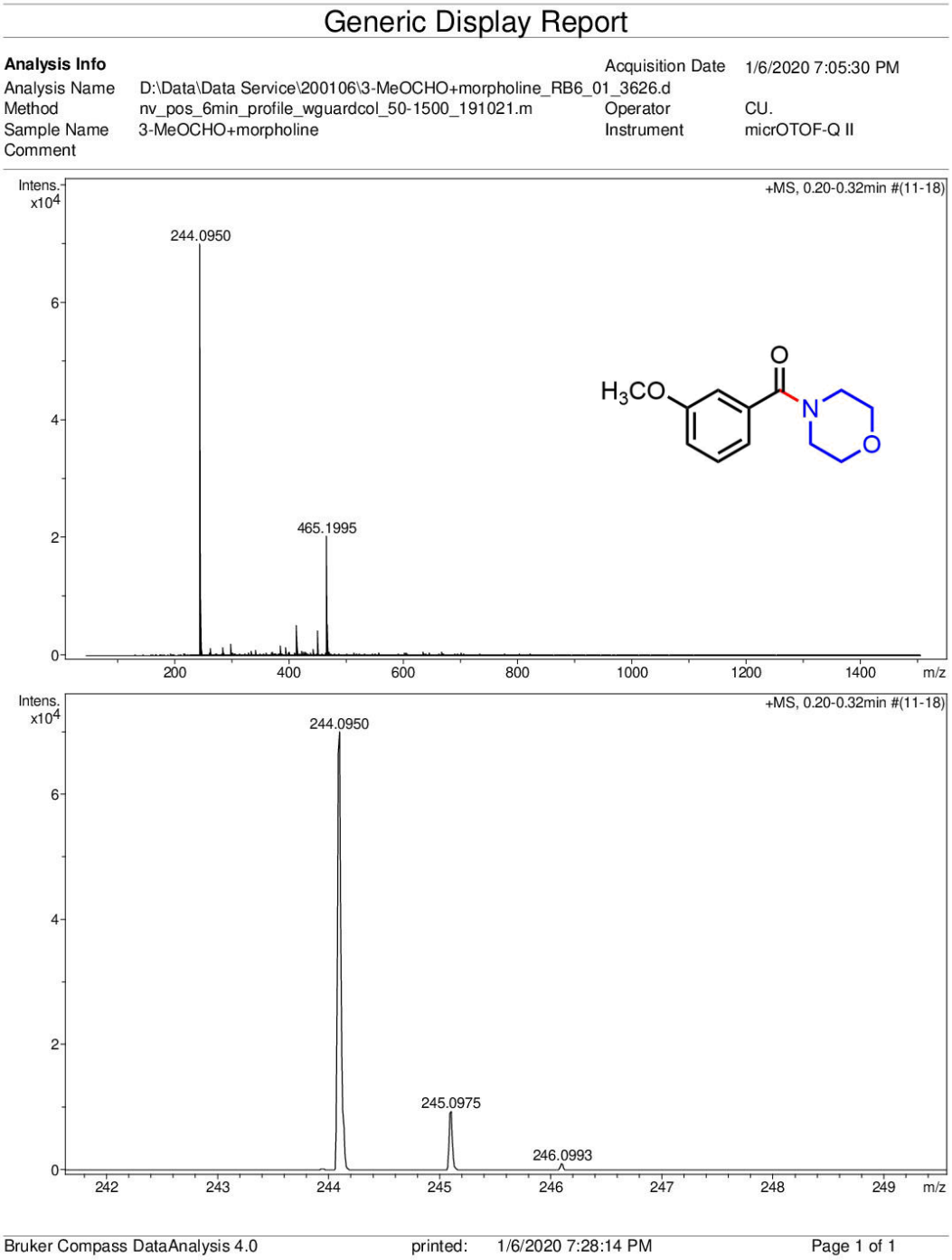

Figure A80 ESI-HRMS spectrum of **3na**

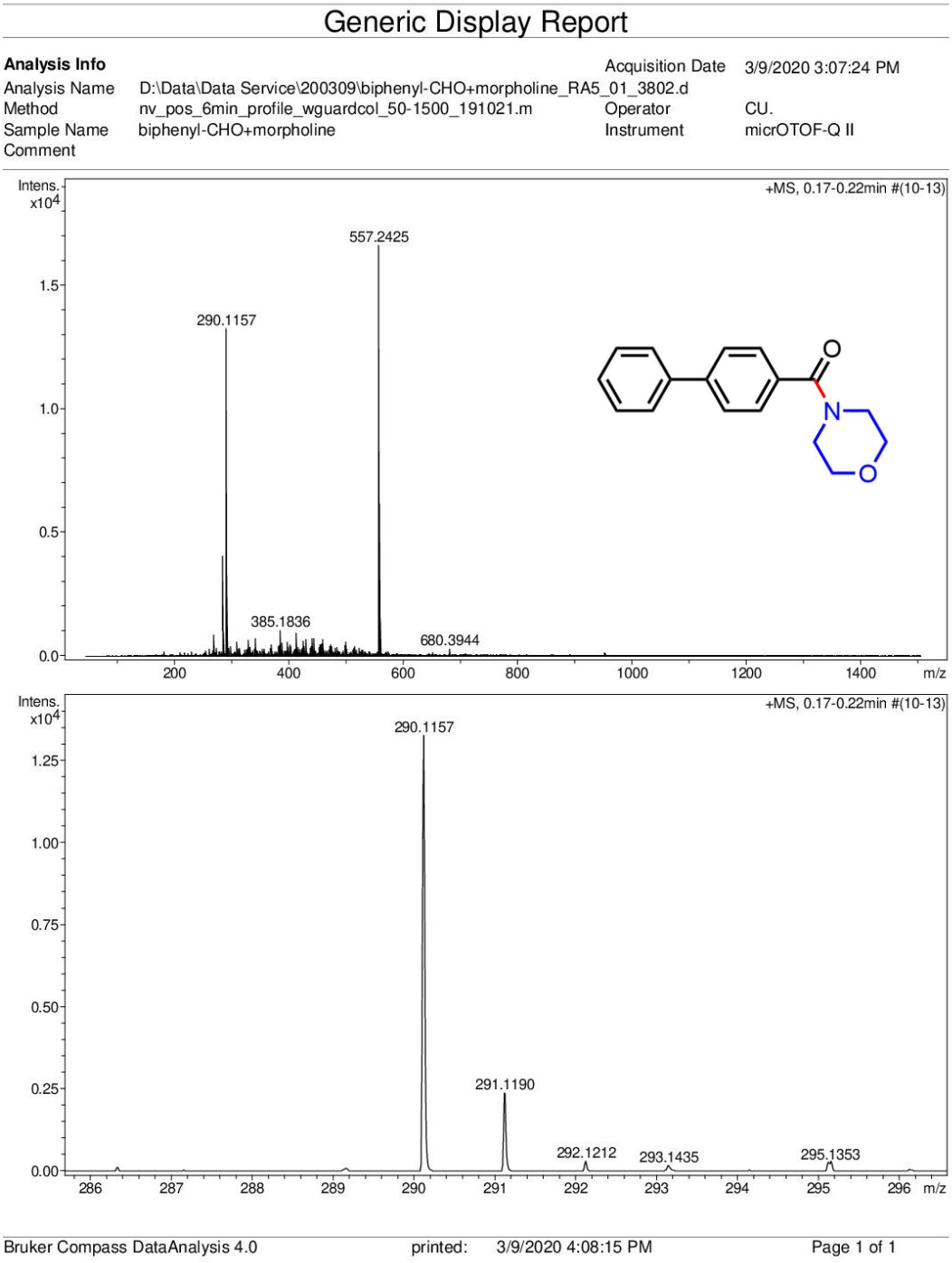

Figure A81 ESI-HRMS spectrum of **3oa**

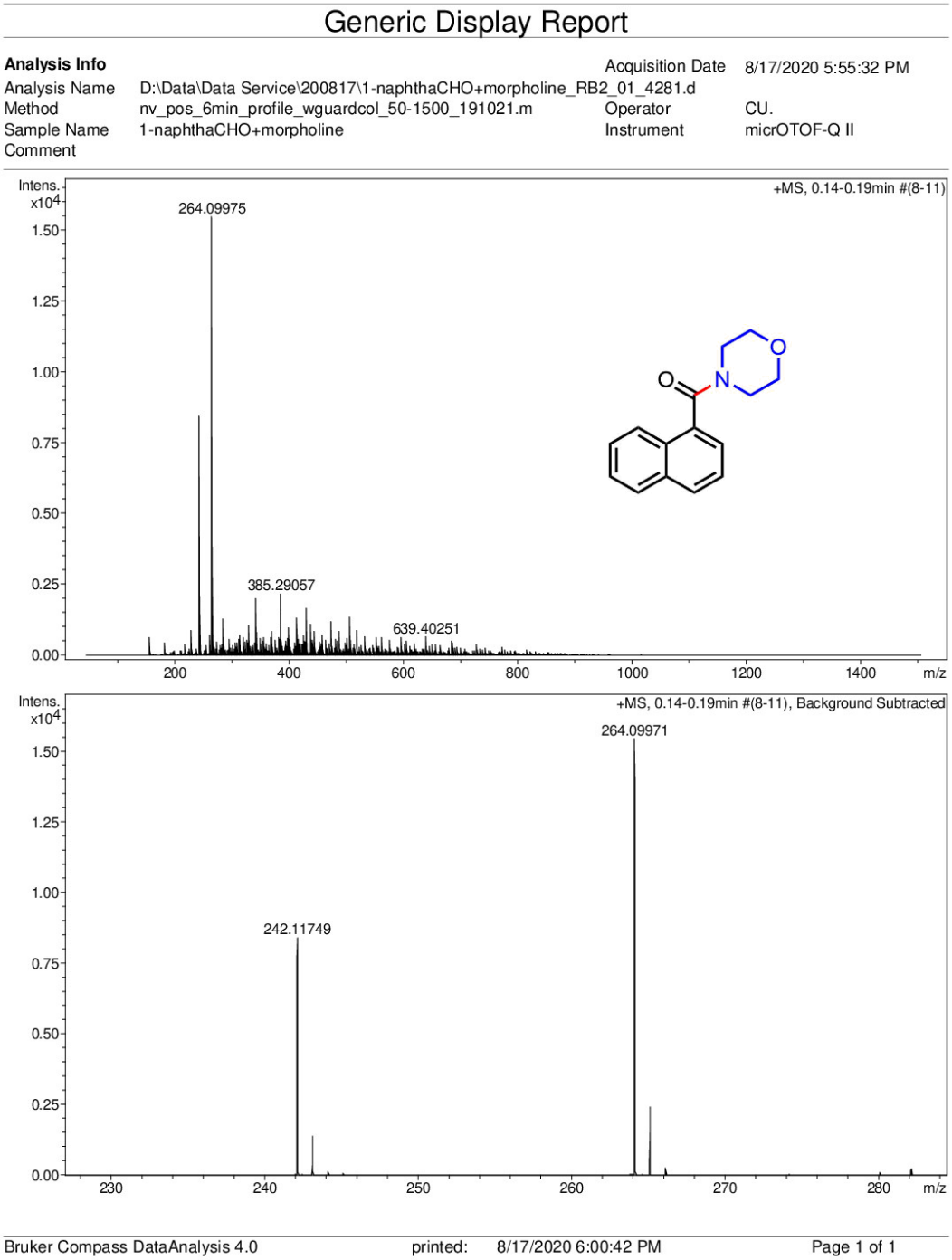

Figure A82 ESI-HRMS spectrum of **3pa**

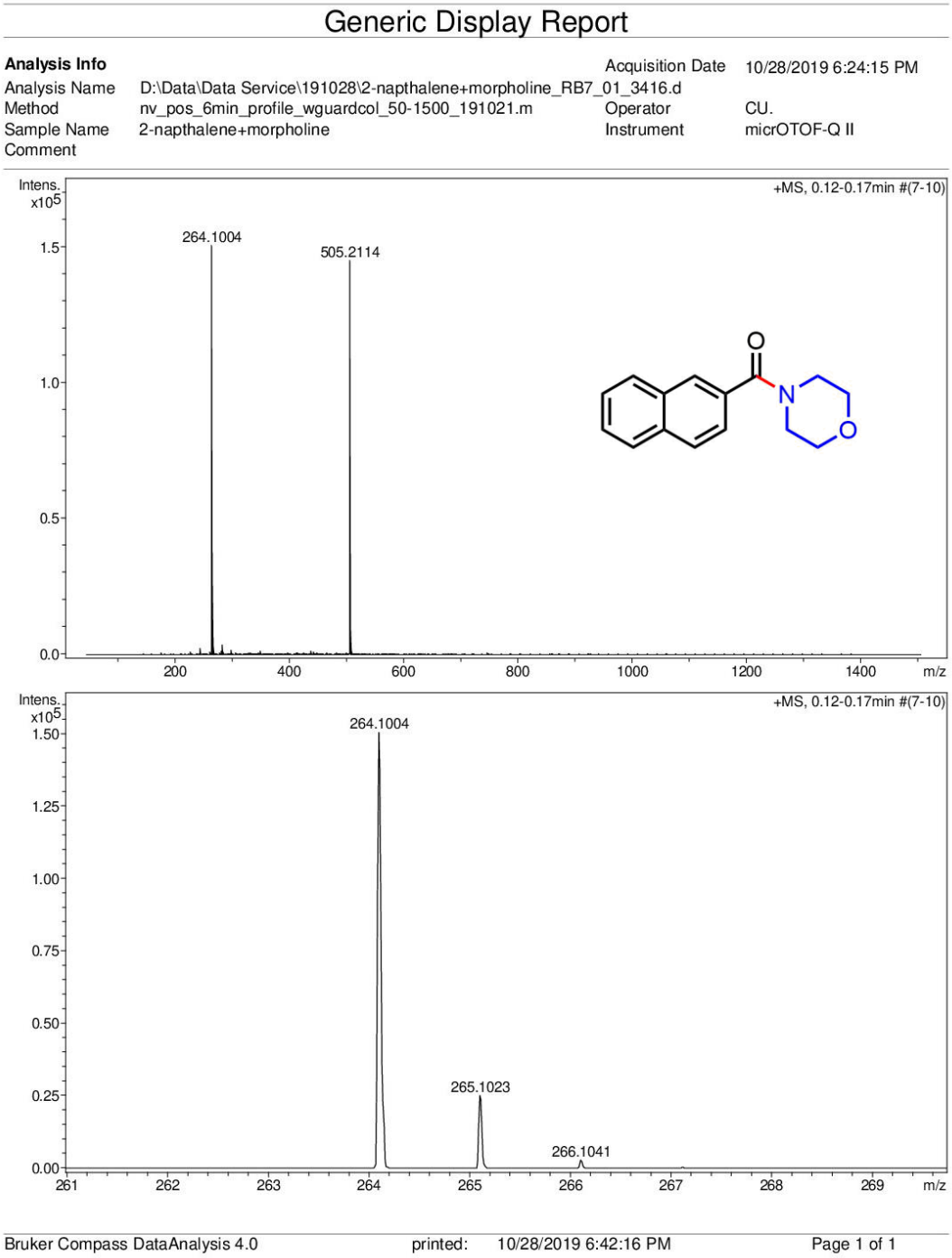

Figure A83 ESI-HRMS spectrum of **3qa**

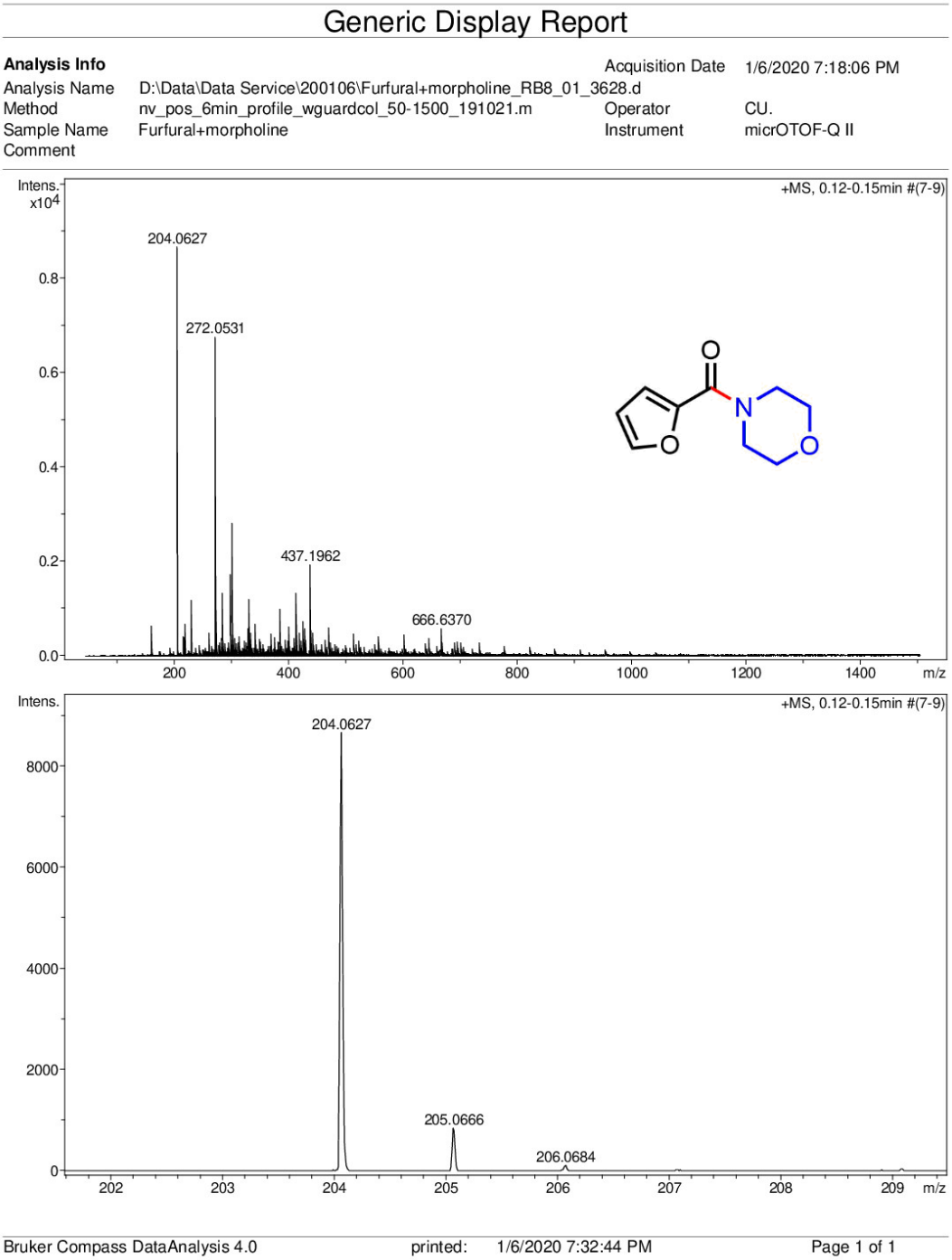

Figure A84 ESI-HRMS spectrum of **3ra**

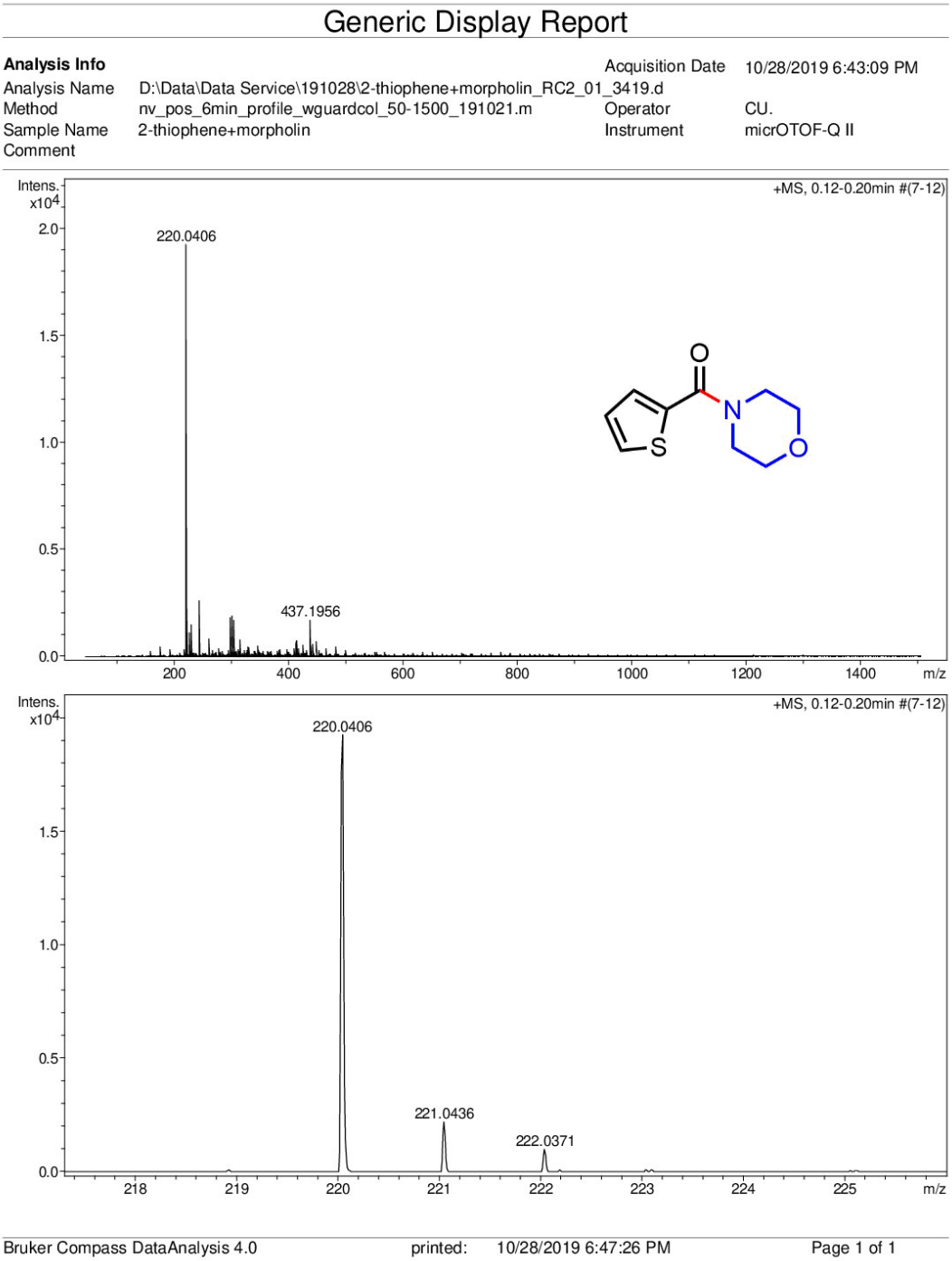

Figure A85 ESI-HRMS spectrum of **3sa**

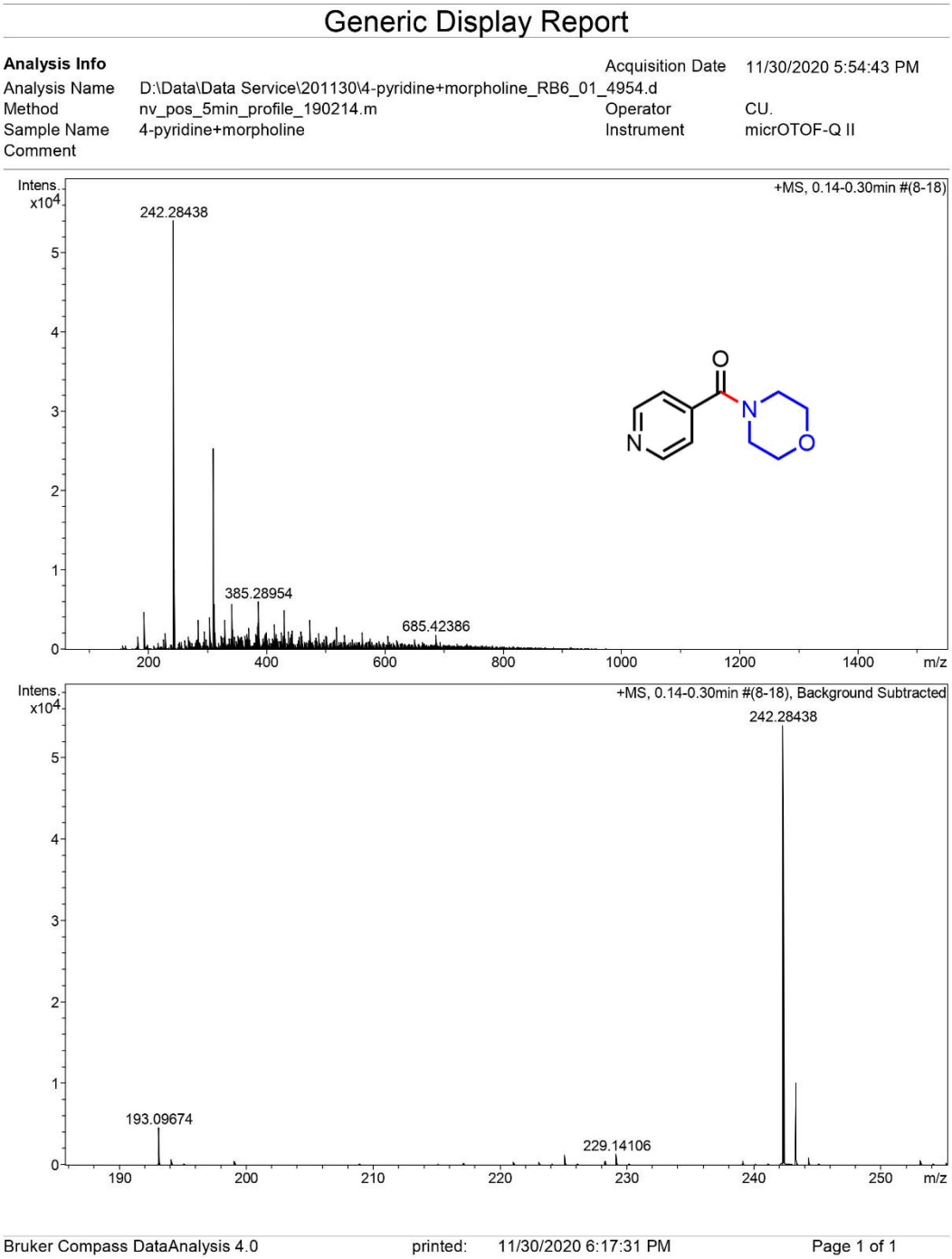

Figure A86 ESI-HRMS spectrum of **3ta**

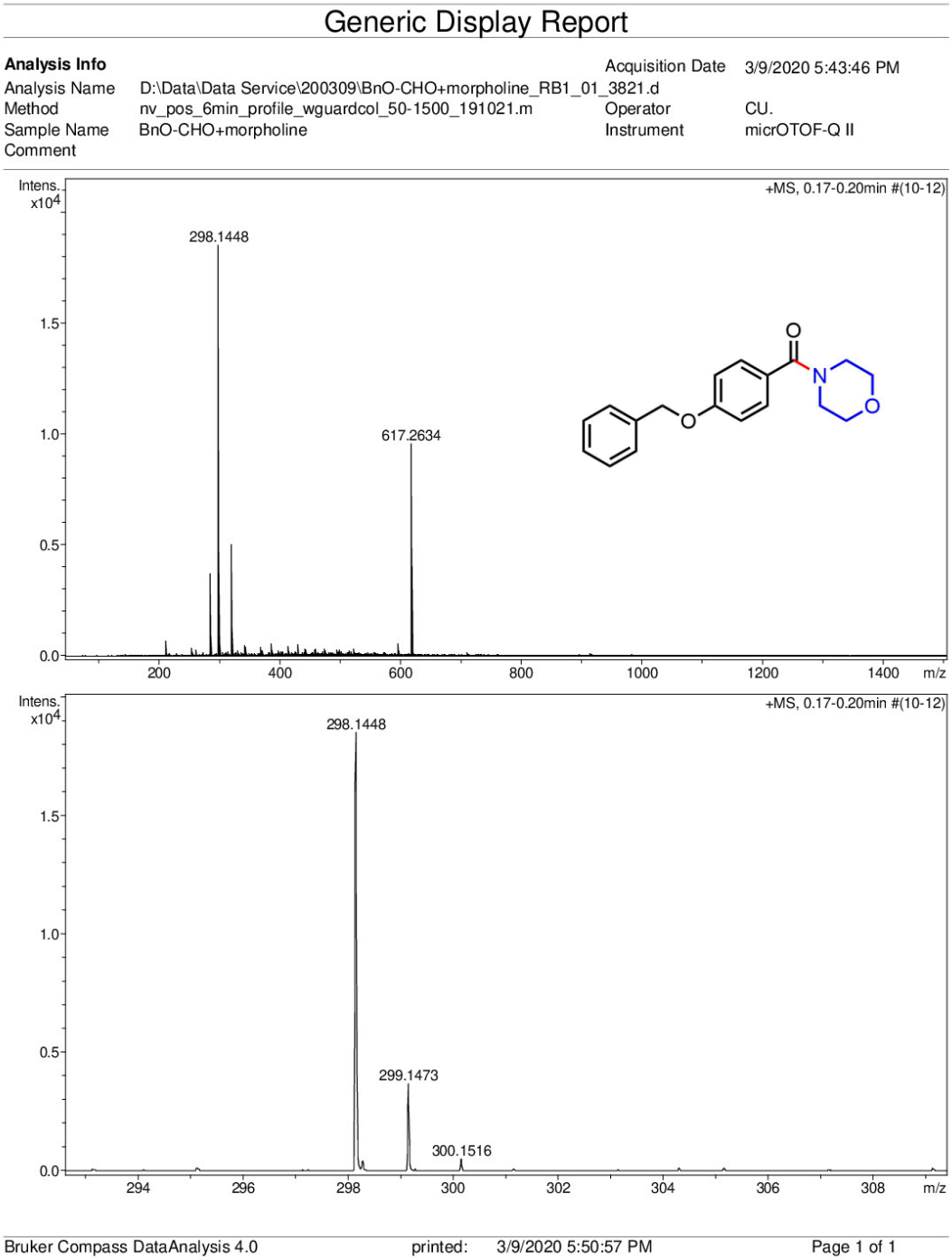

Figure A87 ESI-HRMS spectrum of **3va**

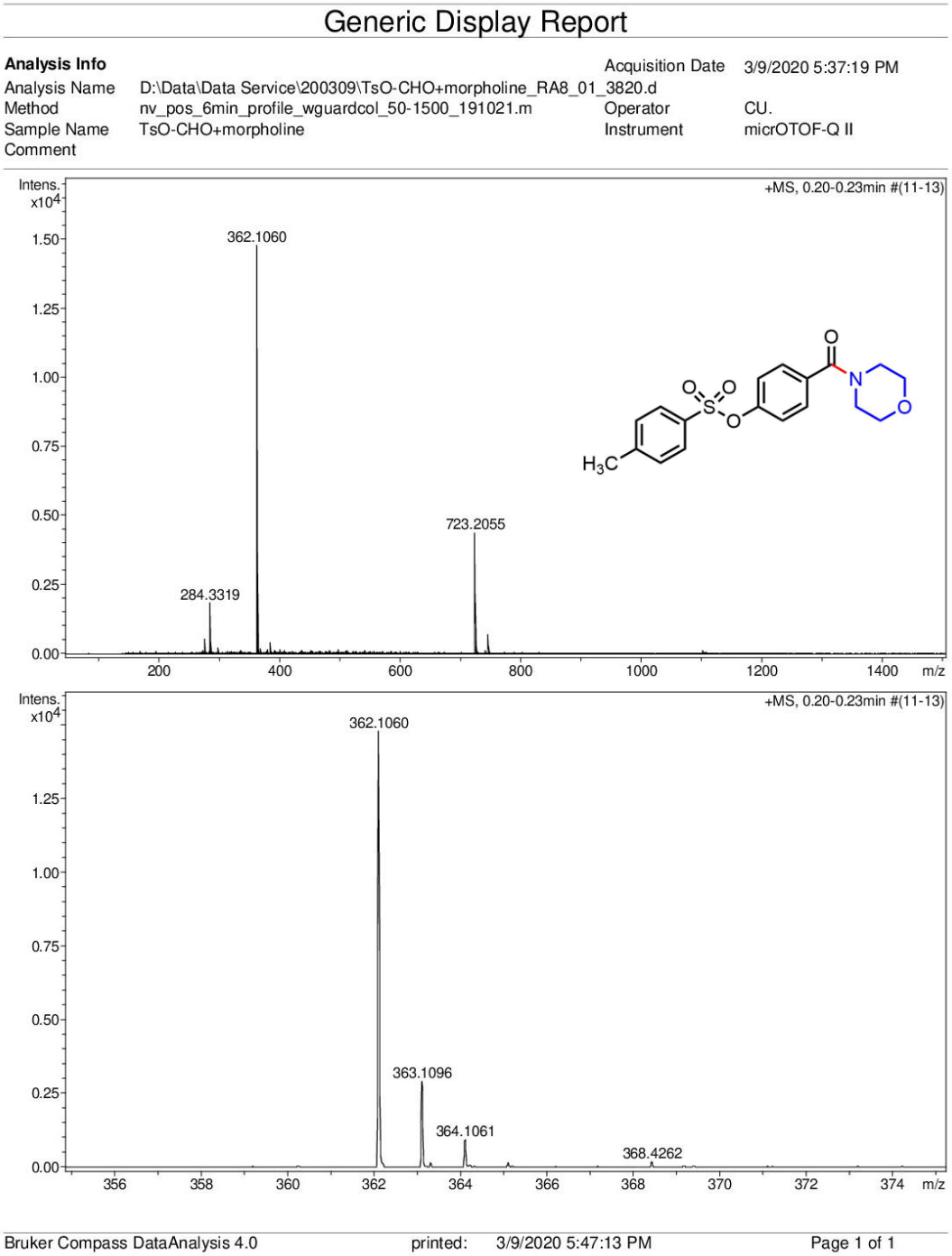

Figure A88 ESI-HRMS spectrum of **3wa**

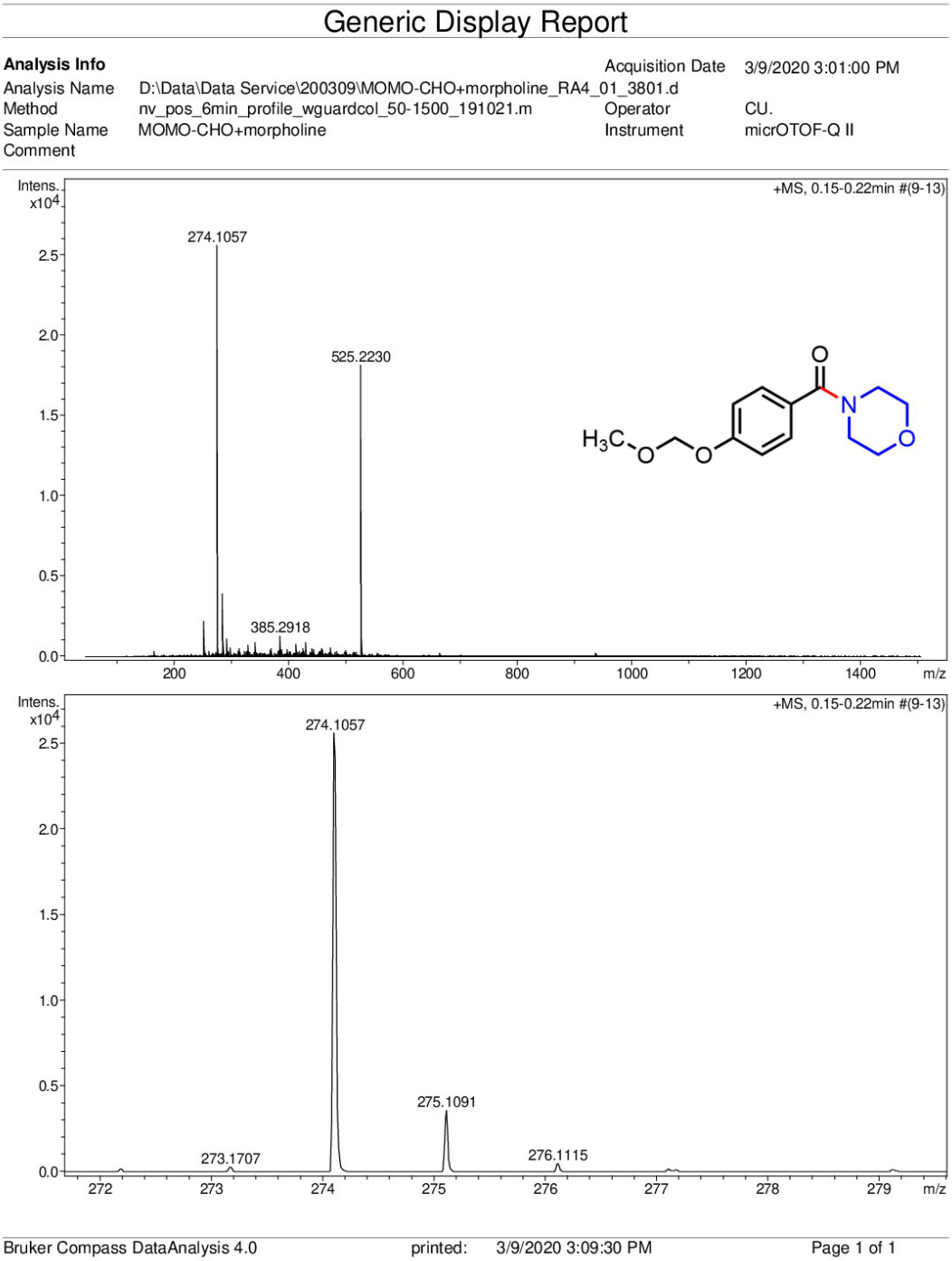

Figure A89 ESI-HRMS spectrum of **3xa**

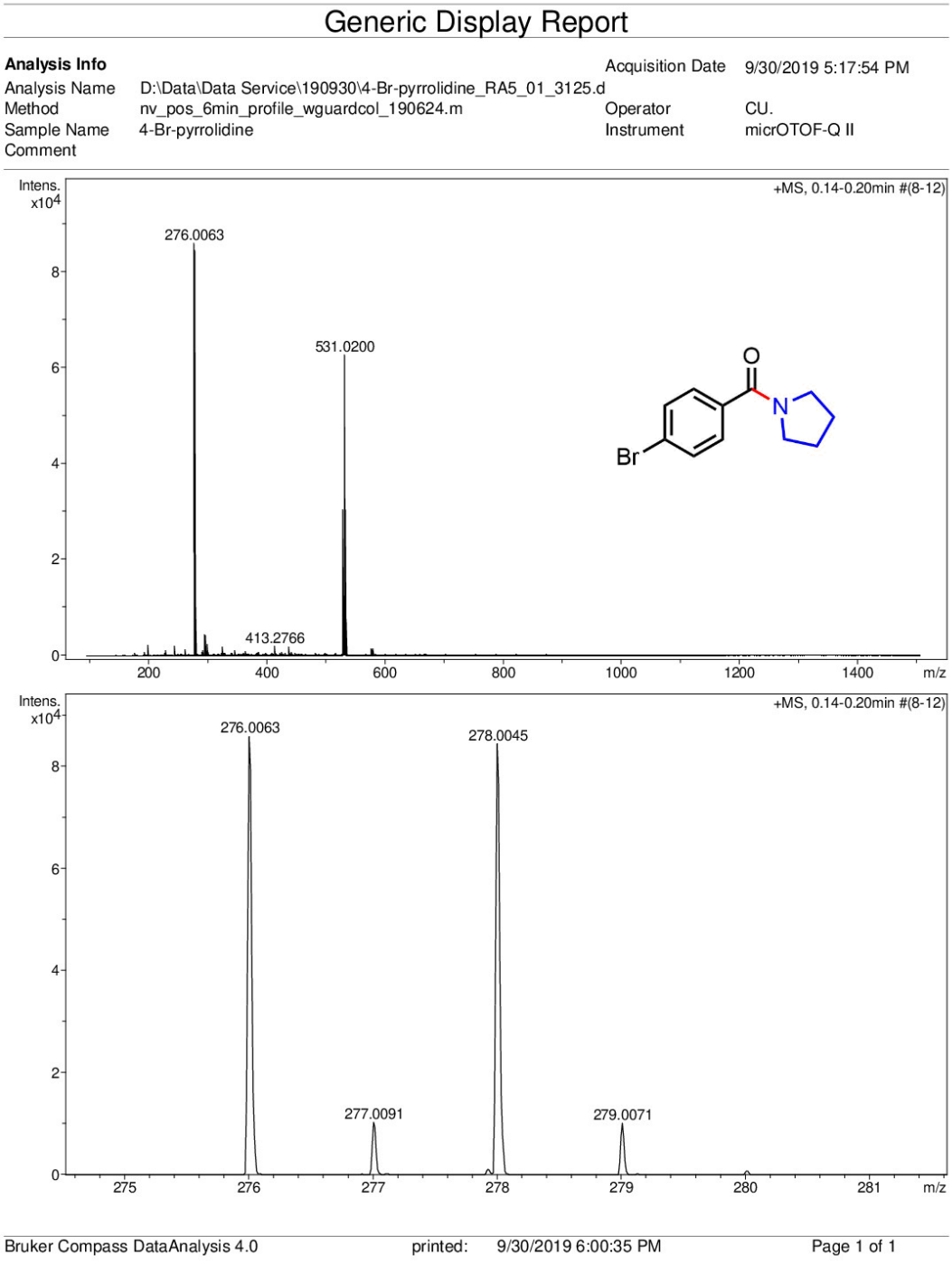

Figure A90 ESI-HRMS spectrum of **3ab**

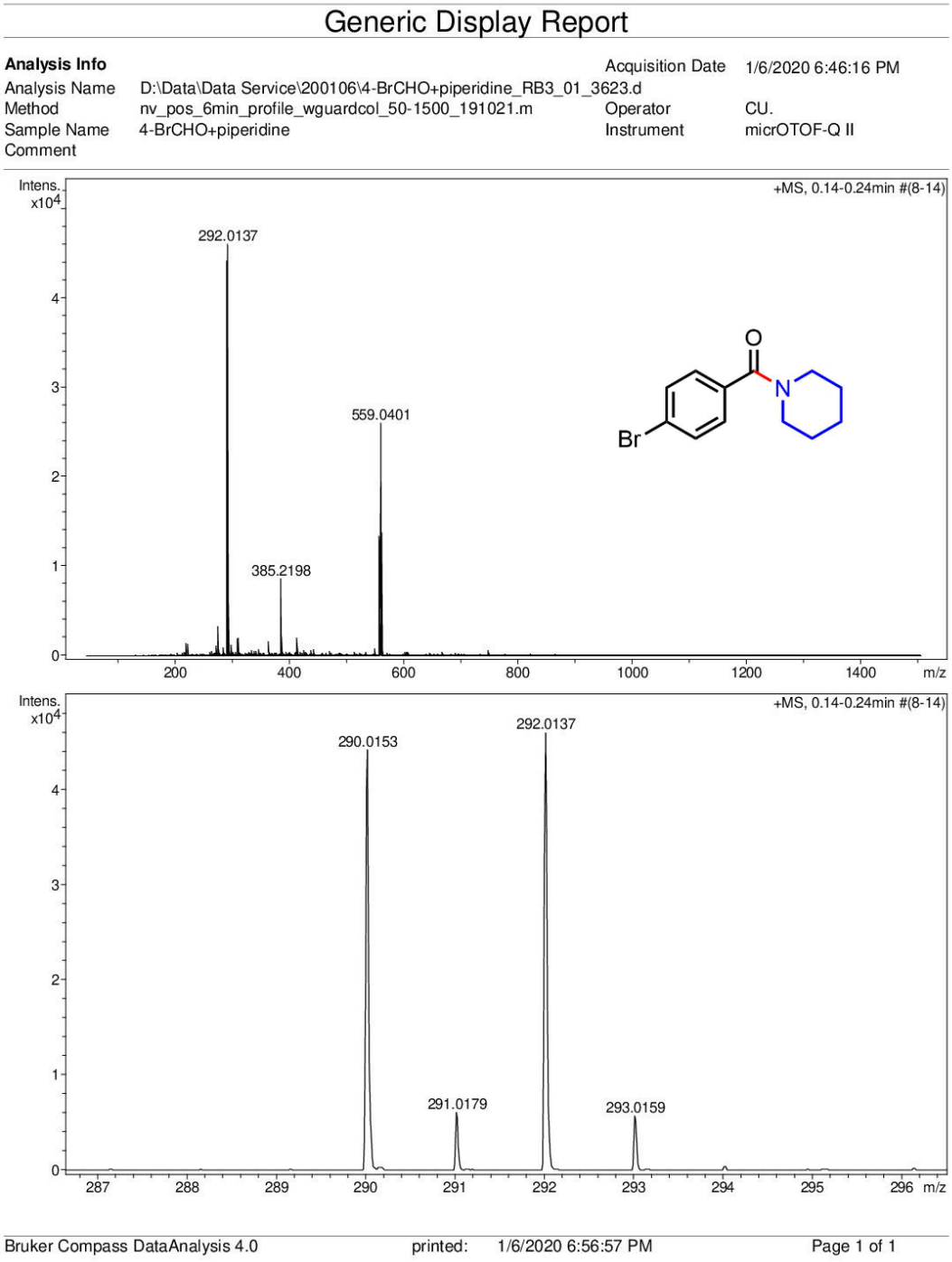

Figure A91 ESI-HRMS spectrum of **3ac**

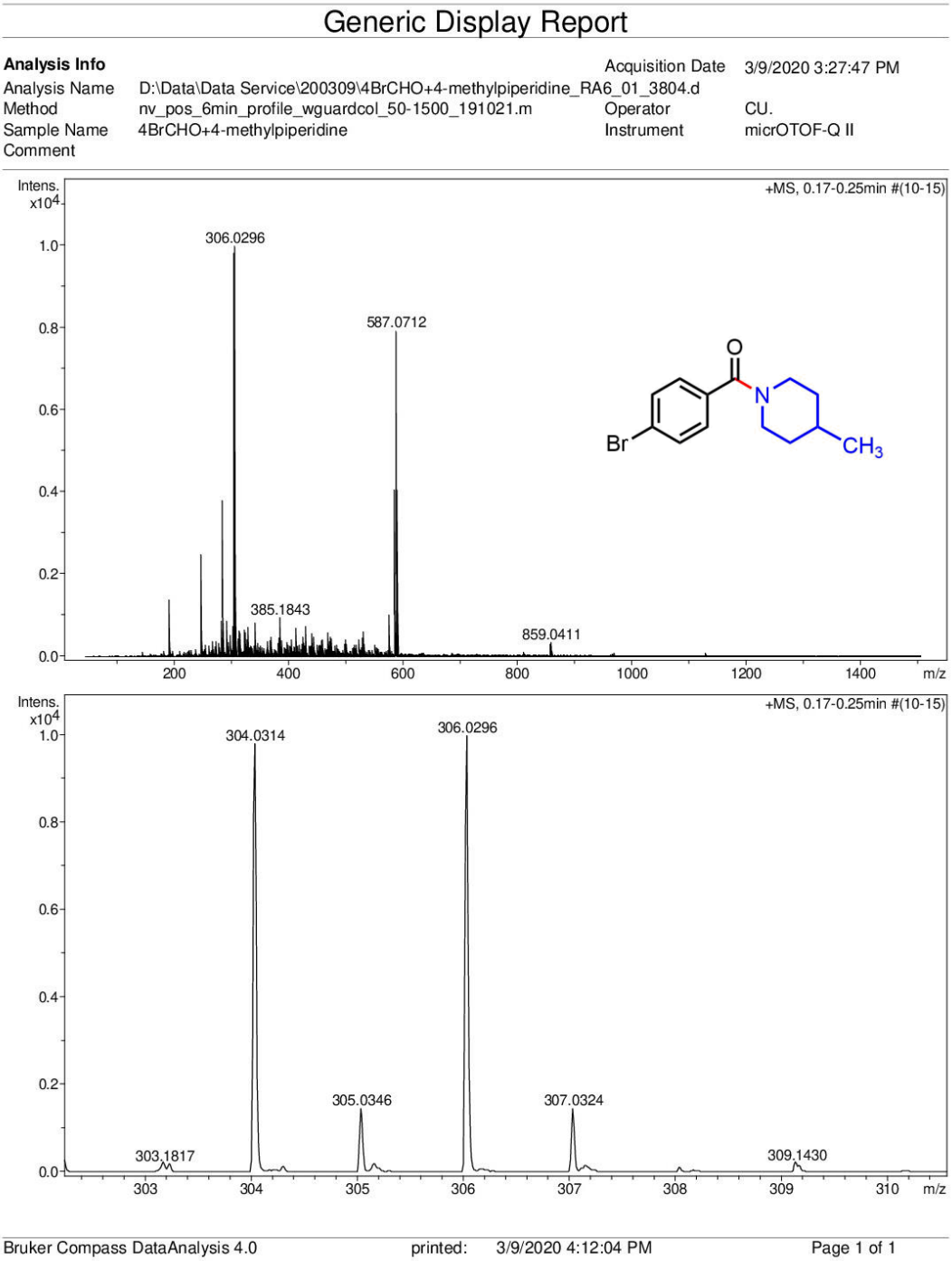

Figure A92 ESI-HRMS spectrum of **3ad**

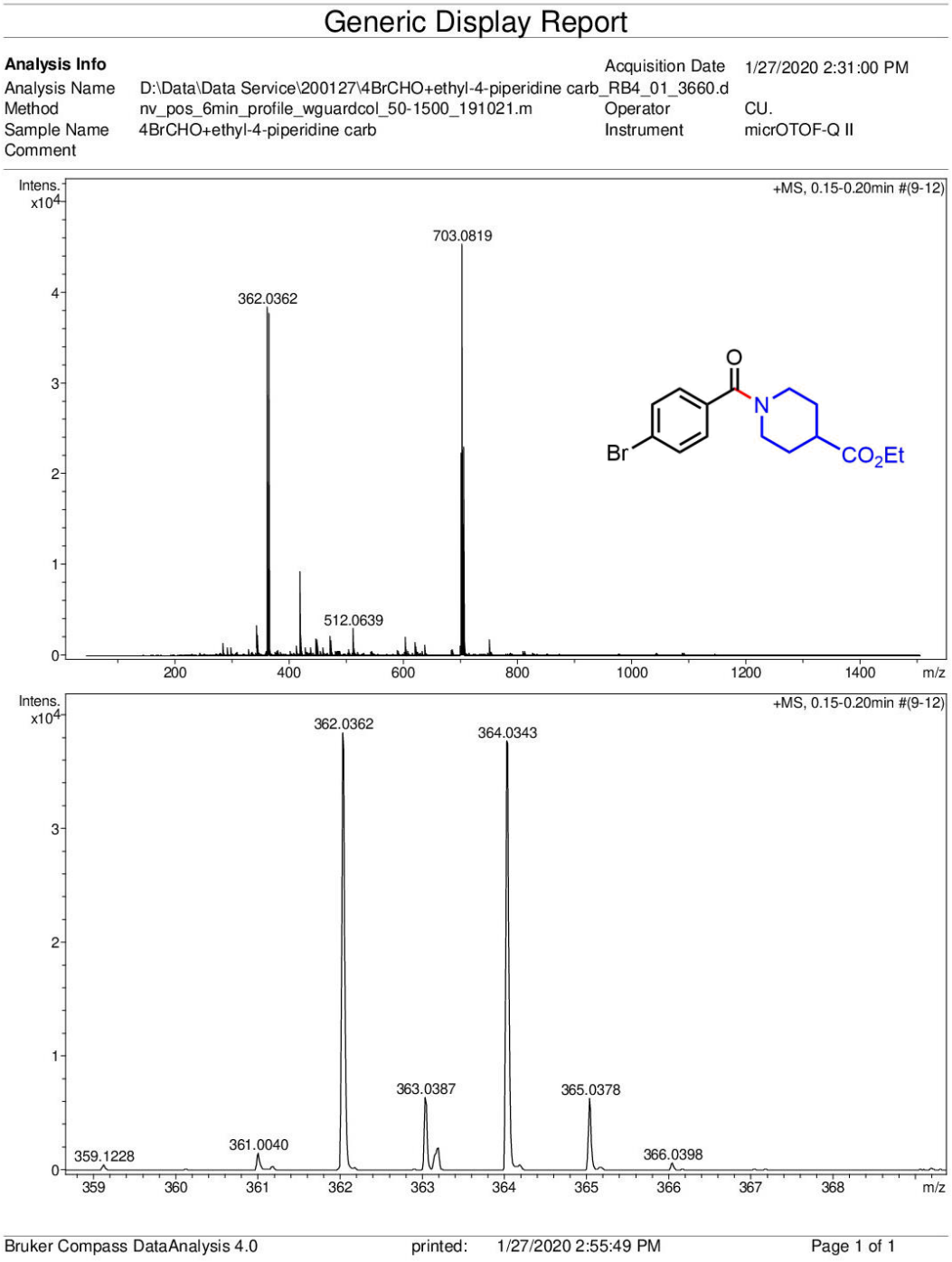

Figure A93 ESI-HRMS spectrum of **3ae**

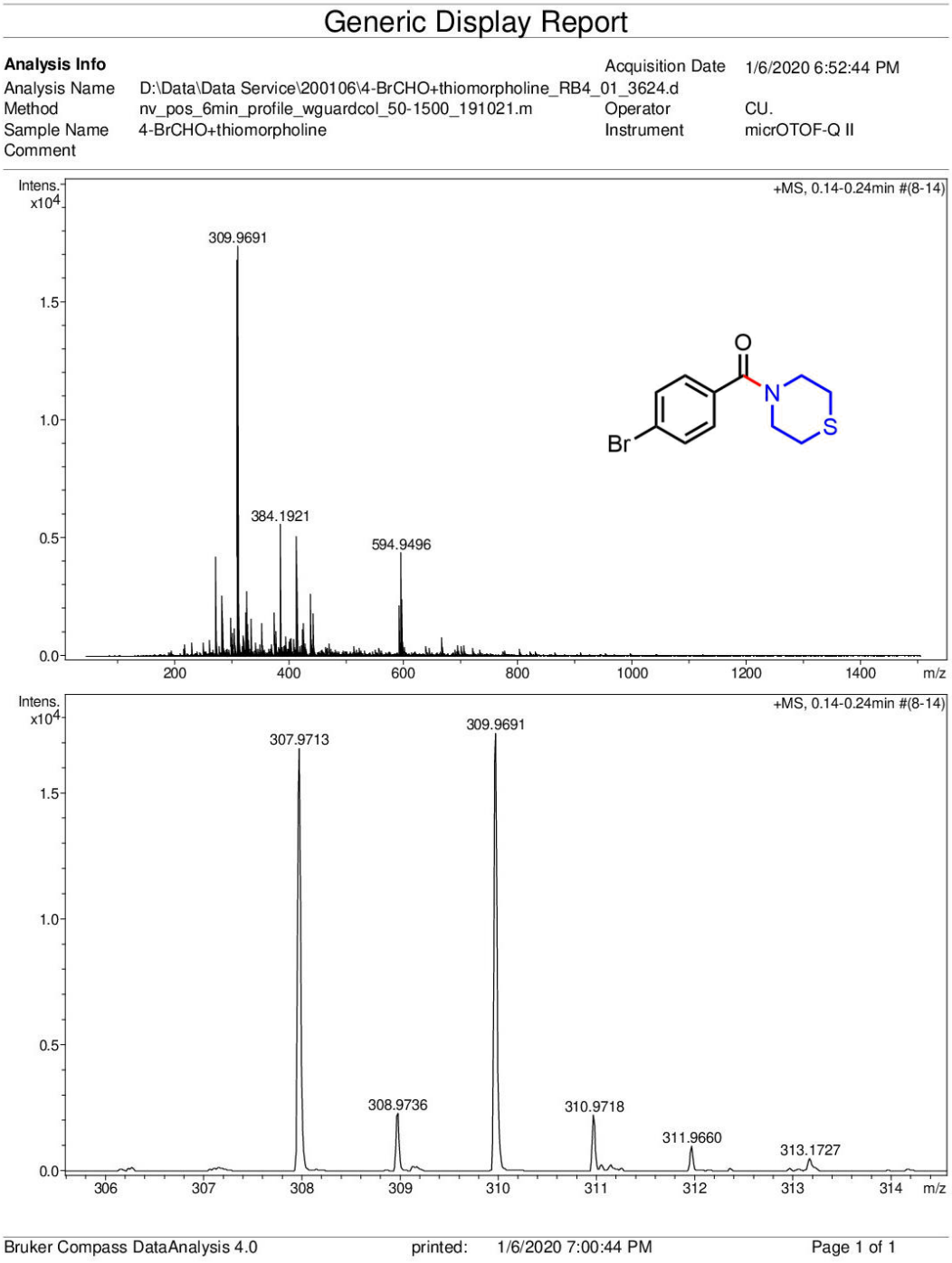

Figure A94 ESI-HRMS spectrum of **3af**

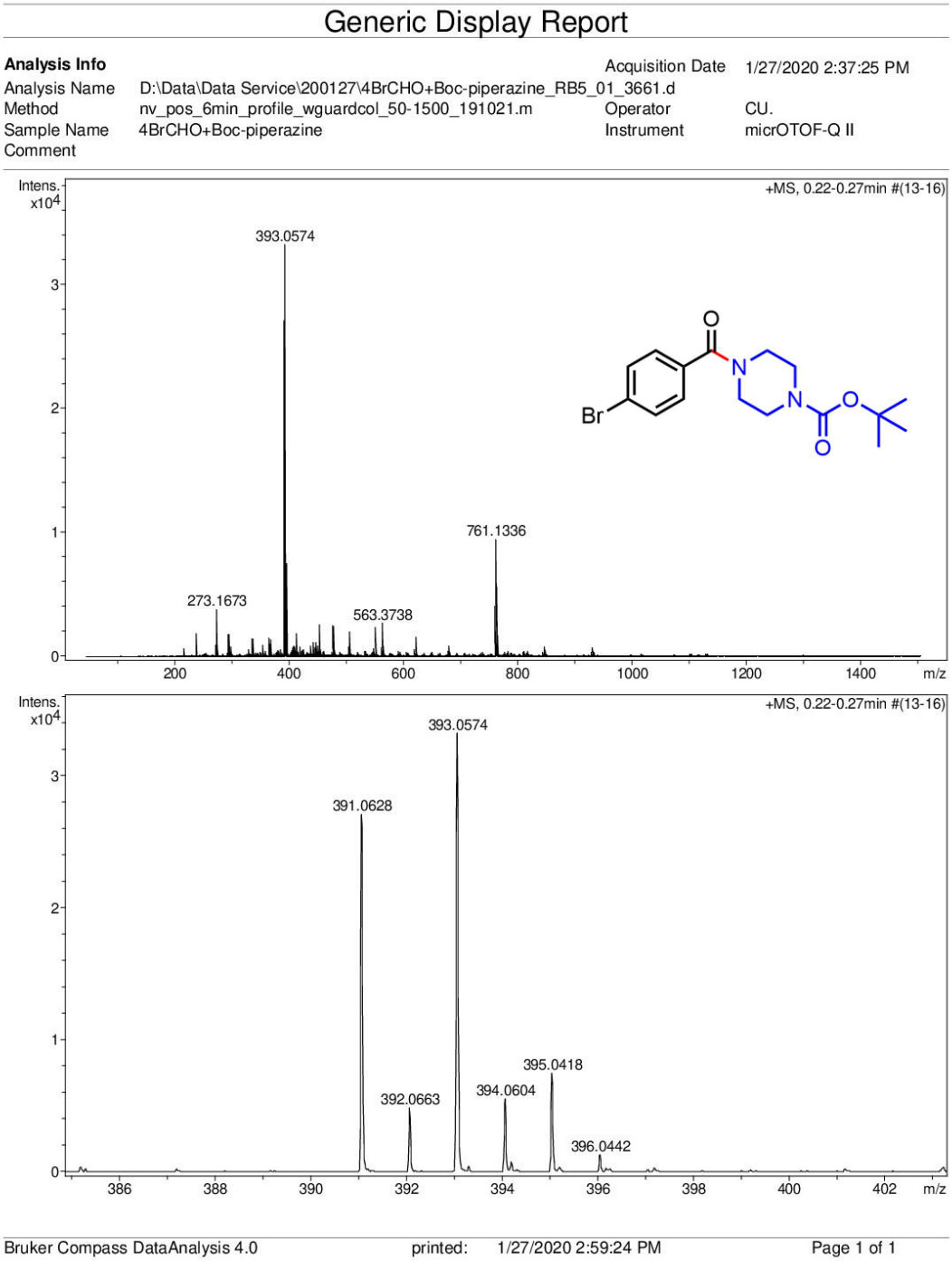

Figure A95 ESI-HRMS spectrum of **3ag**

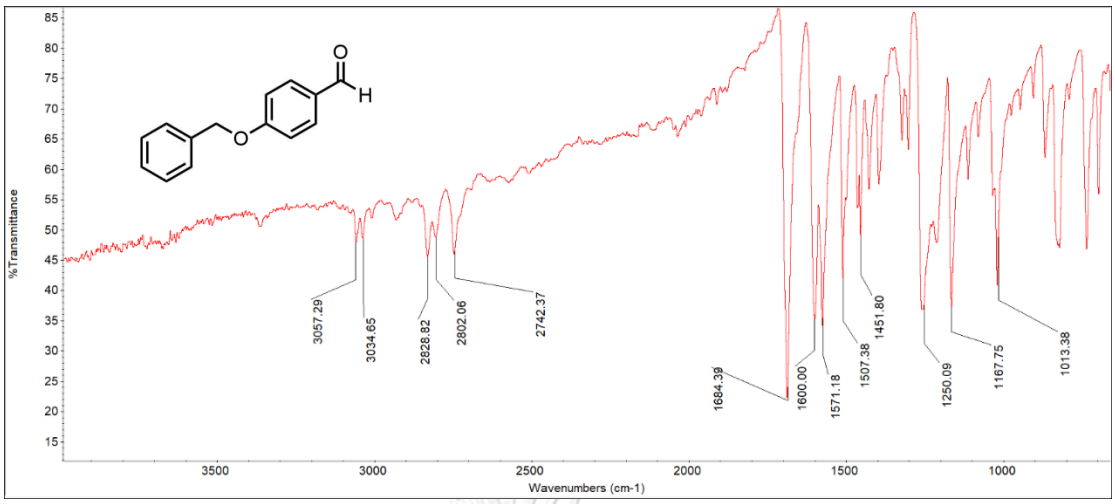

Figure A96 FT-IR spectrum of **1v**

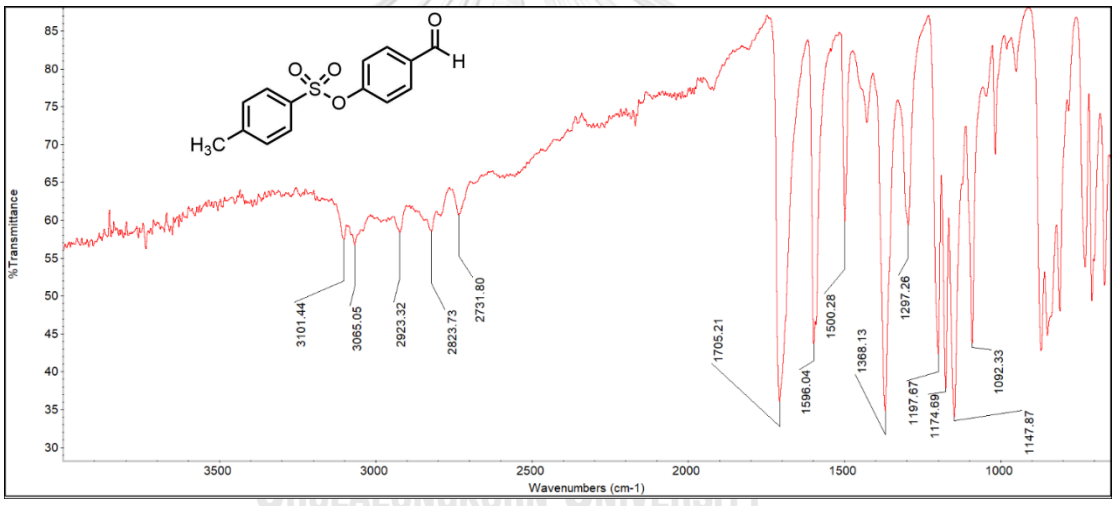

Figure A97 FT-IR spectrum of **1w**

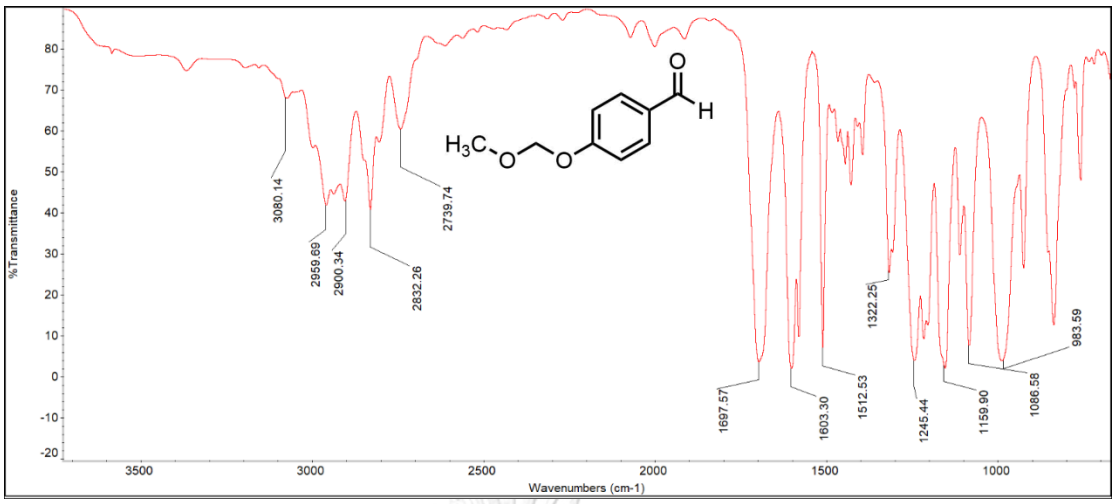

Figure A98 FT-IR spectrum of **1x**

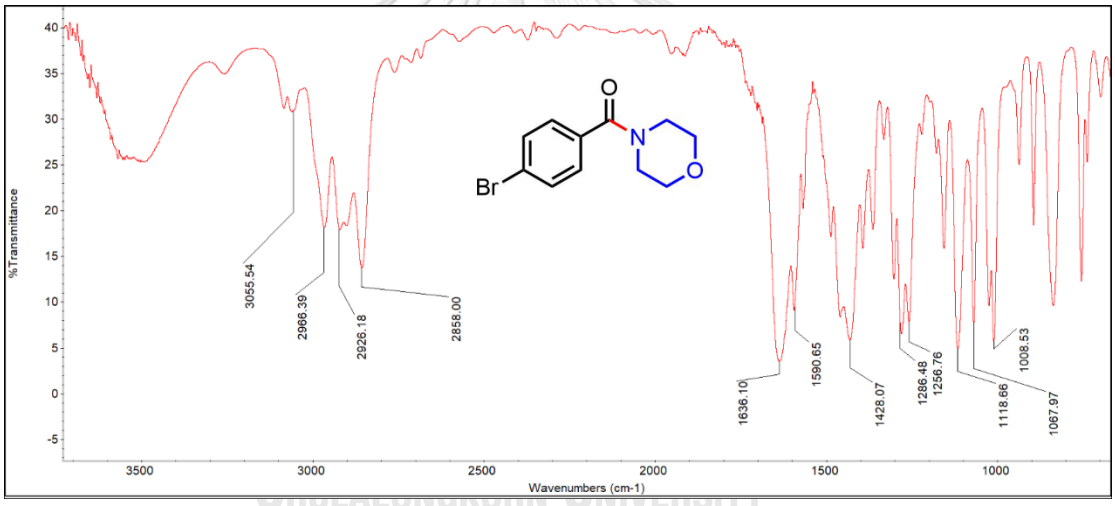

Figure A99 FT-IR spectrum of **3aa**

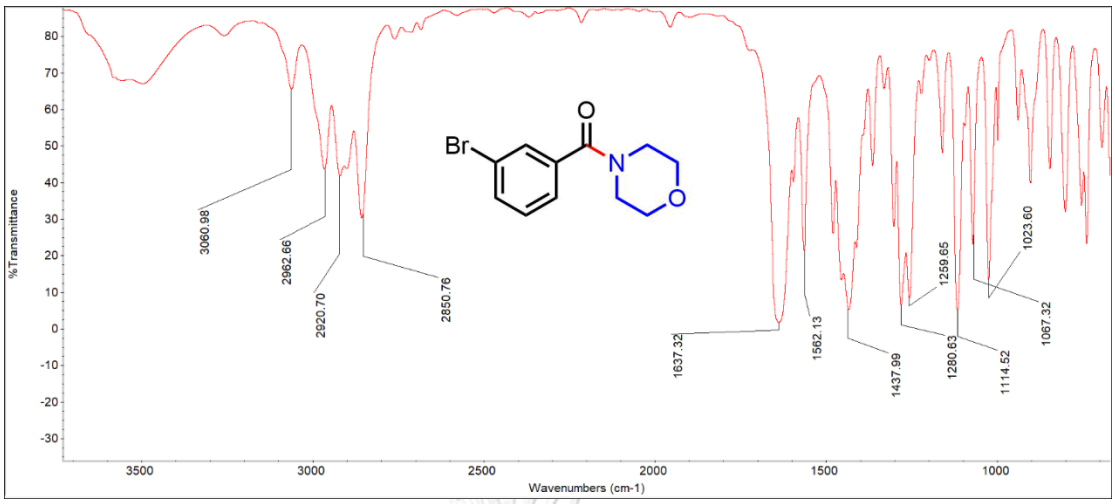

Figure A100 FT-IR spectrum of **3ba**

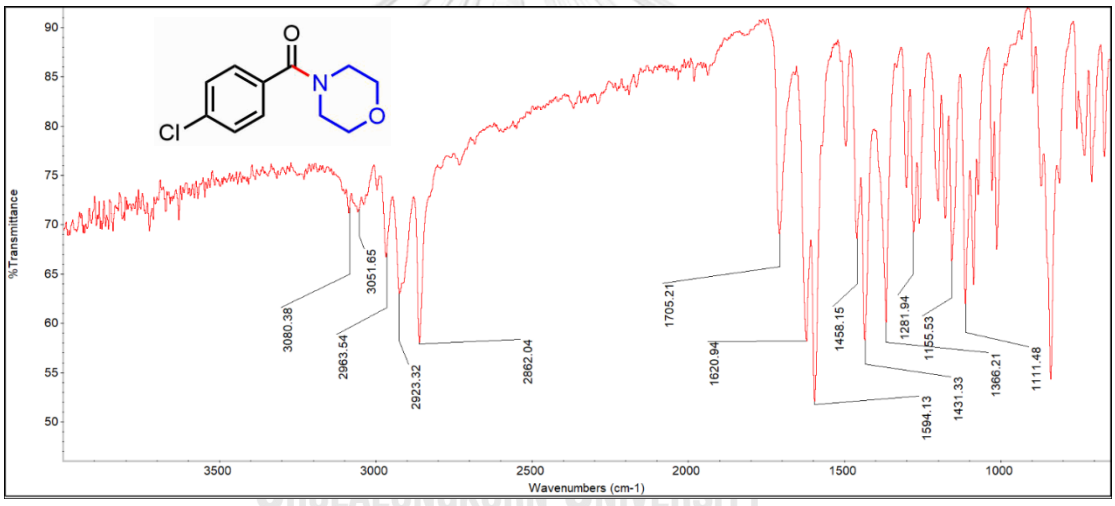

Figure A101 FT-IR spectrum of **3ca**

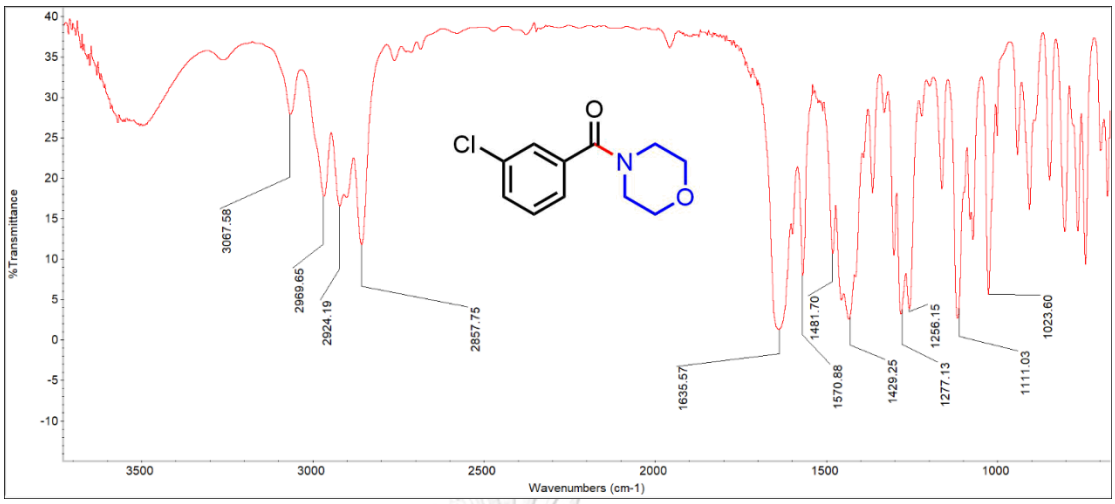

Figure A102 FT-IR spectrum of **3da**

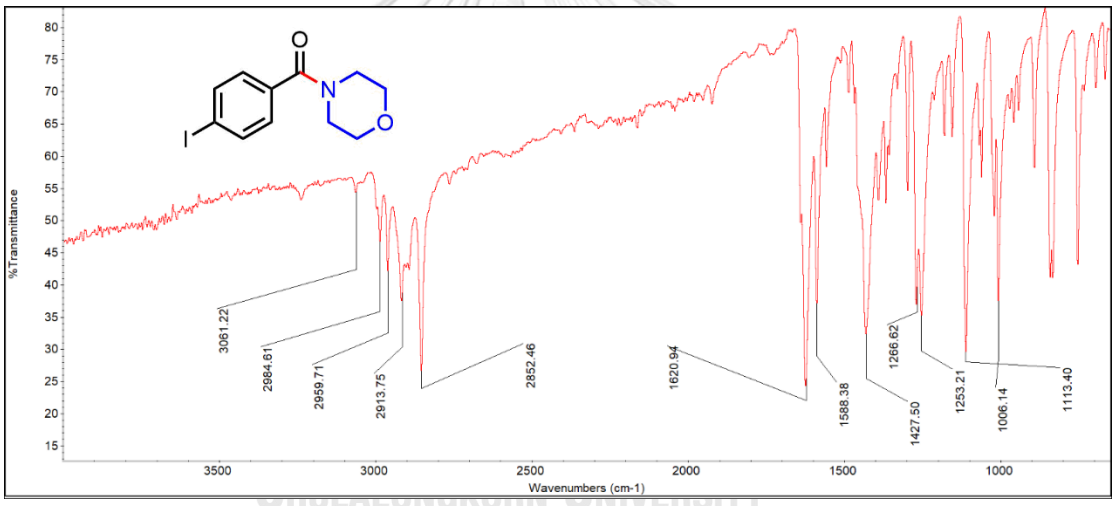

Figure A103 FT-IR spectrum of **3ea**

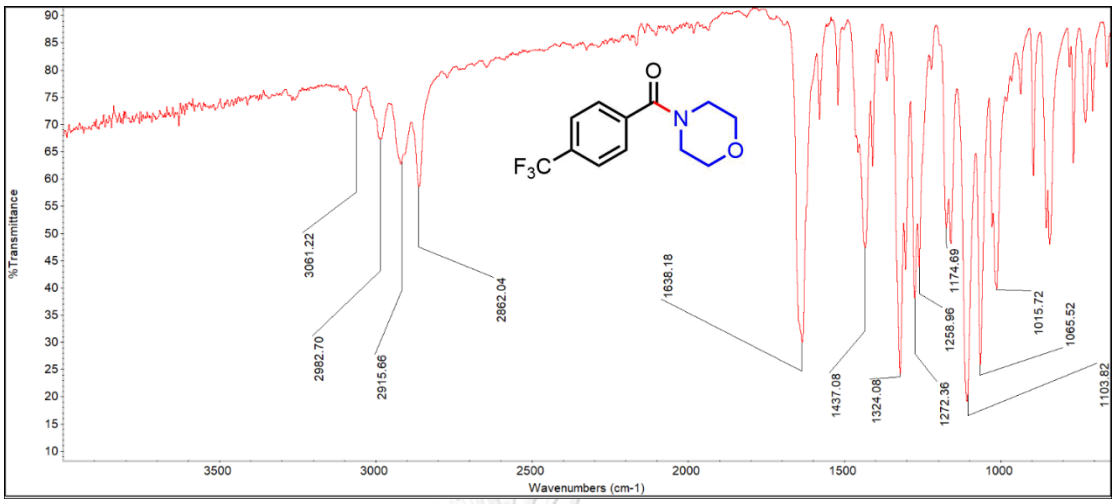

Figure A104 FT-IR spectrum of **3fa**

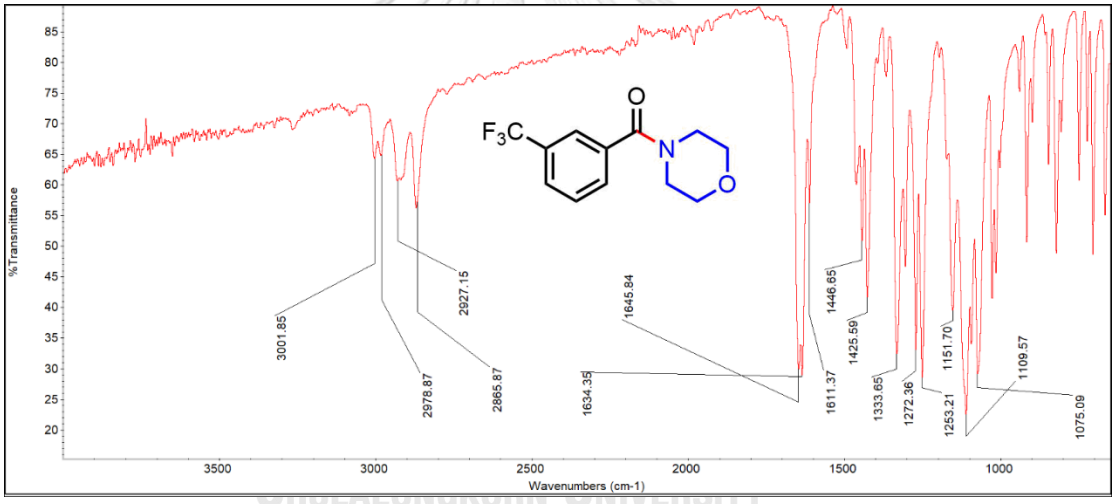

Figure A105 FT-IR spectrum of **3ga**

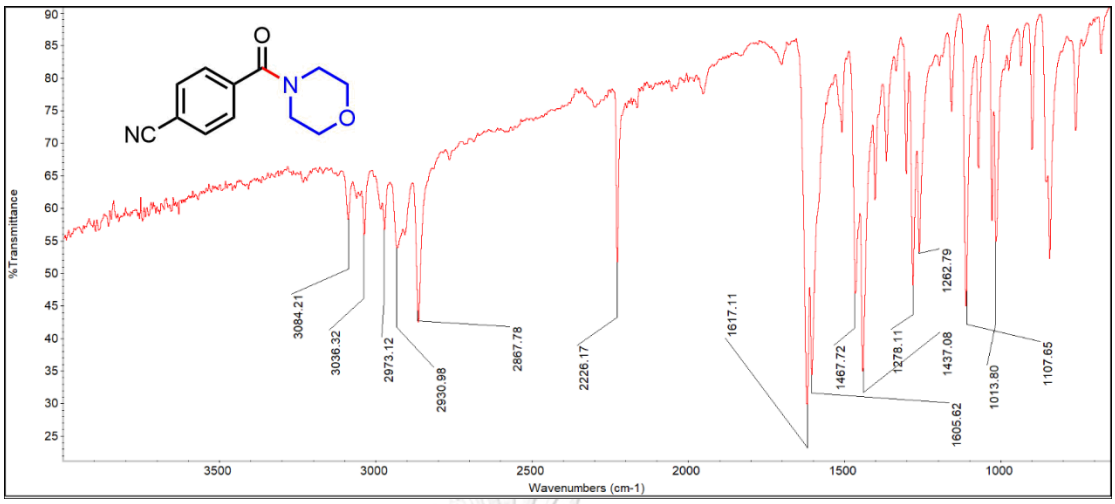

Figure A106 FT-IR spectrum of **3ha**

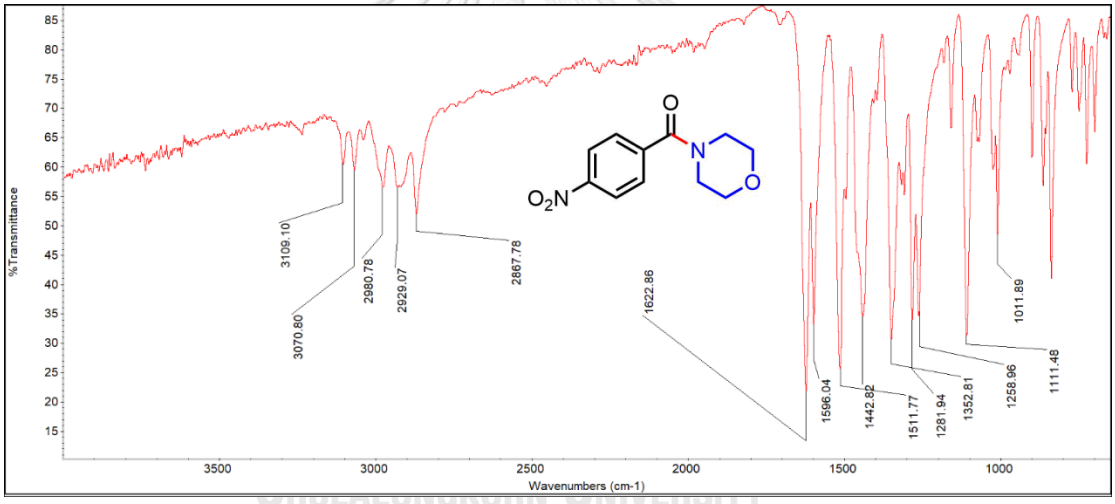

Figure A107 FT-IR spectrum of **3ia**

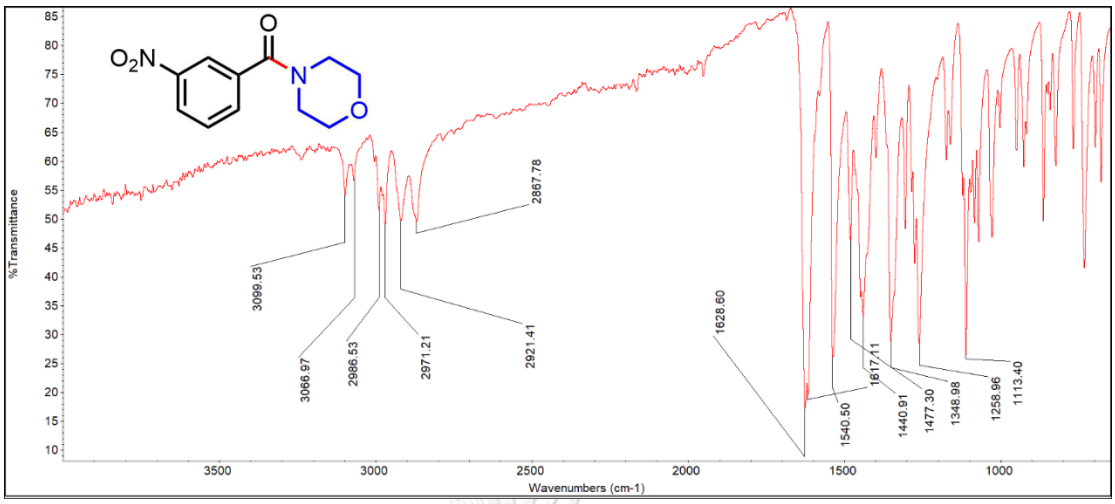

Figure A108 FT-IR spectrum of **3ja**

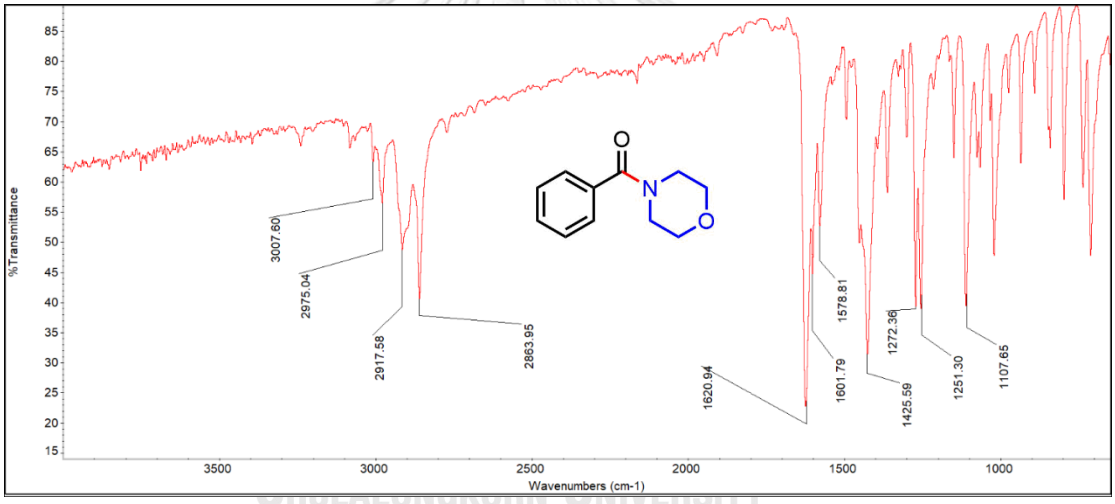

Figure A109 FT-IR spectrum of **3ka**

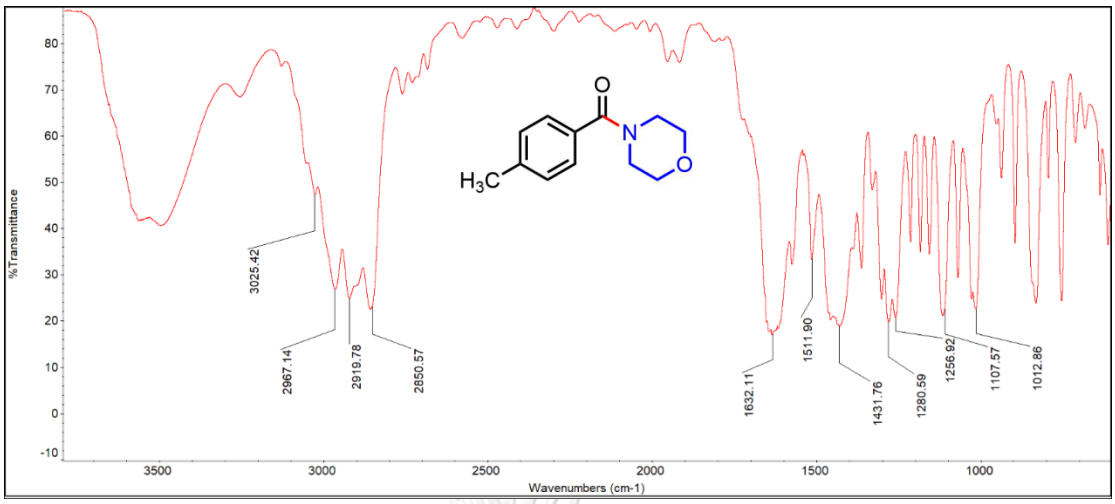

Figure A110 FT-IR spectrum of **3la**

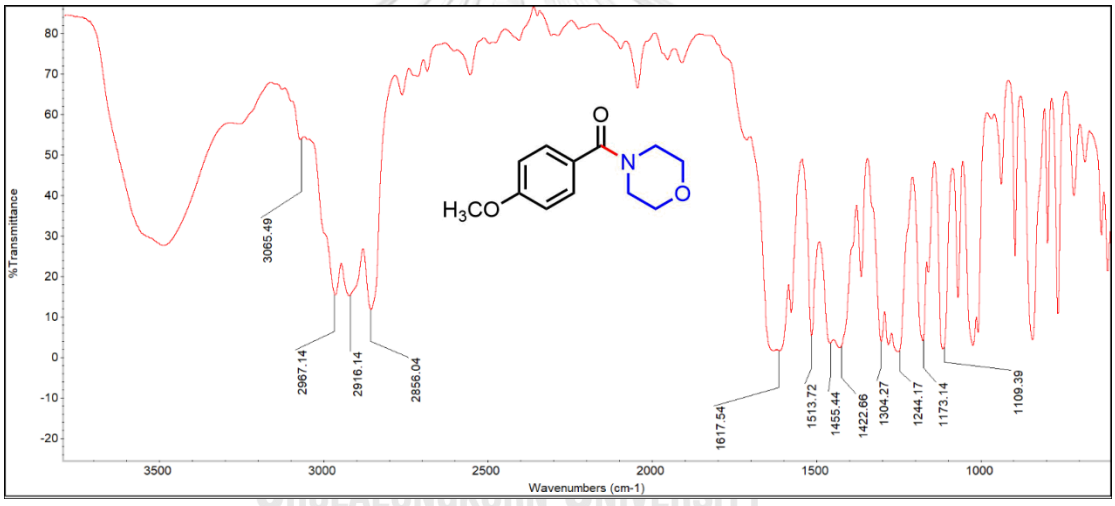

Figure A111 FT-IR spectrum of **3ma**

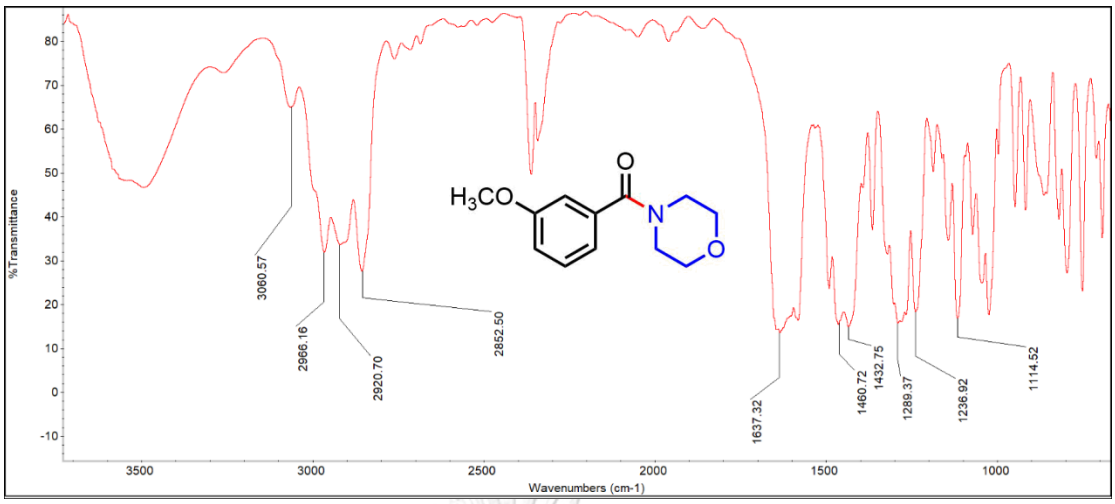

Figure A112 FT-IR spectrum of **3na**

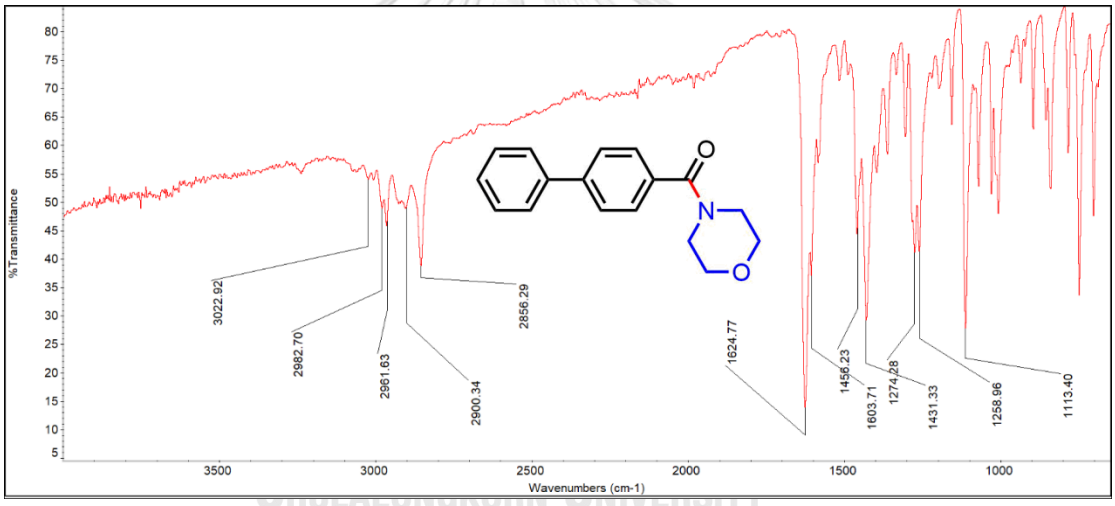

Figure A113 FT-IR spectrum of **3oa**

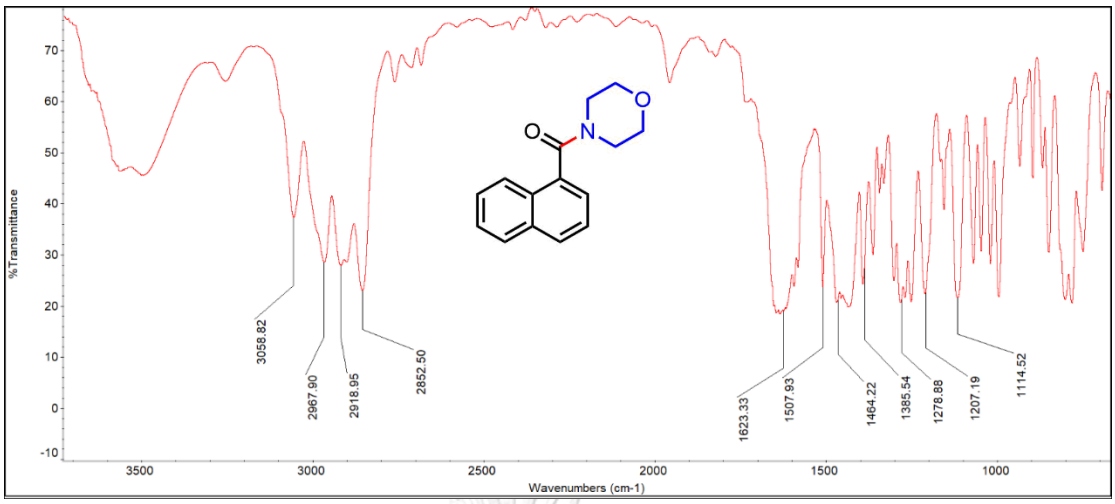

Figure A114 FT-IR spectrum of **3pa**

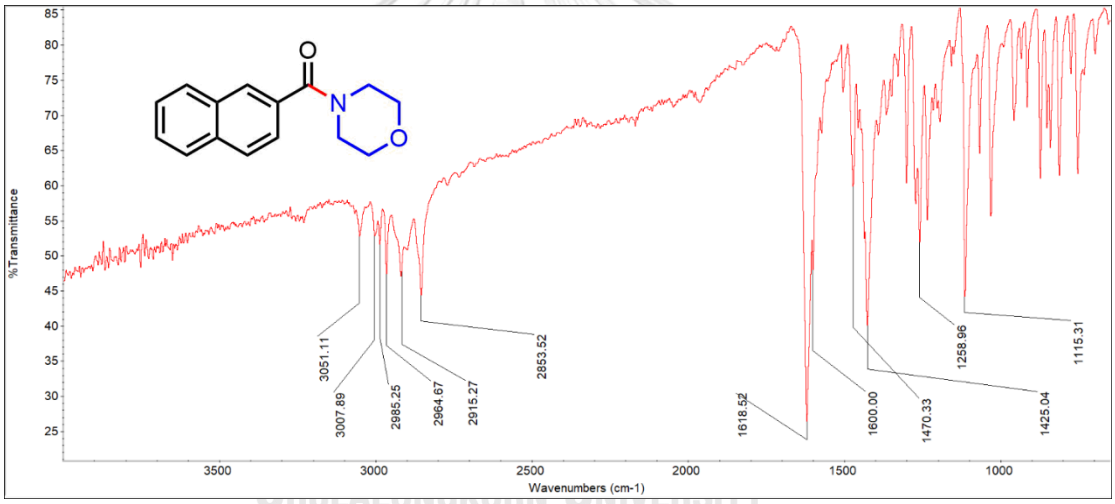

Figure A115 FT-IR spectrum of **3qa**

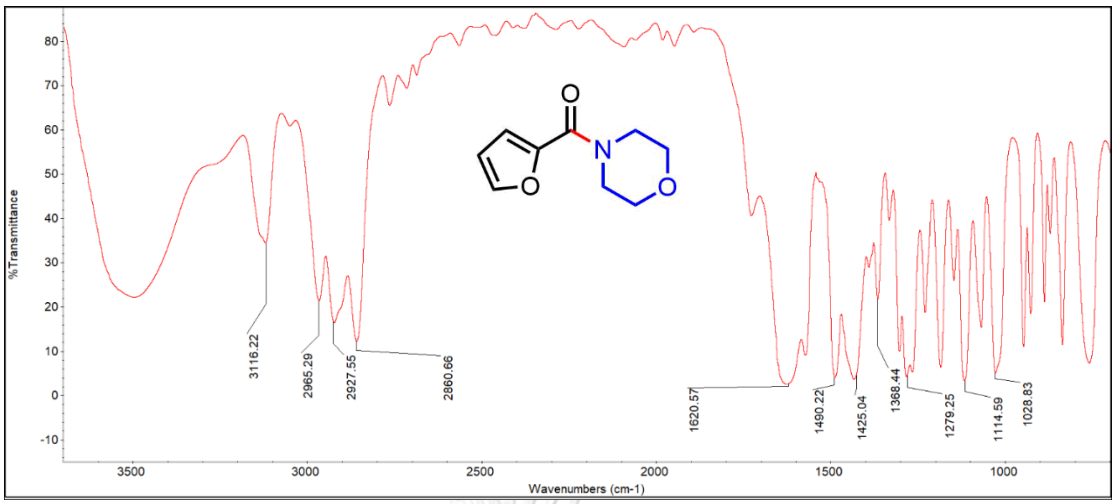

Figure A116 FT-IR spectrum of **3ra**

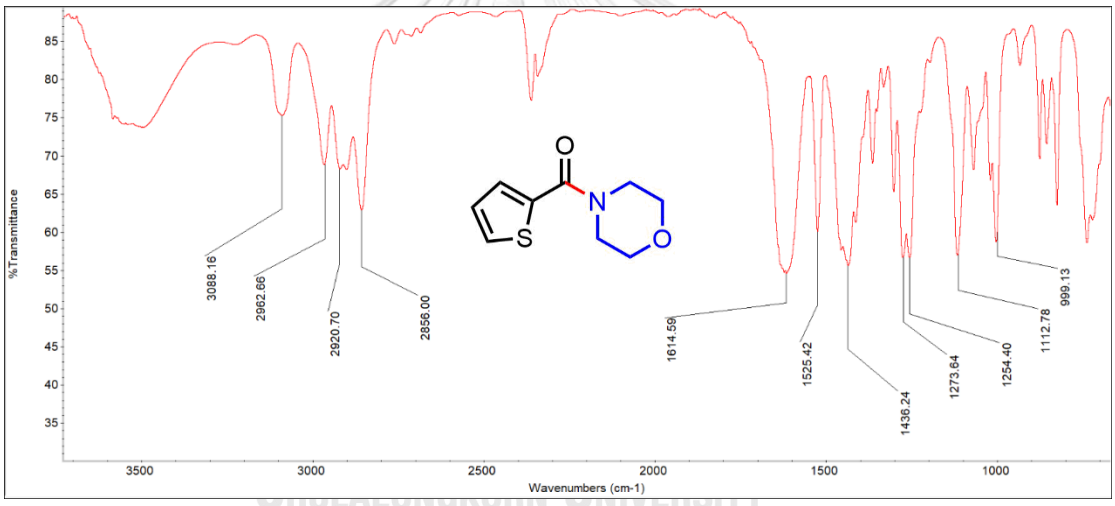

Figure A117 FT-IR spectrum of **3sa**

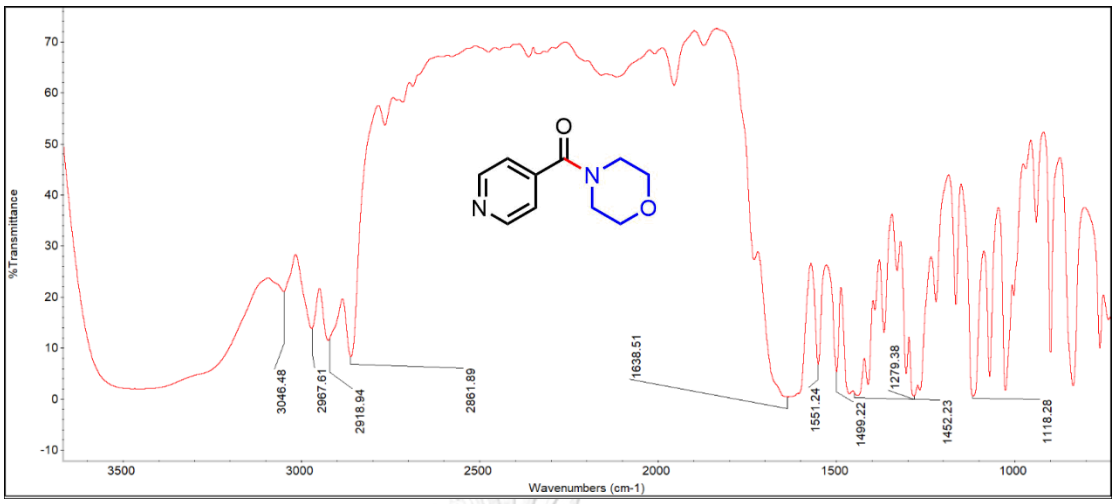

Figure A118 FT-IR spectrum of **3ta**

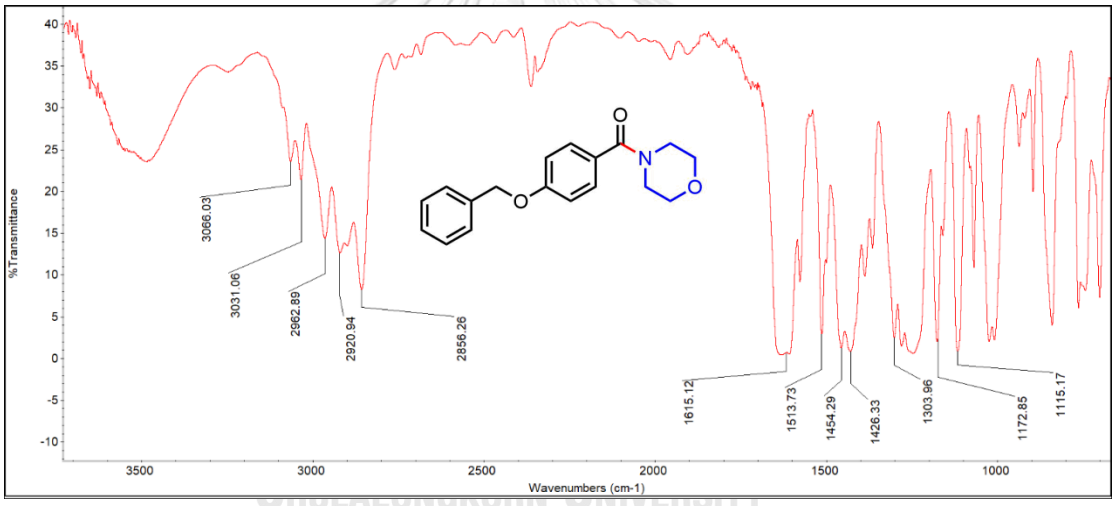

Figure A119 FT-IR spectrum of **3va**

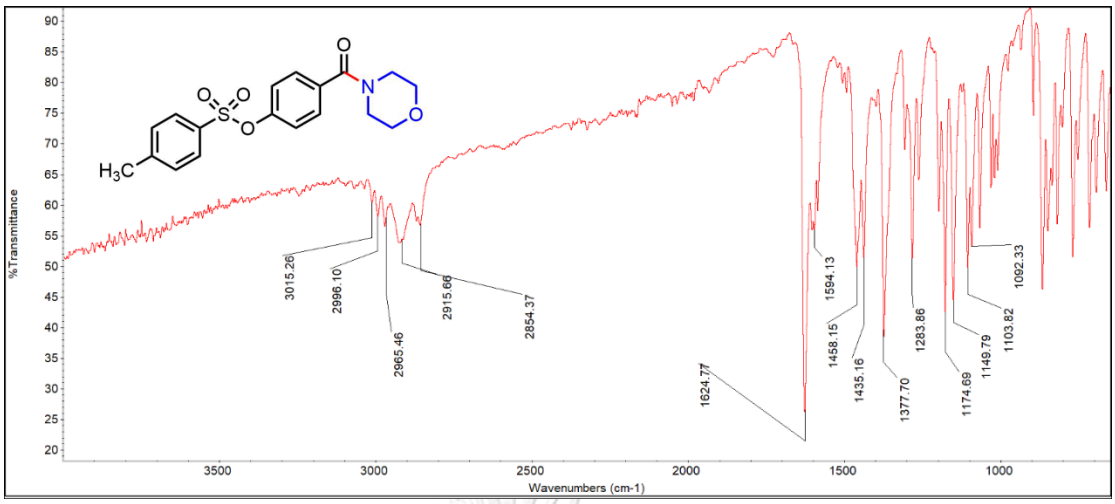

Figure A120 FT-IR spectrum of **3wa**

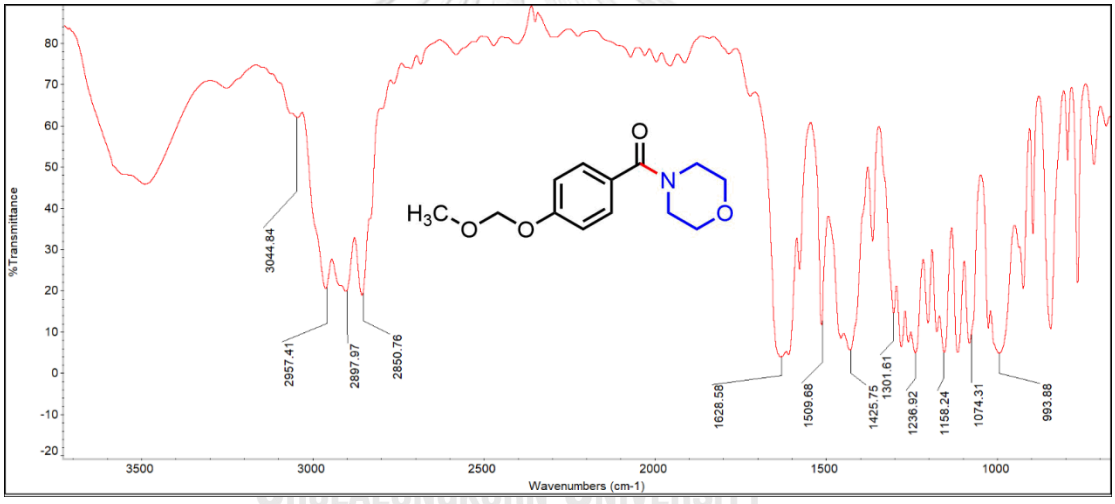

Figure A121 FT-IR spectrum of **3xa**

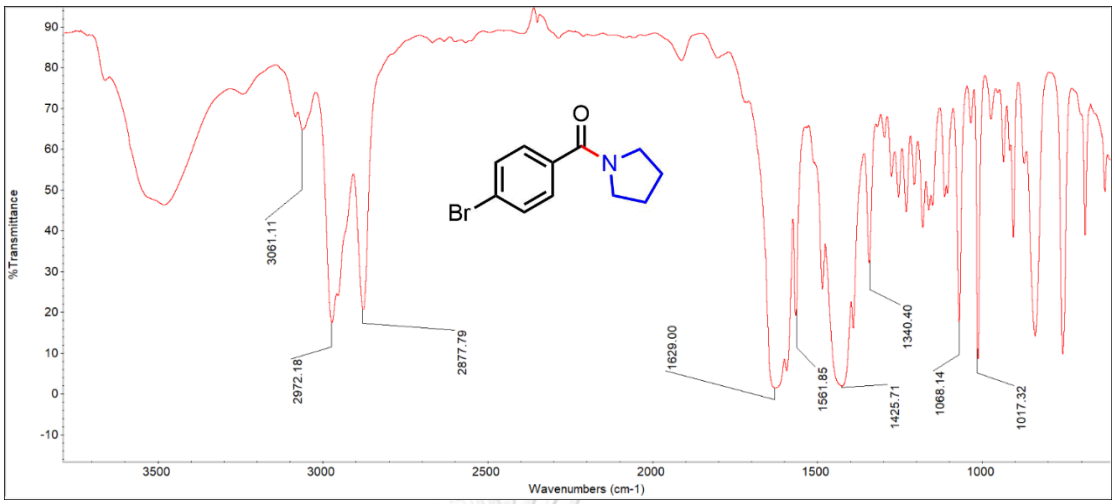

Figure A122 FT-IR spectrum of **3ab**

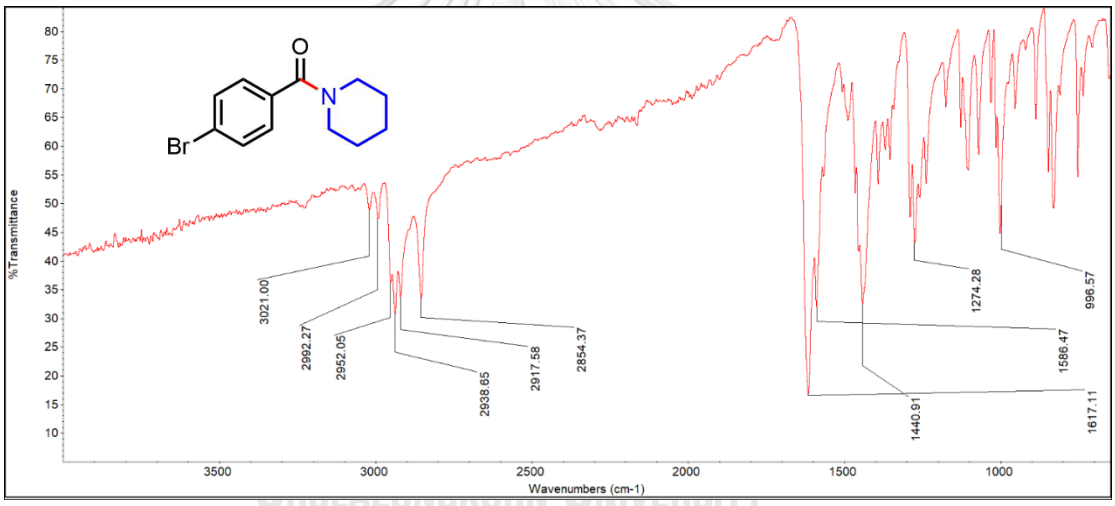

Figure A123 FT-IR spectrum of **3ac**

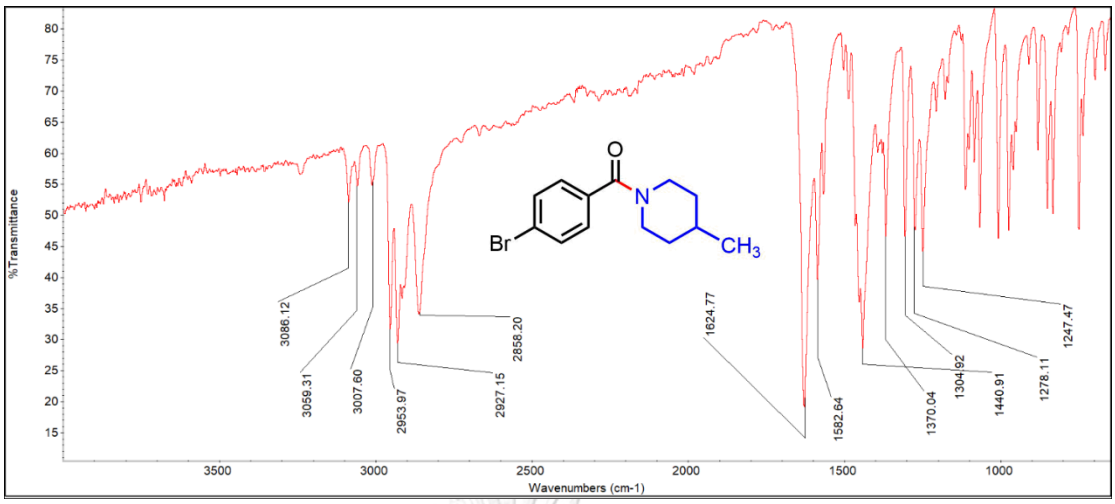

Figure A124 FT-IR spectrum of **3ad**

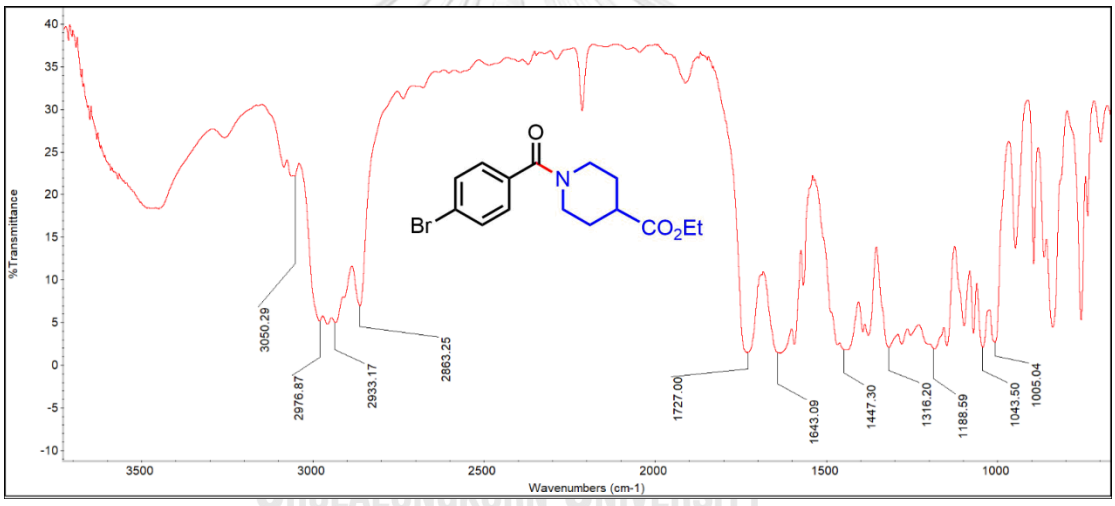

Figure A125 FT-IR spectrum of **3ae**

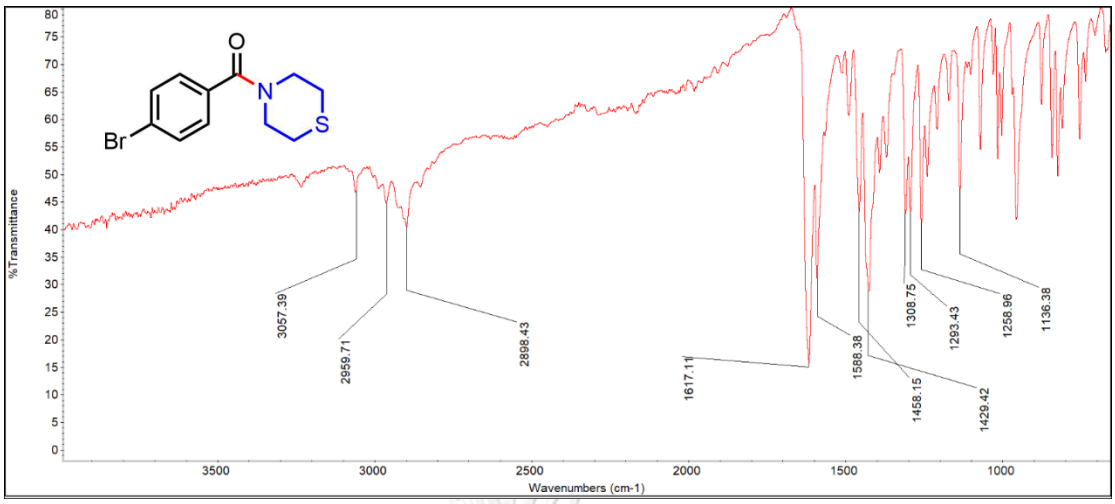

Figure A126 FT-IR spectrum of **3af**

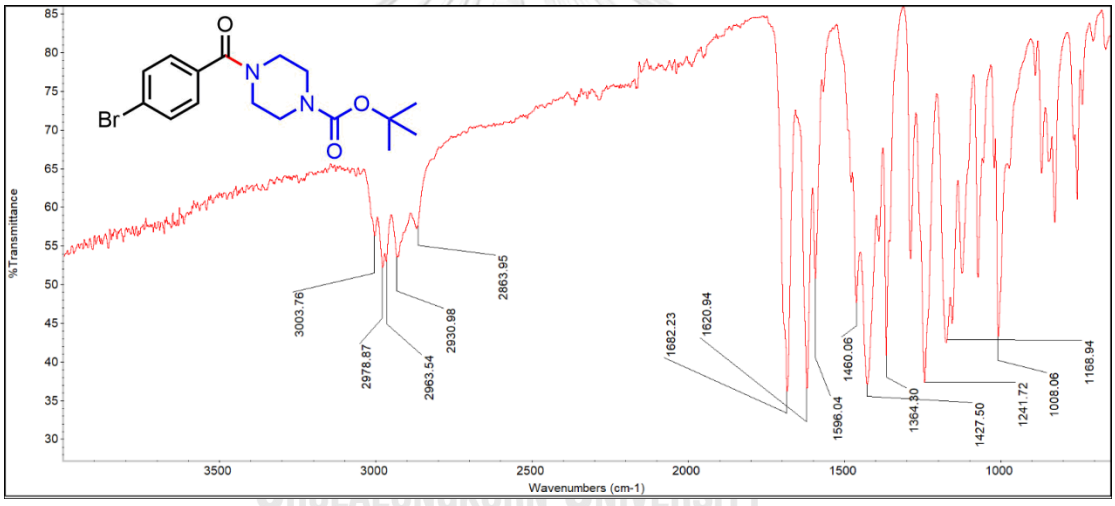

Figure A127 FT-IR spectrum of **3ag**

VITA

NAME	Tanawat Rerkracheneekorn
DATE OF BIRTH	11 December 1996
PLACE OF BIRTH	Bangkok, Thailand
INSTITUTIONS ATTENDED	Chulalongkorn University
HOME ADDRESS	399 Charoen Krung Road, Pom Prap, Pom Prap Sattru Phai, Bangkok 10100
PUBLICATION	1. Rerkrachaneekorn, T.; Tankam, T.; Sukwattanasinitt, M.; Wacharasindhu, S. Tetrahedron Lett., 2021, 70, 153017. 2. Huynh, Nguyen, Thanh, T.; Tankam, T.; Koguchi, S.; Rerkrachaneekorn, T.; Sukwattanasinitt, M.; Wacharasindhu, S. Green Chem., 2021, DOI: 10.1039/D1GC01131F
AWARD RECEIVED	-